

**THE POTENTIAL OF RAMAN SPECTROSCOPY IN  
DISTINGUISHING BETWEEN WOOL AND MOHAIR FIBRES**

By

**Mzwamadoda Notayi**

**(212461753)**

Submitted in fulfilment of the requirements for the

Degree of Doctor of Philosophy

in

The Faculty of Science

at the

Nelson Mandela University

Promoter: Professor Lawrance Hunter

Co-Promoters: Professor Japie A. Engelbrecht and  
Dr Anton F. Botha

December 2020

## DECLARATION

I, Mzwamadoda Notayi, student number 212461753, hereby declare that the thesis for PhD (Textile Science) to be awarded is my own work and that it has not previously been submitted for assessment or completion of any postgraduate qualification to another University or for another qualification.

  
..... (Signature)

04/12/2020  
..... (Date)

Official use:

In accordance with Rule G5.6.3,

**5.6.3** A treatise/dissertation/thesis must be accompanied by a written declaration on the part of the candidate to the effect that it is his/her own work and that it has not previously been submitted for assessment to another University or for another qualification. However, material from publications by the candidate may be embodied in a treatise/dissertation/thesis.

## **DEDICATION**

*This work is dedicated in loving memory of my late father and brother, Phambili Cardwel Notayi and Siviwe John Notayi, respectively, whom not a single day passes without thinking about them. This is also dedicated to the late and my closest cousin Thulani Lucky Mehlwempi.*

## ACKNOWLEDGEMENTS

- ❖ A big word of thanks goes to my supervisor, Prof Lawrence Hunter, for making this work a possibility through his professional guidance and mentorship throughout this study.
- ❖ My sincere word of thanks goes to my co-supervisors:  
Prof Japie A.A. Engelbrecht for his valuable suggestions and for always making time to listen and give valuable inputs throughout the course of this study.  
Dr Anton F. Botha for the samples used in this project, for always having time to listen to my problems and willingness to provide solutions.
- ❖ I would also like to thank Prof Mike Lee for his constructive criticism and the valuable inputs he made which added great value to this research study.
- ❖ The financial support from the National Research Foundation (NRF) and NMU postgraduate scholarship (PGRS) is greatly acknowledged.
- ❖ I would like to also acknowledge Mr Etienne G. Minnaar for his assistance with the Raman analysis and interpretation of the Raman and FTIR spectra.
- ❖ I would like to thank Dr Rudolph Erasmus of Wits University School of Physics for the analysis of wool and mohair samples in their micro Raman system.
- ❖ A word of thanks also goes to Dr Kwezi Mkentane in the Department of Medicine (Hair and Skin Research (HSR) Laboratory) at the University of Cape Town for the FTIR-LUMOS experiments on wool and mohair samples.
- ❖ A sincere word of thanks also goes to the staff of the Council for Scientific and Industrial Research (CSIR), in Port Elizabeth, for all the support.
- ❖ Let me thank Mr Johan Wessels and the whole staff of the NMU Physics Department, for always providing help whenever it was needed.
- ❖ The support of my friends Dr Asanda Mtibe, Dr Teboho Mokhena, Dr Thabang Mokhothu, Dr Ngcali Tile, Dr Jim Rapakgadi, Desmond Katleho Sekonyana, Nontsikelelo Dumakude and Yeki Sibusiso, throughout this study, is greatly acknowledged.
- ❖ A heartfelt gratitude also goes to everyone at city lights church (CLC) in Port Elizabeth for the prayers and all the support throughout the course of this study.
- ❖ Last but not by any means least, I want to thank my family and relatives, whom I love so much, for the patience and for always believing in me throughout the course of my studies.

## ABSTRACT

The possible application of the FT Raman, Raman micro-spectroscopy and ATR-FTIR micro-spectroscopy, have been investigated for distinguishing between wool and mohair. Highly identical Raman and FTIR spectra were obtained from the two fibre types, indicating that indeed they share similar basic molecular structural chemistry. The analysis of the amide I through curve fitting of wool and mohair FT Raman spectra showed that the protein and polypeptide secondary structure exists mainly in the  $\alpha$ -helical structural conformation with smaller proportions of  $\beta$ -pleated sheet and  $\beta$ -Turns. These proportions, however, could not be used to distinguish between wool and mohair, due to the significant overlap observed between the two fibres.

This study also determined the disulphide contents for possibly distinguishing between wool and mohair fibres, with the average and standard deviation values of  $0.20 \pm 0.04$  and  $0.17 \pm 0.03$  for wool and mohair, respectively, being found. Despite the mean values being found to differ statistically significant ( $p < 0.05$ ), a considerable overlap was observed, posing a doubt in the possible application of the method for distinguishing between the two fibres and blend composition analysis of the two fibres.

The application of ratiometric analysis, based on the relative peak heights of certain FT Raman bands, showed that a combination of ratios A ( $I_{2932}/I_{1450}$ ) and D ( $I_{508}/I_{1450}$ ) could hold great potential in distinguishing between wool and mohair fibre samples. The individual values of ratios A and D varied a great deal from one mohair sample to the other and even more from one wool sample to another, with the individual values for ratio A ranging from 2.71-3.68 and 2.35-3.08 for wool and mohair, respectively, while ratio D ranged from 0.18-0.32 and 0.17-0.22 for wool and mohair, respectively. An important observation from this study is that if, for an unknown sample, if individual values of ratios A and D exceed 3.1 and 0.22, respectively, are found then the sample is most likely to be either a pure wool or blend of wool and mohair, whereas if all the values fall below the two threshold values, then the unknown sample can be declared a pure mohair sample.

A Raman spectral database or library of approximately 100 high quality Raman average spectra of wool and mohair fibres has been established for the Bruker 80V FTIR/Raman spectrophotometer at the Nelson Mandela University (NMU). Although this has not been fully validated due to the unforeseen frequent breakdown encountered with the FT Raman system, at this stage, it has been realized that verification of unknown materials is highly possible. A great need for the development of a classification model based on multivariate or chemometrics has been realized.

An ATR-FTIR LUMOS micro-spectroscopic system was also investigated for the possible application in distinguishing between wool and mohair single fibres. The amide I/II band ratios were determined for both wool and mohair fibres to distinguish between the two fibre types. The mean and standard deviation values of  $1.20 \pm 0.02$  and  $1.21 \pm 0.01$  for mohair and wool, respectively, were found and were shown not to differ statistically significant ( $p > 0.05$ ). The secondary structure analysis showed that the content of the  $\alpha$ -helical secondary structure might be different between the two fibre types, with a great overlap of individual values, however, being observed between the two fibre types (wool and mohair), raising concerns in the possible application of the  $\alpha$ -helical content for distinguishing the two fibres.

## TABLE OF CONTENTS

DECLARATION.....	i
DEDICATION .....	ii
ACKNOWLEDGEMENTS .....	iii
ABSTRACT .....	iv
TABLE OF CONTENTS .....	vi
LIST OF ABBREVIATIONS.....	x
LIST OF FIGURES.....	xiii
LIST OF TABLES.....	xvii
CHAPTER ONE .....	1
INTRODUCTION.....	1
1.1 BACKGROUND OF THE STUDY.....	1
1.2 PRODUCTION, QUALITY AND PROCESSING OF SOUTH AFRICAN WOOL AND MOHAIR FIBRES.....	5
1.2.1 South African Wool and Mohair Fibre Production and Quality.....	5
1.2.2 Processing of Raw Animal Fibre.....	6
1.2.2.1 Cleaning and Scouring.....	7
1.2.2.2 Carbonizing.....	9
1.2.2.3 Moth proofing.....	9
1.3 SIGNIFICANCE OF THE STUDY.....	9
1.4 AIMS AND OBJECTIVES.....	11
1.4.1 Objectives.....	11
1.4.2 Thesis Outline.....	11
1.5 THEORY OF VIBRATIONAL SPECTROSCOPY .....	12
1.5.1 Infrared Spectroscopy.....	12
1.5.1.1 Brief Theory .....	12
1.6.1.2 Fourier Transform (FT) IR micro-spectroscopy .....	13

1.5.2 Raman Spectroscopy .....	15
1.5.2.1 Introduction .....	15
1.5.2.2 Instrumentation and Basic Theory of Raman Spectroscopy ...	15
1.6 SELECTION RULES .....	19
1.7 QUALITATIVE AND QUANTITATIVE SPECTROSCOPIC METHODS.....	21
1.8 SPECTROSCOPIC LIBRARIES FOR IDENTIFICATION OF MATERIALS. ....	24
CHAPTER 2.....	26
LITERATURE SURVEY.....	26
2.1 INTRODUCTION.....	26
2.2 PHYSICAL AND CHEMICAL STRUCTURE OF ANIMAL FIBRES .....	26
2.2.1 Physical (Morphological) Structure .....	26
2.2.1.1 The Cuticle.....	27
2.2.1.2 Cortex .....	28
2.2.1.3 Medulla .....	30
2.2.2 Chemical Structure of Natural Protein Fibres .....	30
2.2.2.1 The Peptide Bond .....	30
2.2.2.2 Polypeptide Chain.....	31
2.2.2.1 Secondary Structure of Keratin Fibres .....	39
2.3 ANIMAL FIBRE IDENTIFICATION AND BLEND ANALYSIS TECHNIQUES.....	40
2.3.1 Introduction.....	40
2.3.2 General.....	40
2.3.3 Surface Topography Based Methods .....	43
2.3.3.1 Light Microscopy (LM).....	43
2.3.3.2 Scanning Electron Microscopy (SEM).....	50
2.3.3.3 Atomic Force Microscopy (AFM).....	61
2.3.4 DNA Analysis.....	63
2.3.5 Amino Acid and Protein Analysis Based Methods .....	70



2.3.5.1 Electrophoresis .....	70
2.3.5.2 Chromatography .....	76
2.3.6 Vibrational Spectroscopic Techniques.....	79
2.3.6.1 Infrared Spectroscopy .....	80
2.3.6.2 Raman Spectroscopy.....	86
2.3.7 Other Techniques .....	97
2.4 LITERATURE REVIEW SUMMARY.....	101
2.4.1 General.....	101
2.4.2 Techniques Applied for Animal Fibre Identification and Blend Analysis .....	102
2.5 MOTIVATION.....	106
CHAPTER THREE.....	107
EXPERIMENTAL METHODOLOGY.....	107
3.1 INTRODUCTION.....	107
3.2 MATERIALS.....	107
3.3 WOOL AND MOHAIR SAMPLE TREATMENT .....	110
3.4 EXPERIMENTAL PROCEDURE AND INSTRUMENTATION.....	111
3.4.1 Sample Preparation .....	111
3.4.2 Instrumentation and Experimental Design .....	113
3.4.2.1 FT-Raman Spectrophotometry.....	113
3.4.2.2 Raman-Micro Spectrometry.....	116
3.4.2.3 ATR-FTIR LUMOS Micro-Spectrophotometry .....	118
3.4.3 Data Pre-Processing.....	119
3.5 EXPERIMENTAL FACTORS WHICH COULD AFFECT RAMAN PEAK HEIGHTS.....	123
3.5.1 Comparison of Washed and Unwashed Fibre Spectra.....	124
3.5.2 Fibre Sample Thickness .....	126
3.5.3 Laser Drift During Spectral Acquisition .....	128

CHAPTER FOUR.....	133
RESULTS AND DISCUSSION.....	133
4.1 INTRODUCTION.....	133
4.2.1 FT Raman Spectroscopic Analysis.....	134
4.2.1.1 Curve-Fitting of the Amide I and S-S Stretching Vibrations..	140
4.2.1.2 The Disulphide Content of Wool and Mohair Fibres.....	148
4.2.1.3 Raman Peak Height Ratios for the Identification of Wool and Mohair Fibres.....	151
4.2.1.3.1 Reproducibility of the Ratiometric Analysis .....	169
OSP51 wool.....	176
4.2.1.4 Spectral Database Development and Partial Validation for Wool and Mohair. ....	178
4.2.1.4.1 Vector Normalization .....	123
4.2.1.4.2 Min-Max normalization .....	123
4.2.2 Micro-Raman Fibre Analysis.....	194
4.3 FTIR MICROSCOPIC EXAMINATION OF WOOL AND MOHAIR FIBRES .....	203
4.3.1 Introduction.....	203
4.3.2 Amide Band Analysis for Distinguishing Between Wool and Mohair ..	203
4.3.3 FTIR Spectral Curve Fitting Results .....	205
4.3.4 Secondary Structure Analysis for Wool and Mohair. ....	210
CHAPTER FIVE.....	212
5.1 CONCLUSIONS.....	212
5.2 RECOMMENDATIONS FOR THE FUTURE .....	215
5.3 REFERENCES.....	217
APPENDICES .....	245

## LIST OF ABBREVIATIONS

AATCC	American Association for Textile Chemists and Colourists
ANN	Artificial Neural Networks
ASTM	American Society for Testing and Materials
ATR	Attenuated Total Reflectance
AFM	Atomic Force Microscope
BA	Buenos Aires
BTTG	British Textile Technology Group
CCMI	Cashmere and Camel Hair Manufacturers Institute
CSH	Cuticle Scale Height
CSIR	Council for Scientific and Industrial Research
CMC	Cell Membrane Complex
DNA	Deoxyribonucleic Acid
DSC	Differential Scanning Calorimeter
DWI	Deutsches Wollforschungsinstitut
ESI-MS	Electrospray Mass Spectrometry
FTIR	Fourier Transform Infrared
FTR	Fourier Transform Raman
FWHM	Full Width at Half Maximum
GC	Gas Chromatography
GGG	Gauche-Gauche-Gauche

GGT	Gauche-Gauche-Trans
TGT	Trans-Gauche-Trans
HPLC	High Performance Liquid Chromatography
HQI	Hit Quality Index
IMA	International Mohair Association
ISO	International Standard Organization
IWTO	International Wool Testing Organization
LC	Liquid Chromatography
LM	Light Microscope
LS	Least Squares
MFD	Mean Fibre Diameter
mt-DNA	Mitochondrial DNA
NIRS	Near Infrared Spectroscopy
NMR	Nuclear Magnetic Resonance
PCR	Polymerase Chain Reaction
PCA	Principal Component Analysis
PLS	Partial Least Squares
RFLP	Restriction Fragment Length Polymorphism
SDS-PAGE	Sodium Dodecyl Sulphate-Polyacrylamide Gel Electrophoresis
SEM	Scanning Electron Microscope
SPM	Scanning Probe Microscopy

SCM	S-Carboxymethylation
TEM	Transmission Electron Microscope
TGA	Thermogravimetric Analysis
WRONZ	Wool Research Organization of New Zealand
XRD	X-ray diffraction

## LIST OF FIGURES

Figure 1.1: Origin of speciality animal fibres.....	2
Figure 1.2: A schematic diagram of an FTIR system. ....	14
Figure 1.3: Schematic diagram of an FT Raman spectrometer.....	16
Figure 1.4: (a) Resonance fluorescence and (b) Rayleigh, Raman Stokes and Raman anti-stokes scattering. (0) Denotes the ground electronic state and (1) denotes the first excited electronic state. (v) indicates vibrational energy levels.....	17
Figure 1.5: Baseline method of eliminating background absorption by means of a tangent. ....	22
Figure 2.1: Physical structure of a wool fibre.....	27
Figure 2.2: A detailed typical inner structure of animal fibres. ....	29
Figure 2.3: Formation of peptide bond by condensation reaction.....	31
Figure 2.4: Protein transformation into different structural conformation. ....	32
Figure 2.5: Identification and classification of animal fibres by their fineness.....	49
Figure 2.6: Animal fibre CSH (h) measurement. ....	52
Figure 2.7: Classification and characterization of speciality animal fibres using the SEM. ....	53
Figure 2.8: SEM micrographs of mohair (left) and wool Buenos Aires (right) fibres at 1000X magnification, and close-ups of their cuticle scale edges at 250000X magnification).....	54
Figure 2.9: Summary of CSH measurements on 18 wools and 14 speciality fibres as box-whisker plots.....	56
Figure 2.10: SEM micrographs of (a) Cashmere fibres and (b) CSH. ....	58
Figure 2.11: SEM micrographs of (a) Cashmere and (b) Wool scales. ....	59
Figure 2.12: Microscopic images of descaled animal fibres. ....	60
Figure 2.13: A simplified schematic representation of nuclear and mt-DNA.....	63
Figure 2.14: The steps involved in the isolation, purification and hybridization of DNA.....	64
Figure 2.15: DNA analysis using the dot-blot method. ....	66
Figure 2.16: RFLP profiles of PCR products containing mtcyt b sequences obtained from DNA of cashmere and wool fibre.....	68
Figure 2.17: Steps involved in the isolation of proteins from keratins.....	71

Figure 2.18: Schematic presentation of animal fibre identification and classification procedure.....	73
Figure 2.19: Densitometric traces of different llama/mohair. ....	75
Figure 2.20: Typical FTIR spectra of cashmere fibres.....	85
Figure 2.21: Raman spectra of wool fibers with different stretch ratios: (a) 0, (b) 30, (c) 50, (d) 80, and (e) 110% .....	88
Figure 2.22: Effect of laser power on the FT Raman spectrum of raw Merino wool (A) 400 mW, (B) 350 mW, (C) 300 mW, (D) 250 mW, (E) 200 mW, (F) 150 mW, (G) 100 mW and (H) 50 mW.....	89
Figure 2.23: Typical FT Raman spectrum of untreated wool.....	90
Figure 2.24: SEM micrographs of cuticle cell fragments (top) and cortical cells (bottom) isolated from the Merino wool fibre. ....	93
Figure 2.25: FT Raman spectra of (A) cuticle cell fragments, (B) cortex fragments and (C) whole Merino fibres. ....	94
Figure 2.26: (a): The deconvolution of amide I band obtained from unstretched sulphite treated wool fibres (b): The deconvolution of amide I band obtained from sulphite treated wool fibres stretched 66 %.....	95
Figure 3.1: Optical microscopic images of wool with different orientations.....	112
Figure 3.2: Bruker 80V FTIR/Raman spectrophotometer setup. ....	113
Figure 3.3: Illustration of the extraction Raman peak heights using the baseline method. ....	122
Figure 3.4: FT Raman spectra of unwashed wool (red) and washed wool (black). ....	124
Figure 3.5: Raman spectrum of naphthalene. ....	125
Figure 3.6: Effect of doubling wool sample thickness on Raman spectra.....	127
Figure 3.7: Effect of sample thickness on Raman peak heights.....	128
Figure 3.8: Relative peak height variation along the length of the fibre bundle. ....	129
Figure 3.9: Variation in the Raman peak heights between fibre bundles of the same wool and mohair sample. ....	130
Figure 3.10: An example of the relative peak height variation within the same spot. ....	131
Figure 3.11: Wool Raman spectrum with a strong fluorescence background.....	132
Figure 4.1: Baseline corrected average FT Raman spectra of wool (red) and mohair (blue) in the (a) 2600-3200 $\text{cm}^{-1}$ and (b) 400-1800 $\text{cm}^{-1}$ spectral regions .....	135

Figure 4.2: Raman second derivative spectra of the amide I (top) and the S-S stretch (bottom) spectral regions for wool (left) and mohair (right) fibres. ....	142
Figure 4.3: Amide I curve fitting on (a) wool and (b) mohair Raman spectra.....	143
Figure 4.4: Typical curve fitting results of the S-S stretching vibration for (a) wool and (b) mohair spectra. ....	146
Figure 4.5: Box whisker plot of the disulphide content values for wool and mohair. ....	150
Figure 4.6: Normalized average Raman spectra of wool (red) and mohair fibres, respectively. ....	154
Figure 4.7: Relationship between Raman relative intensities and mean fibre diameter. ....	155
Figure 4.8: Raman band ratios for wool and mohair fibres.....	158
Figure 4.9: Distributions of Ratio A values for wool and mohair. ....	159
Figure 4.10: Ratio B distributions for wool and mohair. ....	161
Figure 4.11: Ratio C distributions for wool and mohair fibre samples. ....	162
Figure 4.12: Distributions of the Ratio D for wool and mohair. ....	163
Figure 4.13: Ratio E distributions for wool and mohair. ....	165
Figure 4.14: Ratio F distributions for wool and mohair. ....	167
Figure 4.15: Ratio G distribution for wool and mohair. ....	168
Figure 4.16(a): The influence of the strongest band in the HQI matching for the same spectrum. ....	181
Figure 4.16(b): The influence of the strongest band in the HQI matching for the same spectrum. ....	182
Figure 4.17: Examples of spectral search result, with the red, blue and green spectra as the query, the first hit of the hit list and the actual match, respectively. ....	184
Figure 4.18(a): Search result of the first query spectrum of the 1052 mohair.....	186
Figure 4.18(b): Search result of the second query spectrum of the 1052 mohair... ..	187
Figure 4.18(c): Search result of the third query of the 1052 mohair. ....	188
Figure 4.18(d): Search result for the fourth query spectrum of the 1052 mohair. ...	189
Figure 4.19: Spectral search result for CBP SS4 merino wool. ....	190
Figure 4.20(a): Wool (red) and mohair (blue) spectra over the spectral range 0-2000 $\text{cm}^{-1}$ . ....	197
Figure 4.20 (b): Wool (red) and mohair (blue) spectra over a spectral range of 2200-3400 $\text{cm}^{-1}$ . ....	198



Figure 4.21: Box whisker plots of micro- Raman peak height ratios (A-G) for wool and mohair fibres.....	200
Figure 4.22: Box whisker of the ratio D values for wool and mohair.....	201
Figure 4.23: Wool and mohair FTIR spectra in the spectral range 500-4000 $\text{cm}^{-1}$ .	204
Figure 4.24: FTIR second derivative spectra of mohair and wool in the 1500-1750 $\text{cm}^{-1}$ spectral range.....	207

## LIST OF TABLES

Table 1.1: World production of wool fibre. ....	8
Table 1.2: Band intensities in the vibration-rotation infrared and Raman spectra ....	21
Table 2.1: Chemical composition of wool fibres. ....	34
Table 2.2: Amino acid composition of Australian cashmere from individual goats and wool.....	36
Table 2.3: A comparison of amino acid composition (wool mol <sup>-1</sup> %) of whole wool, cuticle cells, and the ortho and para cortical cells. ....	38
Table 2.4: Fibre identification tools and targets.....	42
Table 2.5: Methods proposed for the analysis of keratin fibres. ....	43
Table 2.6: Comparison of SEM and LM capabilities in examining animal fibres .....	46
Table 2.7: Amino acid composition of different protein fibres.....	78
Table 2.8: Keratin fibre FTIR chemical bands.....	84
Table 2.9: Raman band assignments of wool and human hair.....	91
Table 3.1: Details of wool and mohair samples tested.....	108
Table 3.2: Operating conditions used in this study and those used in a previous study.....	114
Table 3.3: Band positions with corresponding baselines.....	120
Table 3.4: Comparison between spectra acquired from washed and unwashed wool fibre samples.....	126
Table 3.5: Wool and mohair (all Texas) samples analysed on the Horiba Jobin-Yvon T64000 Raman micro-spectrometer.....	245
Table 3.6: List of wool and mohair samples analysed on the FTIR-LUMOS.....	245
Table 3.7: FTIR-LUMOS operating conditions.....	119
Table 4.1: FT Raman band assignments for wool and mohair, respectively.....	137
Table 4.1 continued... ..	138
Table 4.2: Amide I band components from wool and mohair spectra.....	144
Table 4.3: Raman secondary structure of wool and mohair fibres.....	145
Table 4.4: Raman band components analysis of the S-S stretch band for wool and mohair.....	147
Table 4.5: The disulphide content of wool and mohair fibres.....	148
Table 4.6: Correlation coefficients for the relative intensities against MFDs.....	152
Table 4.7: Raman relative intensities determined from wool and mohair spectra.....	156

Table 4.8: Relative peak height ratios for wool and mohair fibre samples.....	157
Table 4.9: The possible application of Ratio A in practice. ....	169
Table 4.10: Possible applicability of Ratio B in practice. ....	170
Table 4.11: Possible application of Ratio C in practice. ....	170
Table 4.12: Possible application of Ratio D in practice. ....	171
Table 4.13: Possible application of ratio E in practice. ....	172
Table 4.14: Possible application of Ratio F in practice. ....	172
Table 4.15: Possible application of Ratio G in practice. ....	173
Table 4.16: Ratiometric analysis validation results.....	175
Table 4.17: Spectral matching results of normalized spectra. ....	191
Table 4.17: continued... ..	192
Table 4.18: Micro-Raman spectral positions of selected bands for wool and mohair. .....	195
Table 4.19: Micro-Raman relative peak heights for wool and mohair fibres. ....	196
Table 4.20: Amide I/II ratios for wool and mohair. ....	205
Table 4.21: IR spectral band positions for wool and mohair fibres. ....	208
Table 4.22: Band areas and heights determined by curve fitting.....	209
Table 4.23: Summary of the secondary structure analysis.....	210

# CHAPTER ONE

## INTRODUCTION

### 1.1 BACKGROUND OF THE STUDY

There is a group of natural animal fibres, popularly referred to as speciality, luxurious or rare fibres, since they possess an image and properties considered to be superior to those of sheep wool. The family of speciality animal fibres includes cashmere, mohair, camel hair, Angora rabbit hair, alpaca, yak, etc. (Sawbridge and Ford, 1987). Cashmere and mohair fibres are two of the most important of the speciality fibre family due to their outstanding properties, such as fineness and lustre (Phan and Wortmann, 1996). Wool and speciality fibres grow from the skins of their respective animals and these fibre types resemble each other in physical and chemical make-up, hence the difficulty in their identification and classification particularly when blended together. Fibres from different animal species (particularly goat hair, sheep wool or camel hair) are sometimes blended to achieve various effects, such as improved properties (additional beauty, colour, softness, durability or lustre), special effects and often for cost savings (von Bergen, 1963). Unfortunately, the latter benefit, cost savings, has led to certain unscrupulous dealers blending a less expensive animal fibre, such as sheep wool, with a more expensive one, while passing it off as an unblended product, containing 100 % of the more expensive fibre. Wool (sheep hair) is the most widely produced animal fibre (Popescu and Wortmann, 2010). Its core material is  $\alpha$ -keratin, a protein contained in the cortex or the body of the fibre, with the fibre surface covered by a layer of overlapping cuticle scales like roof tiles or fish scales. This also applies to most of the other animal fibres. Nevertheless, the physical dimensions of the scales and the pattern, or form, in which they are arranged on the fibre surface generally vary for different animal fibre types and may even vary for different fibres from the fleece of one animal. The analysis of animal fibre blends has traditionally relied on the use of Light Microscopy (LM) and Scanning Electron Microscopy (SEM), to differentiate between different animal fibre types based upon differences in the fibre surface characteristics. Figure 1.1 shows the animals producing speciality or rare fibres.

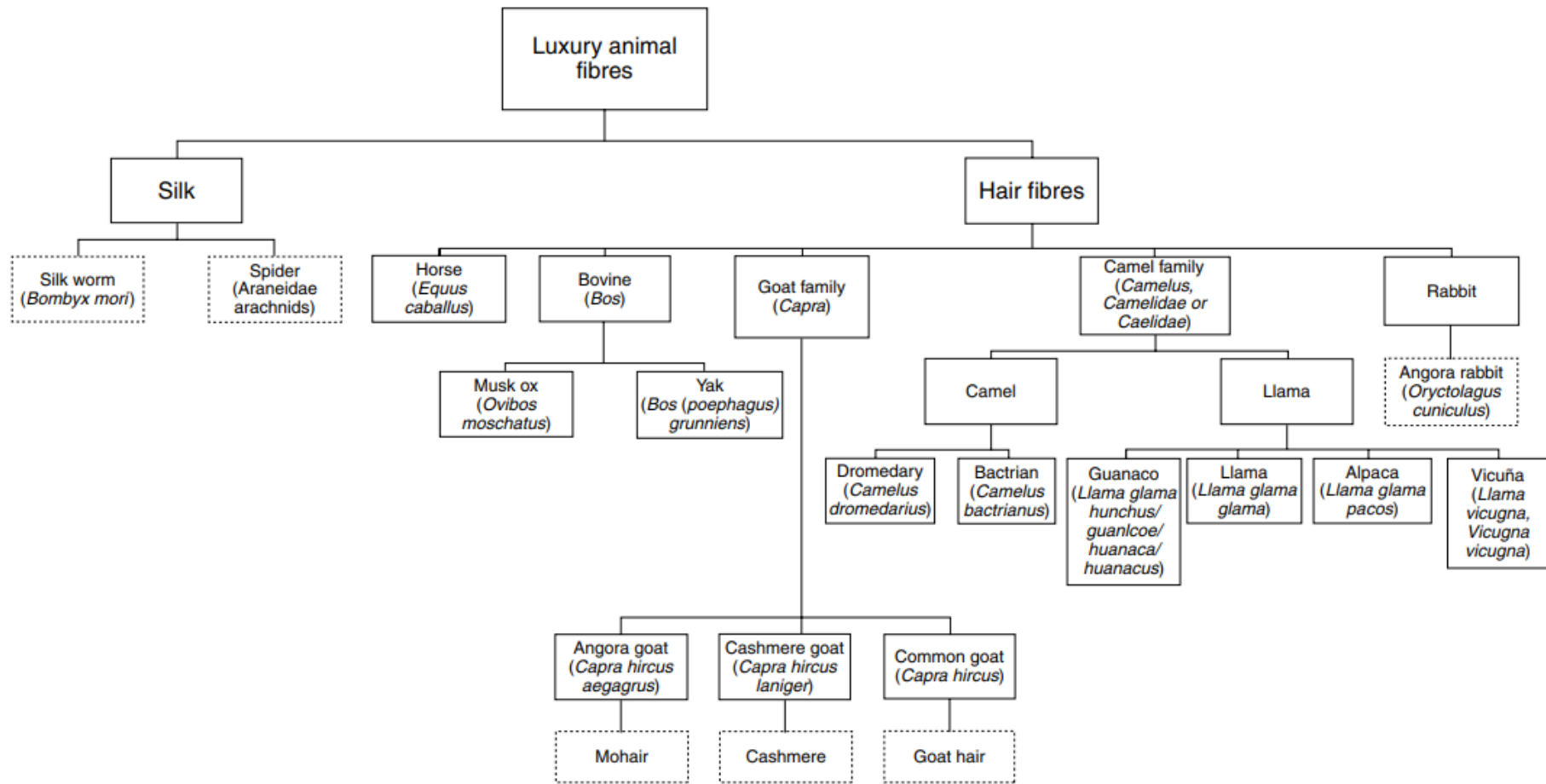


Figure 1.1: Origin of speciality animal fibres (von Bergen, 1963).

The methodologies underpinning these techniques are documented in the International Wool Testing Organization (IWTO-58, 1998), the Technical Manual of the American Association of Textile Chemists and Colourists (AATCC, 1971), American Society for Testing and Materials (ASTM, 1993) and also in the ISO International Standard Organisation (ISO-17751, 2007) test methods. Fibre identification and characterization are not only the problem of the textile industry but are also one facing the forensic science field, where identification of animal and human hairs is crucial for solving criminal cases. The ability to determine the composition of textile materials (fibre, yarn or garment) is of high necessity for various organizations such as textile manufacturers, import and export houses, government agencies, R&D institutes, and academic institutions (for carrying out applied research), investigation such as archaeological studies for identification of ancient textile fibres from various archaeological tracts, case analyses by legal experts, and so on (Zhong and Xiao, 2008). Fibre identification plays a huge and crucial role in the textile industry world-wide, in terms of product labelling and certification, and also in dealing with the problem of unscrupulous adulteration of expensive fibres with less expensive ones and then misrepresenting the blend composition in the product label (Kurabayashi *et al*, 2009). The high demand for speciality fibres, such as mohair and cashmere, their scarcity and their high prices compared to sheep wool are believed to be the main reasons for this unscrupulous adulteration and false labelling of the fibre content of mohair textile products. Misrepresentation or wrong declaration of fibre content in garments represents a multi-million-dollar fraud, and downgrades the image of superb quality of speciality fibres, such as cashmere, mohair and camel hair (Hamlyn, 1998).

An important issue often encountered by customs officials, retailers and consumers, is whether the blend composition specified on the label of a textile product accurately reflects the actual blend composition in the product. This is of particular importance where luxury or speciality fibres, such as cashmere and mohair are involved which carries a price premium and an image of high quality. For example, one of the big questions the textile industry is confronted with is whether the one hundred percent cashmere labels found on textile products are true or just persuasive advertising. The knowledge of the exact fibre making up the fabric or material is of high importance in the value of the fabric and this is because different fibres possess

different properties, which may significantly affect the properties and value of the textile material. For example, a consumer paying for a high price cashmere, mohair or silk material would be mostly unhappy to discover that that the material is made of only polyester. The stringent labelling legal regulations within the EU and the Wool Products Labelling Act have forced the fibre content of yarns, fabrics and garments to be indicated (labelled) in order of predominance, with the corresponding name of the fibre component. Every fibre component greater than five percent in a textile must be stated (McGregor, 2012). Characterization and identification, and hence quantification, of different fibre types present in a textile product is a necessary and an important step in the accurate labelling of such products (Wortmann and Wortmann, 1992). This requires knowledge of all factors defining or distinguishing every type of fibre, animal or otherwise, present in the textile product. Kadikis (1987), in his research article, stated that each type of fibre found in a blend of animal fibres has its own unique set of defining characteristics, or fingerprint, such as the size, shape and frequency of scales, fibre diameter, distribution of pigmentation and fibre medullation, enabling its identification and classification. Nevertheless, in some cases, using such characteristics alone, does not provide for accurate determination of the composition of textile products containing blends of certain animal fibres, such as wool and mohair. A variety of techniques have therefore been proposed and investigated for their applicability in the identification of animal fibres, and various studies have been undertaken to determine the specific characteristics of different types of animal fibres which can be used in their identification. In spite of all these efforts, however, the only internationally accepted technique or method for distinguishing between certain animal fibres, such as wool and mohair, in a blend, and for accurately quantifying the blend composition, is that based on cuticle scale height, using a scanning electron microscope (SEM) (Wortmann and Arns, 1986). This method, however, is slow, labour intensive, and expensive and somewhat depend upon the experience of the operator. Hence, the need for the development of a reliable, accurate, objective and cost-effective method, Hamlyn *et al.*, (1995) stating that a sophisticated and complex high technology solution is a necessity to meet some of these requirements. More specifically, such a technique or method must, for example, be able to distinguish between lustre wools, and speciality fibres (e.g. cashmere, mohair, and rabbit hair), with which they are often blended. It must

also be able to distinguish between different speciality animal fibres, such as mohair, cashmere, camel hair, etc.

## **1.2 PRODUCTION, QUALITY AND PROCESSING OF SOUTH AFRICAN WOOL AND MOHAIR FIBRES**

### **1.2.1 South African Wool and Mohair Fibre Production and Quality**

According to Hudson *et al.*, (1993), the earliest use of wool fibre occurred before recorded history as it is believed that sheepskin, including the hair, was used long before it was discovered that the fibres could be spun into yarns or even felted into a fabric. The major source of the world's wool fibre is Australia, constituting about 25% of greasy wool of the world market. Other countries also contributing considerable amounts include China, New Zealand and Argentina (see Table 1.1). South Africa makes the list of other countries that contribute substantial amounts in the world's total production of wool. South Africa, a vast and beautiful country, prides itself with its rich history of sheep and wool farming. This long history has established wool growers who have a keen appreciation of how to care for their animals and the environment. As a result, the industry consistently generates a high quality, environmentally sound product for international markets. There are various sheep breeds worldwide, making a total of approximately 500 different breeds of domestic sheep, with merino sheep being well known for producing wool of high softness, fineness and their high-quality wool for apparel, with also a wide variety of merino bloodlines found to exist. The textile industry processes substantial amounts of fibre, obtained from a variety of animals, of which wool from sheep is one of the commercially important for South Africa. The composition of wool sheep in South Africa is predominantly merino and Karakul while 74% of wool clip is predominantly merino clip. Coarse and pigmented fibre types, however, are also produced and marketed on a limited stock. More than 50% of South African wool is produced in two provinces, namely the Eastern Cape (34%) and the Free State (24%) followed by Western and Northern Cape at 20% and 13%, respectively (source: DAFF, 2016). The fineness of Merino wool, often used in apparel textile materials, usually ranges from 10-25 microns while coarse ones around 75 microns gets application in making carpets and upholstery.



Mohair is produced by the Angora goat and it is sometimes referred to as “The Diamond Fibre” because of its natural outstanding lustre, due to its relatively large cuticle surface and also the flat scale edges compared to sheep wool (Hunter, 1993). According to Shelton, 1993, it is common knowledge that Angora goats were originally developed in the region known as Asia North Minor, which lies between the Black Sea and the Mediterranean where Turkey is situated. It is believed that these fibre producing goats inhabited the area of Asia Minor for at least 2000 years. In the beginning of the 1600s the Angoras were exported to different countries, mostly in Europe, aiming at establishing mohair industries in these areas. For various reasons, these attempts could not come through and the first major mohair industries were established in South Africa and the United States of America (USA). The first Angora goat imports from Turkey reached South Africa in 1838 (Shelton, 1993). This mohair fibre belongs to a class of fibres popularly known as speciality or luxury animal fibres, as shown Figure 1.1, and is amongst the most ancient fibres known to man. The world’s production amounts to approximately 5000 tons per year and South Africa contributes a major portion than any other country, constituting approximately 53 % of the world’s total production (Musango *et al.*, 2017). Other countries include Texas, Australia, Argentina, Lesotho and New Zealand.

The low flammability, felting, pilling and good durability, elasticity, resilience, resistance to soiling, soil shedding (it brushes clean easily), insulation and comfort are just a few properties making consumers to run after this fibre. Mohair’s outstanding lustre, soil shedding, smoothness, low soiling, and low felting all relate to its faint pattern of its surface scales. The coarseness of this fibre has its limitations when it comes to certain luxury apparel applications when compared to other rare fibres, however it has proved to be virtually unsurpassed when it comes to non-apparel applications such as furnishings, blankets, and upholstery. The mohair grown in South Africa is generally referred to as Cape Mohair and it is widely regarded as one of the best, finest and highest yield in the world (Hunter, 1993).

### **1.2.2 Processing of Raw Animal Fibre**

Before they are made into a finished textile product, animal fibres, such as wool, mohair and cashmere, must go through a number of chemical and physical treatment stages to assist in improving certain properties (Mozaffari-Medley, 2003).

The appropriate treatment depends mainly on the nature of the raw fibre and the intended end-use of the material. These chemical and physical processes may affect the morphological or chemical structure of the fibre which in turn may affect the accuracy of the identification or classification of the fibre. The next section looks at some important processing stages which animal fibres usually undergo.

### ***1.2.2.1 Cleaning and Scouring***

Wool taken from sheep skin is often called “raw” or “greasy” wool because it contains considerable amounts of foreign material or natural contaminants such as sand, dirt, grease, dried sweat popularly known as suint, and pesticide residues from treatment of sheep to prevent disease. Mohair contains far less grease, (about 4-6% compared to about 15% of Merino wool) (Hunter, 1993). The water soluble suint and other heavy dirt particles are removed by washing the raw animal fibre with water at 32 °C to 42 °C and the water insoluble wool grease is removed by treating the desuinted wool with a mixture of detergent and sodium sulphate (or chloride) at 65 °C. As detergent scouring yields waste of very high strength, some wool mills prefer to remove the impurities by solvent scouring wherein the desuinted wool is scoured with organic solvents such as benzene, carbon tetra chloride, ethyl alcohol methyl alcohol or isopropyl alcohol. Although solvent scouring removes grease effectively, dirt is not readily removed. Thus, a detergent wash generally follows solvent scouring.

Table .1: World total production of wool fibre (Wilcox, 2018).

mkg clean	2017	2018f	% change	2019f	% change
<b>“Apparel” wool IWTO countries</b>					
Australia	272.0	269.2	-1.0%	265.9	-1.2%
South Africa	27.0	25.1	-7.1%	25.8	+2.7%
Argentina	26.1	25.9	-0.7%	25.9	+0.1%
Uruguay	17.9	18.3	+2.3%	18.8	+3.0%
USA	6.6	6.4	-4.0%	6.0	-5.3%
<b>“Interior textile” wool IWTO countries</b>					
China	180.0	179.9	-0.1%	180.0	+0.1%
New Zealand	102.8	104.0	+1.2%	104.7	+0.7%
India	33.2	33.4	+0.8%	33.7	+0.9%
UK	25.2	25.8	+2.5%	25.6	-0.6%
Mongolia	18.5	20.5	+11.1%	21.7	+5.6%
Other countries	429.2	432.8	+0.8%	435.0	+0.5%
<b>Global</b>	<b>1,138.3</b>	<b>1,141.3</b>	<b>+0.3%</b>	<b>1,143.1</b>	<b>+0.2%</b>

### **1.2.2.2 Carbonizing**

This is a final processing stage in the removal of vegetable matter in the wool fibres which may have been left behind during the scouring process (Halliday, 2002). The wool fibres, impregnated with sulphuric acid solution, are oven dried at 100 °C to 104°C followed by mechanical agitation. The acid degrades the cellulosic impurities without damaging the wool fibres. During drying, the sulphuric acid becomes more concentrated due to water evaporation resulting in burning of remaining impurities. The fibres are then passed through pressure rollers to crush the solid carbon residue. The loosened carbon residue is removed from the wool by passing it through the mechanical agitators called dusters. The fibres are then rinsed with water, passed through baths containing carbonate solution to neutralize the residual acid, washed again and then dried.

### **1.2.2.3 Moth proofing**

Wool fibres are often treated with standard insecticides to protect them against attack by moths and other insects (Mozaffari-Medley, 2003), with mothballs or naphthalene balls often being used for this purpose. It is common practice that the insecticide is applied in the same manner as a dyestuff (making it bind well with the fabric) for the insecticide to last longer. Naphthalene balls have been used to protect some wool samples that were used in the current study.

## **1.3 SIGNIFICANCE OF THE STUDY**

South Africa is the major producer of mohair, contributing approximately 60% of the world's total production (Department of Agriculture, forestry and fisheries, 2016). Mohair is known for its outstanding superb quality characteristics, such as lustre, resiliency, low wrinkling, low flammability, durability, moisture management and comfort, and this has resulted in a certain positive or superior image and prestige being associated with products on which the label 'mohair', even more so 'Cape Mohair', appears, and for which consumers are generally prepared to pay a premium. Nevertheless, this positive image, together with the associated premium price, has led to certain unscrupulous operators 'adulterating' mohair by blending it with other cheaper and inferior animal fibres, such as lustre wool, but still trading their product as pure mohair. Similar

considerations apply to other luxury animal fibres, notably Cashmere. Because of the damage (financial losses, prestige, image, etc.) caused by such illegal practices, considerable research has been devoted towards developing test methods which can reliably distinguish between different animal fibres, such as mohair and lustre wool, one of the most widely accepted ones being that based on differences in scale height, measured by means of a Scanning Electron Microscope (SEM) at magnifications of up to 25 000X. Other potential methods which have been researched, but which have various potential drawbacks, such as complexity, cost and lack of accuracy, include mitochondrial DNA, lipids and amino acid composition. None of these have as yet received wide acceptance. The purpose of this research is to investigate the possible application of Raman spectroscopy in distinguishing between wool and mohair fibres, particularly when in blends. Traditionally, blend composition of animal fibres relies on the use of the cuticle scale height (CSH) measurement using the scanning electron microscope (SEM). This method has been documented as an international standard (IWTO-58, 2000) for distinguishing between different animal fibre types. However, this test method is slow, labour intensive, and expensive and somewhat depend upon the experience of the operator. Thus, a reliable, accurate, objective and more cost-effective method is required.

Because South Africa is a world leader in the production of quality mohair, it is important to be able to carry out mohair blend analysis and certification locally. In view of this, efforts have been directed towards establishing such a facility and capability in South Africa, specifically, Port Elizabeth. Because of the high expertise and infrastructural and labour costs associated with the SEM method, it is important to search for, and develop, less complicated and expensive, but equally accurate, and preferably automated or semi-automated systems. In this respect, isotope, RAMAN/FTIR and amino acid analysis-based methods would appear to hold potential, the latter also possibly lending itself to engineering mohair quality through appropriate nutrition and breeding.

## **1.4 AIMS AND OBJECTIVES**

This research study was mainly aimed at investigating the possible application of vibrational spectroscopy techniques (Raman and IR spectroscopies) for characterization, classification and identification of wool and mohair fibres and their blend composition analysis.

### **1.4.1 Objectives**

1. To characterize the secondary structure of wool and mohair proteins and polypeptide chains using FT Raman spectroscopy.
2. To investigate the application of the peak height based ratiometric analysis for specific FT Raman spectroscopic bands in distinguishing between wool and mohair fibre samples.
3. To build and validate an in-house FT Raman spectral library or database for pure wool and mohair from different countries (i.e. library calibration and validation) for the Bruker 80V FT Raman spectrophotometer.
4. To characterize wool and mohair fibre properties using Raman micro-spectroscopy.
5. To characterise wool and mohair single fibres using Attenuated Total Reflectance (ATR) Fourier Transform Infrared (FTIR) micro-spectroscopy.

### **1.4.2 Thesis Outline**

This thesis is composed of five chapters, with chapter one providing a general background of the study and also describing the importance of animal fibre identification and quantitative analysis of their blends. The production of wool and mohair fibres worldwide and their processing are briefly explored. The same chapter also outlines the aims and objectives of the study. Chapter one ends off by providing some brief theory behind the operation principles of Raman and infrared spectroscopic techniques. The second chapter, i.e. chapter two, describes the physical and chemical structure of natural animal fibres. It also reviews, comprehensively, previous work of different characterization techniques used in the identification and classification of different animal fibres and composition analysis of their blends. The limitations experienced in

the identification of different animal fibres and blend composition analysis using these techniques are also explored. The chapter ends-off by providing the motivation for pursuing the current research study. In chapter three the experimental plan, sample preparation and the characterization techniques used in the present study are discussed. The possible sources of experimental errors are also briefly described in chapter three. The results from different techniques utilized in the current research study and the comprehensive discussion of these results is provided in chapter four. In this chapter, the comparison of results of this study with the previous literature is done. Finally, chapter five contains the general conclusions of this research and also outlines some recommendations for the future.

## **1.5 THEORY OF VIBRATIONAL SPECTROSCOPY**

Spectroscopy is defined as the study of interactions between electromagnetic radiation and matter. Vibrational spectroscopy is a collective term often used to describe the two analytical techniques, namely infrared (IR) and Raman spectroscopy. These are non-destructive and non-invasive techniques that provide information about the molecular composition, structure and interactions occurring within a sample. Naturally, IR spectroscopy and Raman spectroscopy possess capabilities and some shortcomings which sometime determines which technique to use for a specific application (Chalmers *et al.*, 2012). The theory and basic operation principles behind these two techniques are briefly described in sections 1.6.1 and 1.6.2.

### **1.5.1 Infrared Spectroscopy**

#### **1.5.1.1 Brief Theory**

Infrared (IR) radiation is defined as that part of the electromagnetic (EM) spectrum between the limits of 0.7 and approximately 500 micro-meters and this region is between the visible and microwave regions. This can be subdivided into three sub regions namely near, mid, and far infrared (Potts, 1963). IR spectroscopy is a technique based on the vibrations of the atoms of a molecule. An IR spectrum is acquired by illuminating a sample with infrared radiation and determining what fraction of that

incident radiation has been absorbed at a particular energy (Stuart, 2004). For the quantum of radiation to be absorbed, the molecular vibration frequency must be identical to the frequency of the radiation as shown in equation 1.1 (Potts, 1963):

$$\omega_{\text{quantum}} = \omega_{\text{vibration}} \quad \dots\dots\dots 1.1$$

Where  $\omega_{\text{quantum}}$  is the frequency of the radiation incident on the sample and  $\omega_{\text{vibration}}$  is the molecular vibration frequency. If the frequency of the quantum is not identical to that of molecular vibration, no interaction will occur between the molecule and the radiation which can cause a change in vibrational state. Not only are the correct energy requirements not fulfilled, but consideration of the instantaneous interaction of the changing dipole moment and moving alternating electric field shows that if these frequencies differ such instantaneous interaction eventually will be cancelled by one of exactly opposite phase. An IR absorption spectrum is a result of the two situations where an oscillating dipole absorbs IR radiation whose frequency is the same as its vibrational frequency and the fact that all other frequencies get transmitted unchanged. The intensity of the absorption band is proportional to the change in the dipole moment of the molecule. This technique is widely known as fingerprint of chemical compounds, meaning each compound present in the specimen will show its unique absorption band (Stuart *et al.*, 1996).

#### **1.6.1.2 Fourier Transform (FT) IR micro-spectroscopy**

The first infrared microscope was invented in the mid 1960's. Fourier transform infrared (FTIR) microscopy is an analytical technique with conventional microscope attached to an FTIR spectrometer. FTIR micro-spectroscopy have received great application particularly for the identification and classification of single fibres in the forensic laboratories around the world. Some of the advantages of FTIR microscopes include the fact that they allow for rapid scan rates, multiplexing capabilities, minimal-to-no sample preparation, which have greatly reduced the time and effort required to obtain IR spectra of single fibres, and it is essentially non-destructive. Infrared microscopes share the same basic components as the conventional light microscope systems, namely an illumination source, an aperture, a condenser lens, the sample stage, an objective, an



eyepiece, and a detector. The process of acquiring an infrared spectrum begins with the infrared beam collected by a mirror after leaving the interferometer and is directed through a hole in the side of the spectrometer into the microscope. This beam allows the IR spectrum of the sample to be obtained. The condenser lens focuses this IR beam which is later collected by the objective. After the objective is an aperture which determines the area, on the sample, from which the infrared spectrum will be acquired and the upper aperture helps prevent the stray light from reaching the detector. Figure 1.2 is a schematic diagram of an infrared microscope (Panaioyou, 2004):

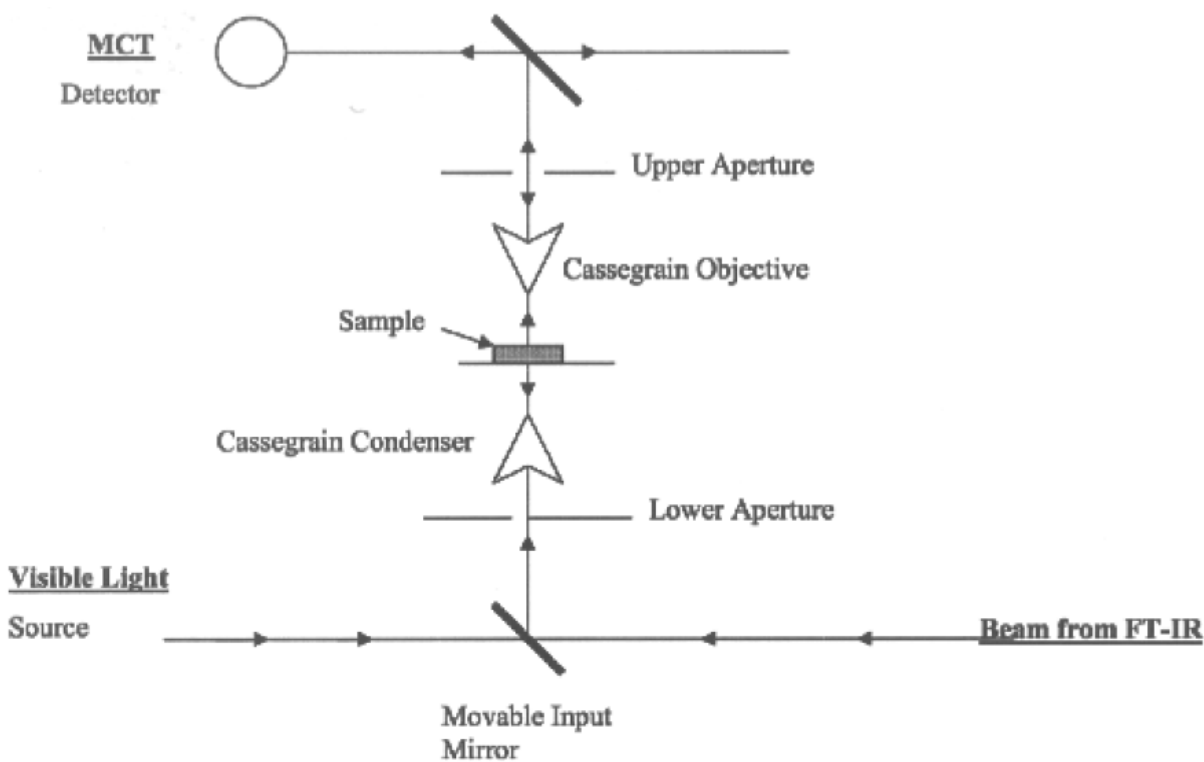


**Figure 1.2: A schematic diagram of an FTIR system (Panaiotou, 2004).**

FTIR microscopes can be used in reflectance or transmission mode. Transmission samples suffer from what is known as “thickness problems” as the ideal thickness of the sample needs to be adjusted between 1-20 microns. The advantage of analysing samples in reflectance is that samples suffer less from thickness problem and as such it is not necessary to flatten the fibre to quite the same degree as in transmission mode. One disadvantage of acquiring spectra in reflectance is the fact that a lot of infrared

beam is scattered by the sample and thus is not collected by the Cassegrain and never reaches the detector. The result is the high noise compared to spectra collected in transmission mode, however the increased number of scans overcomes this problem. All infrared spectra reported in this study were acquired in reflectance mode and the number of scans used fairly improved the signal-to-noise ratio of the spectra (Panaiotou, 2004).

## **1.5.2 Raman Spectroscopy**

### **1.5.2.1 Introduction**

In the late 1920's Chandrasekhara Venkata Raman reported the light scattering effect which has come to be known as the Raman Effect. Raman scattering is a fundamental form of molecular spectroscopy which is used to obtain information about the structure and properties of molecules from their vibrational transitions. The basic principle of Raman spectroscopy is based on the irradiation of a specimen with an intense laser beam in the UV, visible or near infrared region of the electromagnetic spectrum (Ferraro *et al.*, 2003). When this happens, certain wavelengths are absorbed and some scattered, Raman spectroscopy is the study of the scattered radiation. This scattered radiation may be unchanged in wavelength (Rayleigh) or, a very small proportion might be slightly increased or decreased. In simple terms, the principle of the Raman spectroscopy is based on the removal of a certain amount of energy by the molecules present in the sample from the particles of the incident laser light illuminating the sample (Whiffer, 1966). Different types of Raman spectrometers have been developed to analyse these scattered light beams and the results are presented in the form of a spectrum.

### **1.5.2.2 Instrumentation and Basic Theory of Raman Spectroscopy**

When electromagnetic radiation irradiates a molecule or particle, the energy or the frequency of that radiation may be transmitted, absorbed or it may be scattered. Raman Effect is a result of the scattering event when the electromagnetic radiation interacts with matter. Raman spectroscopy is, just like infrared spectroscopy, another powerful technique for determining molecular vibrations. Both of these methods often provide

similar spectra but notable differences also exist leading to the two techniques giving complementary information. Figure 1.3 (Herrero, 2008) illustrates a typical layout of dispersive Raman spectrometer:

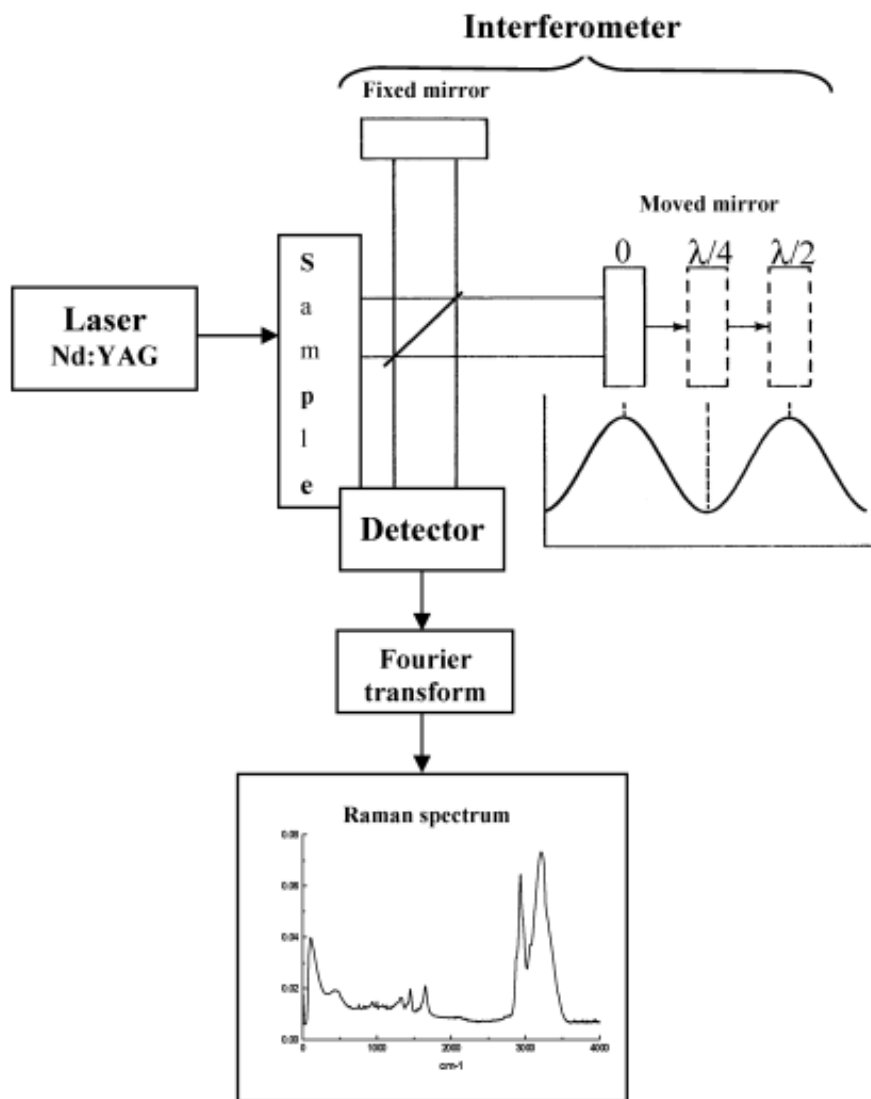


**Figure 1.3: Schematic diagram of an FT Raman spectrometer (Herrero, 2008).**

Different interactions of matter with the electromagnetic radiation make the two methods distinct from each other (Günzler and Gremlich, 2002). When the incident photon interacts with a molecule (of the specimen), the following three events may be observable, namely absorption, emission and scattering.

Absorption: If the energy of the radiation, incident on the sample, is sufficient to excite an electron from a lower energy state to the higher state, then the applied radiation is absorbed.

Emission: Occurs from excited molecule, at some time equal to or greater than the lifetime of the molecule in the initial excited energy state. The energy of the emitted photon corresponds to the difference between the two stationary energy states of the molecule.

Scattering: This is a faster process (occurs in  $10^{-14}$  s) and is due to the interaction of a photon and molecule when the photon energy does not correspond to the difference between any two stationary energy states of the molecule. Scattering may occur without a change in the frequency of the incident photon (Rayleigh scattering) or with some change in the incident photon frequency (Raman scattering) (Barańska *et al.*, 1987). Figure 1.4 illustrates the energy-level diagram showing the states involved in Raman spectra:

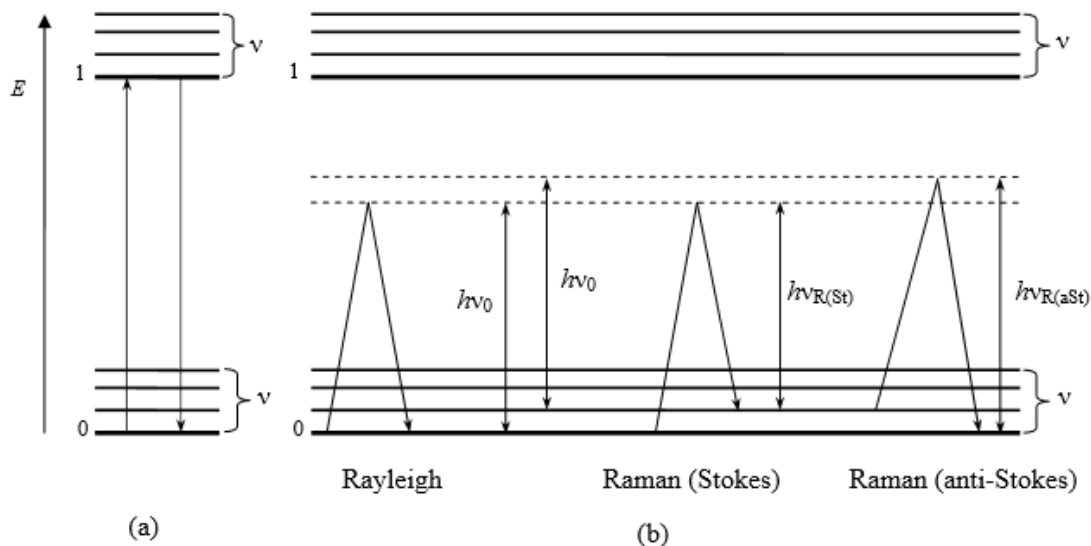


**Figure 1.4: (a) Resonance fluorescence and (b) Rayleigh, Raman Stokes and Raman anti-stokes scattering. (0) Denotes the ground electronic state and (1) denotes the first excited electronic state. (v) indicates vibrational energy levels (Barańska *et al.*, 1987).**

The laser beam can be considered as an oscillating electromagnetic wave with electric vector  $E$  which upon its interaction with the sample induces electric dipole moment  $P = \alpha E$ , which deforms the molecules and facilitates their vibration with characteristic frequency  $\nu_m$ . The monochromatic laser beam of frequency  $\nu_0$ , excites molecules and transforms them into oscillating dipoles. Such dipoles emit light of three different energy or frequency when:

1. A molecule that is Raman inactive absorbs the monochromatic with the frequency  $\nu_0$ . The excited molecule returns back to the same basic vibrational state and emits light of the same frequency as the incident laser beam. This interaction is known as the Rayleigh scattering and is generally very strong.
2. Absorption of the incident monochromatic light of frequency  $\nu_0$ , by a Raman active molecule which at the time of interaction is in the basic vibration state. Part of the incident beam's energy is transferred to the Raman-active mode with frequency  $\nu_m$  and the result is the reduced frequency of the excitation source to  $\nu_0 - \nu_m$  and this Raman frequency is called the Stokes frequency.
3. A photon with frequency  $\nu_0$  is absorbed by Raman-active molecule, which at the time of interaction, is already in the excited state. The excited molecule releases energy and returns to the lower vibrational energy state and the resulting frequency of the scattered light is increased to  $\nu_0 + \nu_m$  and this Raman frequency is called the Anti-Stokes frequency.

Raman scattering (Stokes and Anti-Stokes scattering events), as opposed to Rayleigh scattering, is a very weak process (1 in  $10^7$  photons).

Raman micro-spectroscopy, a technique where a conventional microscope is attached to a Raman sepectrophotometer, allows for the examination of small samples, substantially less than a millimeter in size, allowing high magnification visualization of a sample and Raman analysis with a microscopic laser spot (Baldwin *et al.*, 2001). Raman micro-analysis simply involves placing the sample under the microscope, focus, and make a measurement. Lang *et al.*, (1986 (a) and (b)) were amongst the pionnering researchers to apply Raman microspectroscopy in characterizing natural and synthetic fibres. The intensity of Raman-scattered light is inherently weak, and the strong

wavelength dependence ( $\lambda^{-4}$ ) results in the Ar<sup>+</sup> ion laser (emitting at 514.5 nm) micro-Raman system, used in this study, offering a better Raman efficiency (of a factor approximately 18 times better (Gallimore *et al.*, 2018), when compared to the 1064 nm excitation of the Bruker FT Raman system also used in this study. This implies that at 514.5 nm excitation, shorter scanning or spectral acquisition times are involved compared to the necessary longer acquisition times involved at 1064 nm excitation for FT Raman spectrophotometer (Zhou, 2015).

## 1.6 SELECTION RULES

Both Raman and infrared absorption spectroscopy deal with vibrational transitions of molecules. Raman effect is mostly preferred in spectroscopic analysis due to the fact that not all conceivable vibrational transitions can give rise to absorption lines measured in infrared spectroscopy. The application of both these two spectroscopic techniques provides one with almost complete information about the vibrational spectrum of a molecule in the ground electronic state. These two methods are complimentary due to the nature of the phenomena on which they are based and also because of the differing nature of the measuring techniques involved and their specific usefulness in different structural and analytical problems (Barańska *et al.*, 1987). The complementarity of Raman and infrared spectroscopy results from the different selection rules, which determine the appearance in the Raman and/or infrared spectrum of a band corresponding to a given vibration of the molecule. The selection rules may be summed up in two rules:

- (1) If the vibration causes a change in the dipole moment  $\mu$ , it is active in the infrared spectrum. This occurs when the vibration changes the symmetry of charge density distribution, i.e. if:

$$\left(\frac{\partial\mu}{\partial Q}\right)_0 \neq 0 \quad \dots\dots\dots 1.2$$

- (2) If the vibration produces a change in the molecular polarizability  $\alpha$ , it will be Raman active. This occurs if:

$$\left(\frac{\partial \alpha}{\partial Q}\right)_0 = 0 \quad \dots\dots\dots 1.3$$

where Q is the vibrational normal coordinate. One or both of these conditions may be fulfilled depending on the symmetry of the molecule. There exists the rule of mutual exclusion, which states that if there is a centre of symmetry in the molecule, a vibration that is active in the infrared spectrum is inactive in the Raman spectrum and vice versa. In the case of molecules lacking a centre of symmetry, a number of vibrations will appear in both spectra. These vibrations often differ with regards to their relative intensities. For instance, the vibrations of strongly polar functional groups are more readily observed in the infrared spectrum, while the vibrations of double and triple bonds and the carbon-skeleton of the molecule are better seen in the Raman spectrum. Totally symmetric vibrations are only (or much better) visible in the Raman spectrum. Table 1.2 summarises some of the more common molecular bonds and their relative intensities in Raman and infrared spectra.

**Table 1.2: Band intensities in the vibration-rotation infrared and Raman spectra (Barańska *et al.*, 1987).**

Group	IR (relative absorbance)	Raman (relative intensity)
Polar groups with high permanent dipole moment, e.g. OH, NH, CO	Very strong	Weak
C-S, S-S Si-O-Si	Medium	Strong or very strong
C=C C≡C	Strong	Very strong
Skeletal vibrations	Medium	Strong
Totally symmetric vibrations, particularly of aromatic and alicyclic rings	Very low or zero (forbidden in IR)	Strong or very strong

## 1.7 QUALITATIVE AND QUANTITATIVE SPECTROSCOPIC METHODS

Vibrational techniques are routinely used to qualify or identify chemicals of interest and may also be applied to quantify these chemical groups. IR absorbance and Raman scattered band intensity are both linearly proportional to the number density of the species substance giving rise to the band (Chalmers and Everall, 1993). A variety of techniques are available to users of modern infrared spectrometers which help in both qualitative and quantitative interpretation of IR spectra. Two principal methods exist for determining absorption maxima or peak heights, namely the cell-in-cell-out method and the baseline method (Potts, 1963). The latter is of interest for this study and Figure 1.5 illustrates the base line construction on an infrared spectrum.



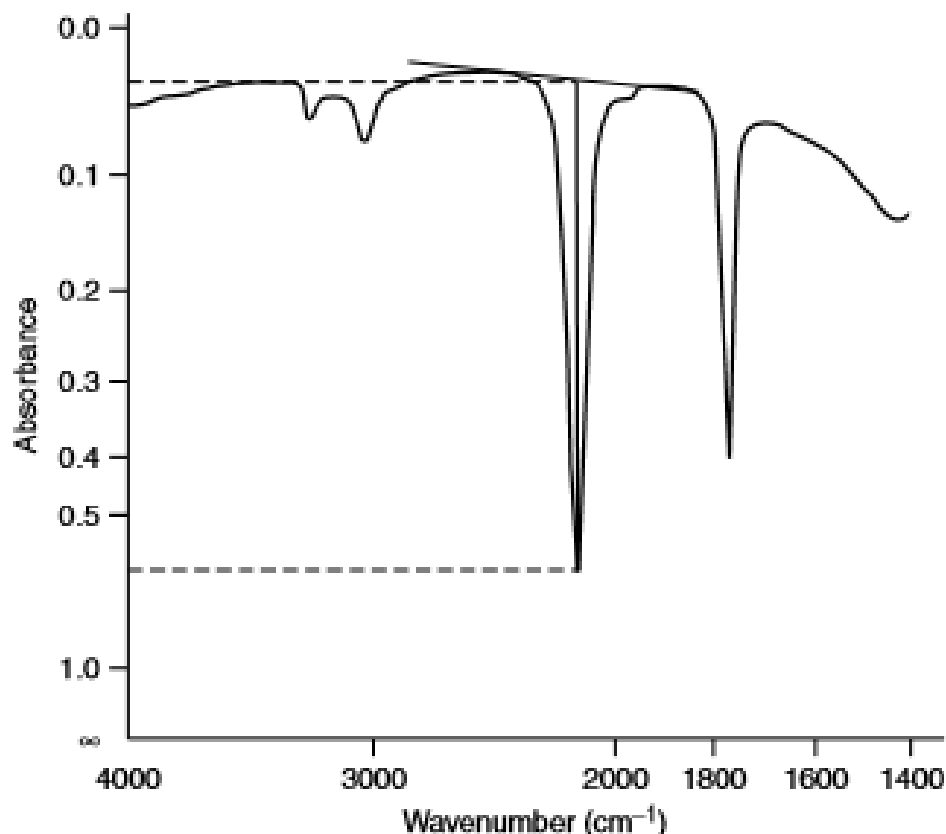


**Figure 1.5: Baseline method of eliminating background absorption by means of a tangent (Stuart, 2004).**

Potts (1963) described the baseline method as a way of determining a closer approximation to the true absorbance of an IR chemical band. This method was adopted in this study to determine Raman relative and absolute peak heights as possible means for distinguishing between spectra acquired from wool and mohair fibres. Various factors may influence the band peak heights or intensities in a vibrational spectroscopic analysis. Kumar *et al.*, (2015) discussed these factors, for FTIR and Raman spectroscopy, in detail. These factors include the background effects, sample effects, substrate effects and the variations in thickness of the sample. The ageing of the excitation radiation source, its improper functioning/alignment or incorrect focusing also significantly affects the intensities or peak height analysis Kumar *et al.*, (2015). These researchers showed an increase in peak heights of certain Raman bands as a result of increased laser powers and argued that performing peak height ratio analysis

(ratiometric analysis) could considerably minimize the effects. It is generally known that Raman scattering is a very weak event, with one Raman photon being produced for every  $10^6$  to  $10^9$  excitation photons incident on the sample (Cebeci-maltaş *et al.*, 2017). Another factor which could possibly influence or interfere with the weak Raman scattering is that of fluorescence, this being more likely to be observed in spectra of the naturally self fluorescent biological materials (Kumar *et al.*, 2015). Sample impurities that are fluorescent may also contribute to the observed fluorescence interference in Raman spectroscopy. Raman scattering strength is inversely proportional to the fourth power of the excitation laser wavelength, and as a result it is expected that a stronger Raman signal should be obtained when an excitation laser of a shorter wavelength is applied (Tuchel, 2016). Raman micro-spectroscopy, a technique where a conventional microscope is attached to a Raman sepectrophotometer, allows for the examination of small samples, substantially less than a millimeter in size (Baldwin *et al*, 2001). Lang *et al* (1986 (a) and (b)) were amongst the pionnering researchers to apply Raman microspectroscopy in characterizing natural and synthetic fibres. Cebeci-maltaş *et al.*, (2017) showed the strong dependence of fluorescence on the excitation laser wavelength, strong fluorescence background being observed at the shortest excitation wavelength (514.5 nm). These researchers also showed that the application of a longer excitation wavelength (1064 nm) strongly suppresses the effects of fluorescence.

## 1.8 SPECTROSCOPIC LIBRARIES FOR IDENTIFICATION OF MATERIALS.

The spectral database searching tool has, over the past years, become one of the powerful available tools receiving application in different spectroscopic (NMR, MS, IR and Raman) and chromatographic techniques for the identification and classification of materials of unknown identities. Spectral searching involves application of various algorithms to match a spectrum of an unknown material, sometimes referred to as query or a test spectrum, with each spectrum from a reference database. The conventional method used for identifying the unknown sample is searching through a list of reference database using a value known as the hit quality index (HQI). This value (HQI) is produced through the application of several search algorithms based on spectral correlation, Euclidean distance, least squares, sum of absolute difference and vector dot product (Stein and Scott (1994); Lee *et al.*, (2013); Howari (2003)) and determines if a correlation exist between an unknown spectrum (query) and the spectra from a large set/collection of known materials or compounds in the reference spectral database (Boruta, 2012). The hit list (a list of similar spectra in the database) is arranged such that the highest HQI values are at the top of the list and the higher the HQI the closer the unknown spectrum to the material/compound in the reference database. Tungol *et al.*, (1990) argued that the most important and essential step in the development of a spectral database or library is based in establishing highly reproducible sampling methods. The current study briefly investigated some of the factors which were found to be posing a threat in the quality of the current spectral library are discussed later in the experimental chapter of this thesis, these including the random unevenness in the thickness of the fibre bundles and the different spectral acquisition time between the query and reference spectra. The traditional HQI search algorithm places more importance on the peak intensity, rather than peak position and other parameters, for identification of spectra of unknown identity. These band intensities may differ, for the same material, because of the difference in excitation wavelengths and conditions used. Recently, a novel scoring method has been developed to minimize the risk of spectral misidentification and misclassification resulting from intensity variations as a result of different excitation wavelengths (Park *et al.*, 2017). This method called segment hit quality index (SHQI), was developed with the aim of mitigating the effects of varying

peak intensities on the HQI scores. An example of spectra of the same material but acquired on different instruments, of differing excitation wavelengths (514.5, 632.8, 785 and 1064 nm), is shown in Park *et al.*, (2017) with different HQI scores. In Boruta (2012), a percentage gap of HQI values between successive hits of the hit list was assessed as the possible means for quantifying the accuracy of spectral matching. The percentage gap was defined by equation 1.4:

$$\text{gap \%} = \frac{\text{HQI}_n - \text{HQI}_{n+1}}{\text{HQI}_1 - \text{HQI}_{100}} \dots\dots\dots 1.4$$

Where  $\text{HQI}_n$  and  $\text{HQI}_{n+1}$  are the successive HQI values of the  $n$ th hit and its successor  $n+1$ , respectively,  $\text{HQI}_1$  and  $\text{HQI}_{100}$  are the first and hundredth hits of the hit list, respectively. This researcher concluded that “compared to the HQI values and the HQI gap between successive hits, the gap % appeared to provide the best results in estimating the quality of the spectral match” compared to using the HQI of the first hit and the gap itself. Perez (2001) argued that the most popular challenge in building spectral libraries is based on the fact that the spectra of solid materials depends not only on their composition but also depends on their scattering geometry, the wavelength of the excitation laser source and the inhomogeneous nature of the samples which brings fluorescence. The spectral database of wool and mohair fibre samples developed in this study is for spectra measured or acquired using the 1064 nm excitation laser source.

## CHAPTER 2

### LITERATURE SURVEY

#### 2.1 INTRODUCTION

This chapter reviews published work and methods dealing with animal fibre identification, classification and blend composition analysis; with the goal of identifying alternative methods or techniques with a potential for rapid and more cost-effective characterization and identification of animal fibres and quantification of their blends. Relevant techniques of particular interest include FT-Raman, Fourier Transform Infrared (FTIR) spectroscopy and the atomic force microscopy (AFM). The ease of use, the non-destructive nature (to samples), together with the fact that these methods are fast compared to the laborious microscopic techniques, are motivating factors to pursue certain of these techniques. Understanding both the morphological and chemical structures of the animal fibres is important for their successful identification and these properties are briefly presented in this chapter.

#### 2.2 PHYSICAL AND CHEMICAL STRUCTURE OF ANIMAL FIBRES

##### 2.2.1 Physical (Morphological) Structure

Natural animal or protein fibres, including wool, mohair and human hair, generally comprises of a hierarchical structure consisting of two physical or structural components, namely the cuticle and the central core known as the cortex, which are morphologically and chemically different (Carter and Edwards, 2001). A central canal, known as the medulla, may also be observed in coarser animal fibres, although it is largely absent from well-bred Merino type wool fleeces and mohair fibres. The properties of fibres are strongly related to the cellular components, both cuticle and cortical cells, and its constituent chemical components, such as proteins and lipids. Another component known as the medulla may also be found in coarse fibres (Popescu and Wortmann, 2010; Rouse and Van Dyke, 2010). The section that follows briefly discusses these structural components.

### 2.2.1.1 The Cuticle

The cuticle surrounds and covers the inner components (cortex) of the fibre and consists of flat cells called cuticle scales. The cuticle scales are arranged in an overlapping fashion, like tiles in the roof or fish scales, and point towards the tip of the fibre (von Bergen, 1963). Each cuticle cell consists of three sub-layers namely the epicuticle, exocuticle and endocuticle, as illustrated in Figure 2.1. During the past decades, the animal fibre cuticle has been widely discussed, and also the subject of many studies (Gralen (1950), Bradbury and Chapman (1964), Bradbury *et al.*, (1965), Fraser and Macrae (1980), Ley and Crewther (1980), with Jones *et al.*, 1990 and (Hallegot and Corcuff, 1993) reporting a high content of sulphur in the cuticle region. The outermost layer of the cuticle, the epicuticle, is 3-6 nm thick, and is presumably derived from the plasma membranes of immature cuticle cells and consists of proteins and lipids. It is hydrophobic and resistant to chemical treatments such as dyeing and bleaching (Carter and Edwards, 2001). According to Marshall (1990), the protein component of this layer is rich in serine, glycine and glutamic acid, with a half cysteine content of 12% residues, which is considerably lower than the 35 % found in the outermost layer of the exocuticle. The detailed morphological structure of wool is shown in Figure 2.1:

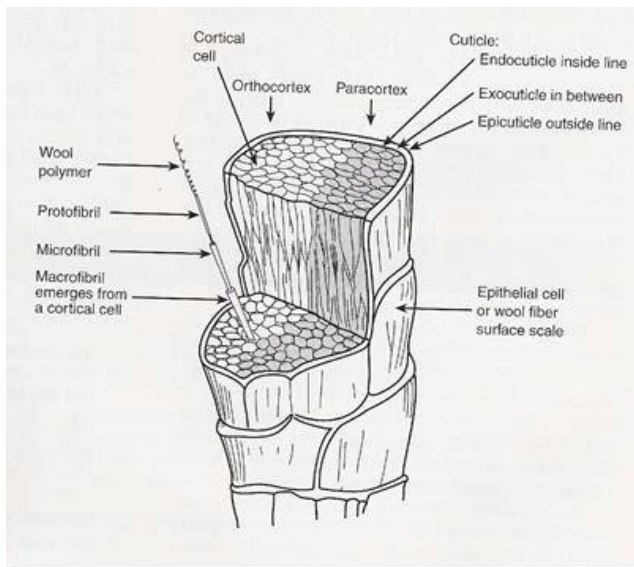


**Figure 2.1: Physical structure of a wool fibre (Bradbury, 1976).**

The exocuticle is a keratinous layer found underneath the epicuticle and is approximately 0.3  $\mu\text{m}$  thick. This is the major constituent of the cuticle and comprises 60 % of the cuticle's total mass. This layer is very rich in cystine. The exocuticle consists of two sublayers, the dense A-layer and the B-layer. The A-layer, which is about 0.1  $\mu\text{m}$  thick, lies adjacent to the epicuticle and is believed to contain more cystine than the B-layer (Bradbury, 1976).

Between the exocuticle and the cell membrane complex (CMC) lies the endocuticle which is approximately 0.2  $\mu\text{m}$  in thickness. The endocuticle represents approximately 40 % of the cuticles' total mass and has very low levels of cystine, and is classified as non-keratinous. This layer, as a result, is mechanically weak and is more susceptible to chemical attack. According to Stewart *et al.*, (1997), little is known about the wool cuticle proteins, due to the difficulty in isolating the cuticle from the wool fibre. Bradbury and Chapman (1964) reported on the ultrasonic disintegration for the isolation of different components of wool.

Separating the cuticle and cortex is the cell membrane complex (CMC), a continuous network primarily consisting of proteins and lipids (Bryson *et al.*, 1992), providing adhesion between the cells. This region is chemically different from the bulk of the fibre. This layer is inert to staining and it is believed that lipids are the major component of the CMC.

### **2.2.1.2 Cortex**

A group of closely packed cells (cortical cells) and pigmented granules, which forms the bulk of the fibre, lie under the cuticle and is known as the cortex (Sawbridge and Ford, 1987). The cortex constitutes about 90 percent of the fibre's volume. Two types of these cortical cells are generally found in keratin fibres, referred to as ortho-cortex and para-cortex, and these exhibit somewhat different physical and chemical properties. Figure 2.2 (Sikorski, 1963) shows the detailed inner structure of an animal fibre, in this case the wool fibre.

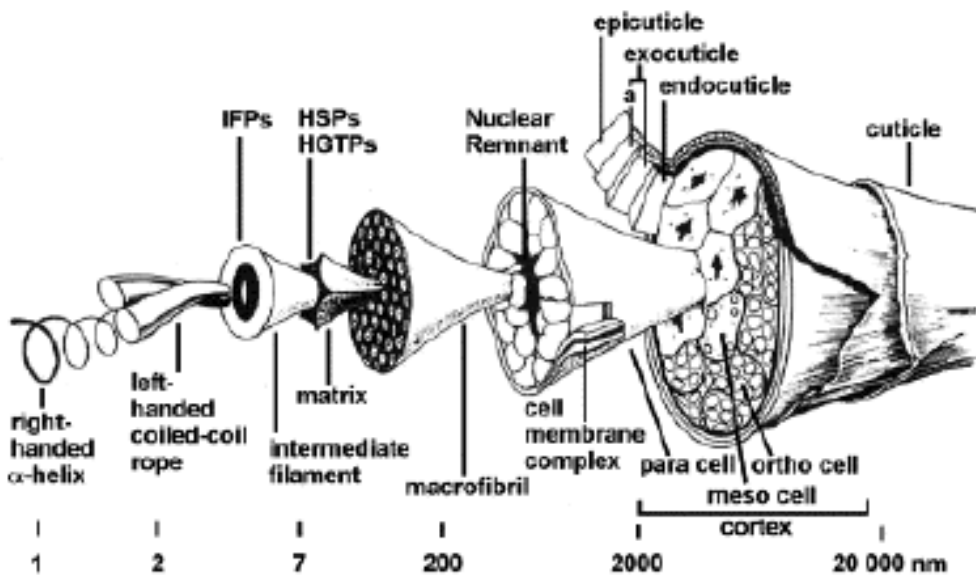


**Figure 2.2: A detailed typical inner structure of animal fibres (Sikorski, 1963).**

The ortho and para-cortex have different cystine contents and differ in their staining and dyeing behaviour, with the ortho-cortex possessing great ability to absorbing dyes compared to the para-cortex (Gohl and Vilensky, 1983). These differences have been presumed to be a result of the different composition and arrangement of the inter-macrofibrillar cement within the two segments (Leeder *et al.*, 1990). In their review paper, Marshall *et al.*, (1991) claimed that apart from the strong ability to absorb dyes the characteristic features of the ortho-cortical cells macrofibrils which are discrete and twisted along their long axis, and intermediate filaments (IFs) which produce a whorl pattern because of twisting of the peripheral IFs around the central core. Through the application of electrophoresis, Dowling (1990) reported that the high sulphur proteins were predominantly found in the para-cortical cells of some merino wool samples, later confirmed by the high tyrosine proteins of the ortho cortex reported by Marshall *et al.*, (1991).



### **2.2.1.3 Medulla**

In certain coarse animal fibres, a hollow or partially filled central canal core, called the medulla, may also be found and the proteins found in this region are non-keratinous, in certain aspects different to those in the cortex (Stapleton, 1992). The cells in the medulla are surrounded by air-filled spaces making them act as thermal insulators and reduce the weight of the fibre. The medulla increases the light scattering ability of the fibre and makes the fabric appear brighter.

## **2.2.2 Chemical Structure of Natural Protein Fibres**

Wool, and other animal fibres, such as cashmere, mohair and camel hair, etc. mainly consist of proteins known as  $\alpha$ -keratins. Keratin proteins are distinguished, from the other proteins, by the high content of the amino acid cystine and can also be classified according to the amount of sulphur in the protein (Carter and Edwards, 2001). In his review, on the general description of the structure of mammalian keratin fibres, Leon (1972) explained the “alpha ( $\alpha$ )” as representing a certain X-ray diffraction pattern in common with various other fibrous proteins. Certain researchers reviewed the chemical structure of animal fibres, including human hair Ward (1955); Panayiotou (2004); Mozaffari-Medley (2003); Douthwaite *et al.*, (1993); Ley and Crewther (1980); Korner (1988); Stapleton (1992); Tucker *et al.*, (1988) and Tucker *et al.*, (1989).

### **2.2.2.1 The Peptide Bond**

The most dominant bond within all keratin protein fibres is the peptide bond and Figure 2.3 is an example or an illustration of how this bond is formed through the condensation or dehydration reaction between the carboxy group of the first amino acid with the amino group of the second amino acid. This bond exhibits an unusual property that significantly influences the rigidity of a polypeptide chain and consequently having an effect on the folding of the polypeptide chain. The peptide bond has a partial double bond character, which is caused by resonance of electrons rapidly moving between the oxygen and nitrogen to make the C-N bond a partial double bond C=N, resulting in the very rigid and a much less flexible character of this bond (Panaiotou, 2004).

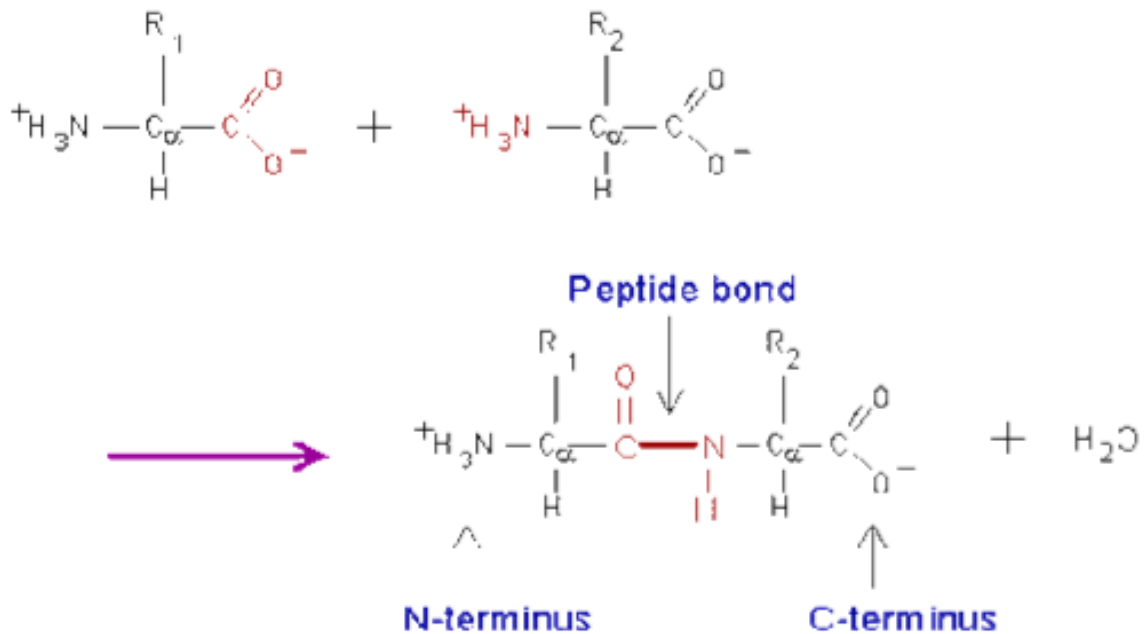


**Figure 2.3: Formation of peptide bond by condensation reaction (Panaiotou, 2004).**

Several distinctive vibrational spectroscopic bands are a result of the vibrations of the atoms of this peptide bond.

### **2.2.2.2 Polypeptide Chain**

Keratin proteins consist of long polypeptide chains, considered to be the backbone of keratin proteins. These are built up from the condensation of twenty different amino acids. Animal fibre keratin proteins contain several different types of polypeptide molecules, and these have been found to have an average molecular weight of about 60 000 (Shenai and Dalvi, 1989). Figure 2.4 (David, 2012) illustrates how proteins transform into different structural conformations from the primary structure.

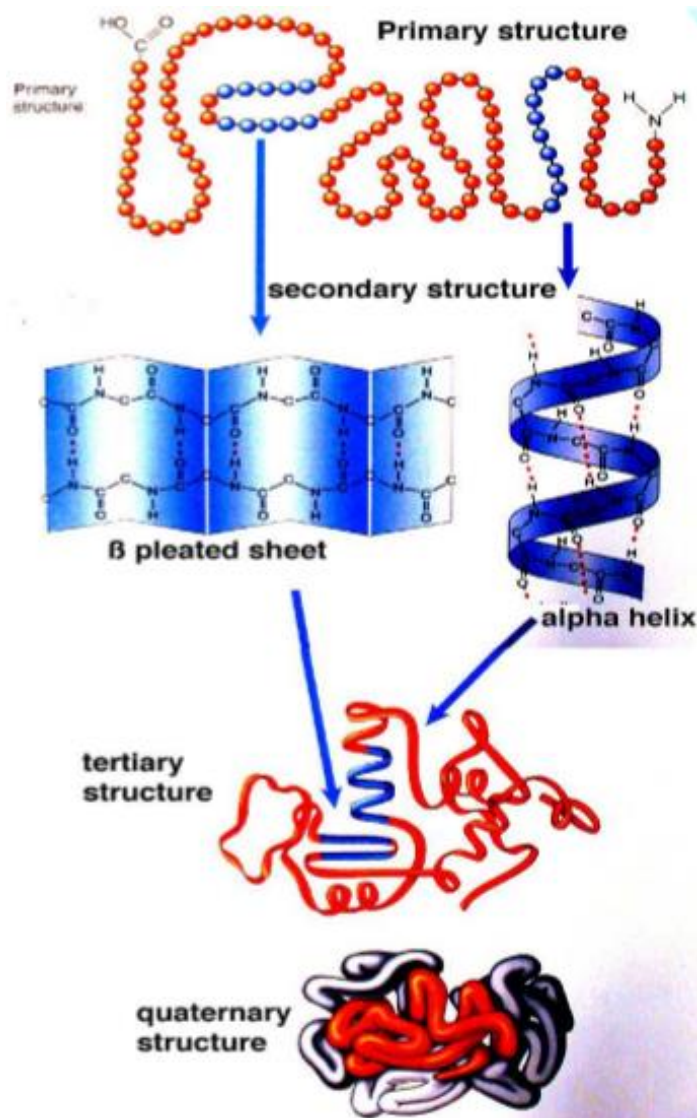


**Figure 2.4: Protein transformation into different structural conformation (David, 2012).**

The protein (keratinous and non-keratinous) material constitutes 99% of the wool fibre, only 1% being non-protein, such as fats and lipids (Rippon, 1992). The chemical (elemental) composition of animal fibres is mainly Carbon (C), Hydrogen (H), Oxygen (O), Nitrogen (N) and Sulphur (S). Three protein groups have been identified, namely low sulphur, high sulphur (rich in cystine) and the high tyrosine (rich in tyrosine and glycine) (Gillepsie and Marshall, 1980). It has also been reported that the cuticle of untreated wool contained 10.7 mol % cystine and the cortex had 5 mol %

(Füchtenbusch and Baumann, 1985). The amino acid composition, expressed as moles per 100 moles, of three classes of proteins found in wool is shown in table 2.1 (Jones and Rodgers, 2006).

**Table 2.1: Amino acid composition of wool fibres (Jones and Rodgers, 2006).**

Amino acid	Low-sulphur SCMKA major fraction	High sulphur Total	High Glycine Tyrosine Total
Alanine	7.7	2.9	1.5
Arginine	7.9	5.9	5.4
Aspartic Acid	9.6	3.0	3.3
Cysteine	6.0	18.9	6.0
Glutamic acid	16.9	8.4	0.6
Methionine	0.6	0.0	0.0
Glycine	5.2	6.9	27.9
Lysine	4.1	0.6	0.4
Phenylalanine	2.0	1.9	10.4
Serine	8.1	12.7	11.9
Threonine	4.8	10.3	3.3
Valine	6.4	5.6	2.1
Proline	3.3	12.5	5.3
Leucine	10.2	3.9	5.5
Tyrosine	2.7	2.1	15.1
Histidine	0.6	0.8	1.1
Isoleucine	3.8	3.6	0.2

The amino acid composition of wool varies to some extent between different qualities, between different samples of the same quality and between different areas of the fleece. The amino acid composition of wool, from different sheep breeds and other protein fibres (cashmere, mohair, alpaca, camel hair, etc.), has also been studied extensively (Tucker *et al.*, 1988), and reviewed by (Hunter, 1993). Table 2.2 compares the amino acid composition of ten different cashmere samples, of different nutrition and different average fibre diameters (Tucker *et al.*, 1988). Popescu and Hocker (2007) showed a considerable difference in the contents of some amino acids, cystine in particular, between wool, cashmere and yak fibres.

**Table 2.2: Amino acid composition of Australian cashmere from individual goats and wool (Tucker *et al.*, 1988).**

Amino acid	Aust. cashmere <sup>a</sup>	Chinese cashmere	Aust. cashgora <sup>a</sup>	Mongolian yak	Camel	Wool	Guanaco	White alpaca	Black alpaca	Llama	Vicuña
Diameter (µm)	12.7–17.9	17.1±2.4	16.2±3.3	18.4±1.9	18.7±2.6	17.1	13.9±1.7	26.4±6.0	40.7±9.8	19.5±2.6	12.3±1.7
<i>Amino acid</i>											
Cysteic acid	0.1–0.2	0.1	0.1	0.4	0.3	–	0.5	0.2	0.6	0.4	0.5
Aspartic acid	6.6–7.1	6.7	7.1	6.6	8.1	6.9	7.2	7.3	6.9	7.2	7.1
Threonine	6.6–7.3	7.0	6.9	6.5	6.6	6.8	6.5	6.3	6.2	7.0	6.4
Serine	10.7–12.7	10.9	11.5	10.3	10.4	12.0	11.1	9.6	10.3	11.3	10.6
Glutamic acid	11.2–13.0	13.0	13.5	12.5	13.6	12.8	13.7	14.6	14.0	16.0	14.3
Proline	8.1–9.0	7.7	7.5	7.5	7.2	8.1	7.9	7.6	7.8	8.4	7.9
Glycine	9.0–10.2	8.8	8.4	9.3	7.8	9.5	8.1	7.9	7.9	5.9	8.1
Alanine	5.8–6.2	5.5	5.7	5.8	5.9	5.8	5.5	5.6	5.4	6.8	5.5
Cystine	4.2–5.6	5.5	4.8	5.4	4.6	4.6	6.0	6.0	7.6	6.3	5.9
Valine	5.0–5.7	5.7	6.0	5.9	5.9	5.2	5.8	6.0	5.9	6.3	6.1
Methionine	0.3–0.5	0.4	0.4	0.5	0.7	0.5	0.5	0.4	0.5	0.5	0.4
Isoleucine	2.6–3.0	3.1	3.2	3.4	3.3	2.8	3.0	3.2	3.0	3.3	3.0
Leucine	7.4–8.4	7.4	7.7	8.0	7.7	7.9	7.2	7.8	7.2	8.3	7.5
Tyrosine	3.4–4.1	4.1	3.5	3.5	3.3	4.0	2.9	2.8	2.6	2.8	2.6
Phenylalanine	2.6–3.0	2.9	2.8	3.2	3.0	2.7	3.1	3.0	2.5	3.2	2.6
Lysine	2.5–3.0	2.8	2.8	3.0	2.7	2.9	2.5	2.8	2.6	2.9	2.7
Histidine	0.6–0.8	0.8	0.6	1.0	0.8	0.9	0.8	0.9	1.0	1.0	1.0
Arginine	6.4–7.2	7.5	7.4	7.5	8.0	6.7	7.7	7.9	8.2	8.7	7.7

Tucker *et al.*, (1988) noted that distinction, between Australian cashmere and pen-grown wool, using the amino acid composition, their cashmere samples exhibiting similar variability in composition as wool. Cuticle and cortical cell amino acid compositions are also different, as shown in Table 2.3 (Church *et al.*, 1997). This difference in composition was also evident in the Raman peak heights of the S-S stretching vibrations (around  $508\text{ cm}^{-1}$ ) for the two structural components.

Hughes *et al.*, (2001) also showed that certain amino acids were predominant in the cuticle, compared to the whole wool or cashmere fibre, and that some significant differences existed in certain surface amino acids between wool and cashmere. The amino acid composition of wool can be influenced by the nutritional status and physiological state of the sheep (McGregor and Tucker, 2010), with the amino acid cystine being particularly susceptible to variation (Tucker *et al.*, 1988). Other factors, believed to influence the variability of the amino acid, include the time of the year and the breed of the animal (Marshall and Gillepsie, 1990). This variability may also be of genetic origin (Frenkel *et al.*, 1974). The presence of cystine in keratin fibres largely determines the mechanical and chemical behaviour of these fibres (Jones *et al.*, 1990), the higher the cystine content the better the mechanical properties (Dowling *et al.*, 1990).



**Table 2.3: A comparison of amino acid composition (wool mol-1 %) of whole wool, cuticle cells, and the ortho and para cortical cells (Church *et al.*, 1997).**

Amino acid	Whole wool	Whole cuticle	Cortex	
			Ortho	Para
Alanine	5.4	5.8	5.6	5.4
Arginine	6.9	4.3	6.8	6.5
Aspartic Acid	6.5	3.5	6.7	6.3
½Cystine	10.3	15.6	10.3	12.9
Glutaminc acid	11.9	8.7	12.1	12.6
Glycine	8.4	8.2	8.6	7.5
Histidine	0.9	0.8	0.7	0.7
Isoleucine	3.1	2.7	3.2	3.3
Leucine	7.7	6.1	8.4	7.3
Lysine	2.9	2.7	2.8	2.3
Methionine	0.5	0.3	0.4	0.4
Phenylalanine	2.9	1.7	2.7	2.2
Proline	6.6	10.5	6.3	7.0
Serine	10.4	14.3	10.2	10.5
Threonine	6.4	4.4	6.1	7.0
Tyrosine	3.8	2.8	3.4	2.4
Valine	5.6	7.5	5.7	5.7

### 2.2.2.1 Secondary Structure of Keratin Fibres

The primary structure of protein is the sequence of a long chain composed of 20 amino acids while the secondary structural conformation occurs as a result of hydrogen bonding between long sequence of amino acids (see Figure 2.4 on page 31). Generally, the protein macromolecules exist in three different structural conformations namely the alpha helix ( $\alpha$ -helix), beta-pleated sheet ( $\beta$ -pleated sheet) and beta turn ( $\beta$ -Turn). The principal structural units in the raw or untreated keratin fibre are the successive turns of the alpha helix. The intrinsic stability of the alpha helix, and thus the fibre, results from intramolecular hydrogen bonds. Proportions of ordered and unordered conformations of the proteins may also be observed (Wojciechowska *et al.*, 1999). These structural conformations and the amino acid compositions have been found to be different in the cortical and cuticle cells. The accurate understanding of the degree of these differences involves isolation of these fibre components (cortical and cuticle cells) from the natural animal fibre (Church *et al.*, 1997). Zhou *et al.*, (2012) determined quantitatively, the contents of the secondary structure of mohair fibres after stretching at different stretching ratios. The content (in percentage (%)) of the  $\alpha$ -helical structure was determined using equation 2.1:

$$p\alpha = \frac{S_{\alpha}}{S_{\alpha}+S_D+S_{\beta}+S_T} \dots\dots\dots 2.1$$

Where  $p_{\alpha}$  is the percentage of the  $\alpha$ -helical conformation,  $S_{\alpha}$ ,  $S_D$ ,  $S_{\beta}$  and  $S_T$  are the band areas of the  $\alpha$ -helical, disordered,  $\beta$ -pleated sheet and the  $\beta$ -turns components of the Raman amide I. Zhou *et al.*, (2012), reported a dominance of the  $\alpha$ -helical conformation for unstretched mohair fibres, this being found to decrease with increased stretching ratios. A content of 58%  $\alpha$ -helical conformation was reported for the unstretched mohair fibres with the gradual decrease to about 14% for fibres stretched to a ratio of 60%, this being accompanied by an increased content of the  $\beta$ -pleated sheet from 20.5 to 44.7%.

## **2.3 ANIMAL FIBRE IDENTIFICATION AND BLEND ANALYSIS TECHNIQUES**

### **2.3.1 Introduction**

For various reasons such as labelling and Mark Certification purposes, it is important to be able to distinguish between speciality fibres such as cashmere, mohair, camel hair, etc. Considerable research effort has been directed over the years, but more particularly since the early 1980's, towards developing reliable methods for distinguishing between luxury fibres, cashmere, mohair, camel hair, etc. with the cheaper fibres such as sheep wool, for accurately quantifying the composition of blends of the luxury fibres and wool. The section that follows comprehensively reviews previous work conducted in the past five decades towards the development of such research techniques.

### **2.3.2 General**

High quality textile products are often intentionally and openly made from blends of wool with luxury or speciality fibres (such as cashmere, mohair, camel hair, angora, etc.). Nevertheless, it is sometimes done clandestinely or fraudulently, mainly for cost and supply reasons. For example, it has previously been shown that substitutes (lustre wools in particular), which were not declared, constituted 10-15% of mohair products (Phan and Wortmann, 1987). The Deutsches Wollforschungsinstitut (DWI) in Germany, one of the laboratories with highly reputable researchers in the field of animal fibre identification and blend composition analysis, found that 50% of the samples they tested in 2004, and the years before, were wrongly labelled (Wortmann and Phan, 2004). The accurate labelling of textile products at all levels of processing relies on the accurate characterization and identification of each fibre type present in the product, this requiring the availability of a reliable and time effective method. Both chemical and physical characterization techniques have previously been investigated in terms of their suitability for wool/speciality fibre blend compositional analysis. Chemical solubility tests make this task a very straight forward one when animal fibre/synthetic or animal/plant fibre blends are under investigation, due to the fact that fibres of different generic types exhibit different chemical compositions and properties, making it possible to select a suitable solvent to preferentially dissolve one component of the blend (Greaves, 1990).

At various times Stratmann (1987), Greaves (1992, 1995), Stapleton (1992), Hunter (1993), Slater (1993) and McGregor (2012) have reviewed the techniques and significant developments in animal fibre identification, classification and quantitative blend analysis, including the use of light microscopy (LM), scanning electron microscopy (SEM), transmission electron microscopy (TEM), Image Analysis, Electrophoresis, Infrared spectroscopy, and Deoxyribonucleic acid (DNA).

Wilkinson (1990) stated that the list of suitable techniques, for animal fibre identification and blend analysis, is shortened considerably if quantitative analysis is performed on samples where contaminants are present in small quantities, with fibre treatments further shortening the list. Various characterization techniques have previously been proposed for both qualitative and quantitative analysis of animal fibre blends. Wilkinson (1990) presented a list of techniques (Table 2.4) which had been discussed in papers on animal fibre identification, presented at the First and Second International Symposia of Speciality Fibres in Aachen, Germany. Table 2.4 shows that microscopic techniques were used to study, for example, the fibre physical dimensions and characteristics (fibre diameter, length, surface, etc.). Microscopy and image analysis techniques provide information on fibre ellipticity, diameter, cross section and surface features (shape of scales, scale frequencies and scale thickness), while chromatography and electrophoresis are powerful tools for protein analysis (Wilkinson, 1990). Satlow (1965) investigated the possibility of applying chemical tests to distinguish between various animal fibres, such as wool, cashmere and mohair. Cystine and cysteic acid contents, alkali solubility, urea-bisulphite solubility, and the effect of acids, alkalies and enzymes, were the tests performed. It was concluded that the differences between the fibres were insignificant. Many of the tests used, however, were not very sensitive and the interpretation of the results was often not easy.

**Table 2.4: Fibre identification tools and targets (Wikinson, 1990).**

Tool	Reference*	Target
Microscopy; light, transmission and scanning electron, image analysis	1, 2 1,2 1,2 1 1 1	Fibre dimensions Ellipticity Surface features Pigment distribution Medullation Cortical segmentation
Chromatography, electrophoresis	1,2	Protein composition
High pressure liquid chromatography	1,2	External and internal lipids
DNA hybridization	1,2	Cell nuclear remnants

\*<sup>1</sup> First International Symposium on Speciality Animal Fibres. <sup>2</sup> Second International Symposium on Speciality Animal Fibres.

Hamlyn *et al.*, (1992) summarized some of the techniques that had previously been investigated and proposed for qualitative and quantitative analysis of animal fibres and their blends (Table 2.5, adapted from Hamlyn *et al.*, 1992).

**Table 2.5: Methods proposed for the analysis of keratin fibres (Hamlyn *et al.*, 1992).**

METHOD	REFERENCE
Amino acid analysis	Sagar <i>et al.</i> , (1990)
Scale height measurement	Wortmann and Arns (1986)
Image analysis	Robson <i>et al.</i> , (1989)
Analysis of extracted proteins using polyacrylamide gel electrophoresis (PAGE).	Wortmann <i>et al.</i> , (1988)
Internal and external lipid analysis	Rivett <i>et al.</i> , (1988)
DNA fibre profiling	Kalbé <i>et al.</i> , (1988) and Hamlyn <i>et al.</i> , (1990)

Section 2.3.3 reviews surface topographic based methods and their application in the identification and classification of animal fibres and the composition analysis of their blends.

### **2.3.3 Surface Topography Based Methods**

#### **2.3.3.1 Light Microscopy (LM)**

Identification and classification of natural animal fibres have always relied on the use of microscopy-based methods. Microscopic techniques are considered to be amongst the most important and useful methods in the characterization of materials (Giri, 2002). Animal fibre identification initially depended on the examination of the fibre surface by light microscopy (LM), for scale frequency (number of scales found in 100 µm fibre length) and scale prominence and pattern (Blankenburg *et al.*, 1979; Hunter, 1993). Wildman (1954) was amongst the first to note that scale pattern and the length of the

fibre scale were significant parameters to take into consideration for a successful identification and classification of animal fibres from different animal species. He described three types of scale patterns, namely Coronal, Corronal-Reticulate and Reticulate scaling, and stated that the Coronal scaling was mostly found in very fine animal fibres, such as merino wool, while Reticulate scaling was mostly found in coarse animal fibres. The use of LM to distinguish between cashmere and wool relies on the fact that cashmere fibres display long, flat scales, wrapping around the fibre, whereas wool fibres have short and thick scales of mosaic appearance (Langley, 2003).

Langley and Kennedy (1981) investigated the possibility of using LM to differentiate between lustre wools and speciality fibres. Relationships between scale length and fibre diameter for mohair, Buenos Aires (BA) lamb's wool, cashmere, camel hair and alpaca were reported. Since certain properties of BA wool, notably lustre, resemble those of mohair, it is widely used as a mohair substitute in textile products, due to its much lower price. The results of this investigation showed that the scale length of BA wool was generally lower than that of mohair, and that the fibre diameter of BA wool tended to be greater than that of mohair. The cube of the scale length (S) divided by the fibre diameter (D), ( $S^3/D$ ) was found to be  $29 \mu\text{m}^2$  for mohair, this value being five times lower than that reported by Skinkle (1936). These researchers concluded that scale length and fibre diameter were unreliable for differentiating between lustre wools and mohair. They also noted that wool possessed thick surface scales and were a little duller or less lustrous in appearance than mohair fibres.

Kadikis (1987) noted that light microscopy was useful and suitable for animal fibre identification, and for determining the content of each fibre present in a blend. Nevertheless, he found that the successful application of LM involved four prerequisites. The first prerequisite was that the analyst should have an understanding of sound sampling techniques. The second was the use of a 500X micro-projector to give a sharp image, with a large field of vision. Third, was a sufficient number of identified fibres to provide statistical validity within the tolerances required by the Wool Products Labelling Act. The fourth prerequisite was the level of experience of the operator: Kadikis stating that the operator must have years of experience and a good visual memory. Ainsworth

and Zhang (2005) noted that a new operator need training of 3-6 months, or even longer, to get to the level of being able to carry out commercial tests. Considerable patience and intellectual honesty, to recognize when a fibre cannot be identified, have also been found to be important. This view has also been emphasised in Langley (2008).

One fibre testing group (EEC Working Party on Names and Labelling, 1988), examined the suitability of LM in animal fibre blend analysis, using round robin trials in the 1970s. After studying the inter-laboratory results, these animal fibre testing experts found that it was difficult to obtain useful information, especially for fibres of which the surfaces have been chemically treated, that could be used in confirming the declared fibre contents in textile materials (EEC Working Party on Names and Labelling, 1988). They concluded that no test, even LM, could precisely quantitatively determine intimate mixtures of wool and other animal fibre at that time. This was later confirmed by Wortmann and Wortmann (1992), who investigated the suitability of LM in animal fibre identification and blend composition analysis. They made use of Round Robin Trial results performed in the seventies and concluded that light microscopy was not a reliable technique for wool/specialty fibre blend analysis. Sich (1990) investigated, and compared, the possible application of both LM and SEM (see Table 2.6), for animal fibre identification and classification.



**Table 2.6: Comparison of SEM and LM capabilities in examining animal fibres (Sich, 1990).**

	SEM	LM
Topography	+	-
Profile edge	-	+
Pigmentation	0	+
Medulla	0	+
Refractive index	0	+
Birefringence	-	+
Staining techniques	0	+
Complete fibre length examination	-	+
Sample preparation	-	+
Speed of examination	-	+
Manipulation during examination	-	+

<sup>0</sup>no capability, + excellent capability, - Moderate capability.

The advantages of each technique were compared, and it was found that the scanning electron microscope (SEM) provided a clear detail of surface features, although it was incapable of providing internal information of the fibre. The researcher concluded that both LM and SEM were needed for undisputed fibre identification.

As a step towards the development of a fast, accurate method and with the aim of reducing the subjectivity of light microscopy, the use of a weighted discriminant analysis, using two fibre properties (fibre diameter and scale frequency) and a three-dimensional cluster analysis, based on three fibre properties (diameter, scale frequency

and scale form), measured using the light microscope [Phan *et al.*, (1988); Wortmann *et al.*, (1989); Hermann *et al.*, (1995); Teasdale, (1988)], were investigated. This technique is aimed at sorting a number of objects which are defined by characteristic data vectors. The first mentioned discriminant analysis was based on the bivariate normal distribution of the two measured parameters (Hermann *et al.*, 1995):

$$P(x, y) = \frac{1}{2\pi s_x s_y \sqrt{1-r^2}} \cdot \exp \left[ -\frac{1}{2(1-r^2)} \left\{ \frac{(x-\bar{x})^2}{s_x^2} - 2r \frac{(x-\bar{x})(y-\bar{y})}{s_x s_y} + \frac{(y-\bar{y})^2}{s_y^2} \right\} \right] \dots\dots\dots 2.2$$

Where x represents the fibre diameter, in  $\mu\text{m}$ , and y the scale frequency (number of scales per 100  $\mu\text{m}$  length),  $s_x$  and  $s_y$  the standard deviations, r the correlation coefficient and  $\bar{x}$  and  $\bar{y}$  the arithmetic means of the two variables, respectively. With all these values in the bivariate function, the discriminant function D(M,W) may be obtained. This function was used to distinguish between different animal fibre types, such as mohair and wool:

$$D(M, W) = \log \frac{PM(x,y)}{PW(x,y)} \dots\dots\dots 2.3$$

Where D(M,W) is the discriminant function for mohair (M) and wool (W), PM(x,y) and PW(x,y) are the values of the bivariate normal distribution for mohair fibres and wool fibres, respectively. Once this relationship is obtained for fibres of known origin, the equal-odds line allows identification of values for unknown fibre blends. In the three-dimensional cluster analysis method, a third variable (scale form) is introduced. Hermann *et al.*, (1990) concluded that both these methods have shown that light microscopy, combined with statistical classification methods, present a potentially valuable fibre blend analysis procedure, but which once again strongly relies on the experience of the operator.

Wilkinson (1990) noted that animal fibre and their blend composition analysis using microscopy-based techniques were limited by the following factors:

- (a) Natural pigmentation and added dye mask features.

- (b) The features vary along each fibre, as well as between fibres from the same animal.
- (c) The features are obscured or removed by weathering.
- (d) Fibre identification strongly relies on the operator's judgement.
- (e) Fibre terminology varies from country to country. Wilkinson stated that "an example is white Iranian cashmere, which is cashmere in Europe but not cashmere in USA".

Different definitions of the cashmere fibre have been studied by Phan *et al.*, (1991) and Phan *et al.*, (1994). Fujishige and Koshiba (1997) developed a light microscopy-based technique for identifying cashmere and Merino wool fibres. Three samples, namely white and naturally dark coloured cashmere fibres from Mongolia and fine Merino scoured wool, were examined. These samples were treated with Basic Blue 7 (about 0.2 wt % in water) dye at 60°C for 1 hour to stain the cuticle scales and to enhance the characteristic scale margins. These were further exposed to heat treatment in the aqueous medium at 80°C for 1 hour in the presence of 0.1 wt % sodium dodecyl sulphate. The researchers found that cashmere fibres had a curvature extended throughout the entire length of the fibre, in contrast to what was observed in Merino wool fibres, where the fibres were crimped, this being revealed by the heat treatment. A bilateral structure, with unstained section in parallel with the stained portion, was observed in cashmere specimens, confirming the results of Chen and Fujishige (1996) that the Merino wool ortho-cortex could not be stained using Basic Blue 7. The research concluded that the technique they developed could form a basis for animal fibre blend analysis and added that the success of the technique required an extremely skilled microscopic analyst.

A round trial was organized under the auspice of the CCMI (Cashmere and Camel Hair Manufacturers Institute /USA) in 1995, where seventeen testing laboratories participated (Phan and Wortmann, 1997). A very low success ratio of 46% was obtained for the LM analysis compared to the 95% of SEM.

Some of the shortcomings in animal fibre analysis, using LM, were summarized by the SGS animal fibre testing laboratory. These include the subjectivity of the method, the

increasing introduction of modified wool and the use of fibres sharing similar morphological characteristics. An important factor, noted by the SGS testing group, was that fibre surface treatments damaged the fibre surface (Ainsworth and Zhang, 2005). The fineness (measured by LM and SEM) of different animal fibres of textile importance has been summarized in the form of bars as shown in the Figure 2.5 (Phan *et al.*, 1988). As evident from the figure, an overlap of diameters is observed between wool and mohair fibres, posing a potential risk of mis-classification of the two fibre types if fibre diameter is used as a sole parameter for classification.

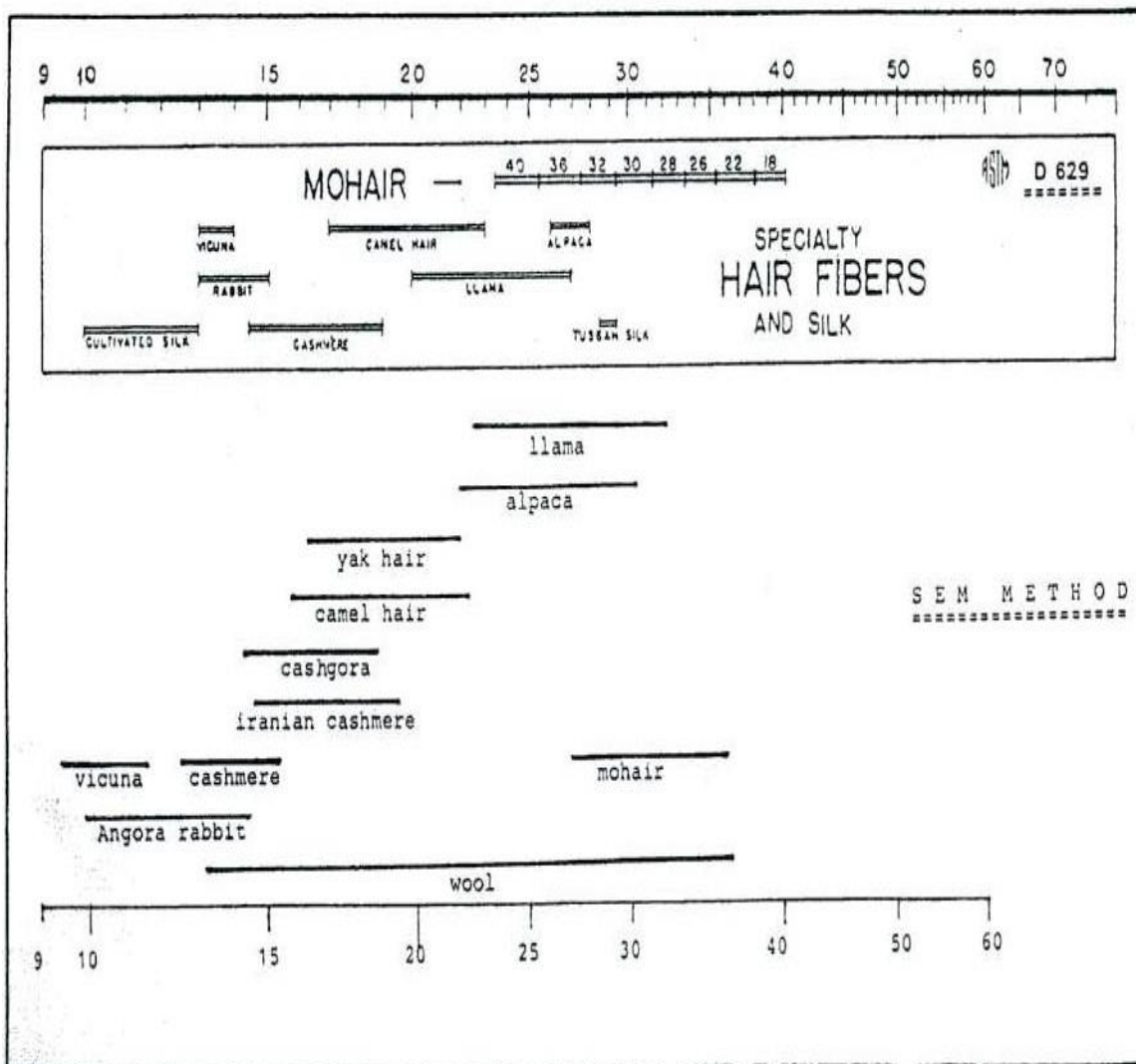


Figure 2.5: Identification and classification of animal fibres by their fineness (Phan *et al.*, 1988).

Scale frequency has also been used in the past as a basis for distinguishing between wool and mohair (von Bergen, 1963). This method was based on the fact that wool was presumed to have a scale frequency (number of scales per 100  $\mu\text{m}$  length) ranging from 9 to 11 compared to about 5 of mohair. Kusch and Arns (1983) found that, depending on breeding conditions, mohair may also have a high scale frequency which may overlap with that of wool. These findings lead to the LM based scale frequency criterion being considered unreliable for animal fibre identification. Phan *et al.*, (1988) claimed that, even though scale frequency was found to be misleading, it could still be considered as an important identifying feature in certain animal fibre analysis. Teasdale (1988) noted that the scale frequency of mohair was about 7/100  $\mu\text{m}$  and was independent of average fibre diameter, while Wortmann *et al.*, (1988) cited in Hunter (1993), found that mohair scale frequency ranged from 5 to 10 per 100  $\mu\text{m}$  with no direct relation to the fibre diameter while a decrease in scale frequency from about 10 per 100  $\mu\text{m}$  for a 16  $\mu\text{m}$  to about 6 per 100  $\mu\text{m}$  for a 35  $\mu\text{m}$  wool was observed. Wortmann *et al.*, (2000) stated that scale frequency varies from 10 to 12 per 100  $\mu\text{m}$  for wool and that of mohair from 4 to about 6 per 100  $\mu\text{m}$ . Fibre profiles may change drastically from root to tip of the fibre and these profiles often overlap for many animal fibres (McGregor, 2012). This fact and the fact that individual fleeces may possess a wide range of fibre diameters and scale patterns, are some limitations to the successful and accurate identification of different animal fibres, using LM based fibre surface characteristics.

### **2.3.3.2 Scanning Electron Microscopy (SEM)**

A technique found to play a vital role in the identification and classification of animal fibres is that of scanning electron microscopy (SEM). This technique offers better resolution and depth of field, which are superior compared to those offered by the traditional optical microscope, enabling valuable parameters such as fibre surface scale heights to be accurately measured. In an SEM, an electron beam of a very small diameter, is irradiated on the surface of the specimen to release secondary electrons which are collected to form the image (Giri, 2002). Sample preparation for the SEM

analysis of animal fibres normally involves the application of a thin layer of a noble metal, such as gold, to the surface of the specimen, prior to the fibre being examined.

In one of the earlier studies, fibre identification method, based on the assessment of the nature of cortical cells by scanning electron microscope (SEM), has been investigated (El-Alfy and Blakey, 1980). This involved a technique, known as plasma-etching, for removing the cuticle of the fibre to reveal the cortex, which was then studied in the SEM. The method involved cutting a flat transverse face to the fibres embedded in any epoxy resin. The face was etched with oxygen plasma, resulting in various subcomponents of the fibres being removed, and then observing the specimen surface in the SEM. It was noted that the cortical cells from camel hair were between 1.5 and 3  $\mu\text{m}$  in width and between 75 and 130  $\mu\text{m}$  in length, those from cashmere were found to be between 2.7 and 4.1  $\mu\text{m}$  wide and between 60 and 80  $\mu\text{m}$  in length. The cortical cell surfaces of wool fibres appeared rougher than those of Angora rabbit hair. The researchers stated that the nature of the cortical cells could be used to identify the origin of the fibre, but this technique has never been adopted in practice.

Dobb *et al.*, (1961) were the first to publish the work which showed that the cuticle scale height (CSH) of animal fibres could be used in distinguishing between them and aid in their classification. The CSH is defined as how far a scale edge protrudes above the surface of the cuticle cell lying under it. Kusch and Arns (1983) discussed some results on wool and mohair CSH measurements obtained from pure samples of untreated sheep wool and goat hair from different countries. Figure 2.6 illustrates CSH measurement on an animal fibre.

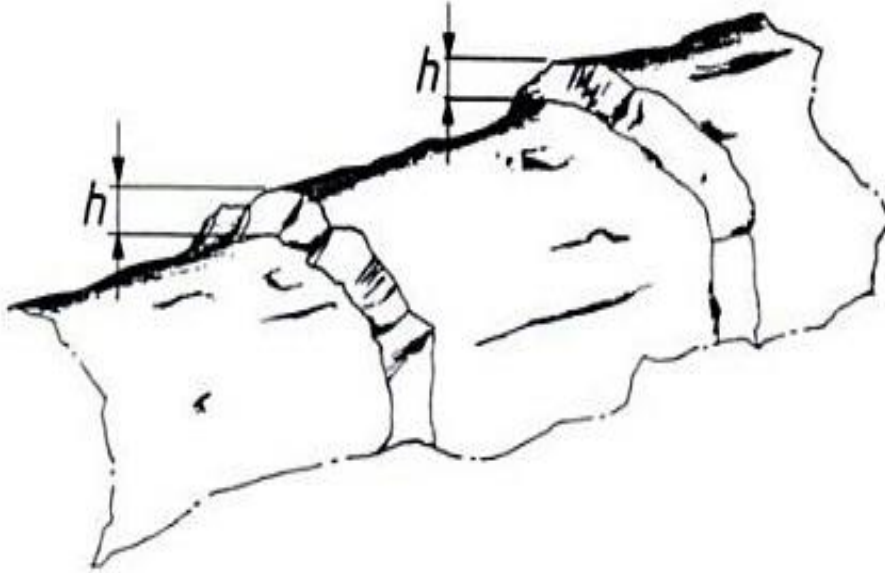


**Figure 2.6: Animal fibre CSH ( $h$ ) measurement (Weideman *et al.*, (1987)).**

Kusch and Arns (1983) found that the CSH of wool ranged from  $0.73 \mu\text{m}$  to  $1.05 \mu\text{m}$  (taking tolerance intervals into consideration), and from  $0.38 \mu\text{m}$  to  $0.49 \mu\text{m}$  for goat hair. There was a difference of  $0.22 \mu\text{m}$  between the lowest wool CSH value and the highest goat hair CSH value. It was therefore concluded that the CSH provided a clear distinguishing property between goat hair and sheep wool. The research was also concerned about the effect of chemical treatment on the CSH, but found that even dyed wool fibres can be distinguished from mohair. Many studies have subsequently been undertaken to investigate the reliability of the SEM based method (Weideman and Smuts (1985); Wortmann and Arns (1986); Weideman *et al.*, (1987); Wortmann *et al.*, (1988); Wortmann and Wortmann (1992); Varley (2006)) for the analysis of pure and blend samples of animal fibres used in textile products. Figure 2.7 presents a system of animal fibre classification developed at DWI in Germany.

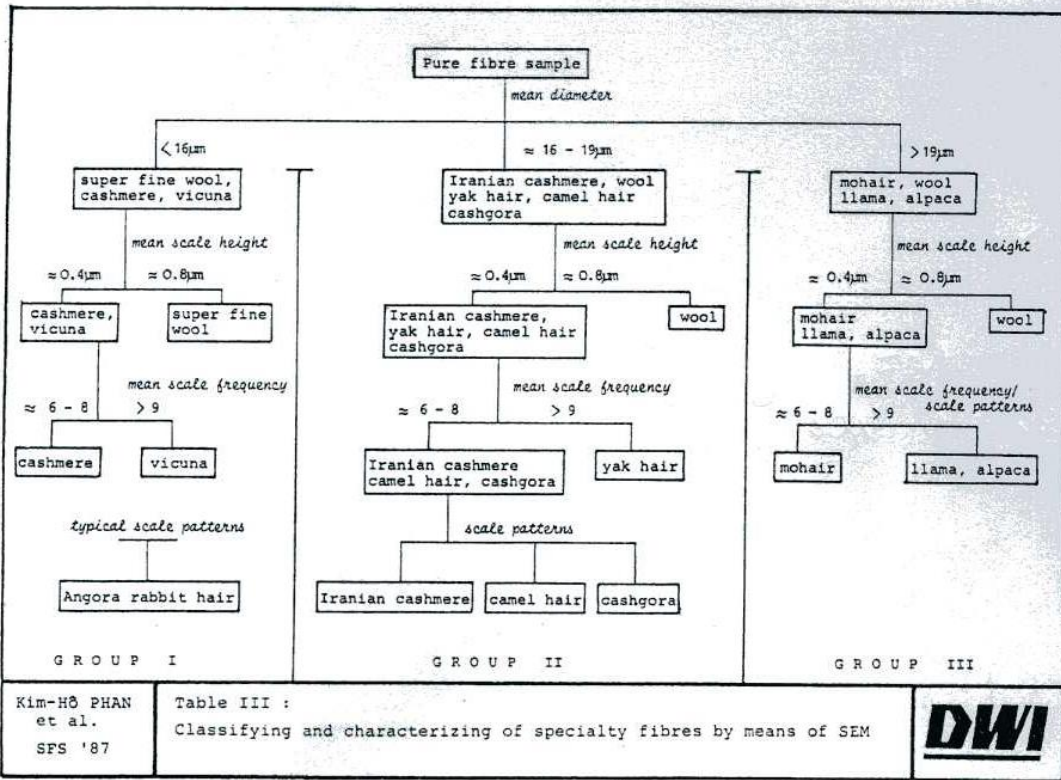


**Figure 2.7: Classification and characterization of specialty animal fibres using the SEM (Phan et al., 1988).**

Figure 2.8 shows SEM micrographs of mohair (left) and Buenos Aires wool fibres (right) at 1000X and 25000X magnifications. This example was chosen because the most frequently found adulteration of mohair is with Buenos Aires fibres. As evident from these micrographs in Figure 2.8 it is through the use of an SEM that mohair and Buenos Aires wool fibres could be reliably distinguished.



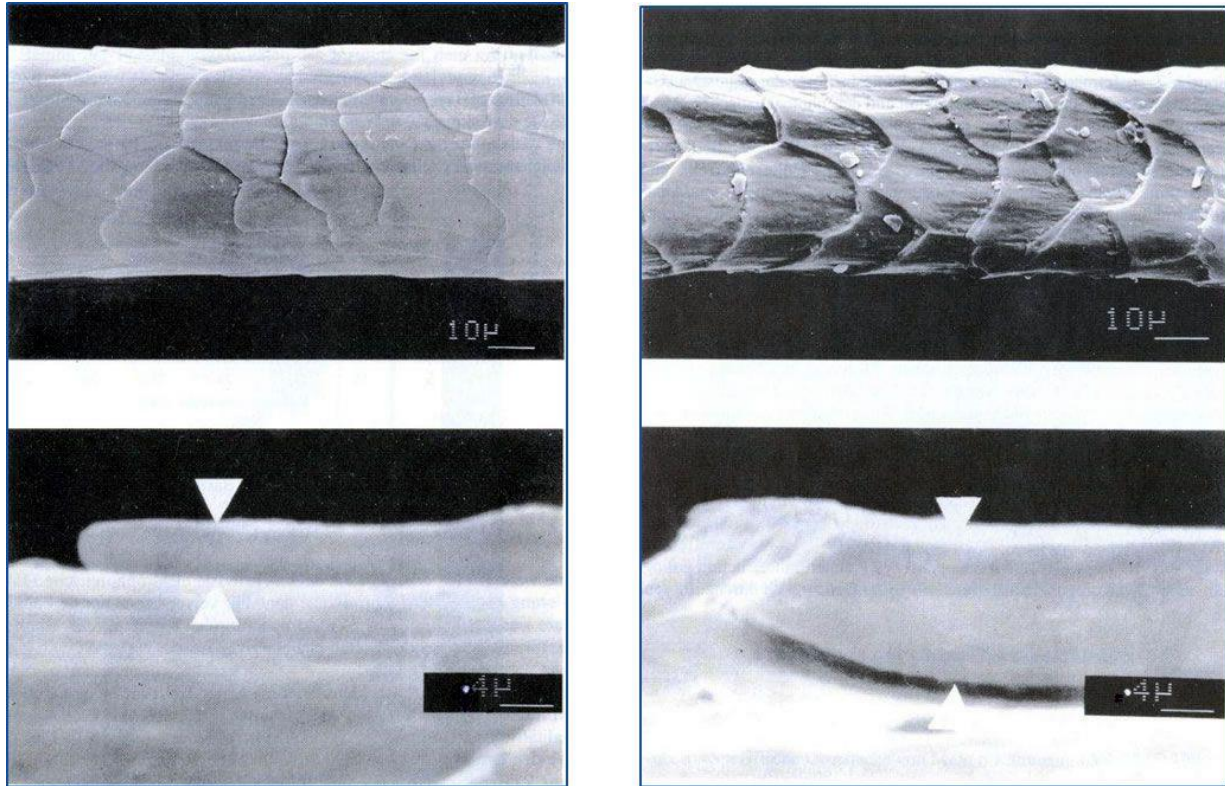


**Figure 2.8: SEM micrographs of mohair (left) and wool Buenos Aires (right) fibres at 1000X magnification, and close-ups of their cuticle scale edges at 250000X magnification) (Wortmann *et al.*, 1988).**

Weideman *et al.*, (1987) investigated the possible sources of uncertainties in CSH measurements by SEM. They noted that variability in scale height could be due to a scale lying on top of another scale, forming a double scale, giving a scale height double the normal scale height. These researchers found that the SEM CSH based method was the most reliable and provided positive identification of different animal fibre types. Nevertheless, a significant overlap in the CSH distributions of wool and mohair was observed. In some cases, scale deformations made it difficult for an accurate measurement on the scale, while in other cases, the scale thickness varied, making it difficult to determine the correct or representative position for measurement on the scale. For this reason, the operator needs to be fully trained and experienced and to have a good knowledge base of animal fibres. Cuticle scale height measurements of 0.5  $\mu\text{m}$  were rare in wool samples examined at the DWI by Wortmann *et al.*, (1988). The observation of CSH animal fibre differences allowed the possibility and limitations of

wool/mohair and wool/cashmere blends to be examined. Fibres, with a CSH exceeding 0.6 µm, were readily classified as wool, and fibres with a CSH less than 0.5 µm were readily classified as mohair. Where classification was difficult, two or three scales were measured on each fibre for more accurate classification. The weight fraction of wool fibres ( $W_w$ ), in a wool/speciality fibre blend, can be calculated from the following Wildman/Bray (W/B) formula (Wortmann and Arns, 1986):

$$W_w = \frac{n_w(d_w^2 + s_w^2)}{[n_w(d_w^2 + s_w^2) + n_s(d_s^2 + s_s^2)]} \dots\dots\dots 2.4$$

Where  $n_w$  and  $n_s$  are the number of wool and speciality fibres counted, respectively, and  $d_w$  and  $d_s$  are the average diameters with  $s_w$  and  $s_s$  standard deviations, respectively of the wool and speciality fibres, respectively.

The speciality fibre weight fraction,  $W_s$ , can be calculated using equation 2.5.

$$W_s = 1 - W_w \dots\dots\dots 2.5$$

The application of the W/B formula (eq. 2.4) in animal fibre blend composition analysis is based on the assumption that the blend components possess circular fibre cross-sections.

Wortmann *et al.*, (1988) discussed some wool/rabbit hair blend analysis results, rabbit hair containing mostly medullated and elliptical fibre cross-sections. It was noted that the analysis had an accuracy which compared well with that of wool/mohair and wool/cashmere blends.

Wortmann and Arns (1986) concluded that the SEM CSH measurement technique was reliable and provided an accuracy which compared well with that of the often-used chemical techniques for wool/mohair blend composition analysis.

The following system in Figure 2.9 of animal fibre identification by CSH, as measured on an SEM, was constructed at the DWI by Wortmann *et al.*, (1988). In this system, cuticle scale heights, for different wool breeds and different speciality animal fibre samples from different countries, are plotted as box-and-whisker plots. No significant

overlap in CSH measurements of different wools and different speciality fibres was observed by Wortmann *et al.*, (1988), in contrast to the observation of Weideman *et al.*, (1987).

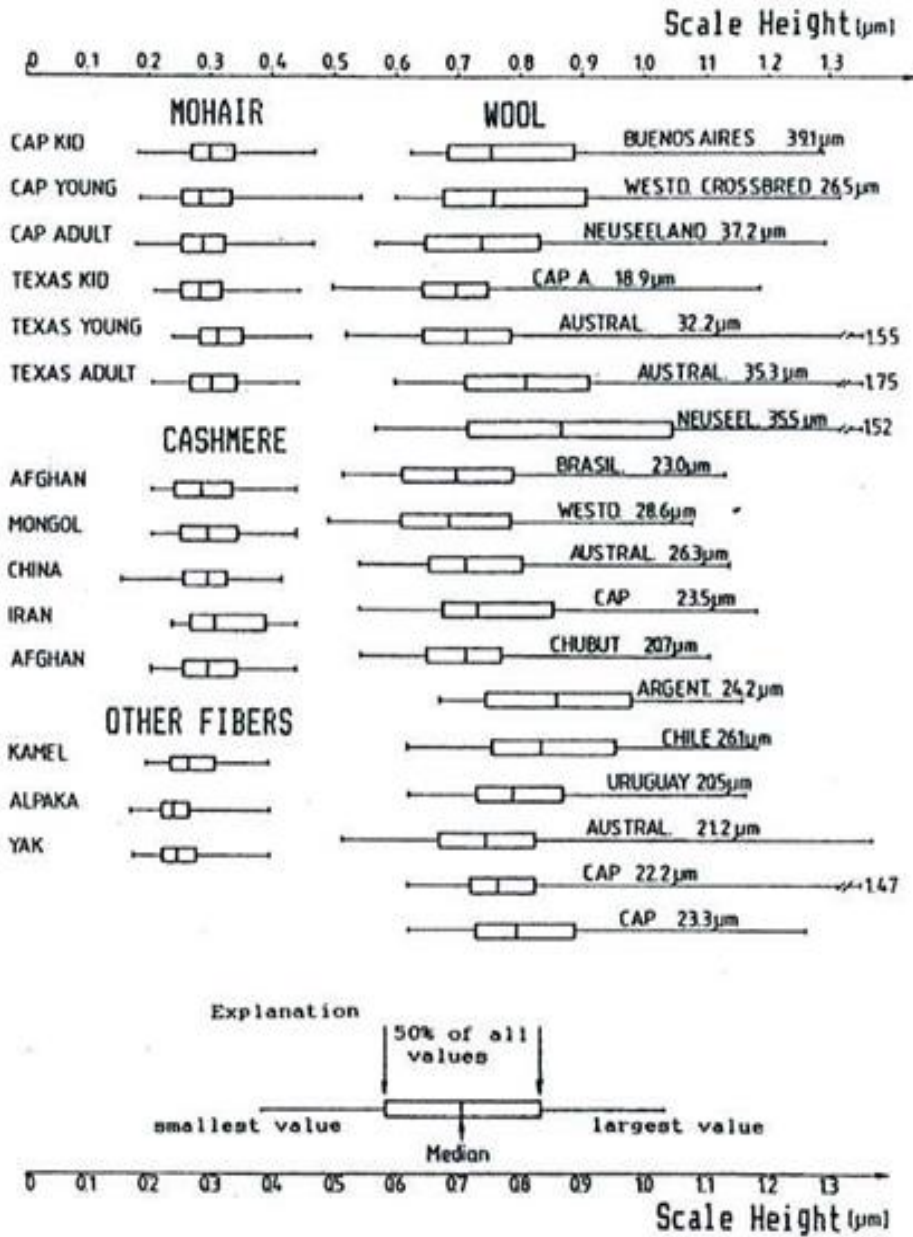


Figure 2.9: Summary of CSH measurements on 18 wools and 14 speciality fibres as box-whisker plots (Wortmann *et al.*, 1988).

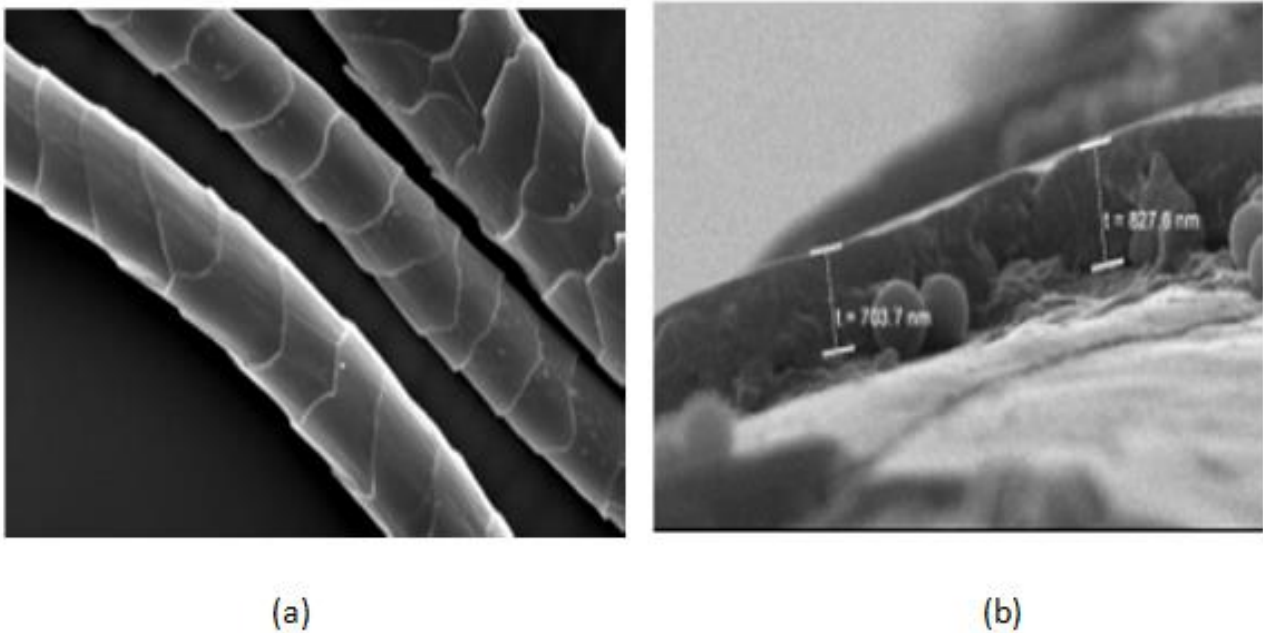
Wortmann (1991) reported results of a round robin trial, involving the composition analysis, of wool/mohair blend samples conducted under the auspices of the International Mohair Association (IMA). The samples were prepared by the CSIR (Division of Textile Technology in South Africa) and the German Wool Research Institute (Deutsches Wollforschungsinstitut, DWI). Wool and mohair fibre snippets of 0.4 mm length were weighed and mixed as described in the IWTO-8 test method. This study showed good agreement between the reference (actual) and the analysis results and indicated that the major component of the analysis error was the random error inherent in the microscopical approach to fibre analysis. Criticism of the CSH technique has been the fact that it gives access to only cuticle scale heights and that it only distinguishes between wool and speciality fibres (Wortmann and Wortmann, 1992). Baker *et al.*, 1998 showed that the use of non-dimensional ratio, based on the ratio of the scale spacing to the fibre diameter, could be useful in distinguishing between wool and cashmere fibres, yielding 89.8 % success rate.

The discovery of the difference in CSH measurements of animal fibres led to the development of the international test method, IWTO 58-00, of the International Wool Testing Organization (IWTO 58-00, 2000). According to this method, animal fibres, lying longitudinally on the SEM stub, are measured for their CSH. A large number (450) of fibre snippets must be examined. Wortmann and Phan (2006) statistically showed that the risk (with a 95% probability) of fibres being incorrectly classified (in a wool/cashmere SEM blend analysis) falls to approximately 0.8 % after the 450 snippets have been analysed. Varley (2006), however, developed a slightly different technique, called the vertically oriented sequential CSH measurement technique, for the examination of animal fibres.

Greaves (2005) argued that a limiting factor in the SEM CSH method for quantitative animal fibre compositional analysis is the fact that these instruments are extremely expensive. This researcher stated that the accuracy of the analytical procedure depends upon the instrument/operator system which is likely to be similar for SEM and LM analyses. According to Greaves (2005), certain fibre modifications (enzyme and plasma shrink-resist processes and fluorocarbon coating treatments) can make animal

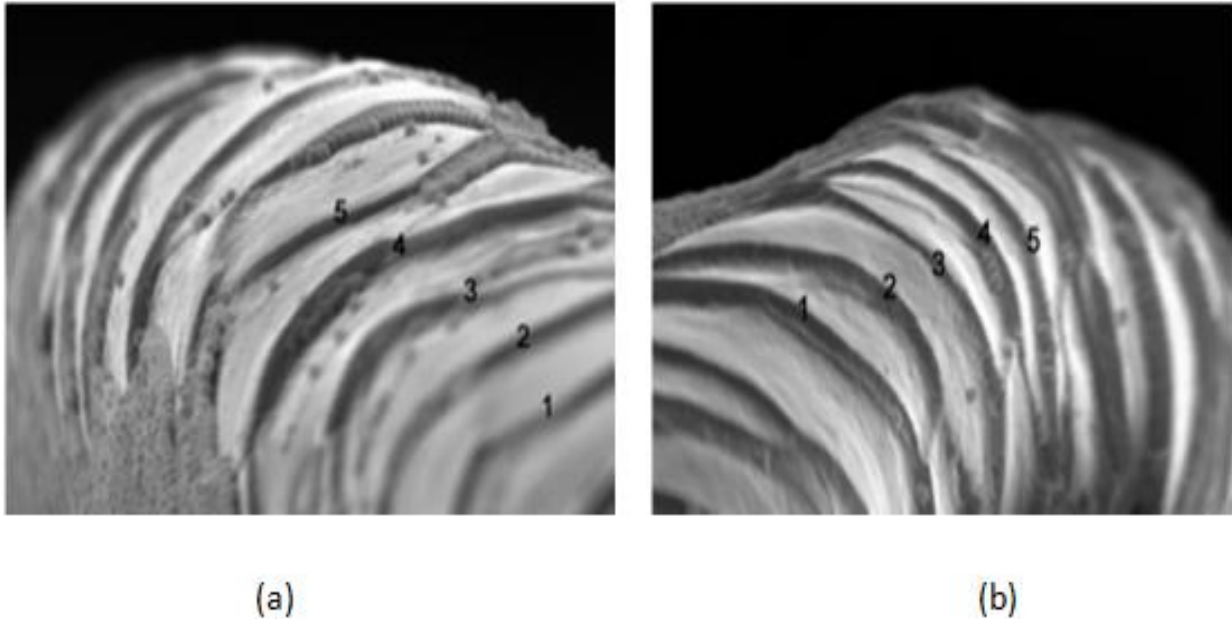
fibre identification, classification and blend compositional analysis difficult. In the research paper by Greaves (2005), LM micrographs are shown which illustrate the distinction between animal fibres based on the scale pattern.

Figure 2.10 depicts some fibres prepared for the conventional longitudinal cuticle scale height measurements, while Figure 2.11 depicts fibres prepared according to the Varley (2006) technique.



**Figure 2.10: SEM micrographs of (a) Cashmere fibres and (b) CSH (Varley, 2006).**

Varley (2006) argued that one of the limitations of the IWTO 58 test method, was certain profile artefacts and limited scale views. Figure 2.11 illustrates that this limitation is largely overcome in the vertical-oriented sequential method proposed by Varley (2006).



**Figure 2.11: SEM micrographs of (a) Cashmere and (b) Wool scales (Varley, 2006).**

Varley (2006) selected six fibres randomly from each of the samples used, and observed an overlap in wool CSH and cashmere CSH, which was contrary to previously reported results (Kusch and Arns, 1983). Varley's vertical-oriented sequential method showed CSH values twice as high the values reported previously by Wortmann and Arns (1986) and Langley (2003). The researcher concluded that the vertical-oriented sequential CSH measurement technique provided CSH measurements in a more objective and accurate manner than those by the longitudinal CSH technique.

Different views have been expressed concerning the effect of chemical treatment of the fibre surface on animal fibre analysis ((Tucker (1997), Wortmann and Phan (1998) and Kim (2008)). According to Tucker (1997)), the application of the SEM CSH method in animal fibre identification and classification, where fibres have undergone chemical treatment, may be misleading and provide unreliable results. To investigate the effect of chemical treatment on animal fibre identification, he treated cashmere fibres with 37.5% hydrochloric acid (HCl), followed by 15 minutes treatment in 3% of hydrogen peroxide. He found that such a chemical treatment lead to increased cuticle scale height values. Nevertheless, the arguments put forward in Tucker's paper were questioned by



Wortmann and Phan (1999) on the basis of their findings on the effect of chemical treatments on the surface of cashmere and wool fibres.

Bahi *et al.*, (2007) found that there was a significant reduction in the cuticle scale height of merino fibres, the reduction being dependent upon the chemical treatment. Another problem with the SEM based CSH method for animal fibre identification is the availability of descaled (as shown in Figure 2.12), stretched and enzyme treated fibres, for which the surface or scale features have been significantly changed (Ki-Hoon, 2008).

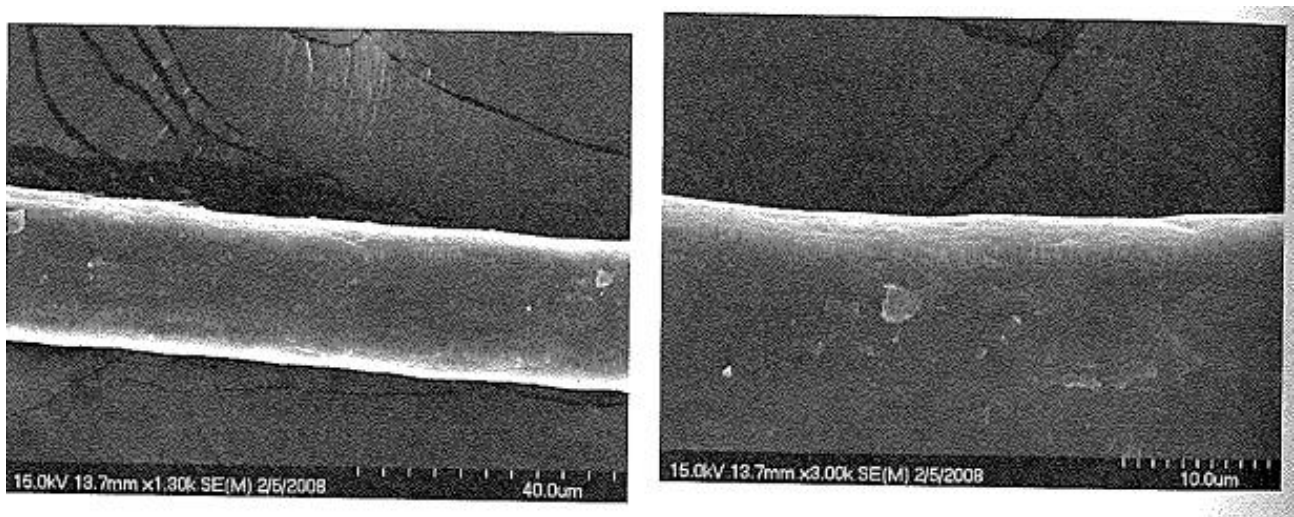


**Figure 2.12: Microscopic images of descaled animal fibres (Ki-Hoon, 2008).**

An analytical method, based on image processing and analysis, has been investigated for its applicability as a possible alternative technique to the existing time consuming and expensive microscopic methods which are sometimes unreliable for the analysis of natural animal fibres (Robson *et al.*, 1989; Robson and Weedall, 1990). This technique is based on the enhancement of fibre images captured from the SEM, to extract useful information leading to more reliable fibre identification and classification. Fifteen scale parameters P1-P15 were successfully extracted from SEM captured images for objective animal fibre identification (Robson, 1997). Amongst these parameters, were fibre width, scale interval, scale circularity, scale orientation and scale elongation, these providing a clear unequivocal description of the fibre scale pattern. The importance of

imaging techniques in cuticle scale measurement has also been investigated (Robson, 2000). Although these microscopic techniques were found to be less subjective, they were still time consuming. Another challenge to the SEM based animal fibre analysis is the deliberate use of de-scaled fine wool fibres to adulterate the expensive speciality hairs, such as mohair and cashmere.

Jin and Hu (2005) stated that quantitative analysis of animal fibres remains difficult when using the traditional microscopic based methods, due to the fact that fine descaled and stretched wool is often unscrupulously adulterated with the expensive rare fibres to reduce costs. These researchers also stated that “an undesirable increase in fibre diameter accompanied by an increase in the height of the scale edge may be observed in some new breeds of cashmere goats, making the differentiation difficult.

In the past two decade, efforts on the development of methods for distinguishing between animal fibres, particularly between sheep wool and speciality fibres, have been on microscopic image processing and computer vision, extracting surface parameters such as fibre diameter, scale frequency, scale heights, scale pattern, etc. (Liu *et al.*, 2019; She *et al.*, 2001; She *et al.*, 2002; Shi and Yu, 2011).

TEM analysis of animal fibres has always been limited by the need for ultrafine cross sections, with Phan (1991) stating that “The chance of getting acceptable whole transverse sections is about 5-10 %, or even less”. Consequently, there has not been enough research over the years on the identification of animal fibres using the TEM.

### **2.3.3.3 Atomic Force Microscopy (AFM)**

The development of the SEM has been considered a huge milestone in the textile industry, particularly in the identification of animal fibres and their blend composition analysis. This method has provided solutions to the limitations of the LM, such as limited resolution and very low depth of field (Ainsworth and Zhang, 2007). Another method that has found great application in the characterization of animal fibres is the atomic force microscopy. The AFM is a form of scanning probe microscopy (SPM) where a tip of a very fine diameter is scanned in a raster pattern (i.e. point-wise and line by line) across the sample surface. Some of the advantages of this method, over SEM,



include the fact that there is minimal sample preparation involved, it is non-destructive and can be operated in different conditions (air and water) (Hilbrick, 2012). Phillips *et al.*, (1995) reported on the changes in the CSH of merino wool fibres when exposed to different conditions, the CSH values ranging from 0.493  $\mu\text{m}$  to 2.039  $\mu\text{m}$  under dry conditions. It was observed that there was an increase in CSH from air exposure to water. CSH values of wool fibres, measured by AFM, have also been reported (Crossley *et al.*, 2000; Maxwell and Huson, 2004; Smith, 1998). The AFM has also been applied to study the effects of bleaching and dyeing on cashmere goat fibres (Javkhlantugs *et al.*, 2009), the results showing an increase in the CSH values for both bleached and dyed fibres compared to the untreated fibres.

Hilbrick (2012) reported on the CSH values of different animal fibres, including wool, cashmere and alpaca, measured using the SPM. One of the objectives of the study was to measure and compare CSH, scale frequency and surface roughness of fibres from wool and speciality fibre tops. Alpaca and cashmere had the lowest average CSH values from wool of similar average fibre diameter and this difference was proved to be statistically significant ( $P < 0.0001$ ). Alpaca fibres displayed higher cuticle interval (defined as the distance between neighbouring scale edges) compared to wool of similar fibre diameter (Hilbrick, 2012). Abdullah (2006) reported AFM based CSH measurements on 20  $\mu\text{m}$  and 18  $\mu\text{m}$  undyed and dyed wool samples, noting a slight increase in CSH values as a result of dyeing. For the undyed fibres, the average CSH was 0.88  $\mu\text{m}$  and 0.85  $\mu\text{m}$  for the 20  $\mu\text{m}$  and 18.5  $\mu\text{m}$  wools, respectively, the corresponding values for the dyed fibres being 0.99  $\mu\text{m}$  and 0.96  $\mu\text{m}$ , respectively. The disadvantage of this technique is that it is very time consuming. Notayi (2014) investigated the possible application of the AFM in animal fibre identification and blend composition analysis. He found that the AFM analysis, though the risk of subjectivity was minimized, was extremely time consuming and could be very expensive. The researcher came to the conclusion that the AFM cannot be considered an alternative to the less time consuming and more subjective LM and SEM methods.

### 2.3.4 DNA Analysis

The need for greater accuracy, reliability and cost effectiveness in animal fibre identification and classification has led to the investigation of a variety of other fibre testing techniques, including deoxyribonucleic acid (DNA) analysis (Kerkhoff *et al.*, 2009). DNA, a species-specific material, contains genetic information of all living organisms. The DNA is a double stranded (two polynucleotide chains) organic complex molecule composed of a repetition of 4 monomers called nucleotides: adenine (A), guanine (G), cytosine (C) and thymine (T). The genetic information is stored in the sequence of these monomers (Kerkhoff *et al.*, 2006). In the living cells of animals, the DNA molecule is found inside nuclei and smaller cellular bodies called mitochondria. The success of animal fibre analysis, using the DNA method, strongly relies on the development of methods for improved extraction of the high molecular weight DNA molecule (Hamlyn, 1998). Two types of DNA test that can be performed, include nuclear DNA and mitochondrial or mt-DNA analysis (see Figure 2.13).

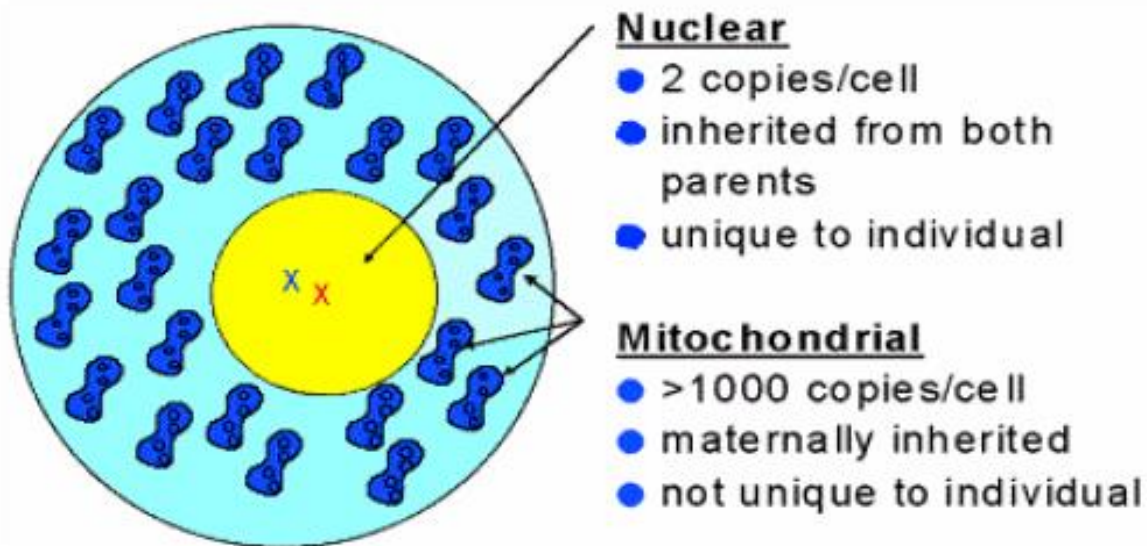


**Figure 2.13: A simplified schematic representation of nuclear and mt-DNA (Panaiotou, 2004).**

In the late 1980s it was discovered that DNA was contained in animal fibre shafts (Kalbé *et al.*, 1988). This was considered an important discovery, as it had previously been believed that DNA was only present in the hair roots and not in the hair shafts. The extracted DNA from the hair shafts made the identification of hair from different species possible. A method for the isolation and purification of DNA from animal fibres has been described (Nelson *et al.*, (1990) and Ley *et al.*, (1988)). Figure 2.14 (Bereck, 1990), summarizes the steps involved in the extraction and purification of DNA and hybridization:

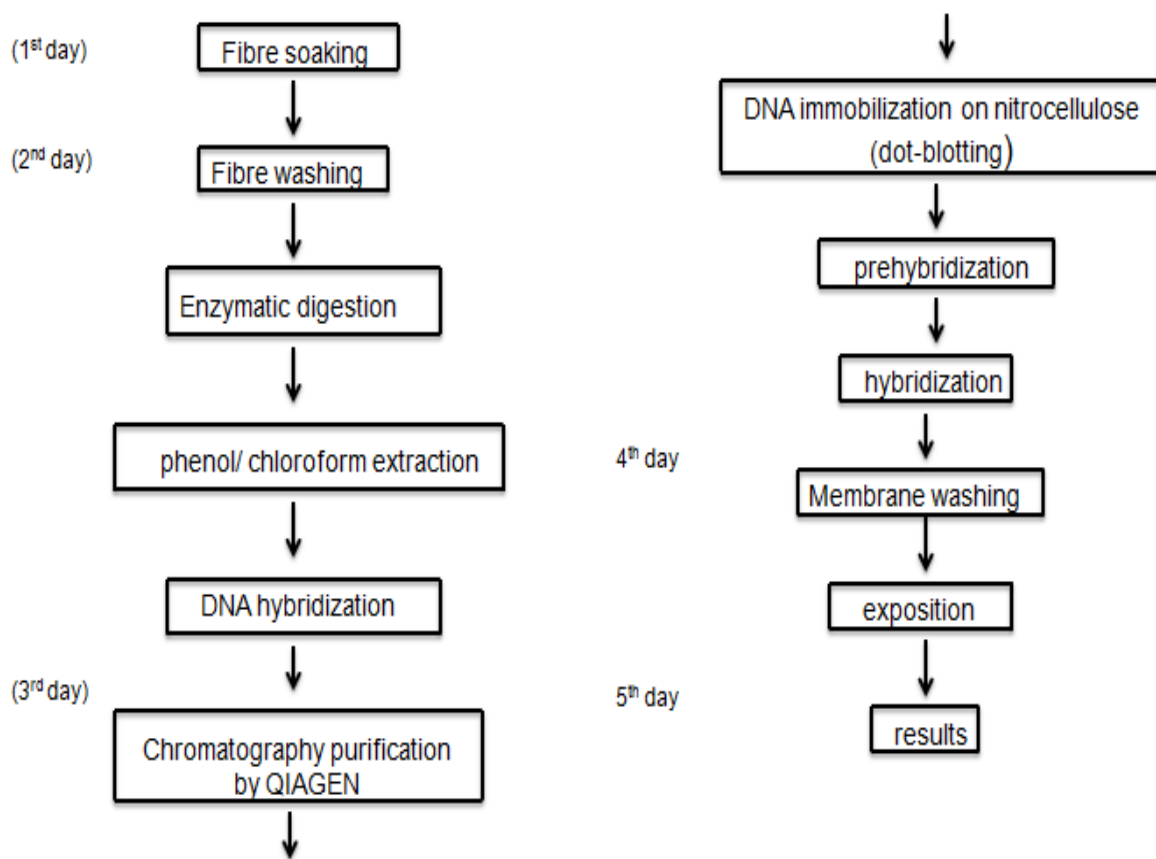
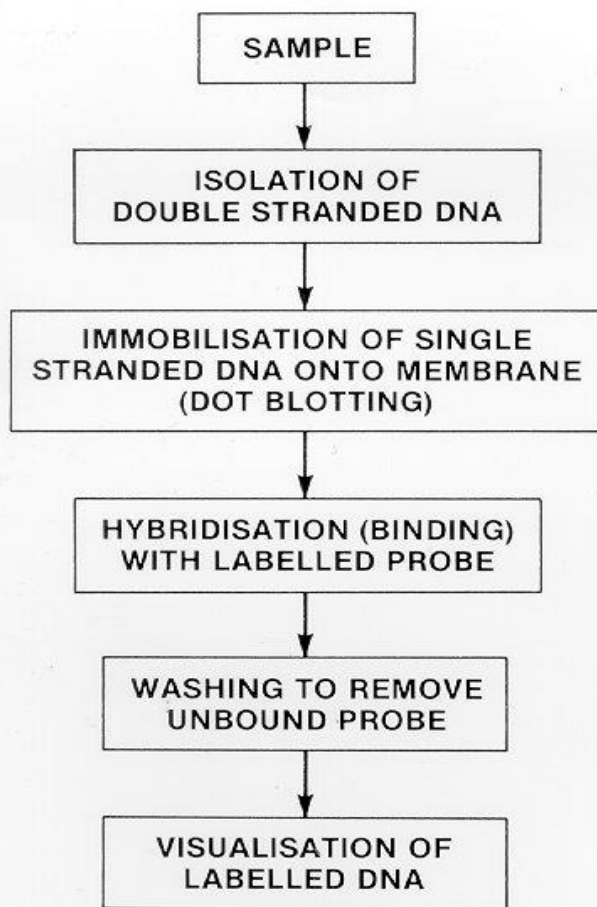


**Figure 2.14: The steps involved in the isolation, purification and hybridization of DNA (Bereck, 1990).**

One of the advantages of DNA analysis, as a means of animal fibre analysis, is that irrespective of any severity of any processing, to which the fibre has been subjected, sufficient DNA still remains for fibre identification, although quantitative fibre analysis

may be impossible (Höcker, 1990). Höcker (1990) claims that the optimised extraction of DNA, of maximum purity, is important and key for animal fibre analysis, and described a method for isolation and purification of DNA from animal fibres. Proteins, lipids, natural pigments and residues are amongst the contaminants that may stick to the DNA, making fibre analysis difficult. Some of the limitations in speciality animal fibre identification and classification, using DNA and other analytical techniques, have been described by Berndt *et al.*, (1990) and Hamlyn *et al.*, (1990). These include DNA degradation, due to thermal and chemical (e.g. oxidation and reduction) treatments, difficulty in the extraction of sufficient DNA and the time required for the analysis.

A DNA dot blot analysis, using species-specific probes to distinguish between DNA extracted from raw and goat fibres, has been developed (Nelson *et al.*, (1992); Hamlyn *et al.*, (1992)), and this technique has received, and still receives, wide application in molecular biology and genetics for detecting bio-molecules. The dot-blotting method is illustrated in Figure 2.15:



**BTTG**

**Figure 2.15: DNA analysis using the dot-blot method (Hamlyn *et al.*, 1992).**

The sample, containing the biological target (mostly proteins or DNA) to be detected, is spotted directly on a membrane (such as nitrocellulose, Nylon 66 and poly (vinylidene fluoride) (PVDF) without prior separation (Laopa *et al.*, 2013). The presence or absence of a specific target can be detected by binding with the probe that can report the binding event by radioactivity, fluorescence, chemiluminescence, or enzyme-based calorimetric assays. Dot blot hybridization requires higher amounts of good quality DNA, which are scarce in processed animal fibres. The absence of a specific target sequence, which will allow a differentiation between DNA isolated from sheep and goat, stimulated the construction of highly sensitive goat-specific oligonucleotides which can be used as

probes to distinguish between DNA isolated from wool and goat fibres (e.g. cashmere and mohair) (Hamlyn *et al.*, 1993). It was found that the prepared goat-specific oligonucleotide probe hybridized very well with DNA extracted from goat hair. These researchers concluded that the oligonucleotide probe was sensitive enough to allow analysis of as little as 100 mg of raw animal fibre and only a few grams of processed material. Further developments of the DNA technique involve the establishment of the polymerase chain reaction (PCR), offering an amplification of high-quality DNA from animal fibres. The PCR is an enzymatic method that can generate thousands or even millions of identical copies of a specified DNA sequence within a very short time. One of the prerequisites for the success of the conventional DNA dot blot hybridization is the extraction of high-quality DNA, and this is not always possible in processed animal fibres. The development of the PCR, where high quality DNA is not a prerequisite, has been of paramount importance in the field. A PCR-reaction consists of approximately 35-50 amplification cycles, where each cycle, in turn, comprises 3 steps, namely Denaturation, Annealing and Detection.

The very high sensitivity, stability and reliability shown by the DNA analysis method, for animal fibre identification, were among other advantages that made this technique a potential alternative tool for replacing the traditional time consuming and expensive microscopic tools for animal fibre analysis (Subramanian *et al.*, 2005). A method for extraction of sufficient DNA from the cuticle of scoured cashmere and wool fibres, using the proteinase K digestion method, as described by Nelson *et al.*, (1992), was employed by Subramanian *et al.*, (2005), who made use of a PCR-RFLP (restriction fragment length polymorphism) technique in distinguishing fibres from goat (*Capra hircus*) and sheep (*Ovis Aries*). Two restriction enzymes, namely BamH1 and Ssp1, were chosen for the analysis, Figure 2.16 (Subramanian *et al.*, 2005), demonstrating their RFLP pattern.

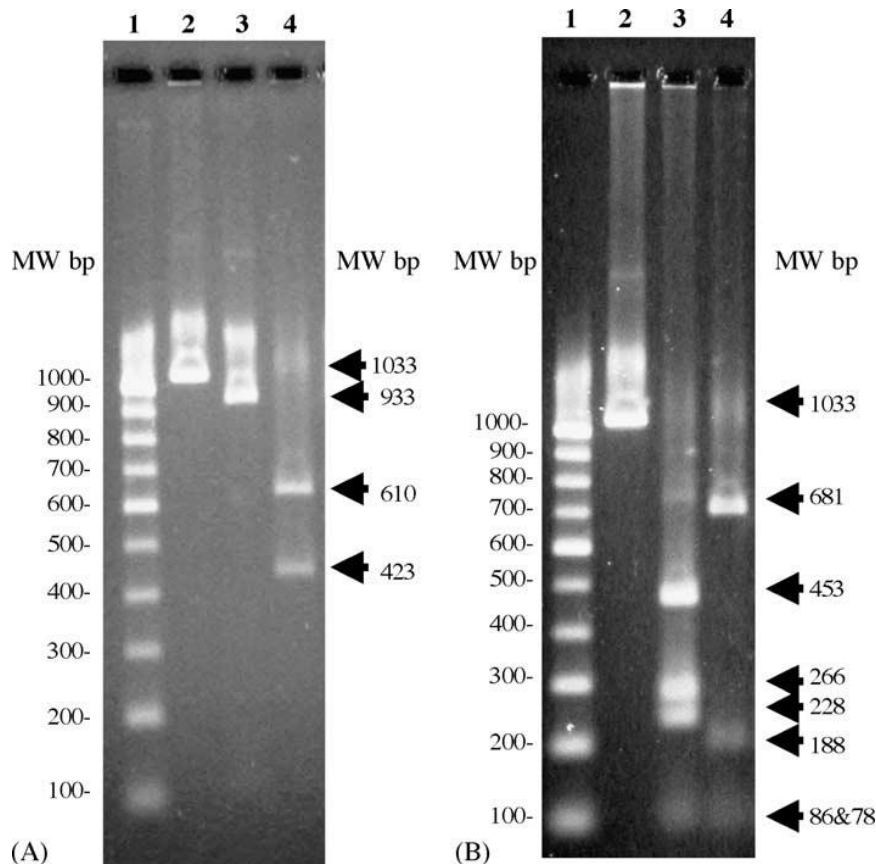


**Figure 2.16: RFLP profiles of PCR products containing mtcyt b sequences obtained from DNA of cashmere and wool fibre (Subramanian *et al.*, 2005).**

Figure 2.16 (A) contains RFLP profile of mtcyt b sequences restricted by BamH1 enzyme- lane 3 and 4: mtcyt b sequences of cashmere and wool, respectively, (B) is the RFLP profile of mtcyt b sequences restricted by Ssp1 enzyme – lane 3 and 4: mtcyt b sequences of cashmere and wool samples, respectively. Lanes 1 and 2 represent the DNA standard (100 bp ladder) and uncut PCR product, respectively. The restricted fragment profiles from wool and cashmere samples clearly showed that there is a difference in the two fibre types. It was concluded that this method differentiated well between wool and cashmere fibres and could qualitatively be applied to detect adulteration in animal fibre blends. Nevertheless, quantitative animal fibre blend analysis, using this technique, seemed impossible.

The DNA analysis of some animal fibre blends, such as cashmere/yak blends, remains a problem and poses a difficulty in the textile industry, due to the similarities of these

fibres. Wortmann *et al.*, (2007) noted that solely relying on DNA analysis may provide unsatisfactory results for the objective judgement of the extent of yak contamination in cashmere products, and recommended that the combination of DNA and microscopic techniques be applied for the objective analysis of animal fibres, especially for blend composition analysis purposes.

According to Phan *et al.*, (2008), amongst others, DNA analysis is one of the important methods in commercial analysis of cashmere and their blends. Even after a mild washing process of a garment, the amount of DNA within the fibres was reduced by a fair amount of nanograms which is one of the reasons why the DNA method got withdrawn from the customer service of DWI (Phan *et al.*, 2008).

Two approaches, qualitative and quantitative, involved in the DNA analyses, have been reported and documented by Yoshioka (2008). In both approaches, a first step involves the application of light microscopy to investigate the presence of fibres from non-animal sources, such as cotton, nylon, etc. Yoshioka (2008) concluded that the quantitative analysis of animal fibres, by the DNA method, was limited to wool and cashmere at the time, also mentioning he was busy developing a method for cashmere/yak quantitative analysis. Yoshioka (2008) noted that DNA analysis was superior to microscopic based methods, when it comes to objectivity.

There have been continuing developments and improvements in DNA analysis of animal fibres over the past few decades, with the more recent advances including the development of a method for the quick extraction of mitochondrial DNA from natural and processed animal fibres (Ji *et al.*, 2011). These researchers also designed two sets of TaqMan PCR primers and probes, which can specifically react to both goat and sheep DNA mitochondrial 12S ribosomal (rRNA) genes. This method could identify cashmere and wool fibres and provide the proportion of each fibre type in cashmere/wool blends. The most recent advances in DNA based identification of animal fibres, involves the development of a highly sensitive method, known as real-time PCR. This technique has also been found useful in the ivory industry in detecting and quantifying DNA from different animal species that have undergone processing (Wozney and Wilson, 2012).



Though the number of copies of mitochondrion tends to vary significantly between different breeds and even between some tissues of an individual, using this technique Tang *et al.*, (2013) showed that this (number of mitochondrion copies) has little effect on the quantification results in animal fibre blend composition analysis. These results indicated that the real-time PCR method can be applied to quantify each fibre type present in animal blends. The DNA method has recently been standardized by the International Organization for Standardization (ISO). The ISO 18074 (2015) method differentiates between wool, cashmere and yak fibres, but only allows qualitative analysis of these fibres in blends.

### **2.3.5 Amino Acid and Protein Analysis Based Methods**

#### **2.3.5.1 Electrophoresis**

Another technique, which has received considerable application in the textile industry, is that involving gel electrophoresis. Some of the applications of the electrophoretic method include the assessment of degradation of animal fibre proteins (Wilrich *et al.*, 1995). The amino acid composition is significantly different, particularly in the cystine and cysteic acid contents, for every animal fibre type, and Tucker *et al.*, (1988) pointed out that this may form the basis for the identification and classification of these fibres when in blends. Electrophoresis is one of the powerful techniques for the analysis of fractionated hair proteins, and some of electrophoretic methods, previously proposed for animal hair identification and classification, include one dimensional polyacrylamide gel electrophoresis, in the presence of sodium dodecyl sulphate (1D-SDS-PAGE) (Wortmann *et al.*, 1986; Laumen *et al.*, 1990), and two dimensional polyacrylamide electrophoresis, in the presence of sodium dodecyl sulphate (2D-SDS-PAGE) (Marshall, 1981; Stephani and Zahn, 1985).

A schematic diagram illustrating a steps-wise procedure involved in the isolation of proteins from keratin fibres is shown in Figure 2.17.

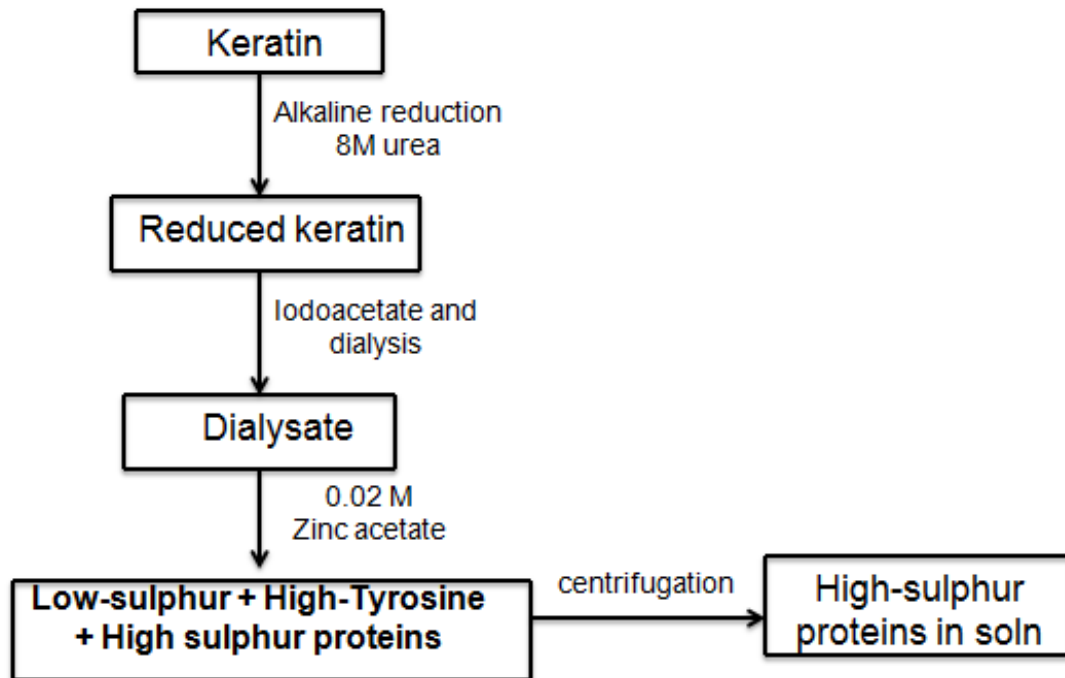


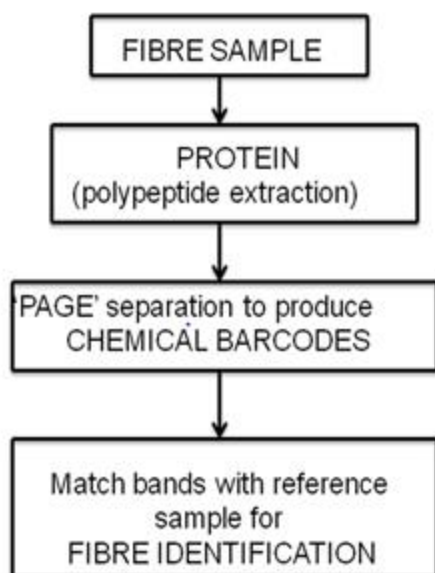
**Figure 2.17: Steps involved in the isolation of proteins from keratins (Marshall *et al.*, 1977).**

Darskus and Gillepsie (1971) applied electrophoretic and chromatographic methods to examine high-sulphur proteins from different breeds of sheep. Proteins from domestic goats were also examined. Differences in the proportions of the components of the patterns, from proteins of different sheep breeds, were observed, which the authors classified as an observation which could aid in distinguishing between different wool breeds. Marshall *et al.*, (1977) investigated the possible application of PAGE patterns in the analysis of high sulphur proteins, as a means for classifying different animal hairs. Among the animal fibres analysed, were sheep wool and goat hair, and these showed different electrophoretic patterns. Differences were also observed in the patterns of non-Peppin fine Merino sheep, housed and given identical diet.

The proteins of animal fibres are chemically dissolved and set apart by S-carboxymethylation (SCM), and fractionated on the basis of molecular weight or electric charge. As part of the textile industry investigation of new fibre testing techniques, in the year 1989 scientists in the British Textile Technology Group (BTTG), through the

merger of the Shirley Institute of Manchester and Wira Technology Group of Leeds, developed a chemically based method for the identification of different animal fibres (Anon, 1989).

Marshall *et al.*, (1984) demonstrated a possible use of the electrophoresis two-dimensional electrophoretic based method, because of its high resolution (Marshall and Gillespie, 1982), for distinguishing between wool and luxury fibres (mohair, camel hair and alpaca hair). The research was able to separate three groups of proteins, namely low-sulphur, high-sulphur and high-tyrosine, in different parts of the electrophoretic patterns, and noted that the results they obtained proved that 2D-PAGE can be useful for investigating the extent of adulteration and identifying the origin of the different fibres. Nevertheless, no quantitative analysis has been reported. Harsh chemical treatments were found to affect the electrophoretic patterns, and the researchers have concluded that further studies on the identification of speciality animal fibres, using electrophoresis, were still required. Bauters (1985) reported on the electrophoretic analysis of wool and mohair fibre proteins extracted by formic acid and aqueous propanol. The proteins extracted from the mohair fibres had the higher proportions of glycine and tyrosine compared to the protein extracts from the wool. The cysteine contents of these two fibre types were significantly different, with wool having the higher content. The research concluded that the proportions of the extracted proteins, as well as the glycine, tyrosine and cystine contents, were different for wool and mohair and could be species specific. The British Textile Technology Group represented their chemically based method of fibre identification as shown in Figure 2.18.



*Schematic representation of speciality fibre identification procedure*

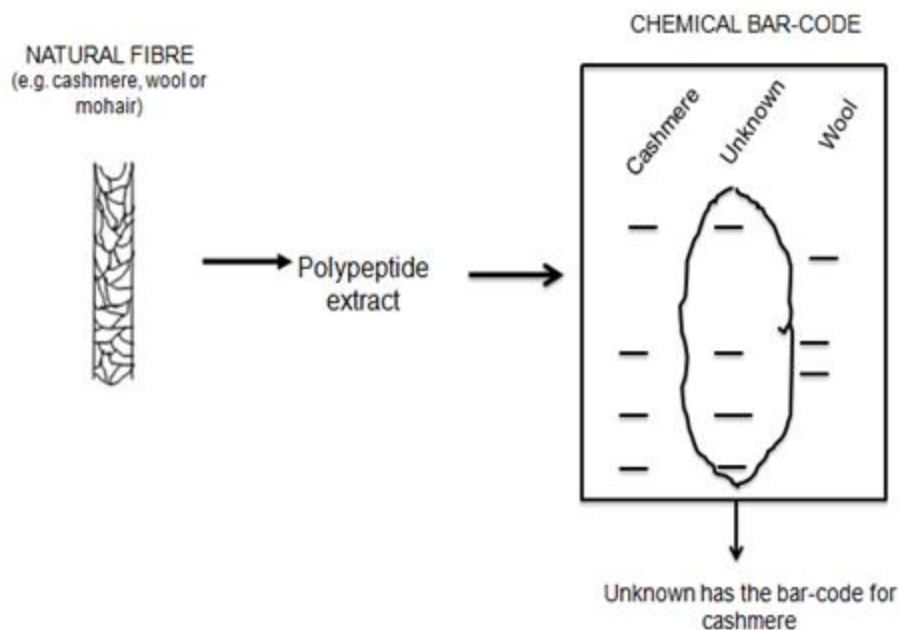


**Figure 2.18: Schematic presentation of animal fibre identification and classification procedure (Anon, 1989).**

A possible fibre identification method, based upon differences in the molecular weights of polypeptides dissolved from different animal fibres, was investigated by Speakman and Horn (1987). The polypeptides (0.2 g) of Lincoln wool, Merino wool, mohair, Alpaca

and cashmere fibres, were dissolved by treating the samples for 18 hr at room temperature in 100 ml of a solution containing 0.2 M mercaptoethanol and 0.1 M disodium hydrogen phosphate, adjusted to pH 11. The dissolved polypeptides were precipitated by acidifying the solutions, re-dissolved, and examined by polyacrylamide-gel electrophoresis (PAGE), in the presence of sodium dodecyl sulphate (SDS), on homogeneous 15% slab gels, Coomassie blue staining being used. The polypeptide extracts of the low sulphur proteins were found very useful in the identification of the individual fibre types covered in the investigation. The polypeptide extracts of the wool fibres had higher molecular weight values, and based on these values, wool fibres could clearly be distinguished from mohair, alpaca and cashmere fibres. Differentiating between fibres from the same breed of animals (e.g. Merino and Lincoln wools) was found to be difficult, because of the overlap in molecular weights of the polypeptides dissolved from these fibres. This difficulty was also experienced in distinguishing between mohair and alpaca. Presumably this method would not work very well for animal fibre blends, particularly unknown blends.

Llama fibres have frequently been substituted for mohair due to their visual similarities, the same applying for cashmere and yak. Laumen *et al.*, (1990) investigated the possibility of differentiating between these fibres by 1D-SDS-PAGE analysis. Figure 2.19 shows electrophoretical patterns published by Laumen *et al.*, (1990):

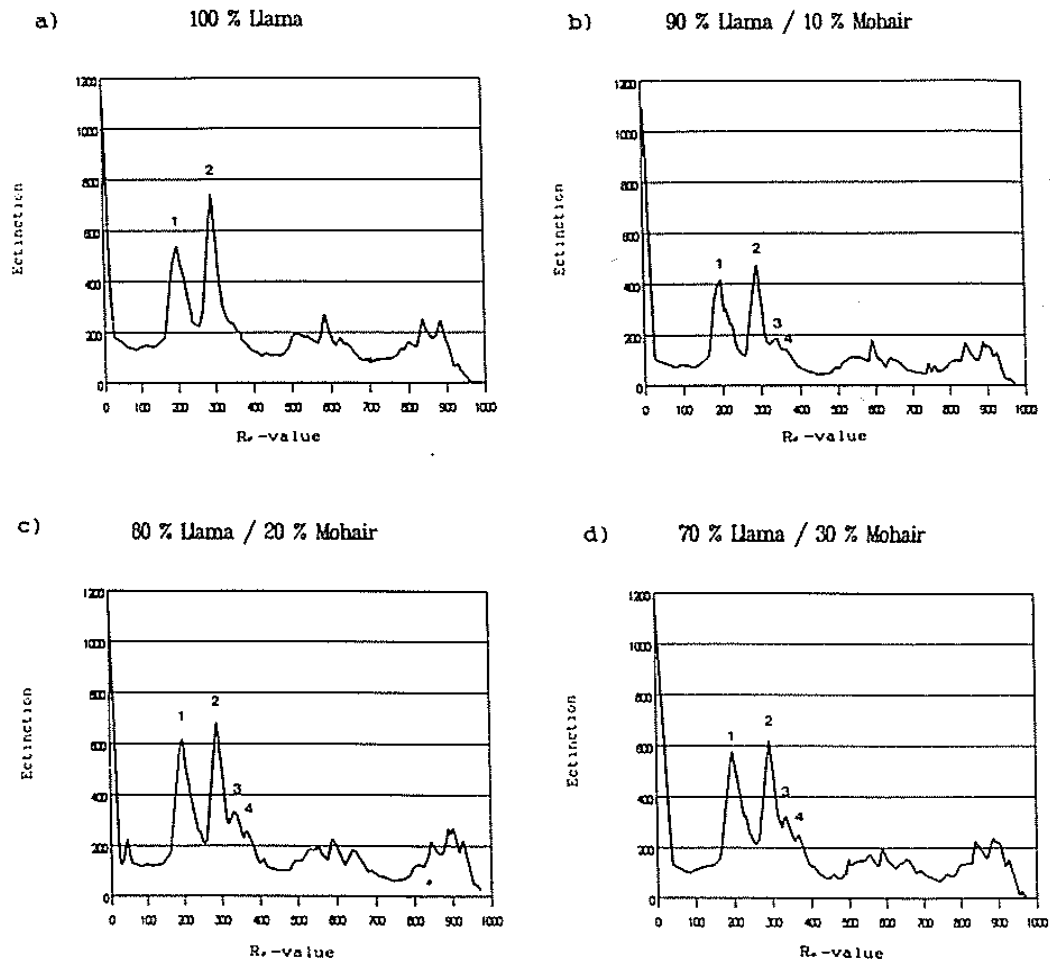


**Figure 2.19: Densitometric traces of different llama/mohair (Laumen *et al.*, 1990).**

Laumen *et al.*, (1990) based their identification on the intensities of peaks 3 and 4, noting that these peaks increased with the increasing proportion of mohair. Rane and Barve (2010) also investigated the possibility of animal fibre identification using SDS PAGE. These researchers applied a different extraction method to those previously reported (Ley and Crewther, 1980; Sagar *et al.*, 1990 and Marshall *et al.*, 1986). Their method enabled 75% of the proteins to be extracted, which was considered an improvement compared to the previous extraction methods. It was, however, concluded that SDS PAGE analysis cannot distinguish between different types of animal fibres present in blends.

Wortmann *et al.*, (2010) reported on a fibre identification method, using SDS Gel electrophoresis, to distinguish between shahtoosh and fine cashmere fibres. The method successfully distinguished between the two fibre types even in the chemically processed state, and they concluded that a combination of their method and SEM could offer an unambiguous means of identifying shahtoosh and cashmere fibres.

### **2.3.5.2 Chromatography**

Corfield and Robson (1955) were among the first researchers to explore the amino acid composition of wool fibres using chromatographic techniques. These researchers supported the contention that wool is not a homogeneous protein, stating that differences in amino acid composition should be expected from different wool samples. Other early applications of chromatographic techniques, in animal fibre analysis, include protein fractionation of reduced Merino wool by Joubert and Burns (1967). Rivett *et al.*, (1988) described, and discussed, fibre identification methods based on the application of High-Performance Liquid Chromatography (HPLC) and Gas Chromatography (GC). Wool and cashmere samples were supplied by the Wool Research Organization of New Zealand (WRONZ) and Dawsons International in Scotland, respectively, for the analysis. These fibre samples were cleaned by sequential extraction with *t*-butanol and heptane, as described by Leeder *et al.*, (1983), after which the internal lipids were collected by soxhlet extraction, using chloroform/methanol azeotrope, as described by Gale *et al.*, (1987). Extracts from total digests were obtained by hydrolyzing the fibre with 2M potassium hydroxide at 60°C. The lipids were obtained by first acidifying the hydrolysate and then extracting with chloroform. The results showed that the major sterols were cholesterol and desmosterol in the internal lipids of wool and cashmere fibres, and that the ratio of cholesterol/desmosterol could form a basis for wool and goat fibre identification. The amino acid analysis of different animal fibres, including mohair and wool, has also previously been investigated using HPLC and Table 2.7 presents results obtained in various studies for the amino acid composition of different animal fibres using different chromatographic techniques (Crewther *et al.*, 1965).

Slight, and statistically insignificant, differences, in the amino acid composition between different sheep breeds and species, were found. Sterol and fatty acid compositions, from wools of different sheep breeds, and from different climatic regions, have also been investigated for fibre identification purposes by Logan *et al.*, (1989), who concluded that sterol and fatty compositions can be of additional value in the animal fibre classification of existing methods.

Using high-performance liquid chromatography (HPLC), Tucker *et al.*, (1990) proposed the use of external and internal lipids as identification and classification features for natural animal fibres. They concluded that the ratios of certain fatty acids, such as palmitic/linoleic or stearic/linoleic acids, could be useful for distinguishing between speciality fibres, such as cashmere and cashgora, and mohair fibres.

An automatic animal fibre identification method, based on the analysis of the profile of internal fatty acid, using gas chromatography, was proposed by Gochel *et al.*, (1995). More than 130 fine samples of different origins (wool, alpaca, cashmere, angora, mohair, yak, cashgora and camel hair) were analysed. They found that the fatty acid proportions could be used to identify and distinguish between different animal hairs. Some of the fatty acids were found in certain protein fibre types and not in others, and these researchers observed that this could also form a basis for classification of animal fibres. However, no information on blend composition analysis was reported.



Table 2.7: Amino acid composition of different protein fibres (Tucker *et al.*, 1990).

Amino acid	Merino 70's <sup>a</sup>		Merino 64's <sup>a</sup>		Corriedale 56's <sup>a</sup>		Lincoln <sup>b</sup>		Mohair <sup>c</sup>		Human hair <sup>c</sup>		Range of variation (% of lowest value)
	I <sup>d</sup>	II <sup>e</sup>	I	II	I	II	I	II	I	II	I	II	
Alanine	3.51	415	3.51	417	4.37	524	4.16	493	3.80	452	2.93	345	49
Ammonia	7.92	937	7.46	887	9.27	1112	7.89	936	6.68	793	6.76	797	26
Arginine	19.35	575	20.32	602	18.21	546	20.00	592	16.52	490	16.15	476	41
Aspartic acid	4.68	555	4.24	503	4.86	584	4.96	588	4.58	544	3.52	415	39
Half-cystine	6.50	768	7.93	943	6.80	817	7.18	852	6.81	808	12.07	1422	86
Glutamic acid	8.54	1011	8.58	1020	9.69	1160	8.79	1040	8.89	1055	7.58	885	28
Glycine	6.60	781	5.80	688	6.40	769	4.80	568	5.43	645	4.34	512	52
Histidine	1.48	59	1.46	58	1.59	63	1.65	65	1.76	70	1.58	62	21
Isoleucine	2.13	252	1.97	234	2.38	286	2.48	294	2.29	272	1.80	212	38
Leucine	5.37	635	4.90	583	5.51	659	5.93	703	5.66	672	3.94	464	51
Lysine	3.19	189	3.25	193	3.72	224	4.46	264	3.75	223	3.02	178	48
Methionine	0.37	44	0.31	37	0.37	44	0.37	44	—	—	—	—	—
Phenylalanine	2.28	270	1.75	208	2.35	284	1.88	234	2.06	245	1.21	143	94
Proline	5.12	605	5.33	633	5.52	662	4.50	533	4.68	557	6.39	753	42
Serine	8.63	1020	7.25	860	7.71	925	6.33	750	6.28	745	7.22	851	37
Threonine	4.12	487	4.61	547	4.84	582	4.23	501	4.06	482	4.58	542	19
Tryptophan	1.38	163	1.73	205	1.80	214	—	—	—	—	—	—	—
Tyrosine	3.09	366	2.97	353	3.11	373	2.00	237	1.64	194	1.07	126	191
Valine	3.56	422	3.57	423	4.50	540	4.29	508	5.59	663	4.16	490	57
Nitrogen (%)	16.57		16.62		16.80		16.58		16.60		16.50		

<sup>a</sup> From Simmonds (1955).

<sup>b</sup> From Thompson and O'Donnell (unpublished data, 1962).

<sup>c</sup> From Simmonds (1958b).

<sup>d</sup> Throughout this table the values designated in column I are given as % total N.

<sup>e</sup> Throughout this table the values designated in column II are given as  $\mu$ mole per gram.

### 2.3.6 Vibrational Spectroscopic Techniques

Over the past three decades, a great deal of research in the textile industry, particularly the speciality fibre industry, has focused on the identification and classification of animal fibres but the textile industry still seeks methods to do so unambiguously, unequivocally, and quantitatively particularly when in blends. With the use of vibrational spectroscopy techniques, it is possible to examine the protein-polypeptide structure (Panayiotou, 2004). These techniques include Infrared (IR) and Raman spectroscopies, certain studies investigating their suitability for the identification of textile fibres. These two techniques (IR and Raman spectroscopy) provide complementary chemical information of materials, and a combination of the methods can provide a large amount of information about the proteins and their respective amino acids. The increased availability of these techniques, particularly IR and Raman microscopes, is believed to have largely influenced their increased application for the investigation of biological samples (Chalmers *et al.*, 2012). Fourier Transform Infrared (FTIR) and Raman spectroscopy can provide considerable analytical data in a very short period, and the problem of handling such extensive amounts of data can be minimized by the application of special data processing methods, such as Chemometrics (Panayiotou, 2004; Zoccola, 2013) and artificial neural networks (Jasper and Kovacs, 1994). Most of the spectral information, gathered from biological samples (such as wool) is due to the protein structure and the small changes in the position and the intensity of the chemical bands (Rintoul *et al.*, 2000). Vibrational spectroscopic techniques have also been used in the evaluation of the effects of proteolytic enzymes on the surface keratin proteins. Different structural conformations of keratin polymer were observed after wool enzymatic treatments in different buffer solutions (Wojciechowska *et al.*, 2004). Some of the research, involving vibrational spectroscopic techniques, is discussed in the following section. It is important to mention that although the main focus of this research is on the application of these techniques in animal fibre studies, such as wool and mohair, reference is also made to human hair due to the great similarities in their chemical and morphological profiles.

### **2.3.6.1 Infrared Spectroscopy**

Another well established and recognized technique in qualitative, and occasionally quantitative, analysis of organic materials, is that employing infrared spectroscopy, particularly in the mid-infrared (MIR) region. This technique offers much to the scientist, such as minimal sample preparation, its non-destructive nature, speed, small sample size and the detailed information about the different types of bonds present in the sample. IR spectroscopy exploits the fact that molecules rotate and vibrate at specific frequencies, depending on their discrete energy levels (Houck, 2009). The IR spectrum is collected by exposing the sample to infrared radiation, over a range of energies within the IR region. IR spectroscopic methods have been widely adopted, especially in the forensic examination of biological materials and in hair research (Pande, 1994), mainly due to its speed and non-destructive nature. Nevertheless, this technique has not been widely applied for characterization of animal fibres due mainly to the fact that these materials produce diffuse and poorly defined spectra. The development of Fourier Transform Infrared (FTIR) instruments, together with IR microscopes, has opened up the possibility for IR analysis of single fibres. FTIR spectroscopy involves a measurement of wavelength and intensity of the absorption of IR radiation by the analyte. The IR spectral data of high polymers are usually interpreted in terms of the vibrations of a structural repeat unit. The vibrations of the polypeptide and protein repeat units give rise to nine characteristic IR absorption bands, namely, amide A, B, and amide I–VII. Of these amide bands, I and II are the two most dominant vibrational bands of the protein backbone. Amide vibrations are characteristic of the peptide bond. The most sensitive spectral region to the protein secondary structural components is the amide I band ( $1700\text{--}1600\text{ cm}^{-1}$ ), which is due almost entirely to the C=O stretch vibrations of the peptide linkages. Therefore, a variation in the composition of fibre peptides should be reflected in the amide bands, these being readily studied through vibrational spectroscopic methods, such as FTIR and Raman spectroscopy. Because the amide II band appears as a very weak feature in Raman spectra of keratin materials, the FTIR spectroscopic analysis was adopted for the analysis of the amide bands.

The initial reports of the applications of IR spectroscopy in studies involving keratin fibres, such as wool and human hair, includes those by Weston (1955), Stein and Guarnacio (1959), Robbins (1967). The IR bands at 1040, 1070, 1125 and 1177  $\text{cm}^{-1}$  were found to be the oxidation products of amino acid cystine to cysteic acid in wool and hair fibres (Signori and Lewis, 1997; Jones *et al.*, 1998). Strassburger (1985) applied FTIR to study the quantitative oxidative damage in human hair after chemical treatment, with the amide III and  $\text{CH}_2$  &  $\text{CH}_3$  bending modes used as the internal standards to which the cysteic acid band was normalized. Brenner *et al.*, (1985) observed that the position of this sulphonic acid band varied from 1042 to 1046  $\text{cm}^{-1}$  and concluded that it could be used to distinguish chemically treated fibres from the untreated.

Some of the first chemical band assignments of the infrared spectroscopic keratin fibre spectra were made by Bendit (1966). Shah and Gandhi (1968) investigated the spectral changes in the IR spectra of Merino wool fibres after 0.4 % and 1% periodic acid treatments, respectively. These researchers noted that there were no changes in chemical bands, especially those that define a typical natural animal fibre IR spectrum, namely the amide I, amide II and the amide III bands. Spectral features that had not been identified prior their work, were observed at 1370  $\text{cm}^{-1}$  and 1040  $\text{cm}^{-1}$ . These bands were presumed to be due to the sulphoxide groups and  $-\text{SO}_3-\dots-\text{H}_3\text{N}-$  or  $-\text{SO}_2-\text{NH}$ , respectively.

The importance of Infrared spectroscopic methods has also been examined for their application in the quantitative analysis of some binary mixtures of fibres, including wool-terylene of unknown blend compositions (Clark and Hickie, 1975). Two methods were used in their study, namely the absorbance and the relative-absorbance method. In the absorbance method, the absorbance of the band was plotted against the fibre content or concentration, while in the relative absorbance method, the ratio of the absorbencies from two bands, one from each component of the binary mixture, was plotted against the fibre content. The absorption of chemical bands, selected for wool and Terylene, were the amide I band, at 1615  $\text{cm}^{-1}$ , for wool, and the  $=\text{C}-\text{O}$  stretching band, at 1225  $\text{cm}^{-1}$ , for Terylene. The choice of bands was such that the band was exclusively from

the fibre component of interest, with no contribution from the other component in the blend. The absorbance method was found to provide satisfactory results, yielding straight line relationships, the absorbance of the amide I chemical band increasing with the wool content in wool/Terylene fibre blend. Clark and Hickie (1975) concluded that the technique may not be applicable to the analysis of fibres belonging to the same generic group, such as wool and mohair, since they will have these share similar absorption spectral information, making it impossible to distinguish between them.

The possibility and applicability of near-infrared photo-acoustic spectroscopy have also been investigated for distinguishing between wool and polyester fabrics, as well as the analysis of wool/polyester blend fabrics (Davidson and King, 1983). These researchers concluded that the photo-acoustic spectroscopy of the near infrared region has a potential for identifying and classifying between wool, polyester and cotton textile materials. It was suggested that techniques, identifying the secondary structure of proteins, would be useful for distinguishing between animal fibres, such as silk and wool.

Based upon their work on wool, cashmere and silk fibres, Jasper and Kovacs (1994) proposed the application of a non-destructive technique, involving near infrared (NIR) spectroscopy and neural networks. They concluded that identification, using this technique, was rapid and fairly reliable.

Wang *et al.*, (2005) reported on the results of various techniques, namely FTIR microscopic analysis, differential scanning calorimeter (DSC) and thermogravimetric analysis (TGA), for differentiating between different types of animal fibres, including cashmere and fine wool from merino sheep. The FTIR analysis showed that animal fibres could be differentiated by using the position of the peak near  $1040\text{ cm}^{-1}$ . This chemical band is due to the S-O stretching cysteic acid residues and appeared stronger at  $1019\text{ cm}^{-1}$  in the Chinese cashmere spectrum, while a weak absorption band was observed at  $1079\text{ cm}^{-1}$  in the Australian cashmere and wool spectra. Žemaitytė *et al.*, (2006) used FTIR for identifying wool from different sheep breeds and different regions, camel hair, llama and some goat hair. These researchers noted that white goat hair

could be distinguished from the rest of the fibres by the absence of the peak at around  $3100\text{ cm}^{-1}$ . A method, based on the application of visible and near infrared spectroscopy (Vis/NIRs), has also been investigated for the rapid and reliable identification and classification of animal fibres (Wu *et al.*, 2008). This investigation involved developing a model using principal component analysis (PCA) and artificial neural networks (ANN). Wu *et al.*, (2008) reported that the model they built was able to discriminate cashmere from wool. They concluded, however, that the method was only applicable to the analysis of pure animal fibre samples and not for blends. Liu *et al.*, (2008) reported on the investigation they conducted on the possible identification of wool and cashmere using FTIR spectroscopy. The accompanying Table 2.8 summarizes their results. The FTIR chemical bands in the table are typical of all keratin fibres.

**Table 2.8: Keratin fibre FTIR chemical bands (Liu *et al.*, 2008).**

Spectral region (cm <sup>-1</sup> )	Chemical bands found
998-1100	S-O vibration and C-H bend
1210-1290	C-O stretching
1361-1470	Amide III, C-N stretch
1500-1572	Amide II, N-H bend
1600-1700	Amide I, C=O stretch
1720-1750	Esters, C-C(O)-OR
2850-3000	=C-H, C-H

Based on the peak heights or intensities of the amide I and amide II bands, Liu *et al.*, (2008) could differentiate between cashmere samples from different countries. These researchers claimed that the C-H, C-N and C-O stretching vibrations may shift, and the shape of the bands may differ, according to the type of animal fibre, and that these features could be used to distinguish different animal fibres. Zhou and Xiao (2008) also claimed that the only spectral feature that could distinguish between cashmere from different origins and some wool samples was the intensities of the S-O stretch which is a component of cysteic acid residues (R-SO<sub>3</sub>). A typical animal fibre FTIR spectra is shown in Figure 2.20.

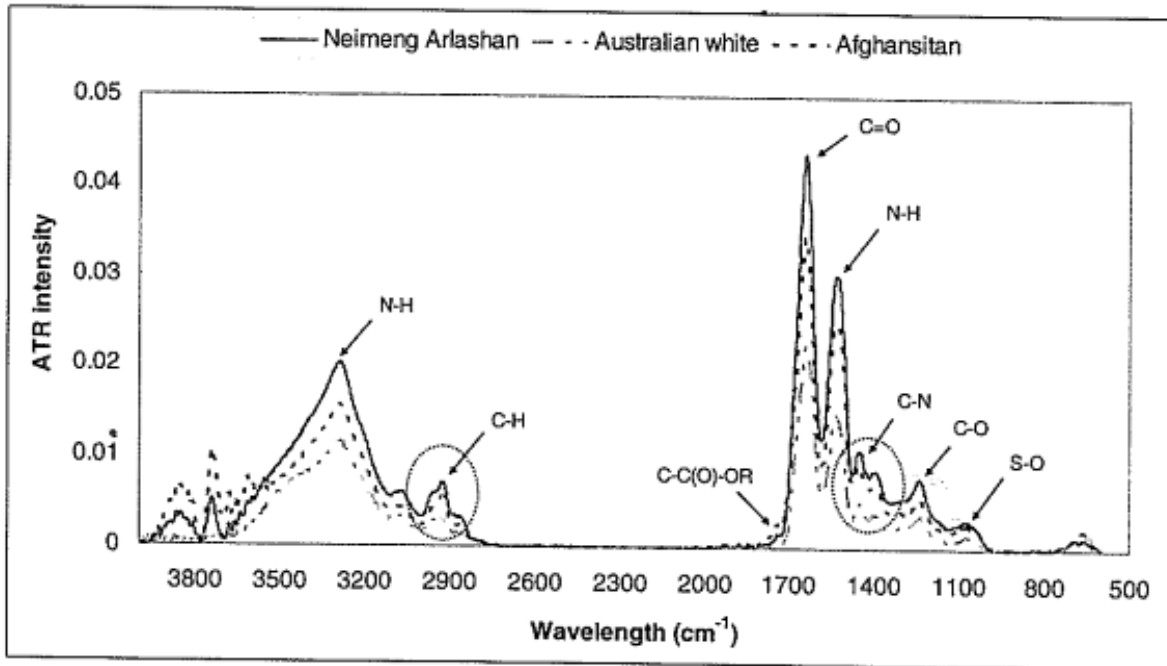


**Figure 2.20: Typical FTIR spectra of cashmere fibres (Liu *et al.*, 2008).**

Near Infrared spectroscopy (NIRS) is one of the spectroscopic analytical methods that have received wide application in studying textile materials, due to their ease of operation and some other advantages. Burns and Ciurczak (2001) reviewed some of the NIRS methods applied in the characterization of textile materials. Yao *et al.*, (2008) made use of FTIR to monitor changes in the wool secondary structure after stretching, in a process used to produce slenderized wool. This study involved treating the wool fibres with a reducing agent,  $\text{NaHSO}_3$ , to break the disulphide bonds and facilitate stretching and fibre deformation. The authors observed shifts in positions of the amide I and amide II chemical bands after such stretching, these being associated with the transformation of the secondary structure, from an  $\alpha$ -helix to a  $\beta$ -pleated-sheet conformation.

McGregor *et al.* (2011; 2017) investigated the possible application of FTIR for identifying different animal fibres, including wool and cashmere from different origins. He found that, even though the intensities of some FTIR chemical bands could significantly distinguish between wool and cashmere fibres, there was a huge overlap which made



the identification of the fibre origin very difficult. He concluded that FTIR did not hold promise as a technique that could be applied in distinguishing between natural animal fibres, particularly wool and cashmere. Liu *et al.*, (2013) noted that the Vis/NIRs can be applied in the identification of keratin fibres, particularly wool and cashmere. However, no quantitative results were reported in their study.

### **2.3.6.2 Raman Spectroscopy**

Raman spectroscopy is another technique that has been applied in the analysis of textile materials. Much like infrared spectroscopy, this technique, analyses vibrational and rotational modes of the sample molecules (Houck, 2009). Though both IR and Raman spectroscopy are vibrational spectroscopies and provide similar information, Raman spectroscopy is often preferred for studying most organic polymers. Many organic polymers possess a highly polarizable backbone and do not have large dipole moments, because of the repeated identical units which cancel adjacent dipoles, and because of this, Raman intensities, associated with the backbone vibrations, are often intense, whereas these appear to be weak in the IR spectra. The fact that most of the very valuable properties of polymeric fibres and films are controlled by the orientation of the polymer backbone, makes Raman spectroscopy more suitable, than IR spectroscopy, for the analysis of such materials (Michielsen, 2001). Another advantage of Raman spectroscopy is that it provides information about the -SS- groups, through oxidation and reduction, which cannot be obtained using IR spectroscopy, and has been valuable in studying changes in the secondary structure of various proteins (Lippert *et al.*, 1975; Mikhonin *et al.*, 2004).

A major challenge, encountered in conventional Raman instruments, is that of fluorescence, which can totally swamp the weak Raman signal, this being particularly common in the analysis of biological materials, such as keratin fibres (wool, mohair, etc.). The development of Fourier Transform (FT) Raman instruments, using near infrared excitation, has made the analysis of molecules and biological materials possible without fluorescence and with a minimum possibility of sample degradation associated with the high laser powers necessary for sample illumination. This technique has also

received wide application in the hair industry, in determining the chemical and structural changes associated with hair treatments (Akhtar *et al.*, 1997). One of the aspects that has gained Raman spectroscopy its popularity, especially in studying organic samples, is its insensitivity to hydration state of these samples. A wide range of studies, covering the application of Raman spectroscopy in the analysis of different types of fibres, for forensic purposes, has been reviewed by Fredericks (2012).

A significant factor, influencing the price of greasy wool, is its wax content i.e. the greasy secretion of the sebaceous glands of the sheep, generally referred to as wool grease. Church *et al.*, (1994) investigated the possible application of Raman spectroscopy for determining the wax content of raw wool samples, solvent extraction and near infrared analysis (NIRA) traditionally being applied for this purpose. These researchers concluded that the Raman based method offered an improved accuracy, and that it was rapid. Raman spectroscopy is also valuable for determining the degradation of keratin fibres (Church *et al.*, 1996; Wilson *et al.*, 1999). Liu and Yu (2005) applied Raman spectroscopy and tensile tests to determine the changes induced by stretching merino wool at different stretching ratios, of up to 110 %. Figure 2.21 shows some of the Raman spectra which they obtained.

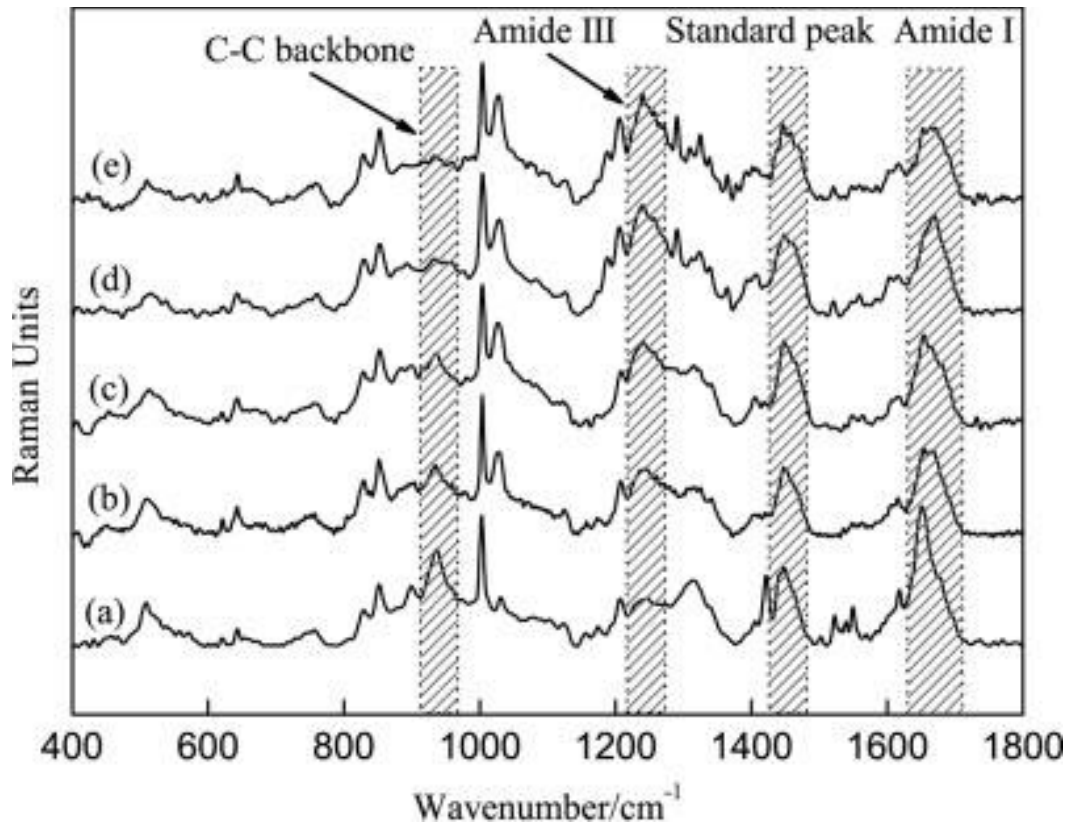


**Figure 2.21: Raman spectra of wool fibers with different stretch ratios: (a) 0, (b) 30, (c) 50, (d) 80, and (e) 110% (Liu and Yu, 2005).**

Liu and Yu (2005) focused on the amide I, amide III and the C-C skeletal vibration regions. Other chemical bands of interest were the S-S and the C-S bond vibration spectral regions. They found that the S-S chemical band at  $513\text{ cm}^{-1}$  gradually decreased with an increase in the ratio of stretching. Their results showed that stretching transformed the secondary structure of wool keratin from the  $\alpha$ -helix into the  $\beta$ -pleated-sheet structural conformation.

Carter *et al.*, (1994) investigated the application of Fourier Transform (FT) Raman spectroscopy in the analysis of wool fibres, which had presented a problem before, because of the fact that wool fluoresces at exposure to visible or UV radiation. A great advantage of the development of the FT Raman spectroscopic systems was the reduction of such fluorescence. Carter *et al.*, (1994) investigated the stability of wool

fibres, at different laser powers, and the optimum conditions for acquiring good wool Raman spectra, their results being summarized in Figure 2.22:

Carter *et al.*, (1994) observed no damage to the wool fibre as the laser power was increased up to 400 mW. An improvement in the quality of spectra was observed with an increase in the laser power, a decrease in the signal-to-noise ratio being observed at laser powers below 200 mW. A 300 mW laser power and 1000 scans were found to be optimum.

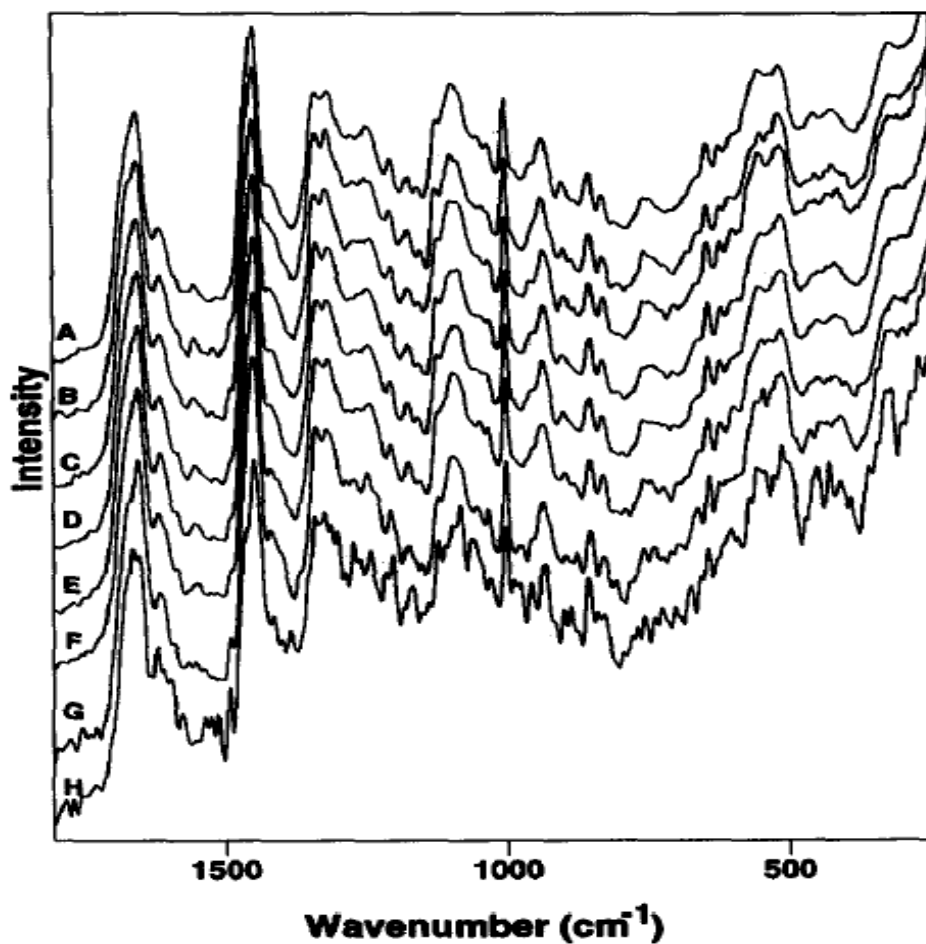


Figure 2.22: Effect of laser power on the FT Raman spectrum of raw Merino wool (A) 400 mW, (B) 350 mW, (C) 300 mW, (D) 250 mW, (E) 200 mW, (F) 150 mW, (G) 100 mW and (H) 50 mW (Carter *et al.*, 1994).

Chemical band assignments, of the Raman-active normal modes of vibrations for wool above the  $1660\text{ cm}^{-1}$  spectral region, were published for the first time by Carter *et al.*, (1994). These include the strong broad band centred at  $3302\text{ cm}^{-1}$  and the sharp chemical band of moderate intensity at  $3062\text{ cm}^{-1}$ , assigned to the N-H stretching vibration (amide A) and the first overtone of the C-H bending vibration (Amide B), respectively. A typical wool Raman spectrum is shown in Figure 2.23.

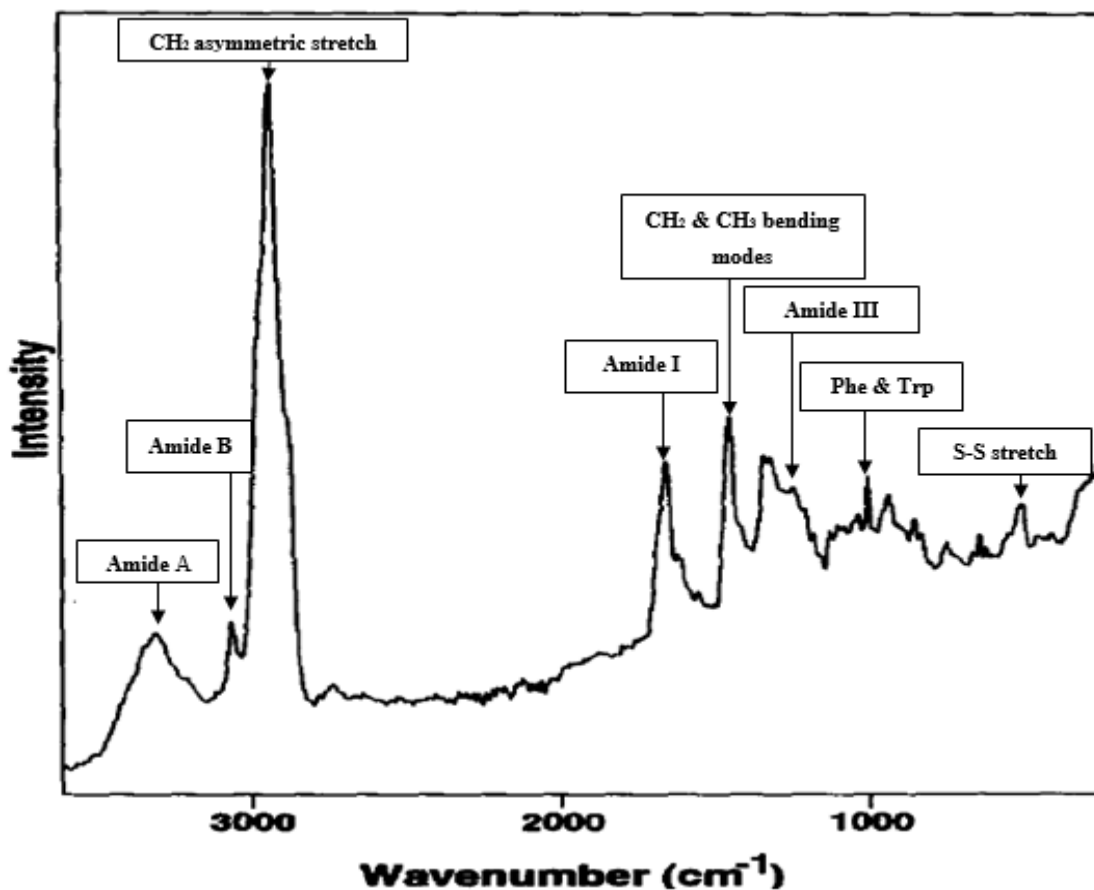


Figure 2.23: Typical FT Raman spectrum of untreated wool (Carter *et al.*, 1994).

The authors detailed a comparison of the conventional Raman spectrum obtained in studies before, in the spectral region below  $1600\text{ cm}^{-1}$ , with that obtained using the FT-Raman system, one of the differences being the position of the amide I band,  $1653\text{ cm}^{-1}$ , previously found in the  $1658\text{ cm}^{-1}$  region.

Jurdana *et al.*, (1995) made use of the confocal laser Raman microprobe in studying wool, human hair and feathers. The main aim of their work was to acquire spectra from various keratin fibres, and to investigate the potential of laser Raman spectroscopy in wool textile research. They also investigated the existence of differences in the wool cuticle and cortex spectra and possible applicability of the confocal Raman microprobe technique for studying the chemical modification over a single wool fibre. In their study, the spectral region between 1740 and 1230  $\text{cm}^{-1}$  was selected, and it is in this region where the characteristic keratin bands, namely the strong amide I, amide III and the C-H bending, occur. The amide III region is conformation sensitive and slight differences in intensities between the cuticle and cortical cell spectra were observed in this chemical band, with the cuticle spectra having higher intensities than the cortex. This was attributed to the cuticle of the wool fibres containing a higher proportion of the amorphous phase. A small shift in the amide band of the cuticle to the cortex region was found to be amongst the minor distinguishing features between the Raman spectra of the cuticle and cortex. A summary of band assignments, and their positions, is given in Table 2.9:

**Table 2.9: Raman band assignments of wool and human hair (Jurdana *et al.*, 1994).**

Wavenumber ( $\text{cm}^{-1}$ )			
Merino wool	Human hair		Vibrational assignments
	Cuticle	Cortex	
1656	1667	1657	Amide I band
1615	1616	1615	tyrosine/tryptophan
1552	1553	1553	Amide II (weak)
1447	1447	1448	$\text{CH}_2$ and $\text{CH}_3$ bending mode
1339	1339	1337	CH bend tryptophan
1316	1303	1312	$\text{C}\alpha\text{H}$ bend
1246	1246	1248	Amide III (disordered)

Jurdana *et al.*, (1995) concluded that the laser-based Raman microprobe/confocal microscope system was a useful technique for identifying minor differences in the protein composition of the cuticle and cortex of wool and human hair. They also applied a procedure, described elsewhere (Lippert *et al.*, 1975), to determine the secondary structure of different keratin fibres, including merino and Lincoln wool. This method is based on the ratios of the relative intensities of the  $1246\text{ cm}^{-1}$  and the  $\text{CH}_2$  and  $\text{CH}_3$  bending mode (near  $1447\text{ cm}^{-1}$ ), these ratios not being different for the merino and Lincoln wool samples, as was expected.

Using the Fourier Transform Raman (FTR) spectroscopy, Church *et al.*, (1997) investigated the chemical changes in the protein structure, especially the secondary structure, of the cuticle and cortical cells of merino wool fibres. The experimental procedure involved in the extraction of cuticle and cortical cells from the wool fibres, Figure 2.24 showing SEM micrographs of the cortical and cuticle cell fragments.

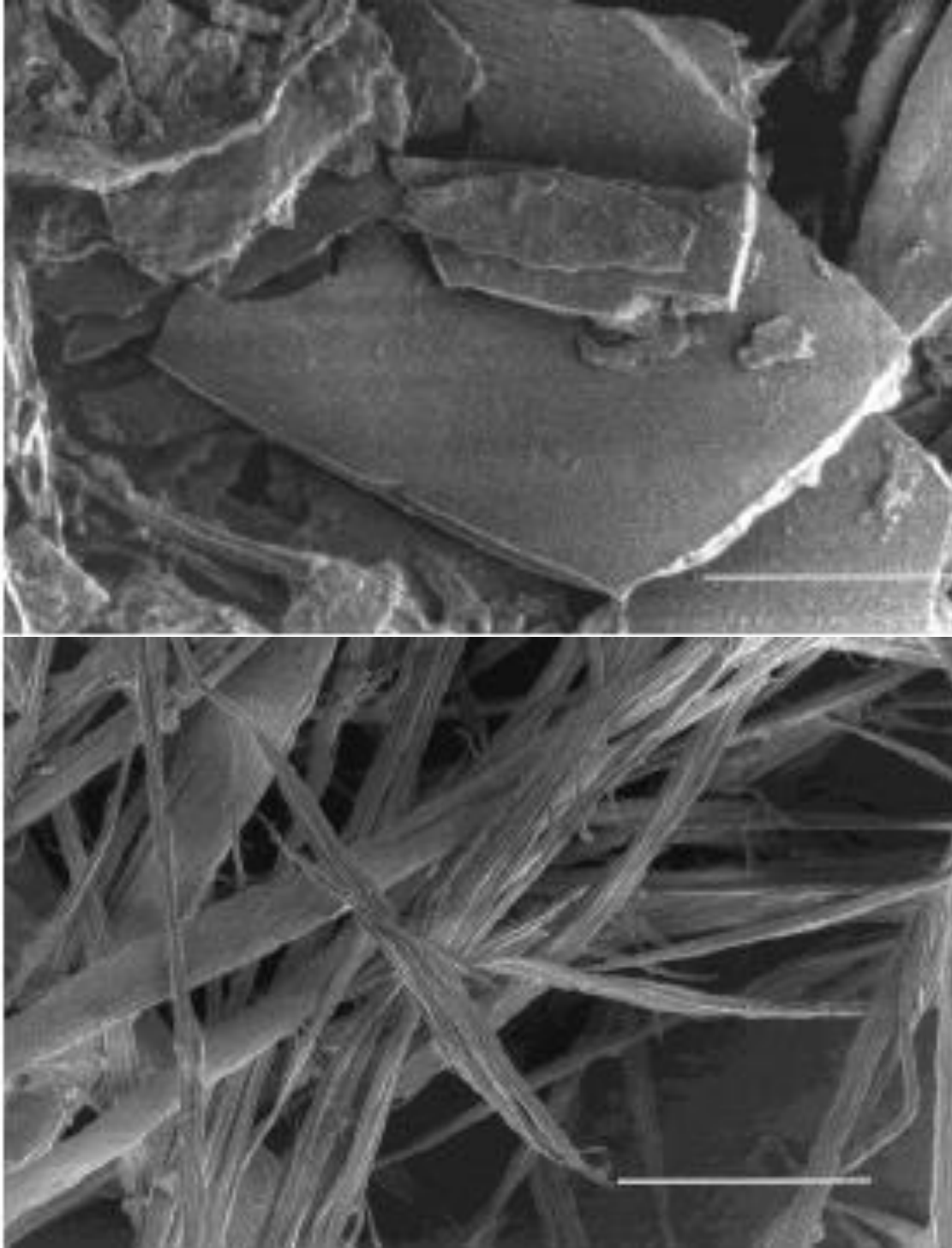


**Figure 2.24: SEM micrographs of cuticle cell fragments (top) and cortical cells (bottom) isolated from the Merino wool fibre (Church *et al.*, 1997).**



Church *et al.*, (1997) collected their Raman spectra, by means of a Bruker RFS-100 FT Raman spectrometer, equipped with an Atlas Nd: YAG laser. Some of the samples were charred at laser powers greater than 100 mW. A spectral resolution of  $4\text{ cm}^{-1}$ , and the averaging of five spectra and 1024 scans, were found to improve the signal to noise ratio. The selected spectral region was between  $1800$  and  $300\text{ cm}^{-1}$ . Similar spectra were observed for the cuticle and cortical cells and the whole fibre (see Figure 2.25). The main characterizing features of an animal fibre Raman spectrum include the amide I (around  $1670\text{ cm}^{-1}$ ), C-H bending (around  $1450\text{ cm}^{-1}$ ), Amide III (around  $1270\text{ cm}^{-1}$ ) and the S-S stretching (around  $512\text{ cm}^{-1}$ ). Some of the observed differences, between the cuticle and cortical cells spectra, were in the shape and the position of the peak maxima of the amide I band.

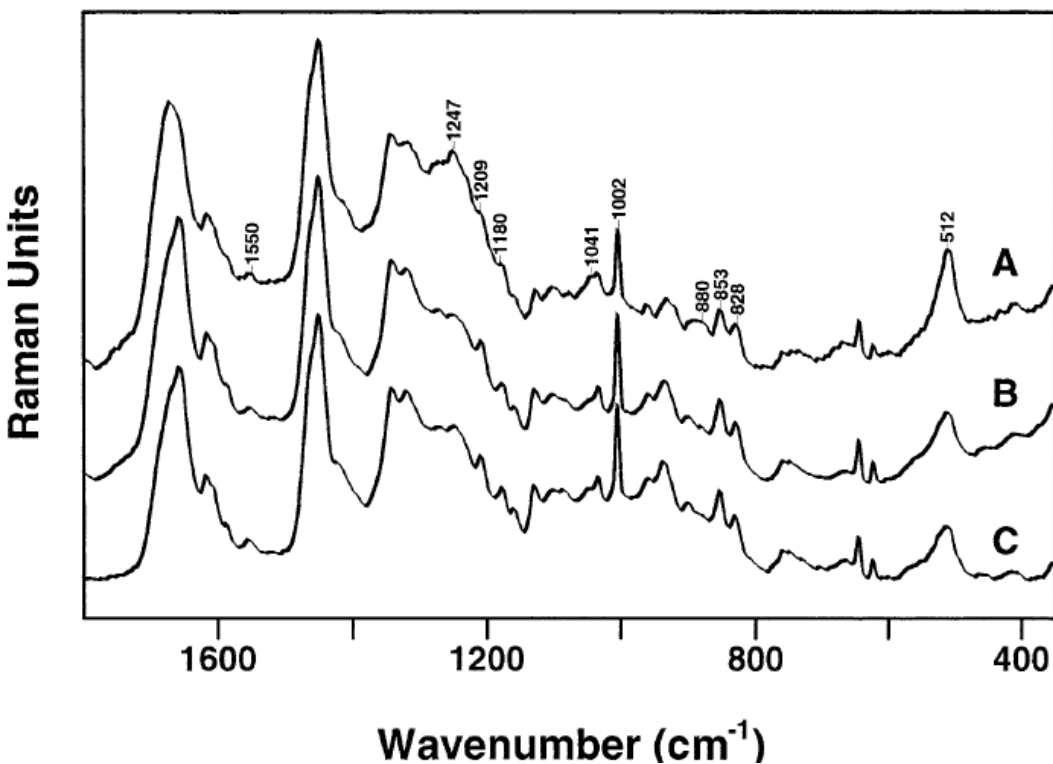


**Figure .25: FT Raman spectra of (A) cuticle cell fragments, (B) cortex fragments and (C) whole Merino fibres (Church *et al.*, 1997).**

The peak maxima of the amide I band for the cuticle and cortical cells were observed at  $1669\text{ cm}^{-1}$  and  $1656\text{ cm}^{-1}$ , respectively. These differences in peak heights were

attributed to the different structural conformations of the peptide chains. The deconvolution studies of the amide I band revealed an increase in the  $1671\text{ cm}^{-1}$  band from the cortical to the cuticle spectra, which was attributed to an increased disordered conformation at the expense of the  $\alpha$ -helical content. The results obtained in this study showed that the wool cuticle contained a higher cystine content than the cortical cells (cortex), as reflected in the strong S-S chemical band at  $512\text{ cm}^{-1}$ , which was stronger in the cuticle spectrum than in the cortical cell spectrum. Church *et al.*, (1997) concluded that Raman spectroscopy is a valuable tool for studying the changes, in the protein secondary structure of wool fibres, induced by stretching.

Subsequently, Church *et al.*, (1998) also conducted an in-depth study, using Raman spectroscopy, to examine the conformational changes caused by stretching wool fibres. The Raman spectra in Figure 2.26 shows the deconvolution of the amide I band, from (a) unstretched and sulphite treated wool fibres and (b) stretched and sulphite treated wool fibres.

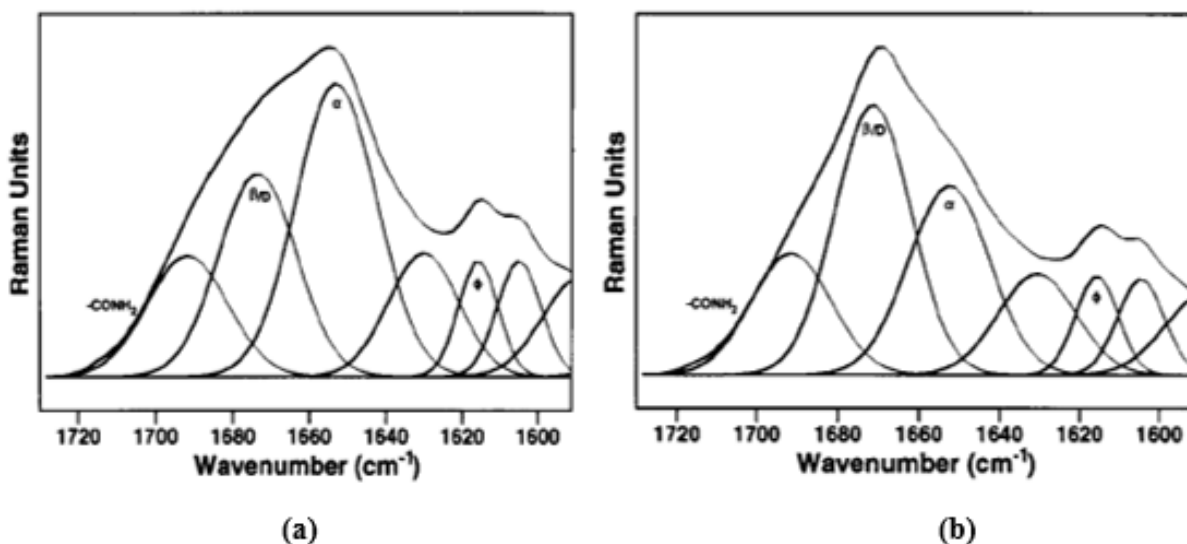


**Figure 2.26: (a): The deconvolution of amide I band obtained from unstretched sulphite treated wool fibres (b): The deconvolution of amide I band obtained from sulphite treated wool fibres stretched 66 %:  $\phi$ = Tyr/Trp side chains,  $\alpha$ =  $\alpha$ -helical,  $\beta$ /D=  $\beta$  pleated sheet and disordered conformations, CONH<sub>2</sub> = amide groups of asparagines and glutamine residues (Church *et al.*, 1998)..**

Significant differences in the band shape and shift in the peak maxima, in the amide I region, were observed by Church *et al.*, (1998), who further observed that these differences were also evident in the amide III region, especially in the  $1247\text{ cm}^{-1}$  peak.

Jones *et al.*, (1998) applied FT Raman and FTIR spectroscopies to study the photo-oxidation of wool keratin fibres and the protective effect of the UV absorber Cibrefast W. A worsted fabric, produced from New Zealand crossbred 35-micron wool, was used in their study. The research made use of a Nicolet 950 Raman spectrometer, equipped with a liquid nitrogen cooled germanium detector and the samples were excited with a Neodymium-YAG laser, operating at 1064 nm wavelength. A laser power of 500mW, and a spectral resolution of  $4\text{ cm}^{-1}$  with 3000 scans (to optimize the signal-to-noise ratio), were used. The intensity of the S-S chemical band (at  $513\text{ cm}^{-1}$ ) decreased with increased light exposure times. After 52, 104 and 208 hours of exposure, the average decrease in intensities of the S-S chemical band were 16, 19 and 28 %, respectively, indicating that photo-oxidation of the amino acid cystine has occurred.

The applicability of vibrational spectroscopic techniques, namely FT Raman, mid-infrared attenuated total reflectance (ATR), mid-infrared diffuse reflectance and near infrared diffuse reflectance, has also been investigated for the quantitative analysis on fabrics of wool/polyester blends (Church *et al.*, 1999). The least squares (LS) and partial least squares (PLS) approaches were used for the analysis of spectral data. The ATR and first derivative NIR techniques were found to be promising for quantitative analysis of wool/polyester blends and these techniques provided useful results when they were applied to commercial samples.

With the purpose of investigating changes induced by dye-keratin interaction, Pielesz *et al.*, (2003) showed the dominance of the  $\alpha$ -helical structure in undyed fibres and fabrics, constituting above 50% of the total secondary structure.

Cho (2007) investigated the use of Raman spectroscopy in the forensic laboratory, wool and silk fibres being sampled. Raman spectra of fibres were acquired in the  $125\text{-}4000\text{ cm}^{-1}$  spectral range at 50s scan time of each fibre sample. The results showed that the

main difference between the wool and silk fibres was the presence of about 11-12 % in the amino acid, cystine, in wool, and none in the silk fibres.

The high content of the diamino acid residue cystine in keratin fibres distinguishes these fibres from other fibrous proteins. Cystine provides keratin fibres with the mechanical and structural stability through the formation of the disulphide S-S linkages (Feughelman, 1997; Kuzuhara *et al.*, 2007). In a typical Raman spectrum of proteins, the S-S stretching band is found in the 500- 550  $\text{cm}^{-1}$  spectral region. Akhtar *et al.* (1997) stated that “in most naturally occurring proteins and peptides the stretching vibration of the S-S bond has a maximum peak at 510  $\text{cm}^{-1}$ , corresponding to the existence of these proteins and peptides in the gauche-gauche-gauche structural conformation, which is the lowest potential energy conformation of the S-S bonds”. Raman band components of the S-S stretching vibration are also observed at around 525 and 540  $\text{cm}^{-1}$  for proteins and peptides, corresponding to the gauche-gauche-trans and trans-gauche-trans structural conformations, respectively (Sugeta *et al.*, 1972; Sugeta *et al.*, 1973). The band resolution of the S-S stretch has been widely recognised, especially in the investigation of changes after chemical treatments of proteins (Kuzuhara, 2017; Kuzuhara, 2005; Wojciechowska *et al.*, 2004; Nakamura *et al.*, 1997).

### **2.3.7 Other Techniques**

Earlier attempts, in the development of a suitable technique for the identification of animal fibres, include the work by Smuts and Slinger (1972), who proposed the use of single fibre against-scale friction as a way of distinguishing between Buenos Aires (BA) wool and mohair. They made use of an unpolished ebonite capstan attached to the A-cell of an Instron tensile tester. Their results showed that BA wool could be differentiated from mohair, even when the two are in a mixture. The use of fibre frictional properties to distinguish and blend compositional analysis of animal fibres was also reported on later (Smuts *et al.*, 1980). This technique has, however, not been adopted to unequivocally distinguish between different animal fibres, mainly due to its highly

specialized and time-consuming nature and the fact that chemical treatments can affect the fibre friction.

A study, aimed at verifying the possible applicability of liquid chromatography (LC) coupled with electrospray mass spectrometry (ESI-MS) in the identification and classification of different animal fibres, was conducted by Paoletta *et al.*, (2013). This technique combines the powerful ability of mass spectrometry to identify molecular structures and the ability of liquid chromatography to separate proteins. Keratin proteins, from cashmere, wool and yak hair fibres, were extracted using a procedure, with slight modifications, described by Nakamura *et al.*, (2002). Keratin proteins, extracted from different animal hair fibres, were enzymatic digested in trypsin, followed by analysis on the LC/ESI-MS. It was found that it was possible to distinguish between cashmere and yak hair fibres, one of the problems faced by the industry of rare animal fibres. One of the problems associated with this method is that some harsh treatments on the fibre damages the keratin and this leads to small yields of keratin during the extraction stage. Paoletta *et al.*, (2013) concluded that more work was necessary, especially on samples of different blend compositions and different fibre/fabric treatments, to improve its accuracy in terms of blend composition analysis. A year later, using a number of samples, with differing blend compositions and different chemical treatments, the method was found to produce satisfactory results and providing a possible means for quantification of cashmere and yak, which is difficult to achieve using the CSH SEM-technique (Vineis *et al.*, 2014).

Other advances in the development of a more accurate and objective technique, in the identification of animal fibres and quantitative analysis of their intimate blends, include the assessment of the PCR-RFLP analysis of the mitochondrial 12S rRNA gene (Geng *et al.*, 2012).

The results, obtained in a preliminary investigation into the possible application of monoclonal antibodies to type II keratins for animal hair fibre identification and classification, proved positive (Paluzzi *et al.*, 2004). A method to objectively identify and classify different animal fibres, such as cashmere and wool, has been proposed (Tonetti

*et al.*, 2012). This approach involved the assessment of three different solvent systems, namely metabisulphite/urea, dithiothreitol DTT/urea and thiourea/urea/DTT, in terms of efficiency and repeatability in the extraction of keratin from animal fibres. The DTT/urea and thio/urea/DTT extraction methods were found to be the more efficient, providing high protein yields. Protein separation was carried out using 1D-electrophoresis. Two kinds of monoclonal antibodies (P21 and I6), named “anti-cashmere”, were tested for both qualitative and quantitative analysis of wool/cashmere fibre blends. The results obtained correlated very well with the results obtained using the SEM. Tonetti *et al.*, (2012) concluded that, depending upon validation, this method could be useful and important for objective identification and classification of animal hair fibres. Nevertheless, this method involves quite a number of preparation steps, which complicate the analysis. The differential scanning calorimetry (DSC) is amongst the technique that have also received application in the analysis of keratin fibres. DSC is a commonly used method in determining polymer crystallinity and usually involves measuring the melting point and related enthalpy. It measures the heat flow that occurs in a sample when it is heated, cooled or held isothermally at constant temperature. Using DSC, it is possible to detect endothermic and exothermic effects; to measure peak areas obtaining information about transition and reaction enthalpies; to determine the specific heat capacity, the melting point, the crystallization behaviour, the glass transitions of amorphous materials and the endothermic effects related to some decomposition reactions. Hence, thermal analysis represents a powerful tool to investigate the thermal modification of the fine structure of complex materials, such as cashmere, wool and hairs (Tonetti *et al.*, 2014). In fact, fundamental relationships were found between thermal behaviour of the main morphological components, fibre properties and associated performances. These researchers concluded that DSC could be used as a rapid and cheap qualitative method of animal fibre identification, but is unlikely to be suitable for fibre blend analysis.

Terahertz spectroscopy represents another technique which has been investigated as a substitute for the existing tedious microscopy-based animal fibre identification methods (Kurabayashi *et al.*, 2009; Kurabayashi *et al.*, 2010). According to Molloy and Naftaly (2013), some of the benefits of the terahertz spectroscopic method include its non-

destructive nature, the ability to analyze a large area of the material, and the fact that the analysis is fast.

Animal fibre surface texture includes scale thickness, scale shape and the scale interval or length. A technique (wavelet texture) based on animal fibre surface texture was developed and proposed by Zhang *et al.*, (2010) for distinguishing between cashmere and superfine wool fibres. This method uses images taken from the SEM, with further work, involving the use of images from a light microscope being planned.

## 2.4 LITERATURE REVIEW SUMMARY

### 2.4.1 General

- Wool, mohair and cashmere belong to a group of natural fibres, popularly known as animal fibres, with wool having the highest global production and application of this group. Animal fibres consist mainly of proteins known as keratins. Keratin proteins are distinguished from other proteins, by the high content of the amino acid cystine.
- Mohair belong to a class of animal fibres known as speciality, sometimes referred to as luxury or rare fibres, due to their low production volumes and the fact that these fibres have an image of outstanding quality and also possess certain sought-after properties, such as lustre and softness. Because of this, rare animal fibres are generally very expensive compared to sheep wool of similar fibre diameter.
- Fibres from different animal species are sometimes blended to achieve various effects, such as improved properties (additional beauty, colour, softness, durability or lustre) and often for cost saving purposes.
- The large price differences between certain animal fibres have led to certain unscrupulous manufacturers blending relatively inexpensive animal fibres, such as sheep wool, with expensive rare fibres (cashmere, mohair, camel hair, etc.) to benefit from the reduced cost while still passing off the product as if it contained only the rare fibre and thereby benefiting from the superior quality image and price benefit of the rare fibre.
- About 10-15 % of undeclared substitutes had been discovered in mohair products tested at the Deutsches Wollforschungsinstitut (DWI) in Germany, with some 50 % of products tested were falsely labelled.
- At present, only the slow, costly, labour intensive SEM CSH based method is internationally accepted for quantitative wool/mohair blend analysis. Hence, the textile industry is in need of a fast, reliable and less subjective technique to analyse



the composition of animal fibre blends. Both physical and chemical techniques have been investigated for their applicability, with none entirely satisfactory in this respect.

#### **2.4.2 Techniques Applied for Animal Fibre Identification and Blend Analysis**

Animal fibre identification has traditionally relied on microscopy-based methods and these have been internationally accepted and standardized in IWTO 58-00, ISO 17751, the AATCC method 20 and various ASTM standards.

- Initially, animal fibre identification relied on the examination of the fibre surface, by light microscope, for scale frequency, prominence and pattern. Nevertheless, not only is this method subjective, labour intensive, time consuming and expensive, but certain chemical treatments can affect the fibre surface scale structure and reliable fibre identification.
- To date, the cuticle scale height (CSH) method, using an SEM, has proved the most accurate in distinguishing between wool and mohair and has been widely accepted by the textile industry internationally, with wool having CSH values generally ranging between 0.5  $\mu\text{m}$  and 1.1  $\mu\text{m}$  while that of mohair generally range from 0.1 to 0.5  $\mu\text{m}$ . This method is described in IWTO 58-00 test method, which is currently the only international standard, used for distinguishing between wool and mohair.
- Although the SEM CSH method (IWTO-58-00) has proved to be both accurate and reliable, and is widely accepted for wool/mohair blend analysis, it is time consuming, labour intensive, expensive and requires an operator with considerable training and expertise. Hence the need for an alternative method which is as accurate, but less operator dependent, time consuming, labour intensive and expensive.
- Atomic force microscopy (AFM) measurement of CSH represents an alternative method to SEM, for distinguishing between wool and mohair, also providing additional fibre surface related information. This technique is, however, even more time consuming and expensive than that based on the SEM and, because of this, has not been adopted for identifying and classifying animal fibres on a routine basis.

- Deoxyribonucleic acid (DNA) analysis has proved to be a potential technique for animal fibre identification technique, and a potential substitute for the time-consuming microscopy-based techniques. Such a technique relies heavily on the extraction of a DNA of maximum purity from the fibre sample. Nevertheless, DNA degradation, thermal and chemical treatments, difficulty in the extraction of a sufficient contaminant free DNA and the time required for the analysis can impact negatively on successful identification of animal fibres using the dot-blot DNA hybridization analysis.
- Within the above context, the development of a DNA analytical method, applying a polymerase chain reaction (PCR), has proved an important step towards a more reliable and accepted test method for routine analysis. Contrary to the conventional dot-blot hybridization method, high quality DNA is not a prerequisite for PCR based methods. The PCR-RFLP (restriction fragment length polymorphism) and real-time PCR DNA based techniques were found to distinguish well between animal fibres, and the latter possessing potential to be applied for quantitative composition analysis of wool and cashmere blends. The DNA method has recently been standardized as an International Standards Organization (ISO) method for qualitative analysis of animal fibres.
- Animal fibre proteins are classified into low-sulphur, high- sulphur and high-tyrosine proteins and the electrophoretic analysis of these showed a significant variability for different species of the same breed and even for fibres from the same animal. Although the various animal fibres contain the same amino acids, they do differ somewhat in the amount of certain amino acids, particularly cystine and cysteic acid contents, which they contain. As a result, considerable research has been devoted to the use of electrophoresis as a tool for animal fibre identification and classification. Mohair extracted proteins were found to be rich in glycine and tyrosine relative to wool fibres. Wool samples contained a high content of the sulphur rich amino acid cysteine. The difficulty to analyze chemically treated fibres, the overlap in the ranges of amino acids, and the impossibility of quantitative analysis of blends are amongst the reasons that this method has never been adopted as an internationally

acceptable technique for animal fibre blend analysis. Nevertheless, the ratios of certain specific amino acids may have potential in this respect, and warrants further investigation, since such a method could lend itself to automation, or at least semi-automation.

- Chromatographic methods confirmed that indeed wool is not a homogeneous protein. Gas and high-performance liquid chromatography showed that distinction between animal fibres, using chemical techniques, is a difficult task. Minor differences have been observed in the peak heights of the chromatograms of internal and external lipids of different animal fibres, but once again it was found difficult, if not impossible, to use this for the accurate identification and quantitative analysis of the composition of blends containing different animal fibres.
- The power of vibrational techniques, such as Infrared (IR) and Raman spectroscopy, in the analysis of biopolymers has been recognised. Mainly because of its speed and non-destructive nature, IR spectroscopy has received wide application in forensic investigations and in the hair industry. It has been utilized in the analysis of animal/synthetic fibre blends, using the baseline method approach. A combination of IR spectroscopy, chemometrics and artificial neural networks (ANN) has been found useful in the qualitative, but not quantitative, analysis of different animal fibres.
- FTIR studies have shown that there might be differences in the positions of certain chemical bands, such as the band at  $1040\text{ cm}^{-1}$ , which appear at different positions in different animal fibres. The relative peak heights and positions of the amide I and amide II bands have also been found to hold potential in the identification and classification of animal fibres. Nevertheless, no successful quantitative analysis has been reported using this method. Some researchers concluded that FTIR related techniques do not hold potential for distinguishing between wool and mohair fibres, because of their similar basic chemistry.
- Raman spectroscopy has found important application in the textile industry, especially in studying wool keratin, for determining wax content in raw wool samples and keratin fibre structure and degradation. This technique has proved useful for

studying changes in the secondary structure of different proteins, including wool and human hair keratin. Stretching may induce changes in the structural conformation of the keratin polymer with the S-S chemical band decreasing with the increase in the ratio of stretching. Minor differences have also been observed, between the cortex and cuticle of some keratin fibres, including wool. Differences included the band shapes and the minor shifts in the peak maxima of certain bands such as the amide I.

- Developments in mass spectrometry and liquid chromatography (LC) based methods for identifying molecular structures and protein separation, respectively, could hold future potential, but further research in these areas is still required.
- Other techniques, based on antigen–antibody specific selectivity (for example, applying monoclonal antibodies named ‘anti-cashmere, Terahertz spectroscopy, wavelet texture and fibre frictional properties, have been investigated as possible substitutes for the laborious LM and SEM methods, but none have, as yet, received significant application or acceptance in practice.

## **2.5 MOTIVATION**

As evident from an exhaustive literature survey, a great deal of research has been directed towards developing alternative techniques for unambiguously distinguishing between various animal fibres and quantitative analysis of their blends. Differences in certain amino acids extracted from the proteins of different animal fibres and the subtle differences in the IR profiles of different fibres, indicates that Raman based technique could hold potential as cost-effective technique for animal fibre characterization and their identification. The simplicity in the operation of Raman spectroscopy techniques, the fact that no sample preparation is required and the non-destructive nature of this technique makes it attractive as potential alternative technique to the existing tedious and laborious microscopic techniques, for identification of different animal fibres. To the best of my knowledge and belief, this thesis contains no material that has been previously published by any other person except where due reference and citation is made.

## CHAPTER THREE

### EXPERIMENTAL METHODOLOGY

#### 3.1 INTRODUCTION

This chapter provides details of the materials, sampling, test methods, procedures and statistical analyses used in this study. It also presents factors that could possibly affect the Raman spectra of animal fibres and provides ways of minimizing the possible effects. One of the most important advantages of the Raman spectroscopic examination of fibres is that very little time is required for preparing the samples for testing.

#### 3.2 MATERIALS

Commercially scoured wool and mohair samples from different countries (listed in Table 3.1) were provided by the Council for Scientific and Industrial Research (CSIR) in Port Elizabeth. The wool samples analysed in this study were in the form of tops, mostly randomly selected from various sheep breeds: including Lincoln, Buenos Aires, Corriedale, Merino and Romney. Among these wool tops are BR lots (tops produced from different merino and merino related sheep breeds), OSP (tops produced from mixtures of fleece wools with non-fleece types or out sorts, such as bellies and backs) and PP (tops produced from producer lots as well as from mixtures of wool differing in either mean fibre diameter or staple length or both) (Botha, 2005). A comprehensive database of mohair samples from various countries of origin is available at the CSIR and the following mohair samples were randomly selected from this database for use in the current study.

South Africa : 25 samples

Texas : 21 samples

Turkey : 6 samples

Lesotho : 1 sample

Argentina : 1 sample

In Table 3.1, a list of wool and mohair samples analysed in the current study, together with their average fibre diameters, is contained.

**Table 3.1: Details of wool and mohair samples tested.**

WOOL		MOHAIR	
Sample ID	MFD ( $\mu\text{m}$ )*	Sample ID	MFD ( $\mu\text{m}$ )*
Dorset horn (DH)	33.8	*SB	30.0
Corriedale	27.4	*742	24.5
Romney marsh	34.5	*376	31.2
Lincoln1 (L1)	33.8	*146	39.6
Lincoln2 (L2)	35.1	*1048	29.1
Lincoln3 (L3)	32.3	*20	32.5
Lincoln4 (L4)	32.9	*712	31.3
BR05	25.3	*1126	28.4
BR11	23.0	*319	31.2
BR14	24.2	1098	36.5
BR20	23.1	1078	29.1
BR28	25.4	1136	34.6
BR36	22.6	1052	35.9
BR41	21.2	1129	34.4
BR42	23.1	1136	34.6
BR43	21.1	1045	26.7
BR44	23.8	1109	28.0
BR45	21.6	1091	30.3
BR55	20.2	1060	29.6
BR58	19.3	1006	31.0
BR59	19.7	1002	33.1
BR65	19.4	1861	29.8
BR66	20.6	1089	35.9
BR71	22.7	Mohair-labs A	25.4
BR74	23.4	Mohair-labs C	39.9
BR81	22.5	Mohair-labs D	31.0
BR82	24.0	1968	32.9

WOOL		MOHAIR	
Sample ID	MFD ( $\mu\text{m}$ )*	Sample ID	MFD ( $\mu\text{m}$ )*
BR83	22.0	1975	35.8
BR85	24.4	TYG1-Istanbul	31.3
BR86	21.0	TYG2-Istanbul	30.8
BR88	24.4	Texas Int. Mohair INC-#705	36.5
BR91	24.1	Texas Int. Mohair INC-#708	33.9
BR95	22.0	Texas Int. Mohair INC-#721	36.3
BR100	23.7	Texas Int. Mohair INC-#737	27.1
BR103	20.4	Texas Int. Mohair INC-#728	29.2
W2 (washed)	26.7	Texas Int. Mohair INC-#734	29.2
W4 (washed)	25.4	Texas Int. Mohair INC-#748	34.8
W10 (washed)	41.0	New Mexico Kid-365	29.8
W16 (washed)	30.5	TA1-Istanbul	35.6
W18 (washed)	35.8	TA2-Istanbul	36.5
W26 (washed)	45.3	TK1-Istanbul	28.0
W28 (washed)	18.4	TK2-Istanbul	28.2
W38 (washed)	41.0	Samil-Samil Combing Lot 1	26.6
W52 (washed)	36.6	Samil-Samil Combing Lot 2	27.0
W54 (washed)	35.4	Samil-Samil Combing Lot 3	34.9
W56 (washed)	29.4	Samil-Samil Combing Lot 4	24.9
OSP21	21.5	Samil-Samil Combing Lot 7	31.0
OSP26	22.8	Samil-Samil Combing Lot 8	33.9
OSP40	22.5	Samil-Samil Combing Lot 11	27.3
OSP49	21.2	Texas super kid-TXSK	23.3
OSP51	22.1	BK11401-Lesotho	48.4
Merino1	18.9	AYG - Argentina Young Goat	29.5
CBP SS6	20.2	1117	28.1
CBP SS4	18.2	1028	32.6
PP66	22.3		
BR47	20.8		
BR54	20.3		

\*MFD: Mean Fibre Diameter



It is worth mentioning that all the samples in Table 3.1 were analysed on the Bruker 80V FTIR/Raman spectrophotometer.

A random selection, which ensures that every sample have an equal chance of being selected (Fienberg, 1989), of five wool and four lustre mohair fibre samples, as shown in Appendix I (a), was made and taken to the University of Witwatersrand for micro-Raman spectroscopic analysis.

Eight wool and eight mohair samples, as shown in Appendix I (b), were also selected, randomly, from the database in Table 3.1 and sent to the University of Cape Town for Attenuated Total Reflection (ATR) Fourier Transform Infrared (FTIR) - LUMOS micro-spectroscopic analysis.

### **3.3 WOOL AND MOHAIR SAMPLE TREATMENT**

The samples in Table 3.1 (except for the W labelled wool samples) used in this study were analysed as received and were not pre-treated (i.e. washed or cleaned) prior to Raman or IR micro-spectroscopic analysis. These samples have all undergone commercial scouring. However, because the W labelled (i.e. W2-W56) wool samples had been stored for some decades, enclosed in glass containers with mothballs (naphthalene) for protection against moths, they had to be re-washed before any spectral acquisition could be performed. Despite the strong odour of naphthalene, these samples deceptively appeared clean in the eye. These W labelled samples were washed using a washing detergent, followed by several rinses in distilled water, ensuring that any traces and the strong odour of naphthalene was removed. After washing, these samples were allowed to dry at room temperature. An FT Raman spectral comparison of these samples before and after they were washed is presented later in section 3.5 of this thesis.

The micro-Raman and the ATR-FTIR spectroscopic analyses of single fibres did not involve any kind of treatment prior any spectral acquisition, fibres were analysed as received.

### **3.4 EXPERIMENTAL PROCEDURE AND INSTRUMENTATION**

The instrumentation, sample preparation and experimental methodology involved in the three characterization techniques used in this study namely Fourier-transform (FT) Raman spectrophotometer, a Horiba Lab-RAM HR Raman micro-spectrometer and the Attenuated Total Reflectance Fourier Transform Infrared (ATR-FTIR) - LUMOS Micro-spectroscopy are described in the section that follows.

#### **3.4.1 Sample Preparation**

One of the most significant advantages of the FT Raman fibre analysis include the fact that no special sample preparation is required. The large sample compartment of the Bruker Ram II FT Raman system can house an extensive range of pre-aligned sampling accessories, designed to accommodate all types of sample formats, ranging from powders to liquids in vials. For this research study a bulk bundle of parallel fibres was drawn from each of the sample bags and prepared by flattening (by use of hand) into approximately 2 mm thickness and was inserted in the sample compartment for analysis, as shown in Figure 3.1 (b) (indicated by arrow). At least three fibre bundle specimens were drawn from different parts of each bag and two measurements were made on each, performing one measurement from each spot along the length of each fibre bundle, making a total of six spectra from each sample.

Raman micro-spectroscopic analysis involved placing a group of individual wool or mohair fibres flat on a glass slide and securing both ends of each fibre onto the slide with an adhesive tape, ensuring that they do not move during spectral acquisition. Fibres were placed in a random manner in the slide, such that they were differently aligned with respect to the plane of polarisation. Figure 3.1 shows light microscopic images of fibres prepared on a glass slide with different orientations.

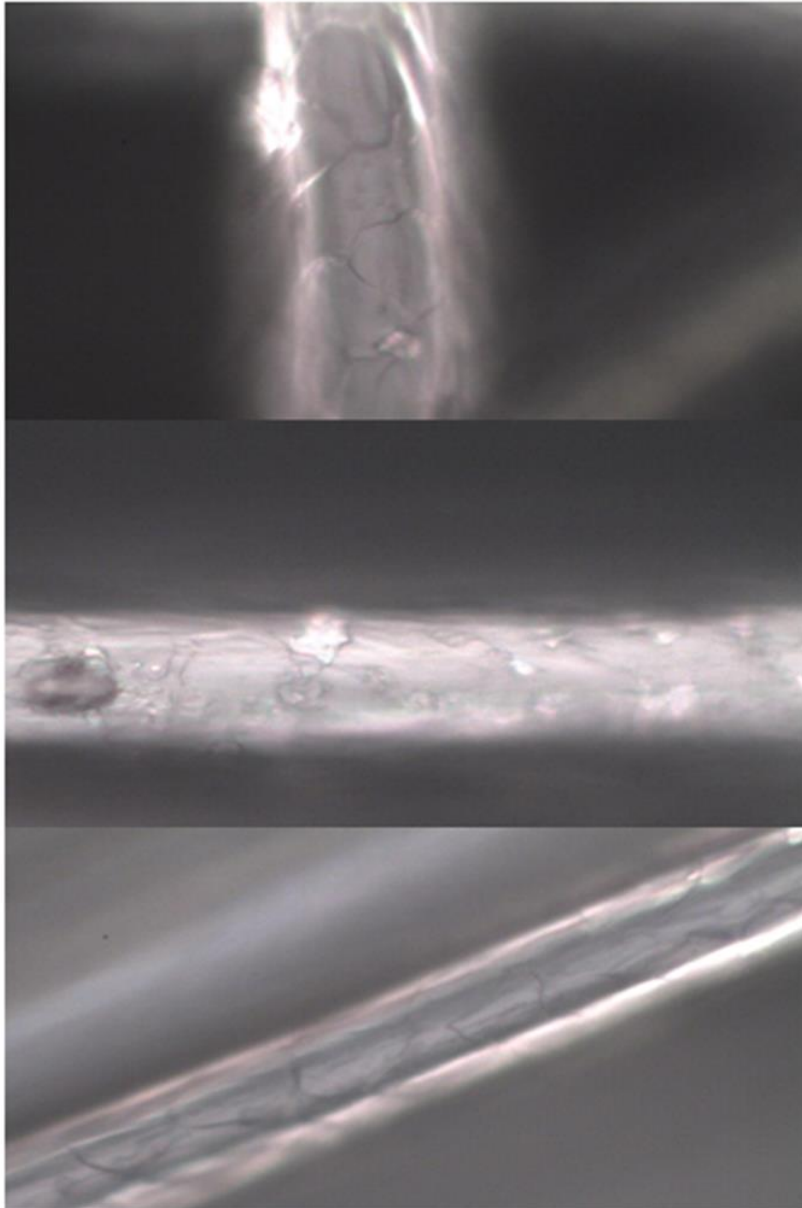


**Figure 3.1: Optical microscopic images of wool with different orientations.**

During the ATR-FTIR LUMOS micro-spectroscopic analysis, the fibre is brought into contact with the tip of the Germanium (Ge) crystal (100  $\mu\text{m}$  in diameter) on all predefined measurement positions. Three positions or spots were chosen from each fibre and these were separated by approximately two centimetres.

### 3.4.2 Instrumentation and Experimental Design

#### 3.4.2.1 FT-Raman Spectrophotometry

- **Instrumentation**

All the samples listed in Table 3.1 were analyzed using the Bruker Ram II FT-Raman module (Figure 3.2a). The Bruker FT Raman system used in this study is a dual-channel FT-Raman spectrophotometer coupled to the VERTEX series multi-range FT-IR spectrophotometers. This system combines fast and easy sample handling with maximum suppression of disturbing fluorescence.

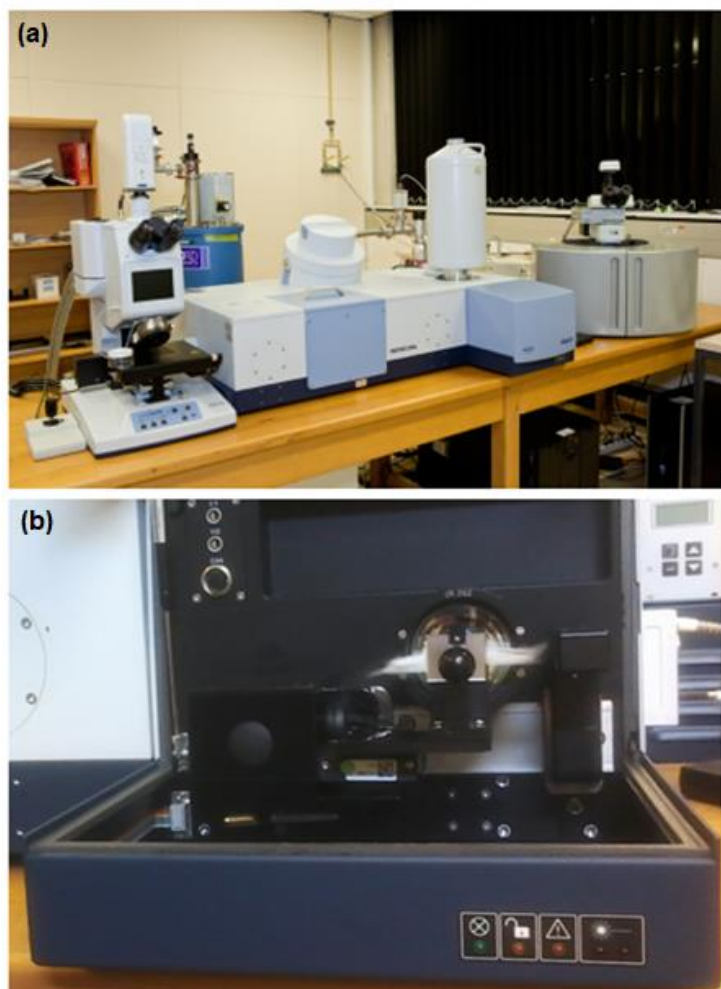


Figure 3.2: Bruker 80V FTIR/Raman spectrophotometer setup.

- **Spectroscopic aspects**

A variety of factors and operating conditions play a role in the signal-to-noise (S/N) ratio or the quality of a Raman spectrum, including the laser power, spectral resolution and acquisition time (number of scans). These conditions were investigated for this research and Table 3.2 summarizes the conditions that were found to be optimal for the current study of wool and mohair samples and well compared with those used by Carter *et al.*, (1994), the first published research involving the analysis of wool fibres using FT Raman spectroscopy. The quality of the spectra obtained in the current research and the wool spectra reported by Carter *et al.*, (1994) were comparable and largely unaffected by the significantly different acquisition time and spectral resolution used in the two studies.

**Table 3.2: Operating conditions used in this study and those in Carter *et al.***

<b>Parameter</b>	<b>Carter <i>et al.</i>, (1994)</b>	<b>This study</b>
1. Laser type	Nd:YAG	Nd:YAG
2. Laser power	50-400 mW	500 mW
3. Laser wavelength	1064 nm	1064 nm
4. Resolution	8.0 cm <sup>-1</sup>	4.0 cm <sup>-1</sup>
5. Acquisition time	4 hours	1 hour

- **Experimental design**

In all FT Raman experiments of this study, a bundle of parallel fibres was mounted and exposed to a monochromatic laser beam by clamping it in front of a silvered mirror. When the laser light strikes the fibre bundle, a portion of this laser light is scattered, with most of it having a similar wavelength as the original incident light (elastic scattering). A minor share of the incident light hits the sample in such a way that it transfers a small quantity of energy to the molecules of the sample (inelastic scattering). In a Raman experiment, this inelastic scattering is detected, giving a plot of the intensity versus the energy difference between the incident laser light and the scattered (detected) light (Raman shift in wavenumbers). On exposure characteristic bands of wool and mohair were observed including the very strong CH<sub>2</sub> asymmetric stretch (around 2932 cm<sup>-1</sup>), the amide I (1654 cm<sup>-1</sup>), the CH<sub>2</sub> & CH<sub>3</sub> bending modes (1450 cm<sup>-1</sup>) and the S-S stretch (around 508 cm<sup>-1</sup>). This research study focused mainly on the comparison of variables extracted from spectra of wool and mohair, these including the band positions (wavenumbers), relative peak heights or intensities and band areas. Initially, comparison of wool and mohair FT Raman spectra was done visually, searching for the absence or presence of spectral bands that could be specific to one fibre type. Table 3.3 contains variables that were extracted from wool and mohair spectra for comparison purposes.

**Table 3.3: Variables extracted from wool and mohair FT Raman spectra.**

Variable	Replication*	
	Wool	Mohair
1. Peak positions	6	6
2. Band areas	1	1
3. Relative peak heights	6	6

\*Number of spectra from each sample.

The Raman spectral peak position or wavenumber analysis was performed on the individual spectra of each sample. A comparison of these peak positions between wool and mohair was conducted for possible shifts that could be specific to one fibre type to help in distinguishing between the two fibres.

The band areas under certain chemical bands were also extracted from wool and mohair Raman spectra. These were also performed on the average spectra for each sample. From these band areas the conformations of the secondary structure of proteins and polypeptides of wool and mohair fibre samples were determined, based on the ratio of the area under amide I band to that of the CH<sub>2</sub> & CH<sub>3</sub> bending modes. The amount of the disulphide –S-S- bonds for wool and mohair were also determined for comparison purposes. According to literature, these could be calculated from the ratios of the area under the disulphide –S-S- stretching vibration to the area under the CH<sub>2</sub> & CH<sub>3</sub> bending modes.

Relative peak heights of certain Raman bands were extracted from wool and mohair spectra. A variation in the relative peak heights was observed from one wool sample to the other and also from one mohair sample to the other and because of this variation, a relationship between these relative peak heights or intensities and mean fibre diameter was investigated. This analysis was performed on the average spectrum of each spectrum.

Relative peak heights, from which the peak height ratios were determined, were extracted from each individual wool and mohair Raman spectra for comparison between the two fibres.

#### **3.4.2.2 Raman-Micro Spectrometry**

- **Instrumentation**

A Horiba Lab-RAM HR Raman micro-spectrometer, equipped with a couple of excitation laser sources for sample irradiation, was used in this study of wool and mohair single fibres.

- **Spectroscopic aspects**

The micro-Raman spectroscopic results presented later in the research findings chapter (Chapter Four) of this thesis were obtained using the green 514.5 nm Ar<sup>+</sup> ion laser. Because the results obtained using the 785 nm laser excitation provided a very bad signal-to-noise ratio, only the results obtained using the green 514.5 nm Ar<sup>+</sup> ion laser are considered for the current study. The measurements were performed using a 50× Olympus objective and a ~ 1 μm spot size diameter. Each spectrum was acquired at 60 seconds acquisition time. An appropriate automated fluorescence suppression and background subtraction method was applied on the Raman scattering measurements. The laser power was deliberately kept low during all measurements to minimize the background fluorescence and possible temperature variation effects on the samples, with a laser power of 4 mW being used. The spectral acquisition and pre-processing were done using the Horiba LabSpec® 5.0 software and Origin Lab 8.0 software packages.

- **Experimental Design**

Similarly to the FT Raman analysis, characteristic bands include the very strong CH<sub>2</sub> asymmetric stretch, the amide I, the CH<sub>2</sub> & CH<sub>3</sub> bending modes and the disulphide S-S stretching vibration. For this research study, the spectral information, of interest, extracted from the micro-Raman spectra included the band positions (wavenumber) and the peak heights for certain bands. Table 3.4 summarizes the variables that were extracted for comparison of wool and mohair single fibres.



**Table 3.4: Spectral information extracted from the micro-Raman spectra of wool and mohair.**

Variable	Replication*	
	Wool	Mohair
1. Peak positions	4	4
2. Relative peak heights	4	4

\*Number of spectra from each sample.

Different fibre orientations (as shown earlier in Figure 3.1), with respect to the polarization plane of the incident laser, may provide variation in the micro-Raman spectra of protein fibres. This may involve changes in the absolute peak height, band position and band shape. In this study, the application of Ratiometric analysis was found to mitigate significantly the effects of different fibre orientations, particularly on the Raman peak heights.

An appropriate automated fluorescence suppression and background subtraction method was applied on the Raman scattering measurements.

Four fibre snippets were randomly selected from each sample on the glass slide and one measurement was performed on each fibre.

### **3.4.2.3 ATR-FTIR LUMOS Micro-Spectrophotometry**

- **Instrumentation**

The IR analysis of single wool and mohair fibres was done using a Bruker ATR-FTIR LUMOS micro-spectroscopic analysis and the instrumental parameters are summarized in Table 3.3. For many samples, as is the case for most keratin fibres, the size of the infrared beam is usually greater than the fibre diameter. The aperture size was reduced from 100 x 100  $\mu\text{m}$  in order to ensure that only spectra of the sample and not of the sample stage/holder were acquired.

**Table 3.3: FTIR-LUMOS operating conditions.**

Software	OPUS 7.5
FTIR Mode	ATR (Germanium crystal)
Number of scans	32
Resolution	2 cm <sup>-1</sup>
Spectral range	400-4000 cm <sup>-1</sup>
Aperture size	50 x 50 μm

Spectra were acquired at three different positions along the length of each wool or mohair fibre. Three single (i.e. individual strands) fibres were randomly selected and analysed from each sample (F1 to F3).

- **Experimental Design**

The characteristic IR bands of wool and mohair include the amide bands I, II and III, the CH<sub>2</sub> & CH<sub>3</sub> bending modes and cysteic acid bands, etc., and in this study the ATR FTIR micro-spectroscopic analysis of wool and mohair focused on the extraction of wavenumbers, peak heights and band area values for the characteristic bands using the baseline method and curve fitting procedure. These were compared for possible differences between the two fibre types using the statistical tools.

### **3.4.3 Data Pre-Processing**

Critical in all experimental procedures, is the careful consideration of pre-processing the data before further analysis. This step is very significant in the analysis of any vibrational spectrum, such as Raman and IR spectra. The most routinely used pre-processing methods include baseline correction, smoothing and normalization. All spectral data pre-processing in the current study was performed using the OPUS 7.2 (Bruker Optik GmbH, Ettingen, Germany) and Origin Lab 8.0 (OriginLab<sup>®</sup> Corporation, 2007) software packages.

The normalization of all Raman spectra of the wool and mohair fibre samples was carried out based on the CH<sub>2</sub> and CH<sub>3</sub> bending modes chemical band (at 1450 cm<sup>-1</sup>), which is insensitive to secondary structure conformation (Church *et al.*, 1997). For each chemical band, the band intensity or peak height was calculated from the peak to a baseline drawn between the points as shown in Figure 3.3. The prominent bands in the Raman spectra of wool and mohair were selected for ratiometric analysis and Table 3.4 summarises their spectral positions (wavenumber) and their baselines.

**Table 3.4: Band positions with corresponding baselines.**

Chemical band	Band position (cm <sup>-1</sup> )	Reference	Baseline (cm <sup>-1</sup> )
CH <sub>2</sub> asymmetric stretch	2932	Carter <i>et al.</i> , (1994)	2804-3112
Amide I	1656	Jurdana <i>et al.</i> , (1995)	1569-1745
CH <sub>2</sub> & CH <sub>3</sub> bending modes	1450	Church <i>et al.</i> , (1997)	1377-1507
Phe & Trp	1004	Carter <i>et al.</i> , (1994)	994-1018
Skeletal C-C stretch	936	Carter <i>et al.</i> , (1994)	912-984
Tyr	644	Carter <i>et al.</i> , (1994)	633-659
Phe	622	Carter <i>et al.</i> , (1994)	613-632
S-S stretch	508	Carter <i>et al.</i> , (1994)	445-613

Figure 3.3 illustrates how the baseline method was applied in determining the Raman band intensities or peak heights from the wool and mohair fibre spectra. The most relevant, a total of eight chemical bands, relative peak heights were extracted from each spectrum.

For micro-Raman analysis of single fibres, the spectrum acquisition and pre-processing was done using the Horiba LabSpec® 5.0 (Horiba Scientific, Edison, NJ, USA) and Origin Lab 8.0 software packages. These included the extraction of the relative peak heights using the baseline method and finding the accurate band positions (i.e. wavenumbers). A similar normalization process as the FT Raman spectra was carried out for the micro-Raman spectra.

The extraction of the peak heights, for the amide I and amide II chemical bands, and accurately locating band positions of ATR FTIR micro-spectroscopic spectra was achieved through the use of OPUS 7.2 and Origin Lab 8.0 software packages. Curve fitting was applied to determine the intensities, wavenumbers and the band areas for the IR bands found in the wool and mohair single fibres.

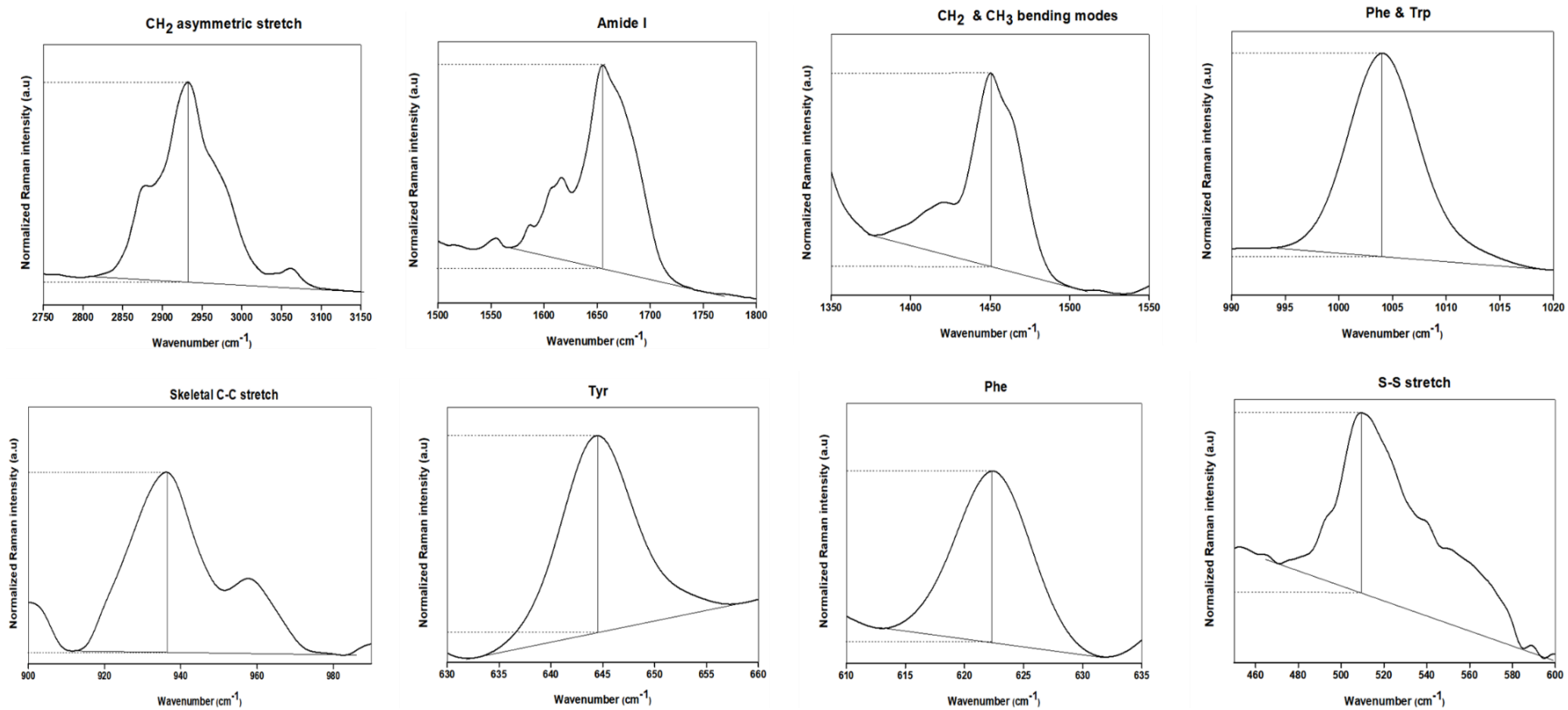


Figure 3.3: Illustration of the extraction Raman peak heights using the baseline method.

### **3.4.3.1 FT Raman Spectral Database**

Later in this thesis, section 4.2.1.4, the possible identification of wool and mohair using a Raman spectral database is presented. This database included average Raman spectra from all the samples contained in Table 3.1. Before all query spectra could be matched with the database, normalization methods had to be performed to assess the influence in the accuracy of the search results, with the available normalization methods including the Vector and the Min-Max normalization methods.

#### **3.4.3.1.1 Vector Normalization**

This normalization method calculates the average y-value of the spectrum. The average value is subtracted from the spectrum decreasing the mid-spectrum to  $y=0$ . The sum of the squares of all y-values is calculated and the spectrum is divided by the square root of this sum. The vector norm of the result spectrum is 1. Vector normalization was assessed for the application prior the spectral search study. The application of this normalization technique was accompanied with a decrease in the hit quality index (HQI) values, compared to the Min/Max normalization.

#### **3.4.3.1.2 Min-Max Normalization**

This is often used with spectra which optical layer thickness varies, to be able to compare these spectra with each other. For example, the spectra of a powder sample which have been compacted unequally during separate measurements. The shape of the single spectra remains, and the difference between the spectra can be detected more easily. An appropriate derivative can be selected from the list, these including a no derivative, first derivative or second derivative. These were assessed for the improvement in the accuracy of the spectral search results and the results are given later in section 4.2.1.4 of this thesis.

### 3.5 Experimental Factors Which Could Affect Raman Peak Heights

A major problem often encountered in the conventional Raman spectroscopic analysis is that of fluorescence which can totally swamp the very weak Raman signal. This is common phenomenon when studying biological materials such as in this case wool and mohair fibres. The influence of this fluorescence and other factors such as variation in sample thickness in Raman spectral features are presented in this section.

#### 3.5.1 Comparison of Washed and Unwashed Fibre Spectra

A comparison of spectra from washed fibre sample and the unwashed fibre sample is shown in Figure 3.4, with the only observable difference being the weak spectral feature found around  $1380\text{ cm}^{-1}$  of the spectra from the unwashed fibre sample.

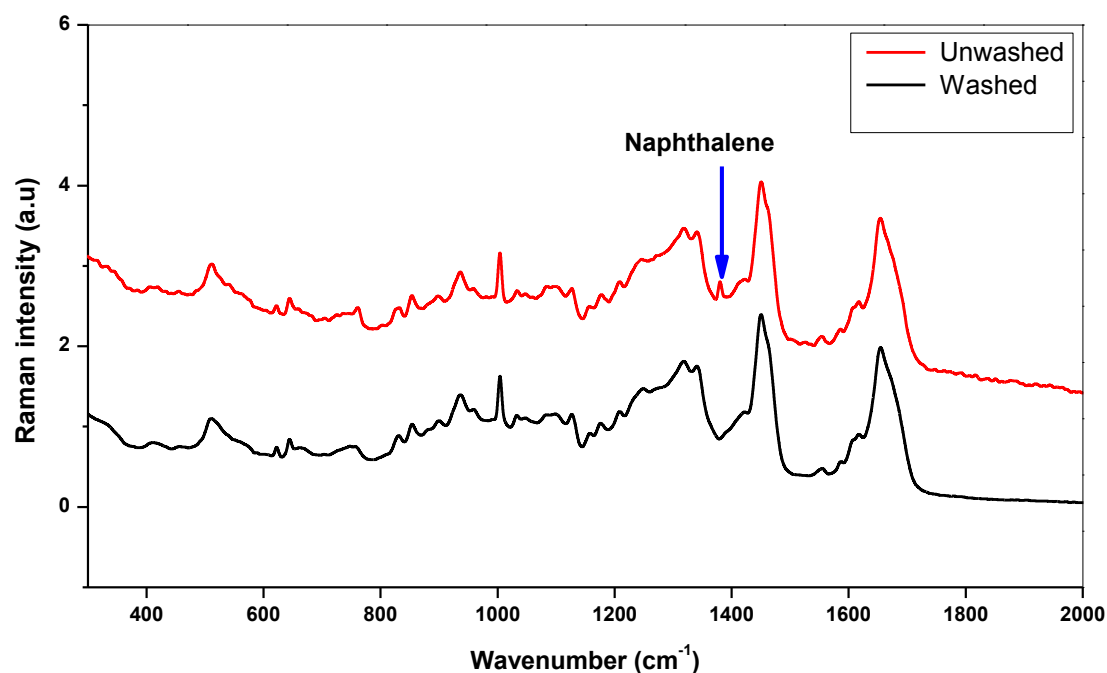


**Figure 3.4: FT Raman spectra of unwashed wool (red) and washed wool (black).**

This peak was consistently observed for all the samples that have been kept in the bottle containers (W labelled samples in Table 3.1) with moth balls (naphthalene). A Raman spectrum of naphthalene (moth ball) is shown in the Figure 3.5 (McCain *et al.*,

2008). The spectrum is characterized by the dominant or very strong and sharp peak around  $1380\text{ cm}^{-1}$ .

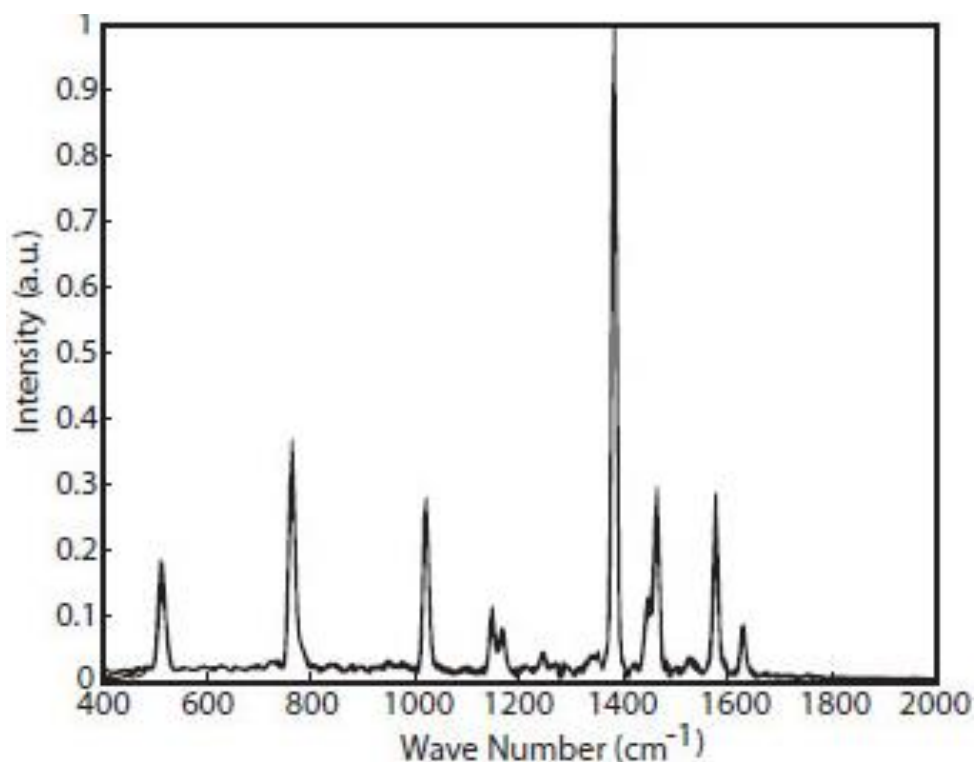


**Figure 3.5: Raman spectrum of naphthalene (McCain *et al.*, 2008).**

The black spectrum in Figure 3.4 confirmed that after these samples were washed all the remains or traits of naphthalene were completely removed. Three wool (W) samples were examined before and after they were detergent washed, the most prominent Raman chemical bands being chosen for this analysis. A spectral comparison, using peak position and relative peak heights, was conducted for a few of the W labelled wool samples before and after they were re-washed the results are presented in Table 3.4. It was found that, for all the analysed samples, there were no changes in the peak positions after they were washed, only small and insignificant increase in the peak heights or intensities of the skeletal C-C stretch and the amide I bands being observed after washing. Statistical comparison of average values proved that these were statistically insignificant ( $p > 0.05$ ). The average relative intensities of the S-S stretch band decreased slightly after the samples were washed. Nevertheless, the observed difference, in the mean values, was proved to be statistically insignificant ( $p > 0.05$ ).



**Table 3.4: Comparison between spectra acquired from washed and unwashed wool fibre samples.**

Chemical band	Before cleaning		After cleaning	
	Peak position (cm <sup>-1</sup> )	Peak height (a.u)	Peak position (cm <sup>-1</sup> )	Peak height (a.u)
CH <sub>2</sub> asymmetric stretch	2932	4.925	2932	4.992
Amide I	1655	1.657	1655	1.670
CH <sub>2</sub> & CH <sub>3</sub> bending	1450	1.760	1450	1.757
Phe & Trp	1004	0.601	1004	0.616
Skeletal C-C stretch	936	0.316	936	0.343
Tyr	644	0.189	644	0.186
Phe	622	0.116	622	0.116
S-S stretch	512	0.435	508	0.403

### 3.5.2 Fibre Sample Thickness

A challenge encountered in this investigation at the initial stages of this research was keeping the thickness of the fibre bundles fairly constant and the initial investigation of this study involved examining the influence of varying sample thickness on the wool and mohair FT Raman spectra. A simple experiment was carried out, during which the thickness of the wool or mohair fibre bundles (test specimens) was deliberately varied to determine the effect on the Raman bands. A fibre bundle (FB1) was drawn from the

container and inserted on the instrument for spectral acquisition and after the acquisition the same fibre bundle was folded once to produce a test sample approximately double in thickness (FB2). Kumar *et al.*, (2015) argued that variations or fluctuations in sample thickness are most likely to occur in practice, irrespective of how carefully the sample has been prepared and that could affect the peak height. It was also found that, in the current study, the main challenge experienced was to keep the thickness of the fibre bundles approximately constant. As evident in Figure 3.6, doubling the thickness of the fibre bundle, was accompanied by a vertical shift in the Raman spectra, resulting in increased peak heights or intensities of not less than 10% for all the analysed Raman bands.

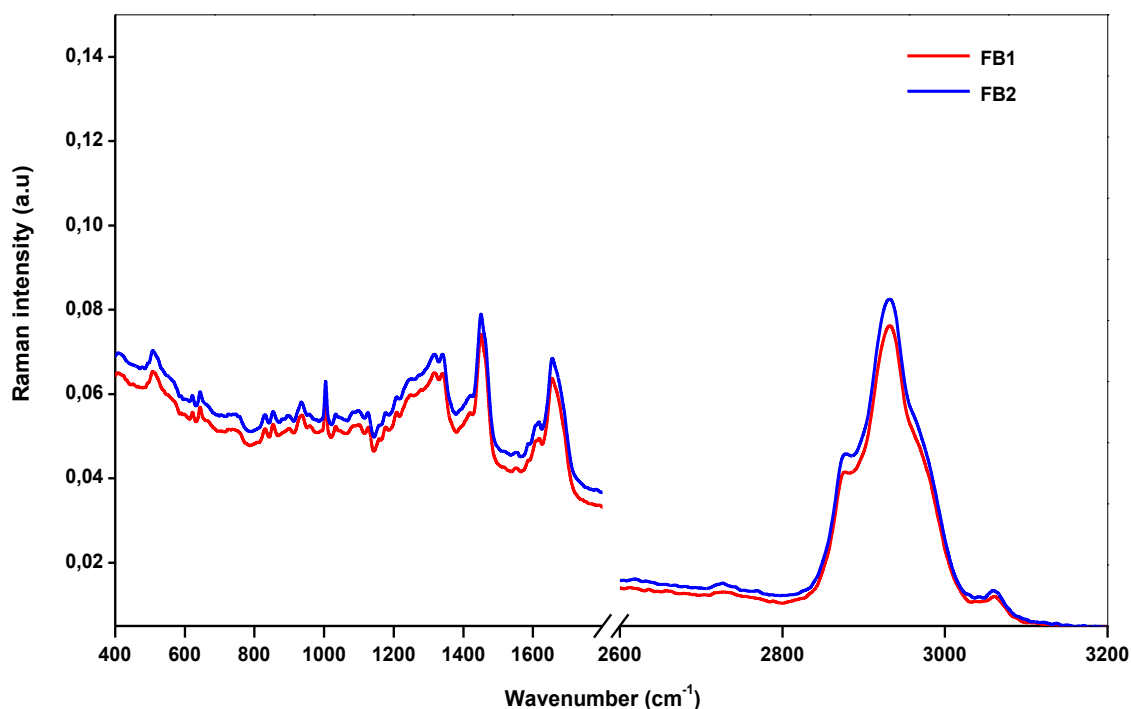


**Figure 3.6: Effect of doubling wool sample thickness on Raman spectra.**

When a third fibre bundle (FB3) was constructed by folding FB2 once, a further increase in the absolute band intensities was observed (Appendix 2 (a)) and occasionally a considerably large decrease of peak heights was also observed which might probably be attributed to the significantly large absorption of the excitation laser photons, resulting in very small backscattered signal reaching the detector. According to Kumar

*et al.*, (2015), the simple approach of taking peak height or intensity ratios (ratiometric analysis) can significantly reduce the effect of the sample thickness variation. This is illustrated for the present study in Figure 3.7:

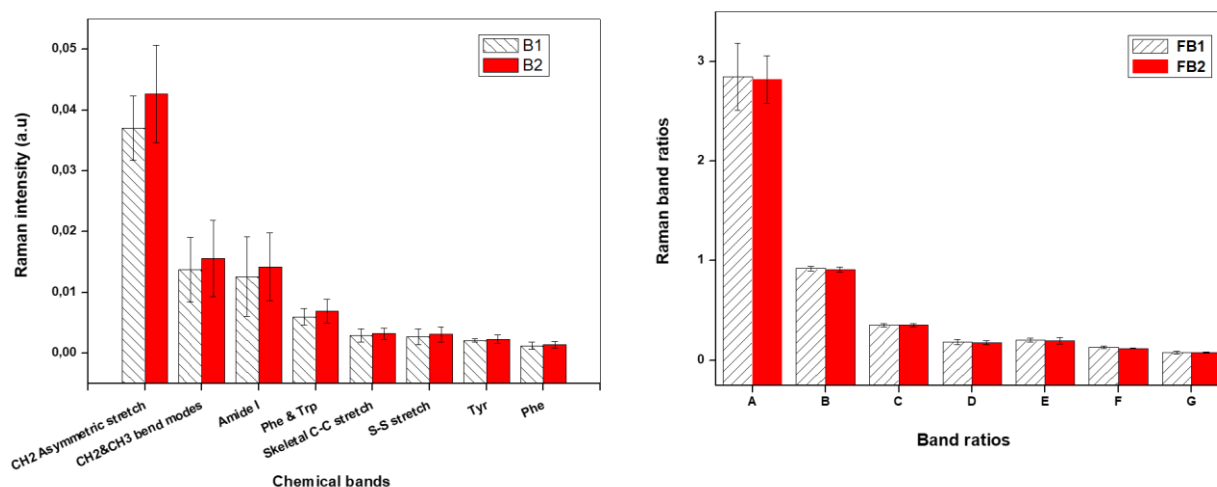


**Figure 3.7: Effect of sample thickness on Raman peak heights.**

In Figure 3.7, b, the Ratios A-G represent the absolute intensities of the very strong CH<sub>2</sub> asymmetric stretch, the amide I, Phe & Trp (around 1004 cm<sup>-1</sup>), skeletal C-C stretch, disulphide S-S stretch, Tyr (near 643 cm<sup>-1</sup>) and Phe (at 622 cm<sup>-1</sup>), respectively, as a ratio of the intensity of the CH<sub>2</sub> and CH<sub>3</sub> bending modes.

### 3.5.3 Laser Drift During Spectral Acquisition

The wavelength of the laser must remain constant during spectral acquisition in order to avoid deterioration of the spectral resolute. The laser drift was also investigated as a possible factor which could influence the variation of the fibre Raman spectral features. Raman band relative intensities, extracted using the baseline method, were then analysed for variability for each of the fibre bundles and spots. Figure 3.8 shows, as an example, baseline corrected Raman spectra for wool and mohair fibre bundles. Most notable is the random change in the average relative peak heights from spot to spot (a, b or c) within the same fibre bundle. This may be as a result of the existing

heterogeneity of wool fibres which could not only be observed in fibres of different individual animal but along the length of the same fibre (Marshall and Gillespie, 1988).

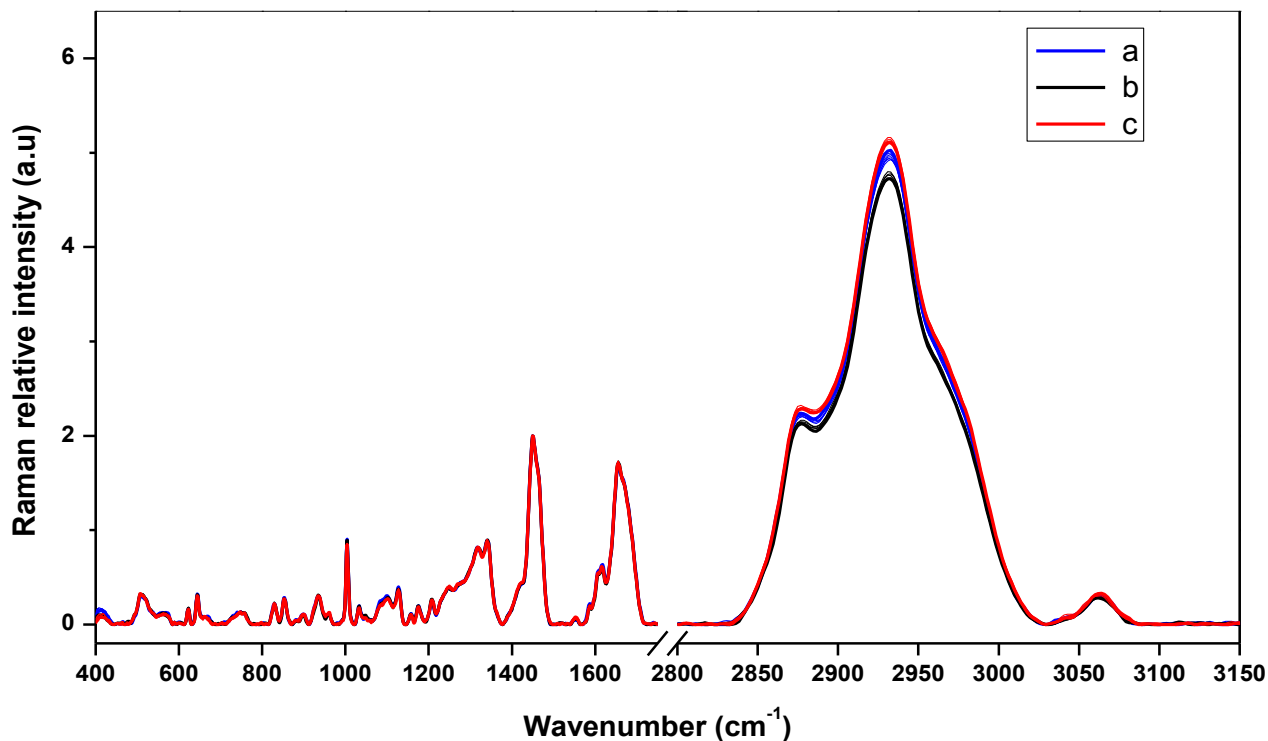


**Figure 3.8: Relative peak height variation along the length of the fibre bundle.**

The statistical comparison of the average peak heights/intensities between the two fibre bundles drawn from the same sample container always proved that the two fibre bundles indeed have been drawn from the same fibre container for all the samples involved in this analysis, the student t-test proving statistical insignificance ( $p > 0.05$ ) in the comparison of the mean relative intensity values of the two fibre bundles. This was the case for all the samples involved in the investigation.

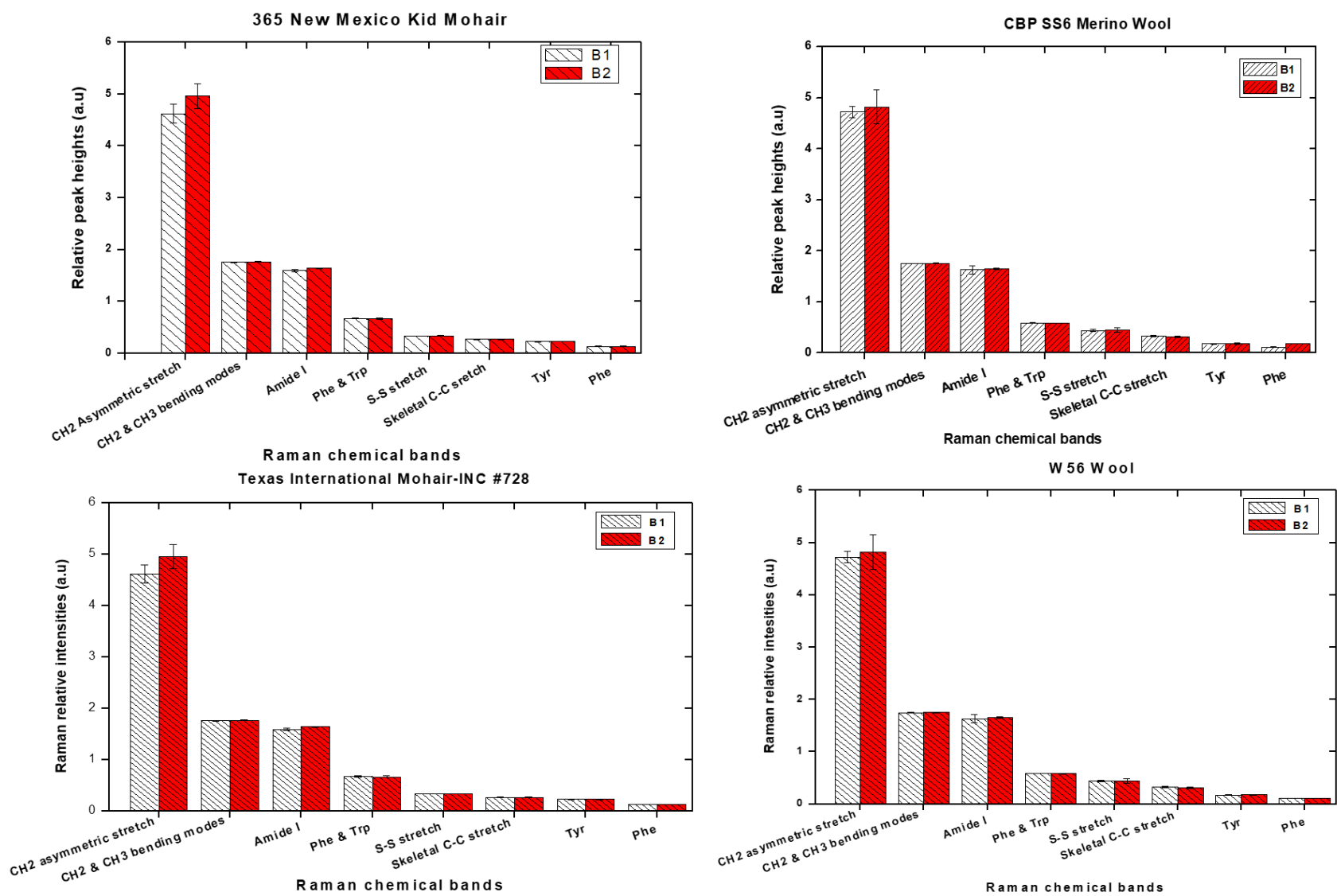
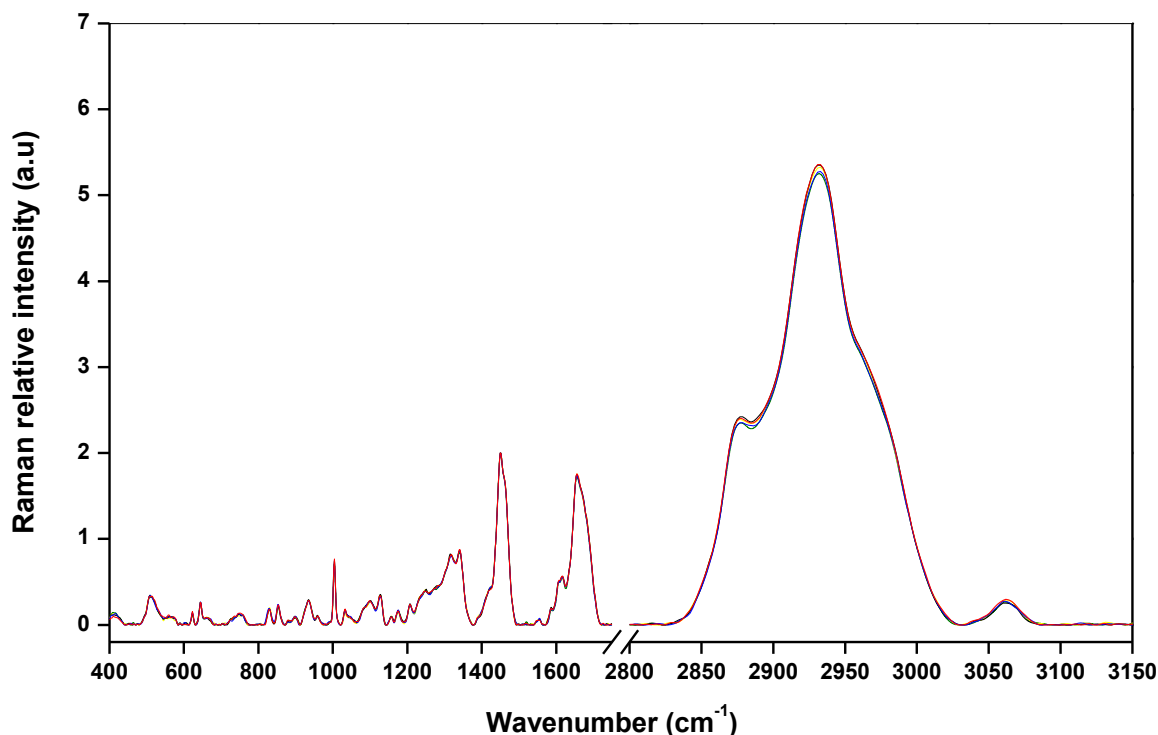


Figure 3.9: Variation in the Raman peak heights between fibre bundles of the same wool and mohair sample.

In Figure 3.10 five spectra acquired from the same spot in a fibre bundle (365 New Mexico Kid mohair sample) are shown. Generally, it is noticeable that only very minor (i.e., insignificant) variations occur between the relative peak heights obtained from the same spot (see Figure 3.10 and Appendix 2). The relative peak heights, for all the analysed bands, were found to vary less than 2% at any single spot. The observed small variations were random and might probably be due to the possible shift in focus of the laser beam during spectral acquisition.



**Figure 3.10: An example of the relative peak height variation within the same spot.**

Spectra with strong fluorescence background (Figure 3.11) were also found to potentially contribute in the variation of the relative peak heights. There was a great difficulty in identifying and analysing the weak Raman bands, these including the S-S stretch ( $508\text{ cm}^{-1}$ ), the Tyr ( $644\text{ cm}^{-1}$ ) and Phe (around  $622\text{ cm}^{-1}$ ) bands. Because of this, a decision to ignore such spectra was taken; the relative peak heights presented throughout this study does not include data taken from such spectra.

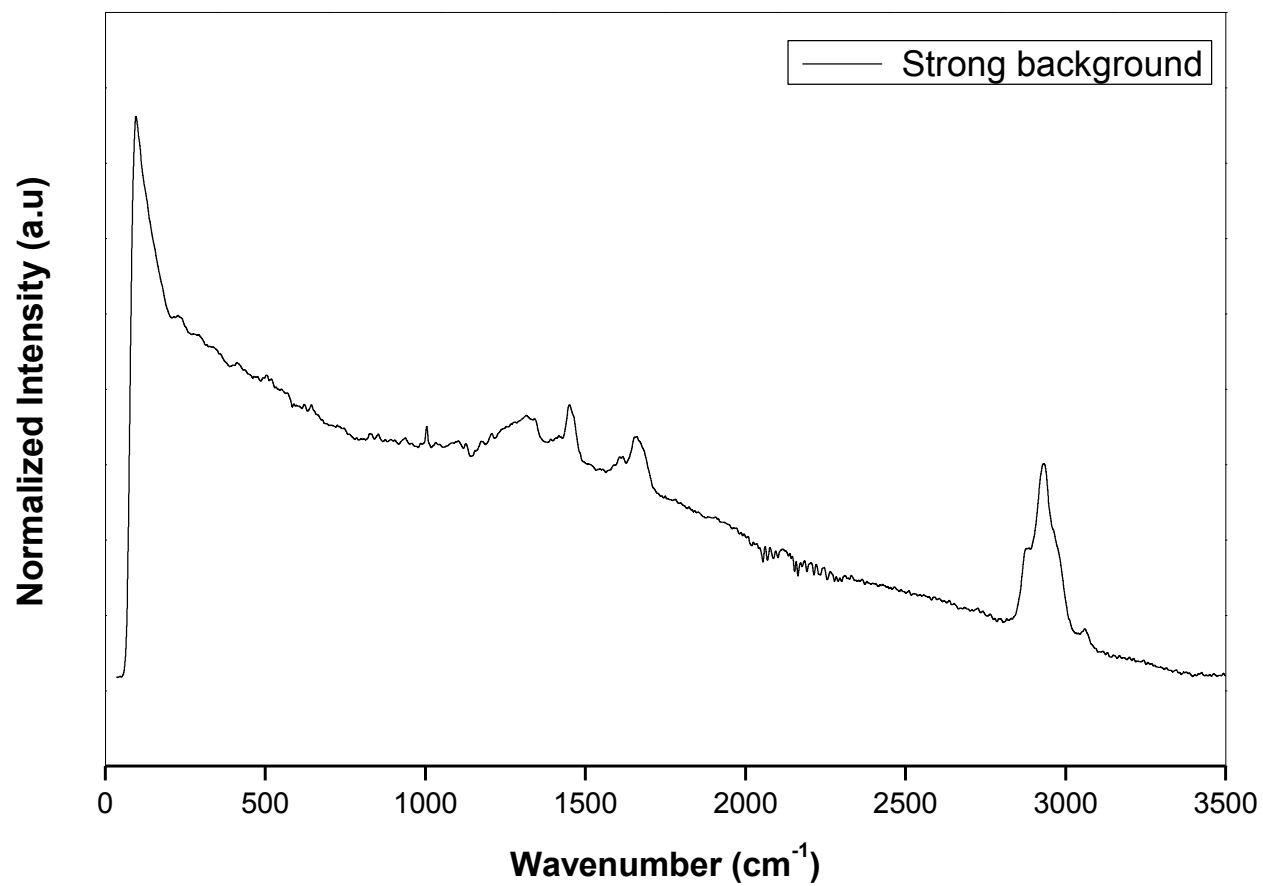


**Figure 3.11: Wool Raman spectrum with a strong fluorescence background.**

## CHAPTER FOUR

### RESULTS AND DISCUSSION

#### 4.1 INTRODUCTION

The detailed results obtained on scoured wool and mohair fibre samples examined using the Bruker Ram II FT-Raman module, Horiba Lab-RAM HR Raman micro-spectrometer and Bruker ATR FTIR-LUMOS micro-spectroscopy, are presented and discussed in this chapter, within the context of determining which of these provide a possible means for distinguishing between wool and mohair. The Bruker Ram II FT Raman system is the main Raman characterization technique and focus of this research because it is quick, easy to operate, reliable and could reduce cost of animal fibre identification tests. The analysis on the Bruker Ram II FTR system, moreover, does not require complex sample preparation. The latter becomes an important consideration in terms of cost reduction. The fact that the results also do not suffer from the risk of fluorescence is another added advantage of the Bruker Ram II FTR system. One of the disadvantages of the 1064 nm excitation wavelength used in the Bruker Ram II FTR is the inherently weak Raman bands, which is due to the strong dependence of the band intensity on the excitation wavelength.

It should be noted that some of the Raman spectra to be presented in this chapter were acquired on a Horiba Lab-RAM HR Raman micro-spectrometer from the Raman Laboratory in the School of Physics at the University of the Witwatersrand in Johannesburg, and the results are briefly compared with the results obtained on the Bruker FTR spectroscopic system.

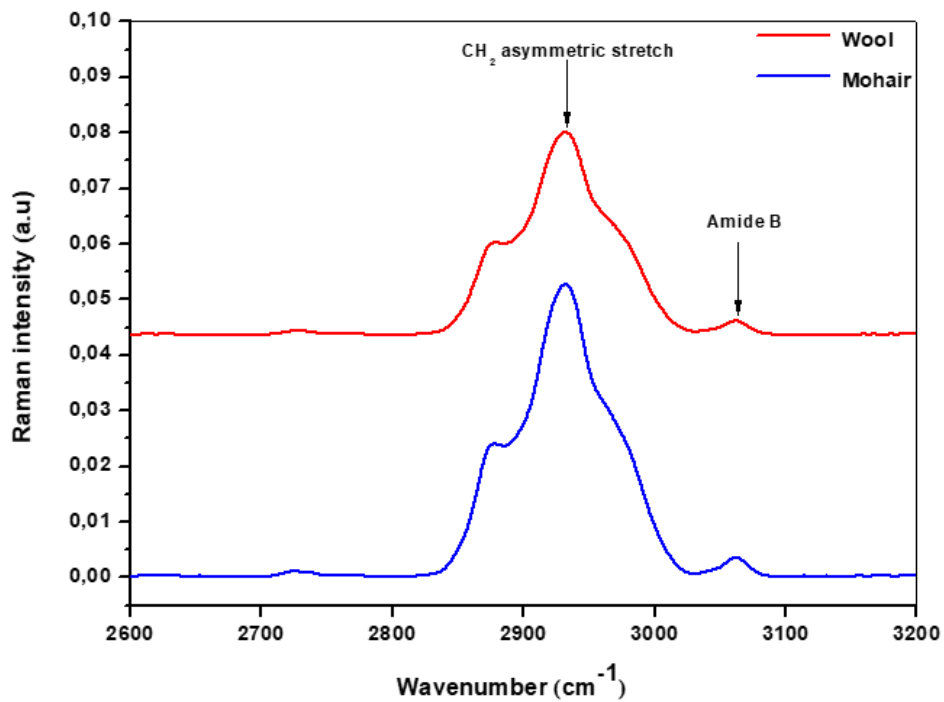
The results obtained from the micro-FTIR analysis aimed at investigating the possible application of the amide band ratio (amide I/amide II) for wool and mohair fibre identification and classification are also presented in this chapter, these having been performed at the Dermatology Department of the University of Cape Town (UCT), as detailed earlier.



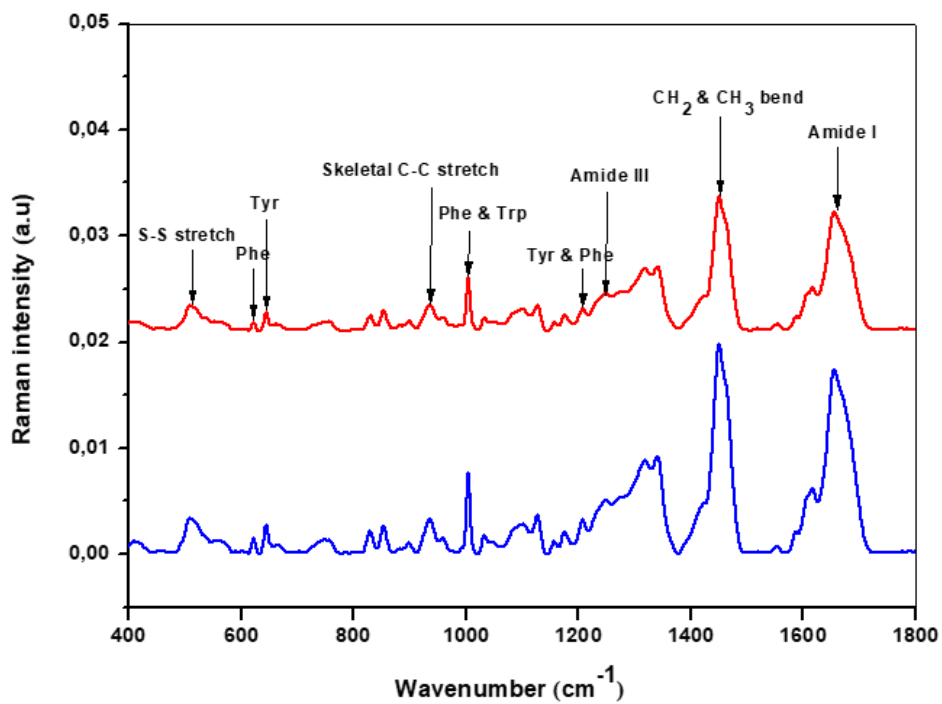
### 4.2.1 FT Raman Spectroscopic Analysis

Wool and mohair fibres share similar basic chemistry, comprising mainly keratin proteins, thus, making it extremely difficult to distinguish between them using chemical techniques. The current research project investigates the possible application of vibrational spectroscopic techniques, especially FT Raman spectroscopy, to distinguish between wool and mohair. The extensive literature review presented earlier in this research showed the huge reduction in fluorescence as the chief advantage of using FT Raman spectroscopy to study keratin fibres. Literature has also showed that differences exist in the amino acid composition of different keratin fibres, such as wool and mohair due to genetic, diet and environmental factors and also in the different fibre structural components (i.e. cuticle and cortex), with some researchers showing that these differences could be reflected in the Raman spectra, particularly in the intensities of the bands associated with respective amino acids. With these facts in mind, this research was initiated to assess the application of Raman spectroscopy for distinguishing between wool and mohair fibres. Compared to the traditional microscopic methods, which are time consuming and costly, and highly dependent on the experience of the operator, Raman spectroscopy is fast and does not require an experienced operator.

Plots of wool and mohair average Raman spectra, obtained in this study, are shown in Figures 4.1 (a) and (b) representing the n(CH) regions 2600–3200  $\text{cm}^{-1}$  and the 400–1800  $\text{cm}^{-1}$ , respectively. These spectral regions contain spectral features that are characteristic of protein or keratin fibres, including the amide I and III features and information about the skeletal backbone, including the disulphide S–S crosslinking modes of the cystine residues. In the spectral regions 0–400  $\text{cm}^{-1}$  and 1800–2600  $\text{cm}^{-1}$  there are no spectral features of interest and have therefore been omitted in the spectra. The spectra were acquired with 2000 scans (equivalent to 1 hour acquisition time), using the maximum laser power (i.e. 500 mW), and a spectral resolution of 4  $\text{cm}^{-1}$ . These acquisition parameters produced spectra of adequate signal-to-noise ratio and were also highly reproducible.



a



b

Figure 4.1: Baseline corrected average FT Raman spectra of wool (red) and mohair (blue) in the (a) 2600-3200  $\text{cm}^{-1}$  and (b) 400-1800  $\text{cm}^{-1}$  spectral regions.

There were no observable differences in the Raman band shapes of wool and mohair spectra obtained in this study (as shown in Figure 4.1). Generally, wool and mohair have identical FT Raman spectral features which cannot in any way be distinguished with the naked eye as these fibres share similar chemical compositional information, there being no chemical band which is specific to one fibre type. Manually locating the exact spectral band positions of the characteristic bands in a spectrum can be time consuming and often in-accurate and often requires use of a software. A peak picking command in the OPUS 7.2 software package was used in this study to locate specific band positions of wool and mohair, both accurately and rapidly.

Table 4.1 compares the wool and mohair band positions observed in this study with those found in other studies, namely those found for wool by Carter *et al.* (1994), one of the earliest published research studies on FT Raman analysis of wool fibres and those for mohair reported by Michielsen (2001), the only research article found containing Raman spectral information on mohair fibres.

**Table 4.1: FT Raman band assignments for wool and mohair, respectively.**

WOOL		MOHAIR		Band Assignments	Intensity
This study	Carter <i>et al.</i> , (1994)	This study	Michielsen (2001)		
3062	3062	3062	N.O	Amide B, C-N-H bend overtone	S
2976	2975	2976	N.O	CH <sub>2</sub> asymmetric methine stretch	S, Sh
2932	2931	2932	2930	CH <sub>2</sub> asymmetric stretch	VVS
2880	2880	2880	2879	CH <sub>3</sub> symmetric stretch	S
2848	2848	2848	N.R	CH <sub>2</sub> symmetric stretch	W, Sh
1655	1653	1655	1653	Amide	VS
1616	1614	1616	N.R	Tyr and Trp	M
1555	1553	1555	N.R	Trp	W
1450	1448	1450	1450	CH <sub>2</sub> & CH <sub>3</sub> bending modes	VS
1340	1338	1340	N.R	CH <sub>2</sub> bend, Trp	S
1318	1318	1318	1310	C <sub>α</sub> -H bend	S
1277	1281	1277	N.R	Amide III (α)	W
1248	1244	1248	1245	Amide III (unordered)	W
1208	1207	1208	1208	Tyr & Phe	M
1176	1176	1176	N.R	Tyr	W
1156	1155	1156	1157	C-N stretch	VW, Sh

**Table 4.1 continued...**

WOOL		MOHAIR		Band Assignments	Intensity
This study	Carter <i>et al.</i> , 1994	This study	Michielsen 2001		
1126	1126	1126	N.R	C-N stretch	W
1083	1079	1079	1079	C-N stretch	W
1033	1031	1033	1035	Phe	W
1004	1002	1004	1003	Phe & Trp	S
959	952	959	959	CH <sub>2</sub> rock	W
936	934	936	935	Skeletal C-C stretch ( $\alpha$ )	S
899	897	899	901	Skeletal C-C stretch ( $\alpha$ )	W
882	881	881	881	Skeletal C-C stretch ( $\alpha$ )	VW
854	851	854	855	Trp	M
830	828	830	833	Tyr	W
758	752	758	758	Trp	M
662	661	662	661	Cys C-C stretch	VW
645	642	645	647	Tyr	W
622	618	622	622	Phe	W
541	546	541	N.R	Cys S-S stretch	W, Sh
530	527	530	N.R	Cys S-S stretch	W, Sh
509	512	508	512	Cys S-S stretch	M

**W-Weak, S-Strong, VS-Very Strong, VW-Very Weak, M-Medium, Sh-Shoulder, N.O-Not Observed, N.R-Not Reported.**

As shown in the table (Table 4.1), the results of this study were found to compare well with results of the two earlier studies (i.e. Carter *et al.*, 1994 and Michielson, 2001), with minor variations in the band positions. Raman spectra of wool and mohair are characterized by the very strong CH<sub>2</sub> asymmetric stretching modes found around 2932 cm<sup>-1</sup>, which is due to the C-H stretching of the lipid alkyl chains. The position of the maximum peak of this band was found to vary slightly (between 2931 and 2933 cm<sup>-1</sup>) in this study, for both wool and mohair. The strong amide I band, with the maximum peak position typically found around 1654 cm<sup>-1</sup>, is another spectral feature dominating the Raman spectra of natural animal or protein fibres. The amide I mode is predominantly due to the peptide carbonyl stretching vibration of the CONH unit, together with an out-of-phase C-N stretching component, with some contribution also coming from the C-C-N deformation. In the current study, the position of the amide I peak maximum also varied slightly between 1654 and 1656 cm<sup>-1</sup>, corresponding to the dominance of the  $\alpha$ -helical secondary structure of protein fibres (Church *et al.*, 1997). This variation was observed in the Raman spectra of both wool and mohair and could not be associated with either fibre type. The amide I spectral region is rich in band components, including components around 1670 and 1690 cm<sup>-1</sup>, corresponding to different secondary structural conformations. These are resolved by a curve fitting procedure discussed in section 4.2.1.1 of this thesis. Another Raman band of strong intensity observed in all the spectra in the current study is the CH<sub>2</sub> & CH<sub>3</sub> bending modes, which was always found around 1450 cm<sup>-1</sup> for both wool and mohair. This band is believed to be due to the CH<sub>2</sub> and CH<sub>3</sub> deformation of the protein and lipids (Wang *et al.*, 2016). Spectral features, of weak and medium strong intensities, from the aromatic amino acids were also observed in the 1300-1400 cm<sup>-1</sup> spectral region. These include Raman bands due to aromatic amino acids, phenylalanine (Phe), tryptophan (Trp). Those of interest in this research are the overlap of the ring breathing modes of both phenylalanine and tryptophan (Phe and Trp found around 1004 cm<sup>-1</sup>), Tyr found near 644 cm<sup>-1</sup>, and the Phe (around 622 cm<sup>-1</sup>). Another band of high significance in the Raman spectrum of natural animal fibres is the amide III band, which was always observed in the 1230-1310 cm<sup>-1</sup> spectral region for both wool and mohair in the current research study. This spectral region produced a very complex pattern of bands due to the overlap of the frequency ranges characteristic

of the  $\beta$ -sheet (1230-1245) and random coil (1240-1255) (Herrero, 2007). The amide II band, which is very strong in the IR spectrum of keratins, appears as a very weak band around  $1555\text{ cm}^{-1}$  in both the wool and mohair spectra. Raman spectra for keratin fibres also show the disulphide S-S stretch vibration (near  $512\text{ cm}^{-1}$ ). The position of the main component of the disulphide S-S stretch band was found to vary between 506, 507, 509, 510 and  $512\text{ cm}^{-1}$  in the current study. These band positions are consistent with those found in the literature (Kuzuhara and Hori, 2002; Sugeta *et al.*, 1973) for untreated wool fibres, being proof of the existence of wool protein structure in the gauche-gauche-gauche (GGG) structural conformation.

Although there were some minor variations in the band positions (i.e. wavenumbers) between the wool and mohair spectra, these variations were not consistent and were not specific to one fibre type to allow them to be used in distinguishing between wool and mohair. The most complex bands, amide I and the S-S stretch, were analysed utilizing curve-fit OriginLab 8.0 and OPUS 7.2 software packages based on the Levenberg-Marquardt (LM) algorithm, the Gaussian peak shape being employed. The positions (wavenumbers) and the intensities of the amide and the S-S stretching vibrations, with those of their band components, have previously been found to be associated with the micro-structure of protein fibres. The deconvolution or curve fitting of the two bands was conducted with the aim of finding out whether any differences exist in the conformation of the secondary structure of the two fibre types.

#### **4.2.1.1 Curve-Fitting of the Amide I and S-S Stretching Vibrations**

In this section, the amide I and the S-S stretch vibrations from the Raman spectra of wool and mohair fibres are analysed in detail using the curve fitting technique. The shape, position, width and the height of a spectral band all contribute to the complete description of the IR or Raman spectrum. Friesen *et al.* (1991) stated that curve-fitting is an essential tool in the accurate description of several band components contributing to different bands in the entire spectrum. The curve fitting results were compared for the wool and mohair spectra for potential differences in the protein secondary structures, characterized by slight differences in the position and band shape of the amide I band

(Akhtar *et al.*, 1997). The spectral range selected for the fitting of the amide I band was between 1550 and 1750  $\text{cm}^{-1}$ .

The spectral range 450-600  $\text{cm}^{-1}$  was selected for fitting of the S-S stretching vibration. Because of the complexity of the amide I and the S-S stretch Raman bands, resolution of the two bands into their components was necessary. This was achieved by the curve fitting procedure, which was carried out using the OPUS 7.2 and Origin Lab version 8.0 software packages. All bands in the normalized spectra were fitted with Gaussian curve, which provided very low errors compared to the Lorentzian curve fit. The band positions were estimated based on previous literature (Church *et al.*, 1997; Rintoul *et al.*, 2000; Wojciechowska *et al.*, 2004) and the second derivative analysis. The quality of the fit was estimated by the reduced chi ( $\chi^2$ ) value and the coefficient of determination (COD  $R^2$ ) (see Table 4.2 and 4.3).

**Table 4.2: The accuracy of wool and mohair FT Raman amide I curve fitting.**

Statistic	Mohair		Wool	
	COD ( $R^2$ )	Reduced $\chi^2$ values	COD ( $R^2$ )	Reduced $\chi^2$ values
Average	0.999	$3.54 \times 10^{-5}$	0.999	$2.69 \times 10^{-5}$
Standard deviation ( $\sigma$ )	$2.22 \times 10^{-16}$	$1.33 \times 10^{-5}$	$2.87 \times 10^{-4}$	$8.24 \times 10^{-6}$

**Table 4.3: The accuracy of wool and mohair FT Raman S-S stretch curve fitting.**

Statistic	Mohair		Wool	
	COD ( $R^2$ )	Reduced $\chi^2$ values	COD ( $R^2$ )	Reduced $\chi^2$ values
Average	0.997	$4.95 \times 10^{-5}$	0.998	$1.53 \times 10^{-5}$
Standard deviation ( $\sigma$ )	$1.44 \times 10^{-3}$	$2.65 \times 10^{-5}$	$1.43 \times 10^{-3}$	$2.97 \times 10^{-5}$



The amide I band (around  $1654\text{ cm}^{-1}$ ) and the S-S stretch (around  $512\text{ cm}^{-1}$ ) components, found in wool and mohair spectra are summarized in Tables 4.4 and 4.6, respectively. The second derivative analysis was carried out to help locate band components in the amide I ( $1550\text{-}1750\text{ cm}^{-1}$ ) and the S-S stretch ( $480\text{-}550\text{ cm}^{-1}$ ) spectral regions. Figure 4.2 shows some examples of the typical FT Raman second derivative spectra for wool and mohair, respectively. These clearly indicates that the selected spectral ranges namely the amide I and S-S stretching vibration, indeed have identical spectral features for both wool and mohair.

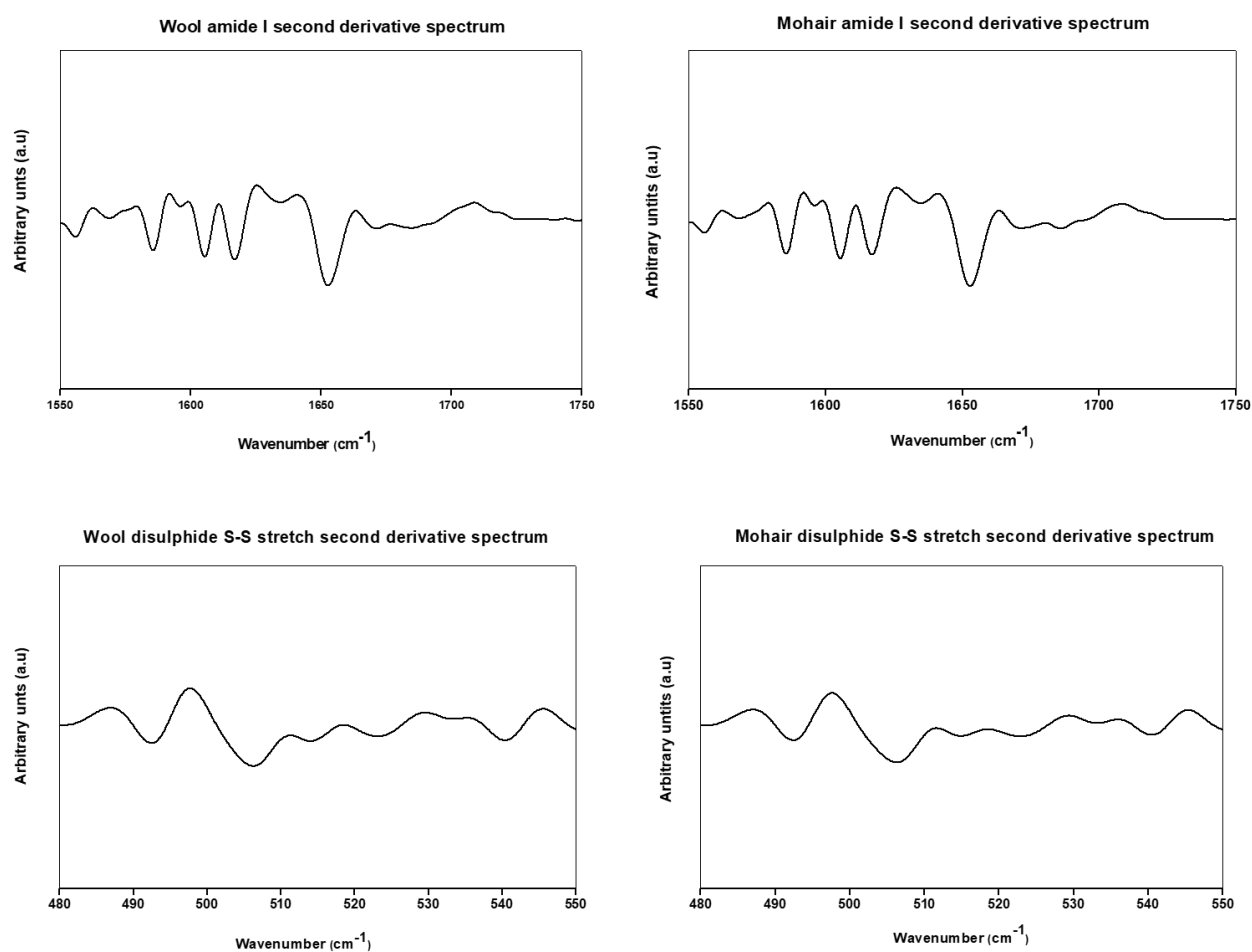


**Figure 4.2: Raman second derivative spectra of the amide I (top) and the S-S stretch (bottom) spectral regions for wool (left) and mohair (right) fibres.**

According to these second order derivative spectra, the wool and mohair amide I and the S-S stretch spectral regions contain the same number of band components in the

same spectral positions, and hence cannot be used to distinguish between them. During curve fitting procedure, all parameters could vary except the component peak shape which was always kept at 100 % Gaussian. The best curve fitting results show that the amide I band has eight band components of different intensities and full width at half maximum (FWHM) in both wool and mohair spectra.

Notably, there were no unique band components specific to one fibre type which could be used to qualitatively distinguish between wool and mohair. The amide I band curve fitting (Figure 4.3) results were identical for both the wool and mohair spectra, with a peak maximum near  $1652\text{ cm}^{-1}$ , corresponding to the  $\alpha$ -helical structural conformation of the protein or polypeptide chain. Zhou (2012) showed that the unstretched mohair Raman spectrum is dominated by the 1658 and the 1648, confirming the dominance of the  $\alpha$ -helical structural conformation. The amide I band of wool and mohair which has contributions from the  $\beta$ -sheet structural conformation, may also have contributions from segments of disordered polypeptides (Church *et al.*, 1997). This band component is found to slightly vary between  $1669$  and  $1671\text{ cm}^{-1}$  in both the wool and mohair spectra.

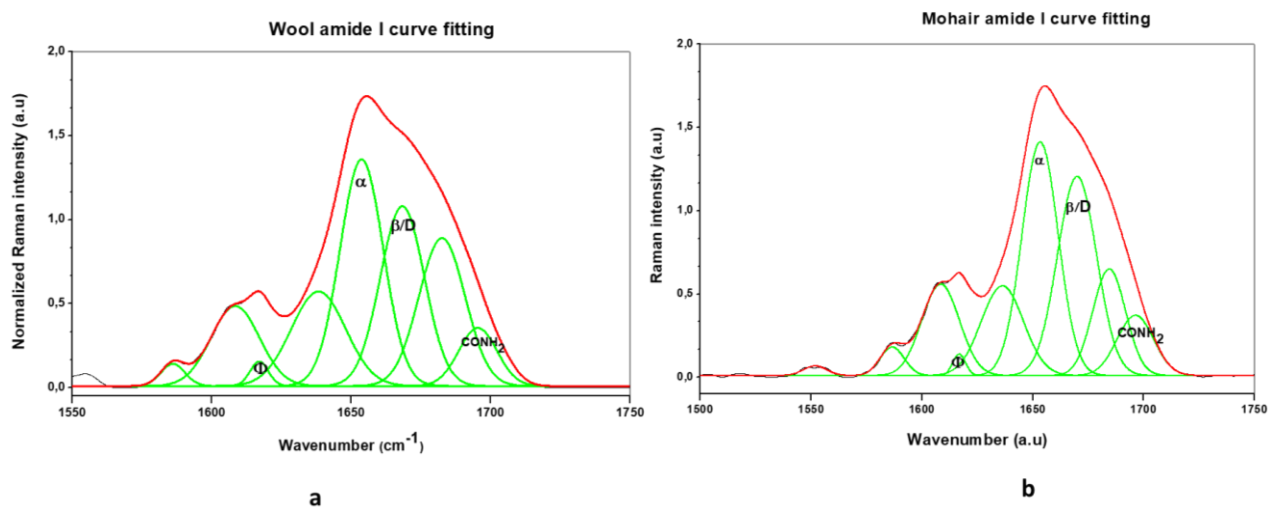


**Figure 4.3: Amide I curve fitting on (a) wool and (b) mohair Raman spectra.**

The COD and chi-squared values are shown in the statistics shown in appendix III, with the COD values ranging These results are a confirmation that wool fibres and other keratin fibres, such as mohair, when in their natural state, exist predominantly in the form of an  $\alpha$ -helical secondary structure (Carter and Edwards, 2001; Church *et al.*,

1997; Edwards *et al.*, 1998). Table 4.4 summarizes the amide I band resolution results for the wool and mohair. The weak Raman band around  $1586\text{ cm}^{-1}$ , previously assigned to the C=C olefinic stretching modes (Edwards *et al.* (1995); Pezolet *et al.* (1976)), was found to differ in the relative intensity between wool and mohair spectra. The band area of this band varied from 0.48 to 1.86 for wool fibre samples while these varied from 1.24 to 3.56 for mohair, with the mean values of 0.96 and 2.29 for wool and mohair fibre samples, respectively. These average values were found to differ significantly ( $p < 0.05$ ).

**Table 4.4: Amide I band components from wool and mohair spectra.**

Band component	Wool			Mohair		
	Height	FWHM	Peak area	Height	FWHM	Peak area
1586	0.12	7.62	0.96	0.17	10.17	2.29
1607	0.38	15.95	8.91	0.54	16.91	9.94
1617	0.20	7.44	1.99	0.18	6.76	2.04
1636	0.41	15.21	10.29	0.55	16.76	11.81
1653	1.28	16.28	24.52	1.40	15.77	33.88
1670	1.04	16.72	18.64	1.05	16.69	19.24
1685	0.71	16.01	17.84	0.79	16.45	16.29
1695	0.30	12.57	3.56	0.33	15.97	5.08

The band component at  $1695\text{ cm}^{-1}$ , assigned to the amide group of the asparagine and glutamine side chains, was observed in both wool and mohair. The amide I band components in the low wavenumbers, including the  $1617\text{ cm}^{-1}$  ( $\phi = \text{Tyr/Trp}$ ) assigned to be due to the ring breathing modes of the tyrosine and tryptophan, were also included in the observed. The  $1608\text{ cm}^{-1}$  component has been associated with the amino acid

tyrosine (Tyr) vibrations. A statistical comparison of the average relative intensities of the 1653  $\text{cm}^{-1}$  band component, between wool and mohair, proved that these differed significantly ( $p < 0.05$ ). The intensities of the band associated with the  $\beta$ -sheet/or disorder (1670  $\text{cm}^{-1}$ ) protein structure, did not differ for wool and mohair ( $p > 0.05$ ). The band component around 1685 has been assigned to the  $\beta$ -Turn.

The contents of the  $\alpha$ -helical and  $\beta$ -pleated sheet protein structure of wool and mohair were also analysed in this study, with the  $\alpha$ -helical structure having been defined as the band area ratio of the 1654  $\text{cm}^{-1}$  component of the amide I to that of the  $\text{CH}_2$  &  $\text{CH}_3$  bending modes (around 1450  $\text{cm}^{-1}$ ) while the content of the  $\beta$ -sheet structure has been previously defined as the band area ratio of the 1670  $\text{cm}^{-1}$  of the amide I to that of the  $\text{CH}_2$  &  $\text{CH}_3$  bending modes (Panaiotou, 2004). Table 4.5 summarizes the results of the protein secondary structure for wool and mohair fibres.

**Table 4.5: Raman secondary structure of wool and mohair fibres.**

<b>Fibre type</b>	<b>Wool (Mean (%))</b>	<b>Mohair (Mean (%))</b>
$\alpha$ -helical	40.5	49.3
$\beta$ -pleated sheet	29.7	27.2
$\beta$ -Turn	29.8	23.5

Evident from the Table 4.5, mohair samples possess high contents of the  $\alpha$ -helical protein structure compared to wool. The reason for this could stem from the fact that the ratio of intermediate filaments (IFs) (rich in the  $\alpha$ -helical proteins) to the matrix (which is rich in the high-sulphur proteins), IFs/matrix, is high in ortho cortical cells than in the para-cortex (Marshall *et al.*, 1991). The application of these secondary structure quantities in blend composition analysis of wool and mohair, however, seem potentially difficult if possible, at all. The application of different characterization techniques, such as X-ray diffraction (XRD) and solid-state NMR, may be essential to determine and

confirm the quantities of the protein structural conformation for the two fibres, wool and mohair.

Figure 4.4 illustrates typical curve fitting results of the S-S stretching vibration for wool and mohair.

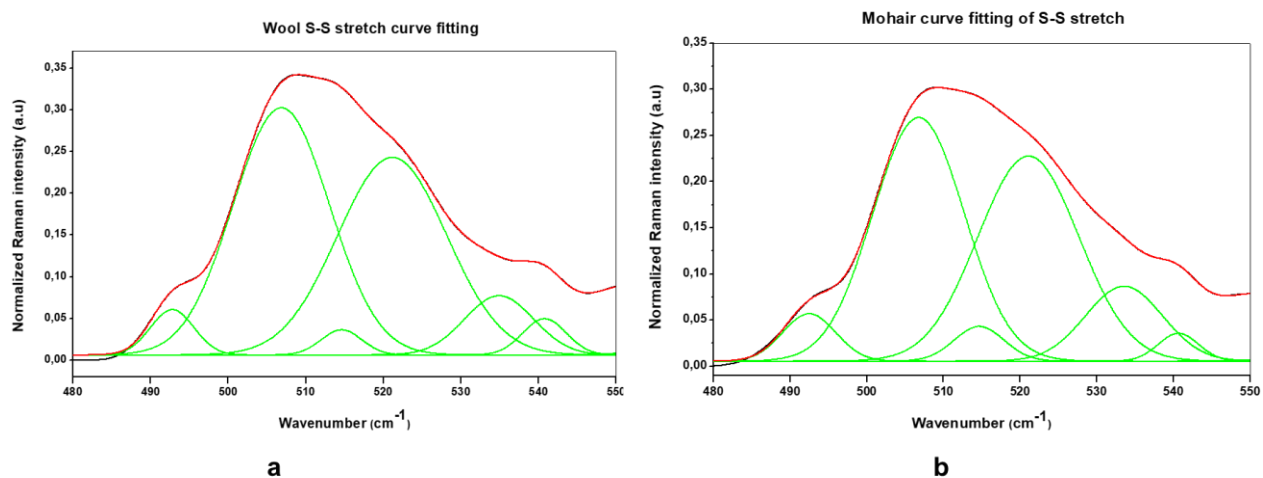


**Figure 4.4: Typical curve fitting results of the S-S stretching vibration for (a) wool and (b) mohair spectra.**

Clearly, the S-S stretching vibration components from wool and mohair spectra are similar in both shape and band positions but slightly differ in intensities or peak heights (as shown in Figure 4.4). Table 4.6 summarizes the results of the S-S stretch curve fitting results for wool and mohair:

**Table 4.6: Raman band components analysis of the S-S stretch band for wool and mohair.**

Band component	Wool		Mohair	
	Height	FWHM (cm <sup>-1</sup> )	Height	FWHM (cm <sup>-1</sup> )
493	0.06	4.92	0.05	5.17
507 <sup>a</sup>	0.27	10.40	0.22	11.62
515	0.11	5.68	0.10	5.45
533	0.06	5.90	0.07	6.20
523 <sup>b</sup>	0.14	10.16	0.15	10.23
540 <sup>c</sup>	0.07	5.82	0.06	5.59

<sup>a</sup> Assigned to the gauche-gauche-gauche (g-g-g) conformation of the S-S stretching.

<sup>b</sup>Assigned to the gauche-gauche-trans (g-g-t) conformation of the S-S stretching.

<sup>c</sup>Assigned to the trans-gauche-trans (t-g-t) conformation of the S-S stretching.

Wool and mohair, generally have a maximum intensity at around 507 cm<sup>-1</sup>, confirming the claim made by Sugeta *et al.*, (1973) that untreated keratin fibres generally exist predominantly in the gauche-gauche-gauche structural confirmation. The spectral position of this band component was also varied between 506, 507 508, 510 and 512 cm<sup>-1</sup>. Differences in the intensities of the band components for wool and mohair were also analysed by means of the application of the statistical student t-test. The difference in the average relative intensities of the most dominant band component (at 507 cm<sup>-1</sup>) was found to be statistically significant (p<0.05), this band being more dominant in the wool than in the mohair spectra. Although, the relative intensity average values of this band component were different, the individual values overlapped greatly between wool and mohair. In practice, this great overlap would make the application of this band component in distinguishing between wool and mohair, a difficult task, with the blend composition analysis being even more difficult or even impossible.

#### 4.2.1.2 The Disulphide Content of Wool and Mohair Fibres

Literature has provided evidence that genetic, diet and weathering related factors cause variations in the levels of certain amino acids, Leon (1972) stating that the main variations occur in the amino acids cystine, proline and glycine. Simmonds (1958) has shown that such variations, in certain amino acids, occur between wools of different merino sheep. Reis and Schinckel (1963) reported that different nutritional supplements, such as sulphur-rich diets, maybe the source of the variation in the amino acid contents. The average Raman spectra from each of the wool and mohair samples in Table 3.1 was analysed for disulphide content which is related to the amino acid cystine. A method (Kuzuhara, 2005) for estimating the disulphide content was applied for some of the fibre samples in this study. This was inspired by the differences observed in the peak intensities of the disulphide S-S stretch vibration. The method is based on the ratio of the peak area of the S-S stretching vibration (near  $507\text{ cm}^{-1}$ ), calculated from the peak to a baseline that was drawn between  $450$  and  $610\text{ cm}^{-1}$ , divided by the peak area of the  $\text{CH}_2$  &  $\text{CH}_3$  bending modes (at  $1450\text{ cm}^{-1}$ ), calculated from the peak to the baseline drawn from  $1375$  to  $1507\text{ cm}^{-1}$ . Table 4.7 summarizes the results obtained from this investigation.

**Table 4.7: The disulphide content of wool and mohair fibres.**

Fibre type	Band area		Ratio B/A
	A: $\text{CH}_2$ & $\text{CH}_3$ bend	B: S-S stretch	Disulphide (S-S) content
Wool	62.28	12.20	0.20
Mohair	65.59	11.02	0.17

Table 4.8 contains descriptive statistics for the disulphide analysis.

**Table 4.8: Descriptive statistics for the disulphide analysis of wool and mohair.**

<b>Statistic</b>	<b>Wool</b>	<b>Mohair</b>
1. Mean	0.20	0.17
2. Standard deviation ( $\sigma$ )	0.04	0.03
3. Lowest	0.14	0.11
4. Highest	0.31	0.24
5. Count	50	54
6. Confidence level (95 %)*	0.01	0.01

**Confidence level refers to the 95% confidence interval of the mean.**

The ratios of the area under the C-H band to that of the S-S stretching vibration varied between 0.11 - 0.24 for mohair fibres, with a mean and standard deviation of  $0.17 \pm 0.03$ , while for wool they varied between 0.14 - 0.31, with a mean and standard deviation of  $0.20 \pm 0.04$ . The statistical comparison, using the student t-test of the mean values (shown in Appendix IV), proved them to be statistically significantly different ( $p < 0.05$ ).

This result is to be expected as the low cystine contents are associated with the predominantly ortho-cortex (rich in tyrosine proteins) of mohair fibre than the para-cortical cells (rich in high-sulphur proteins) of wool (Marshall *et al.*, 1991; Hunter, 1993). Nevertheless, the individual values were found to overlap greatly as shown in Figure 4.5, which brings into question the practical applicability of the disulphide content in distinguishing between wool and mohair.



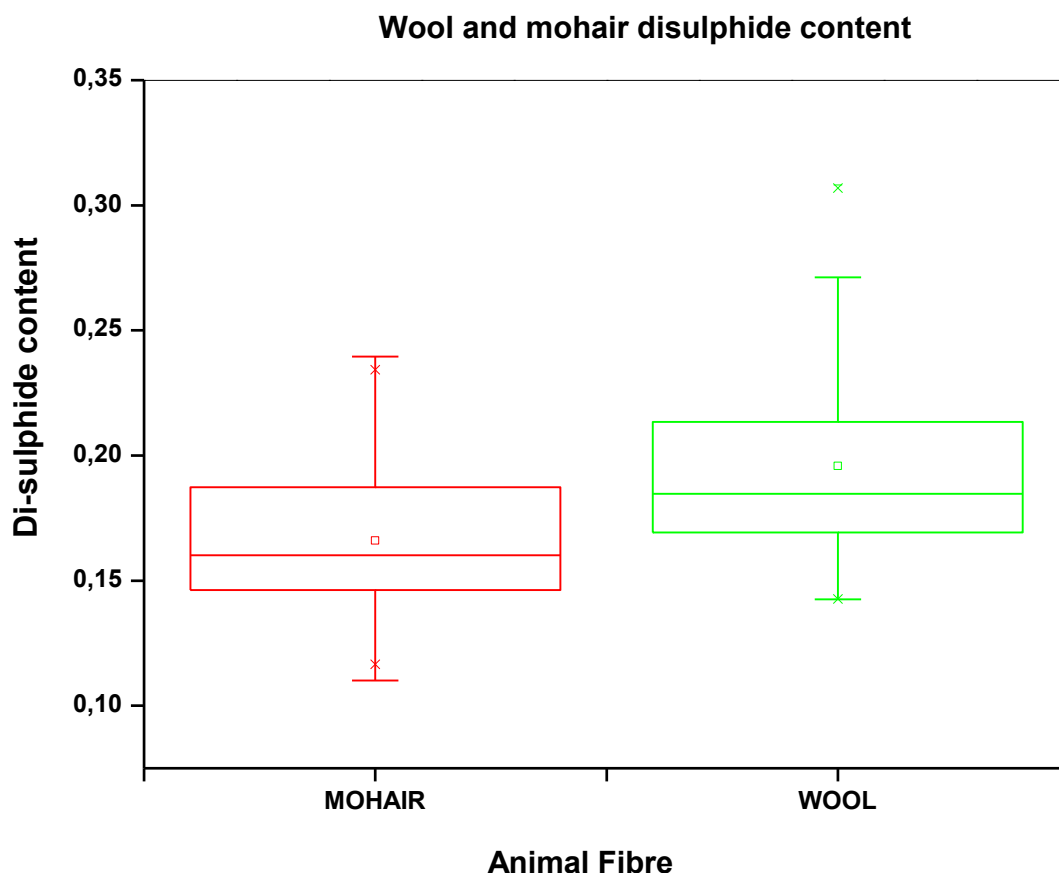


**Figure 4.5: Box whisker plot of the disulphide content values for wool and mohair.**

Furthermore, wool and mohair blend composition analysis, would be an even more difficult task. It therefore appears that this method, based on the disulphide content, is not reliable for the analysis of the composition of wool and mohair blends. A comprehensive amino acid analysis, however, using chromatographic or electrophoretic techniques, of the samples used in this study would be very important, as this would provide a correlation of the estimated cystine or disulphide content obtained here with the results of the conventional techniques (chromatographic or electrophoretic) for amino acid analysis, which are often time consuming. The chromatographic or electrophoretic analysis of the wool and mohair samples used in this study is recommended for the future research studies.

### 4.2.1.3 Raman Peak Height Ratios for the Identification of Wool and Mohair Fibres

The close visual comparison of both wool and mohair Raman spectra (Figure 4.1) indicated that there might be a difference in their band peak heights and this section presents results for certain band intensities/peak heights determined using the baseline method. The student t-test was adopted throughout this research as a means for statistically determining the significance of the differences in the results of wool and mohair. The size of the difference between the two mean values was quantified in terms of Cohen's *d*, defined as the difference between the mean values divided by the pooled standard deviation (equation 4.1) (Cohen, 1988).

$$d = \frac{M_a - M_b}{SD_{\text{pooled}}} \dots\dots\dots 4.1$$

Where  $M_a$  and  $M_b$  are the mean values of the groups being compared,  $SD_{\text{pooled}}$  is found as the root mean square of the two standard deviations (Cohen, 1988). The effect size, *d*, has been defined as small when the value of *d* is equal to 0.2, moderate when *d* is 0.5 and large when it is equal to or great than 0.8.

Kumar (2015) discussed, in detail, factors that may cause variations in the spectroscopic peak heights or intensities, the variation in sample thickness being one potential source of peak height variations. The current research study confirmed the claim made by Kumar *et al.*, 2015 who stated that ratiometric analysis mitigates significantly the effects of unevenness of sample thickness on the peak heights. The laser drifting during spectral acquisition was not found to significantly influence the results obtained in the current study.

Fifty (50) scoured wool and fifty four (54) scoured mohair samples of different origins and average fibre diameters (see Table 3.1) were analysed for their Raman peak heights which were extracted for eight Raman chemical bands (shown in Figure 4.6). These were selected on the basis of prominence and the ease of defining the baseline reproducibly. All spectra used in this analysis were acquired with 2000 scans (equivalent to 1-hour acquisition time) and the thickness of the fibre bundle was kept as constant as possible. Generally, the relative peak heights correlated poorly (see Table

4.9 for the correlation coefficients  $R^2$ ) with the mean fibre diameters for some of the Raman bands analysed in this study. Plots of the relative peak heights against mean fibre diameters (MFDs) are illustrated in Figure 4.7.

**Table 4.9: Correlation coefficients for the relative intensities against MFDs.**

<b>Correlation coefficients (<math>R^2</math>)</b>		
<b>Relationship</b>	<b>Wool</b>	<b>Mohair</b>
CH <sub>2</sub> asymmetric Stretch v MFD	0.01	0.02
CH <sub>2</sub> & CH <sub>3</sub> bend v MFD	0.02	0.01
Amide I v MFD	0.03	0.01
Phe & Trp v MFD	0.44	0.04
Skeletal C-C stretch v MFD	0.01	0.09
Tyr v MFD	0.50	0.12
Phe v MFD	0.05	0.17
S-S stretch	0.16	0.02

A moderate positive correlation was only observed for the wool Tyr band, with a 0.5 correlation coefficient being observed. The correlation of the MFD with the Phe & Trp (around 1004 cm<sup>-1</sup>) relative peak heights produced  $R^2$  values of 0.44 and 0.04 for wool and mohair, respectively.

Relative peak heights of various bands were determined with the view of possibly distinguishing between wool and mohair fibres. The list of the analysed bands included the CH<sub>2</sub> asymmetric stretch, the amide, the S-S stretch of the disulphide cystine linkages and the Phe & Trp vibration (around 1004 cm<sup>-1</sup>). The normalization was done

based on the CH<sub>2</sub> & CH<sub>3</sub> bending modes (near 1450 cm<sup>-1</sup>), suggested in literature (Lippert *et al.*, 1976; Kuzuhara and Hori, 2003 and Church *et al.*, 1997).

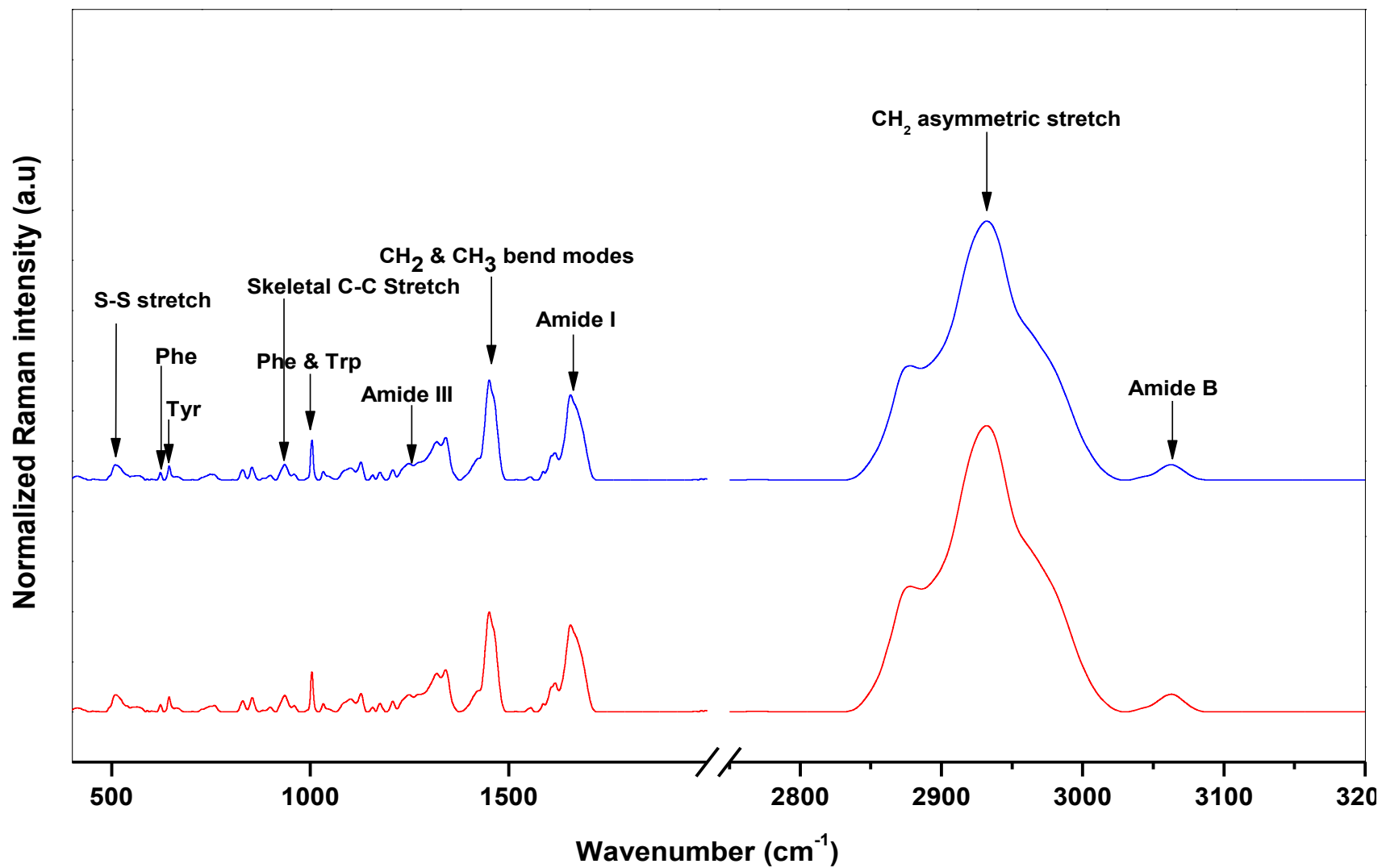
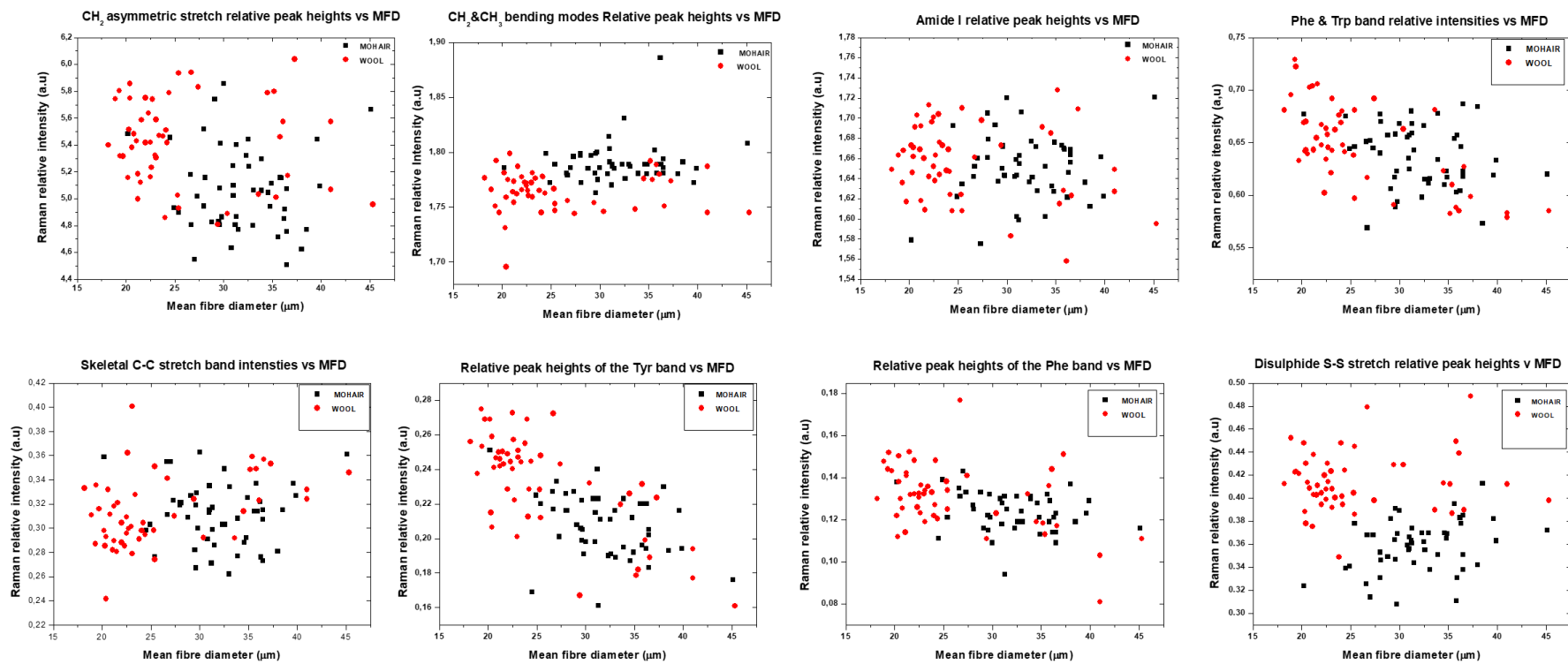


Figure 4.6: Normalized average Raman spectra of wool (red) and mohair fibres, respectively.



**Figure 4.7: Relationship between Raman relative intensities and mean fibre diameter.**

Crucial dissimilarities in the features of the normalized spectra of wool and mohair fibres seem to be very scarce, making the possibility of distinguishing between the two fibre types a very difficult task. The ratios of the peak heights of the Raman chemical bands, listed in Table 3.3, to those of the CH<sub>2</sub> & CH<sub>3</sub> bending modes (around 1450 cm<sup>-1</sup>) were determined for each individual wool and mohair spectrum to investigate the possibility of using this criterion for distinguishing between the two fibre types. For each spectrum, eight peak height measurements were made, results being presented as the average values together with their standard deviations (see Table 4.10):

**Table 4.10: Raman relative intensities determined from wool and mohair spectra.**

Raman band	Wool		Mohair	
	Mean	Std dev ( $\sigma$ )	Mean	Std dev ( $\sigma$ )
CH <sub>2</sub> asymmetric stretch	5,07	0,31	5,42	0,32
CH <sub>2</sub> & CH <sub>3</sub> bend	1,76	0,02	1,79	0,02
Amide I	1,66	0,04	1,65	0,03
Phe & Trp	0,65	0,04	0,64	0,03
Skeletal C-C stretch	0,31	0,03	0,31	0,03
Tyr	0,24	0,03	0,21	0,02
Phe	0,13	0,02	0,12	0,01
S-S stretch	0,42	0,03	0,35	0,02

The statistical comparison of the relative peak heights showed that the CH<sub>2</sub> asymmetric stretch (around 2932 cm<sup>-1</sup>), the CH<sub>2</sub> & CH<sub>3</sub> bending modes (at 1450 cm<sup>-1</sup>), the amide I (1655 cm<sup>-1</sup>), Phe and Trp (around 1004 cm<sup>-1</sup>), the skeletal C-C stretch (around 936 cm<sup>-1</sup>) and the Phe (at 622 cm<sup>-1</sup>), all did not differ statistically significantly ( $p > 0.05$ ) between the two fibre types. The mean values of the S-S stretch (near 508 cm<sup>-1</sup>) differ statistically significantly ( $p < 0.05$ ) between wool and mohair. It is important to mention that these relative peak heights tended to vary significantly even within the sample fibre sample. A specific group of mohair samples, (\*) labelled samples in Table 3.1, tended to possess high relative peak height values which were in the same order of magnitude as those for the wool samples. Because of this, the relative peak height ratios with their standard deviations were determined (see Table 4.11 and Figure 4.8):

**Table 4.11: Relative peak height ratios for wool and mohair fibre samples.**

Symbol	Ratio	Wool	Mohair
A	$I_{2932}/I_{1450}$	3.11 (0.23)	2.81 (0.23)
B	$I_{1655}/I_{1450}$	0.94 (0.03)	0.91 (0.02)
C	$I_{1004}/I_{1450}$	0.37 (0.03)	0.35 (0.02)
D	$I_{508}/I_{1450}$	0.24 (0.03)	0.20 (0.01)
E	$I_{936}/I_{1450}$	0.17 (0.02)	0.18 (0.01)
F	$I_{644}/I_{1450}$	0.14 (0.02)	0.12 (0.01)
G	$I_{622}/I_{1450}$	0.08 (0.01)	0.07 (0.01)

In this study, the assignment of symbols to the specific relative peak height ratios was adopted, with symbol A assigned to represent the ratio of the relative peak height of the very strong CH<sub>2</sub> asymmetric stretch band ( $I_{2932}$ ) to that of CH<sub>2</sub> & CH<sub>3</sub> bending modes ( $I_{1450}$ ). Symbols B and C represents ratios of the relative peak height of the amide I band ( $I_{1655}$ ) to that of the CH<sub>2</sub> & CH<sub>3</sub> bending modes ( $I_{1450}$ ) and the relative peak height of the Phe & Trp ( $I_{1004}$ ) to that of CH<sub>2</sub> & CH<sub>3</sub> bending modes ( $I_{1450}$ ), respectively. Symbol D is the ratio of the relative peak height of the S-S stretch ( $I_{508}$ ) to the peak height of the CH<sub>2</sub> & CH<sub>3</sub> bending modes ( $I_{1450}$ ). E, F and G symbolises ratios of the relative peak heights of the skeletal C-C stretch ( $I_{936}$ ), Tyr ( $I_{644}$ ) and Phe ( $I_{622}$ ) all to that of the CH<sub>2</sub> & CH<sub>3</sub> bending modes ( $I_{1450}$ ).

The individual values of ratio A varied a great deal, indicated by the standard deviation values in brackets of Table 4.8, from one mohair sample to the other and also from one wool sample to another, wool samples varying more than did the mohair. The individual values ranging from 2.71-3.68 for wool and from 2.35-3.08 for mohair. A considerable variation was also observed in ratios within the same sample, with the greatest wool variation of 2.72-3.22 observed for the Lincoln1 sample and while for mohair the widest variation of 2.41-3.03 was observed for the Mohairlabs D sample.



The largest ratio A value for wool ( $3.45 \pm 0.20$ ; 95 % confidence limits) was found for a Dorset horn wool, while the lowest was for the BR81 CSIR wool top ( $2.91 \pm 0.20$ ). The largest ratio A value ( $2.97 \pm 0.20$ ; 95% confidence limits) for mohair was for the Texas mohair (20 lustre mohair), while the lowest ( $2.54 \pm 0.22$ ; 95 confidence limits) was for the South African mohair sample (SAMIL SAMIL Combing Lot2).

Both the mean and standard deviation of ratio A for wool and mohair were found to be  $3.11 \pm 0.23$  and  $2.81 \pm 0.23$ , respectively. The application of the student t-test proved them as significantly different ( $p < 0.05$ ), with a Cohen's d value of 0.91 being found which indicates a large difference between the two mean values. The graphical representation of these average values, shown in Figure 4.8, indicates a clear difference of ratio A between the two fibre types.

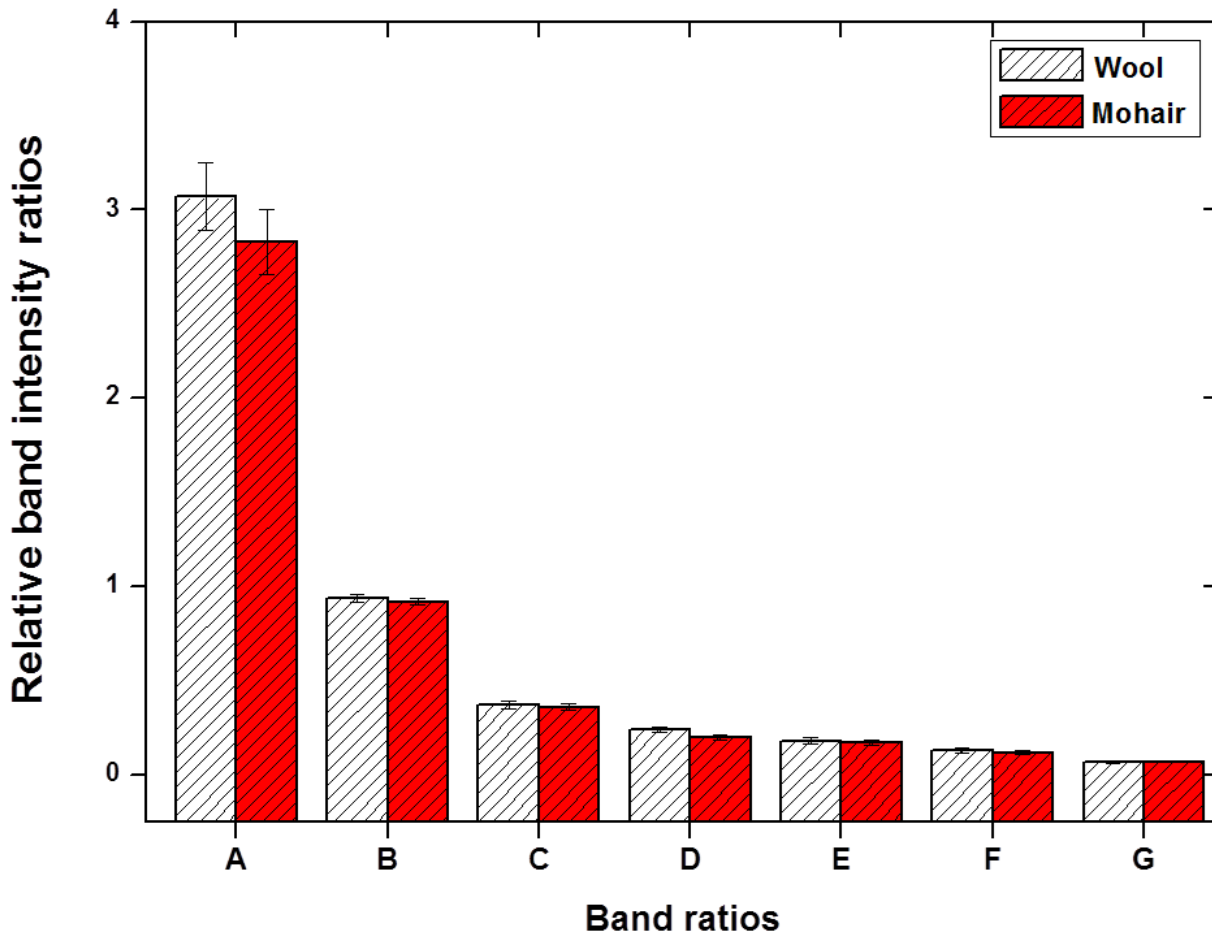
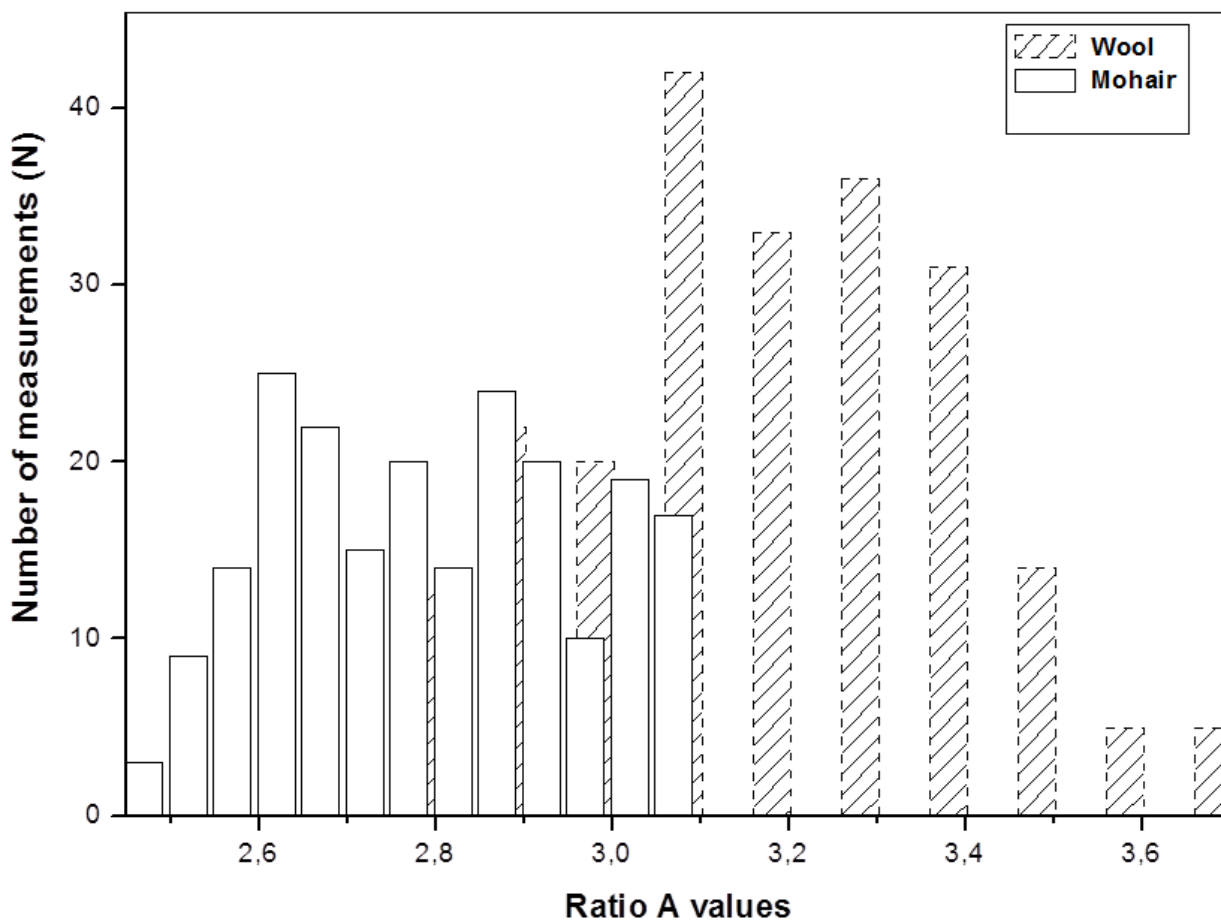


Figure 4.8: Raman band ratios for wool and mohair fibres.

These differences could be a result of the difference in the amounts of the internal lipid contents existing between the two fibre types. However, there was a considerable overlap of the individual wool and mohair values which virtually rules out the possibility of the application of ratio A for quantitative wool/mohair blend analysis. This study has shown that wool lots are characterized by the presence of some relatively large ratios, particularly beyond the value of 3.2, while the mohair lots were all found to be below the threshold of 3.1 (see Figure 4.9).



**Figure 4.9: Distributions of Ratio A values for wool and mohair.**

Nevertheless, using this in wool-mohair blend composition analysis would present problems in practice although a qualitative approach for determining the presence of any wool in a supposed 100% mohair may be possible. The application of this band ratio in answering the question of whether a sample is a pure mohair or not seem to hold a great potential. However, for the application of this band ratio in practice, a relatively larger number of minimum spectra, from each sample, is highly recommended, compared to the minimum of

six spectra acquired from each sample in this study. This would minimize the observed variation between spectra of the same sample. An interesting point to emerge from this research study relates to establishing whether a sample is pure mohair or a possible mixture of wool and mohair. It has been noted that if a threshold value of 3.1 is selected for ratio A and it is found that for a sample of unknown identity, none of the values exceed this threshold value, the sample can be declared to be a pure mohair sample. Conversely, if a sample of unknown identity is examined and possesses ratio A values that exceed this threshold, then the sample cannot be a pure sample. Figure 4.9 shows the distribution of values of Ratio A determined from some 50 wool and 54 mohair samples. The figure indicates that all mohair individual ratio A values are found below the 3.1 threshold whilst wool samples are characterized by the presence of values exceeding the threshold of 3.1.

Amongst the peak height ratios investigated in this study is ratio B ( $I_{1655}/I_{1450}$ ), determined for both wool and mohair as a possible means of distinguishing between them. Figure 4.9 illustrates the distributions of the individual ratio B values for wool and mohair fibre samples.

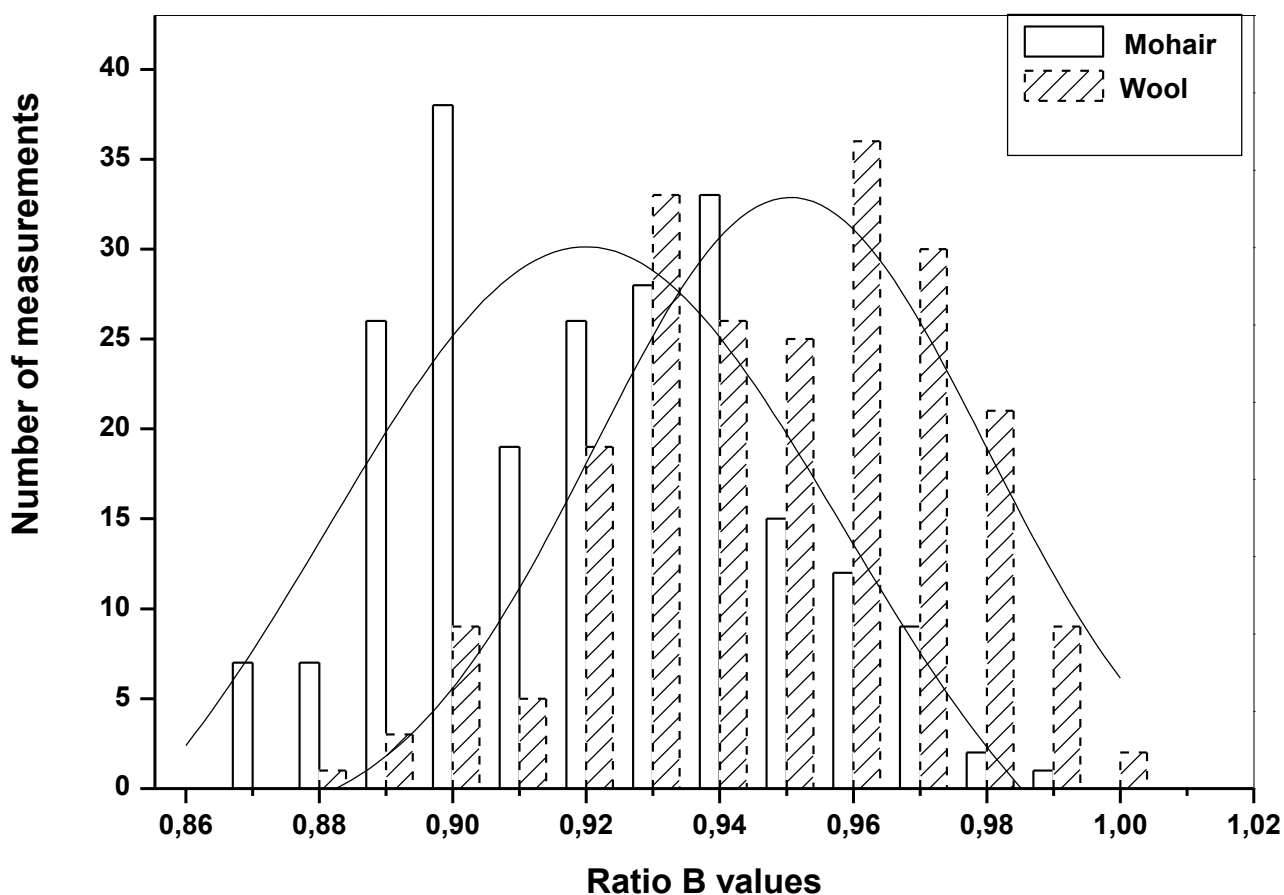


**Figure 4.10: Ratio B distributions for wool and mohair.**

The amide I is one of strongest bands in Raman spectra of protein fibres, so based on its prominence it was also selected for this analysis. Ratio B values were found to vary considerably for both fibre types, with a wide variation also being observed in values obtained from the same fibre sample analysed. A great overlap of individual values was observed, with wool ranging between 0.88 and 1.00 for wool while mohair ranged between 0.86 and 0.99 (as shown in Figure 4.10). The average value and standard deviation of  $0.94 \pm 0.03$  were found for wool while these were found to be  $0.92 \pm 0.02$  for mohair fibre samples, with the application of the student t-test proving the observed difference in the mean values to be statistically significant ( $p < 0.05$ ). A Cohen's d value of 0.57, proving a moderate difference between the two mean values. Because of the observed overlap of the individual values, it can be concluded that the application of this relative peak height ratio does not seem possible in the identification and classification of wool and mohair, particularly when the two fibres are in a blend.

This study also investigated the potential of the application of the ratio of the peak height of the Phe & Trp (near  $1004\text{ cm}^{-1}$ ) band to that of the  $\text{CH}_2$  &  $\text{CH}_3$  bending modes (at  $1450\text{ cm}^{-1}$ ), ratio C, in possibly distinguishing between wool and mohair fibre samples. The individual values varied considerably between wool and mohair; these are shown in the distributions illustrated in Figure 4.10.

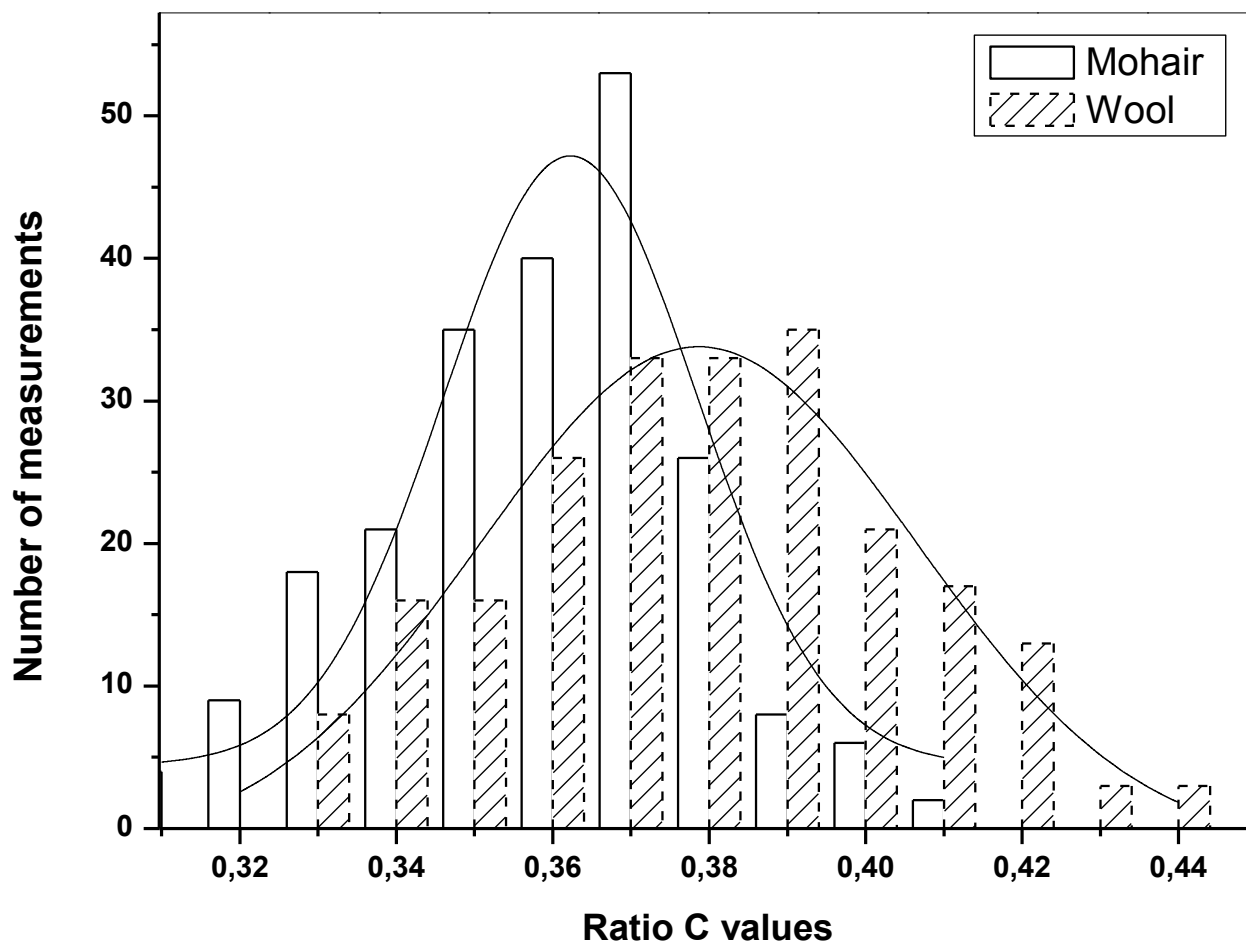


**Figure 4.11: Ratio C distributions for wool and mohair fibre samples.**

The individual values for wool were found to range from 0.33 to 0.45, while those of mohair ranged from 0.31 to 0.41, with a considerable variation also observed between ratios of the same fibre sample. The widest variation, within a sample, in wool was observed for the values of one of the CSIR BR lots (BR71), ranging from 0.33 to 0.41, while in mohair samples the only sample that possessed an alarming variation is the South African (SAMIL SAMIL Combing Lot3) mohair sample, ranging from 0.31 to 0.38. The largest ratio was for the BR65 wool top with  $0.40 \pm 0.03$  (95% confidence limits) and the lowest for the Dorset horn wool,

0.34 ± 0.01. The largest ratio for mohair was found in the 1126 lustre mohair with 0.39 ± 0.01 while the lowest was for the Lesotho mohair with 0.32 ± 0.02. The mean and standard deviation values were 0.37 ± 0.03 and 0.35 ± 0.02 for wool and mohair fibres, respectively, with the means comparison proving the observed difference to be statistically insignificant ( $p < 0.05$ ). A cohen's d value of 0.28, indicating a very small difference. The great overlap of the individual values observed in Figure 4.10, proves that the possible identification or distinction between the two fibre types would be extremely difficult in practice.

The relative peak height ratio D ( $I_{508}/I_{1450}$ ) could be related to the content of the disulphide bonds or the amino acid cystine within keratin fibres (Barani and haji, 2015). The distribution of the individual ratio D values, found in the current research study, from wool and mohair fibre samples is illustrated in Figure 4.12.

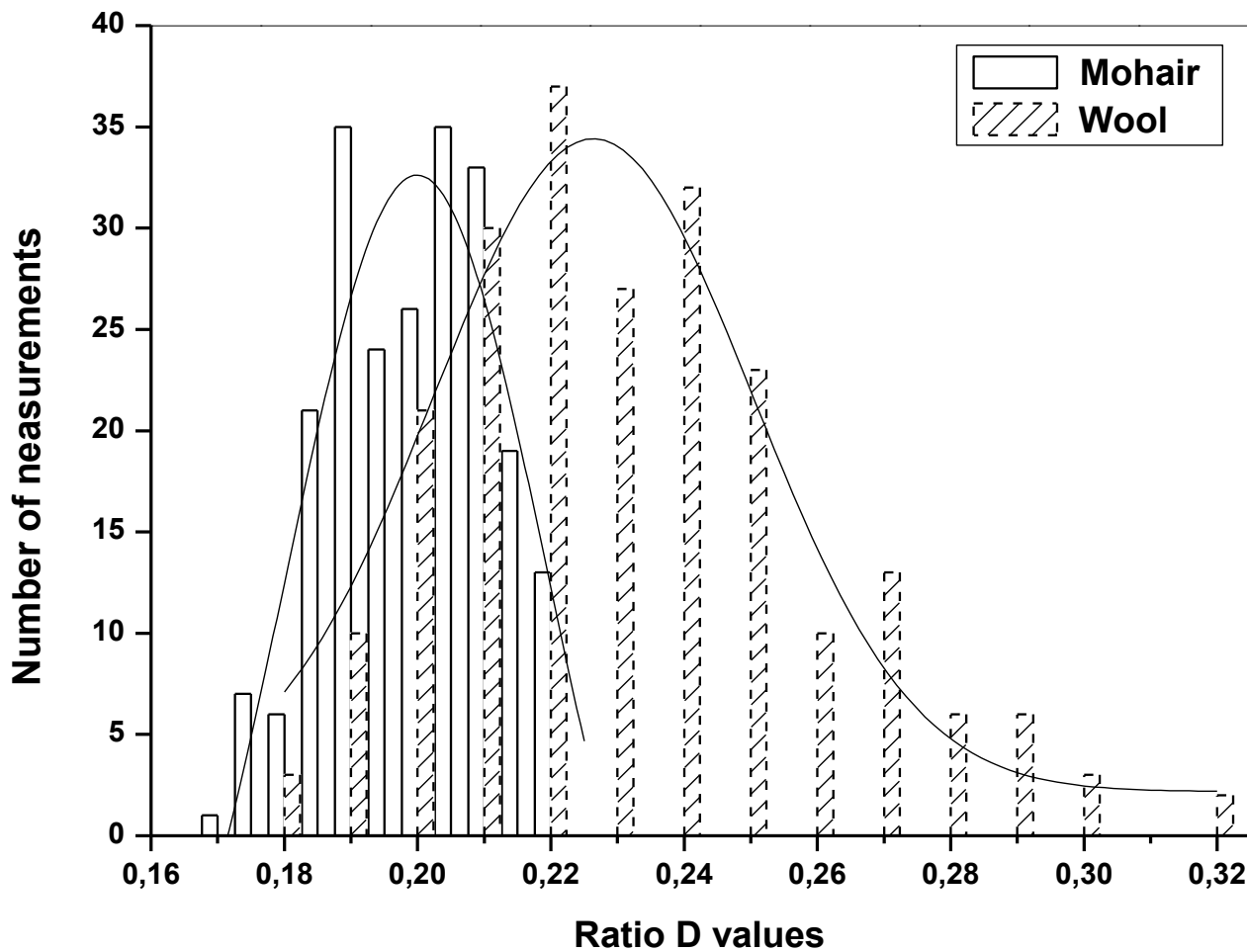


Figure 4.12: Distributions of the Ratio D for wool and mohair.

The individual values were found to vary greatly for both wool and mohair, with wool ranging between 0.18-0.32 while mohair ranged between 0.17-0.22 (see Figure 4.12). For this peak height ratio as well, almost identical variations were observed in spectra acquired from the same sample. For wool, the widest range of 0.18-0.26 was observed for the Lincoln wool (L1) sample while for mohair a variation of 0.17-0.22 was observed for one Lesotho mohair (BK11401) sample. The largest ratio D value for wool was found for the Dorset horn sheep wool with a value of  $0.28 \pm 0.04$  (95% confidence limits) and the lowest ( $0.21 \pm 0.03$ ) for a Lincoln (L1) wool. The largest peak height ratio D for mohair was observed for the South African (SAMIL SAMIL Combing Lot3) with  $0.20 \pm 0.02$  (95% confidence limits) while the lowest was also for one of the SA mohair samples (1028 mohair) with a ratio of  $0.17 \pm 0.01$ .

The overall mean and standard deviation values were found to be  $0.24 \pm 0.03$  and  $0.20 \pm 0.02$ , for wool and mohair, respectively. Despite the considerable overlap (see Figure 4.12) of the individual values has been observed, the statistical comparison of the mean values proved them to be statistically significant ( $p < 0.05$ ). A Cohen's d value of 1.41 was obtained, indicating a large difference between the two mean values.

The quantitative analysis or blend composition analysis of the two fibre types seem a potentially difficult task, especially if the blend consists of only wool and mohair. The need of a considerable number of spectra from each sample is highly recommended to reduce the variation that exist within the band ratios of the same sample.

This result indicate that ratio D may be useful in detecting possible counterfeiting in mohair fibre samples. The application of this band ratio, in practice, would be based on the selection of a threshold of 0.22, where the absence of values exceeding this value would imply the possibility of the sample being a pure mohair and conversely, the presence of ratios exceeding the 0.22 threshold value implying the possibility of the sample being a pure wool or a mixture of the two fibre types. Keratin fibres which have been subjected to chemical treatments have a tendency of possessing reduced disulphide S-S contents of the amino acid cystine, this being due to oxidation of these disulphide S-S linkages (Joy and Lewis, 1991; Wojciechowska *et al*, 2004). With this fact in mind, the possible application of this band ratio in examining chemically treated samples is still to be extensively investigated in future

research studies. Furthermore, a comprehensive chromatographic or electrophoretic analysis for determining the amino acid contents, particularly cystine, of the samples used in this research study would be beneficial in determining the correlation that may exist between the ratio D and the cystine contents determined by chromatographic or electrophoretic methods. This task is recommended for the coming research studies. Some of the possible advantages of this ratio would offer include the rapidness and potentially reduced cost involved in the fibre identification tests. Another advantage is the fact that the success of the fibre identification does not require a highly skilled Raman spectroscopist.

This study also examined Ratio E for its possible application in the identification of wool and mohair, with this ratio being found to also vary considerably between wool and mohair fibre samples, with wool ranging from 0.14 to 0.24 while mohair ranged between 0.13 and 0.22, as shown in Figure 4.13.

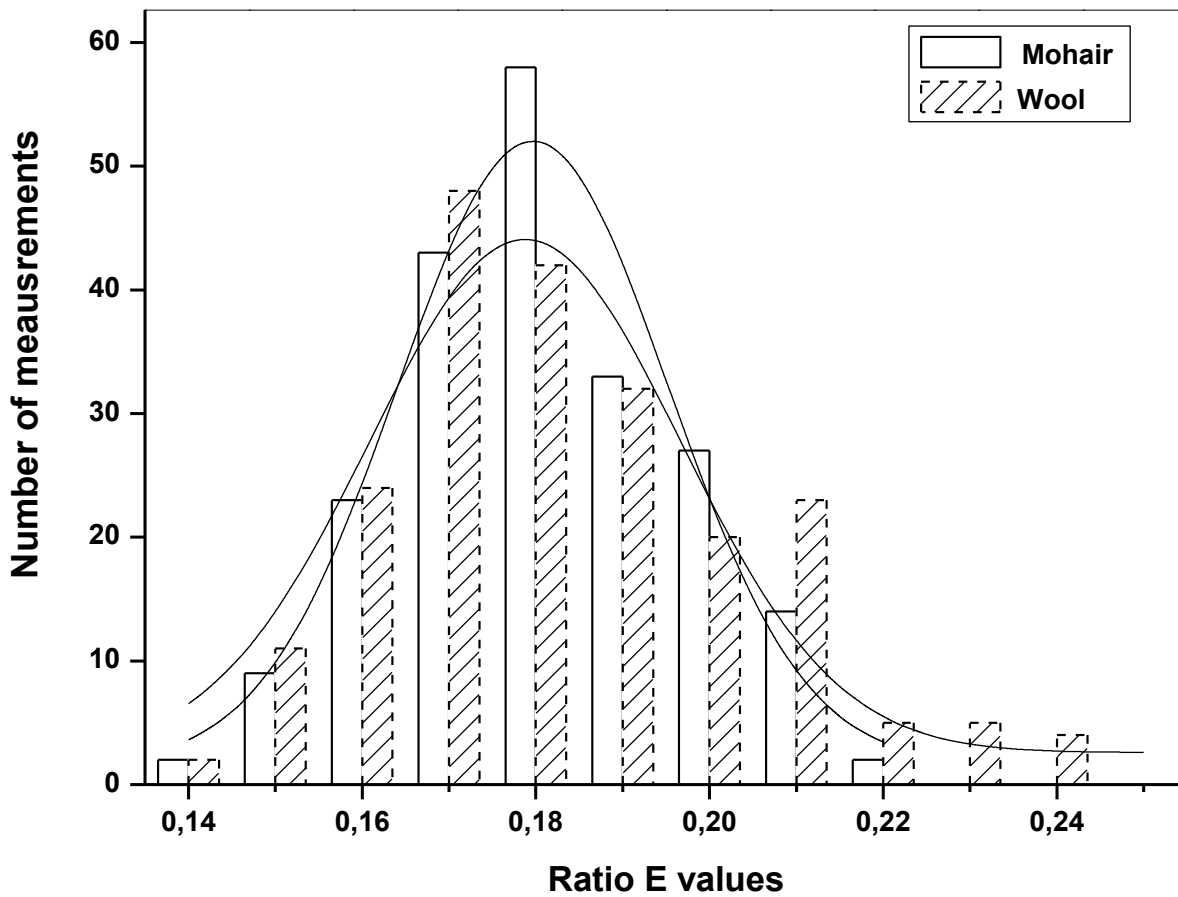
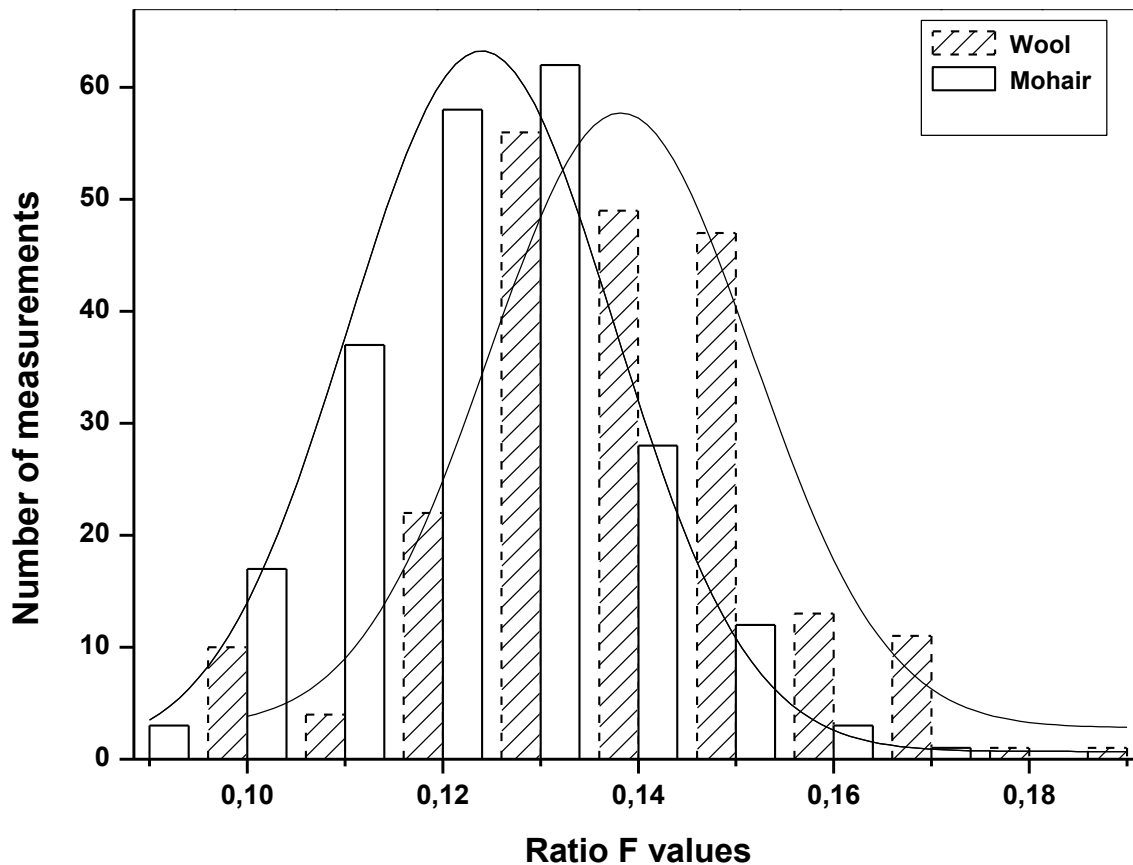


Figure 4.13: Ratio E distributions for wool and mohair.



The greatest wool value was found for the BR20 wool top, with a value of  $0.22 \pm 0.01$  (95% confidence limits) and the lowest for the BR55 wool top with  $0.14 \pm 0.01$ , while for mohair, the greatest was found for the 1028 South African mohair with  $0.20 \pm 0.01$  (95% confidence limits) and the lowest for the Texas Int. Mohair INC- #734 sample with a value of  $0.14 \pm 0.01$ . The average values were found to be  $0.18 \pm 0.02$  and  $0.17 \pm 0.01$  for the wool and mohair, respectively. A great overlap (see Figure 4.13) was also observed for individual values between the fibres and the student t-test showed that the means did not differ significantly ( $p > 0.05$ ). This may be attributable to the similar contents of the  $\alpha$ -helical secondary structure between the two fibre types (Wang et al., 2013). This study has, earlier, indicated that the two animal fibres studied in this research share similar secondary structural conformation (dominated by the  $\alpha$ -helical structure), and this may be the reason for this observed overlap in this peak height ratio. The possible application of this band ratio in the identification or classification of wool and mohair fibre samples seems extremely impossible, due to the observed overlap of the individual values.

This research study also investigated the possible application of the band relative intensity ratios F and G in distinguishing between wool and mohair. Ratio F values varied between 0.09 - 0.20 and 0.08 - 0.17 for wool and mohair, respectively, with the mean values of  $0.13 \pm 0.02$  and  $0.12 \pm 0.01$ . Figures 4.14 and 4.15 illustrates the distribution of ratios F and G, for wool and mohair.



**Figure 4.14: Ratio F distributions for wool and mohair.**

A statistical comparison of these means proving them as statistically significant ( $p < 0.05$ ), with a cohen's d value of 0.30 indicating a small difference. The application of this band ratio in distinguishing between wool and mohair seem to hold a great potential, particularly in declaring the purity of mohair fibre samples, this being based on the selection of 1.5 does not seem possible due to the observed overlap of the individual values. At the moment, because of the considerable overlap observed in the individual values, the application of the ratio seem highly impossible. More research studies, however, will need to be conducted towards realizing the full potential of the application of ratio F ( $I_{644}/I_{1450}$ ) in practice.

The individual values of Ratio G were found to range between 0.04 to 0.13 and 0.04 to 0.09 for both wool and mohair fibres, respectively. The average values of  $0.08 \pm 0.01$  and  $0.07 \pm 0.01$  were obtained for wool and mohair, respectively, with a very low cohen's d value of 0.20. Wool samples were characterized by the presence of a very few ratios exceeding 0.10, while mohair values were always found below this value. Despite the small difference between the

mean values, the application of the t-test proved that these differ significantly ( $p < 0.05$ ) between wool and mohair fibre samples. The application of this ratio G in practice would be extremely difficult due to the considerable overlap observed in the individual values between wool and mohair.

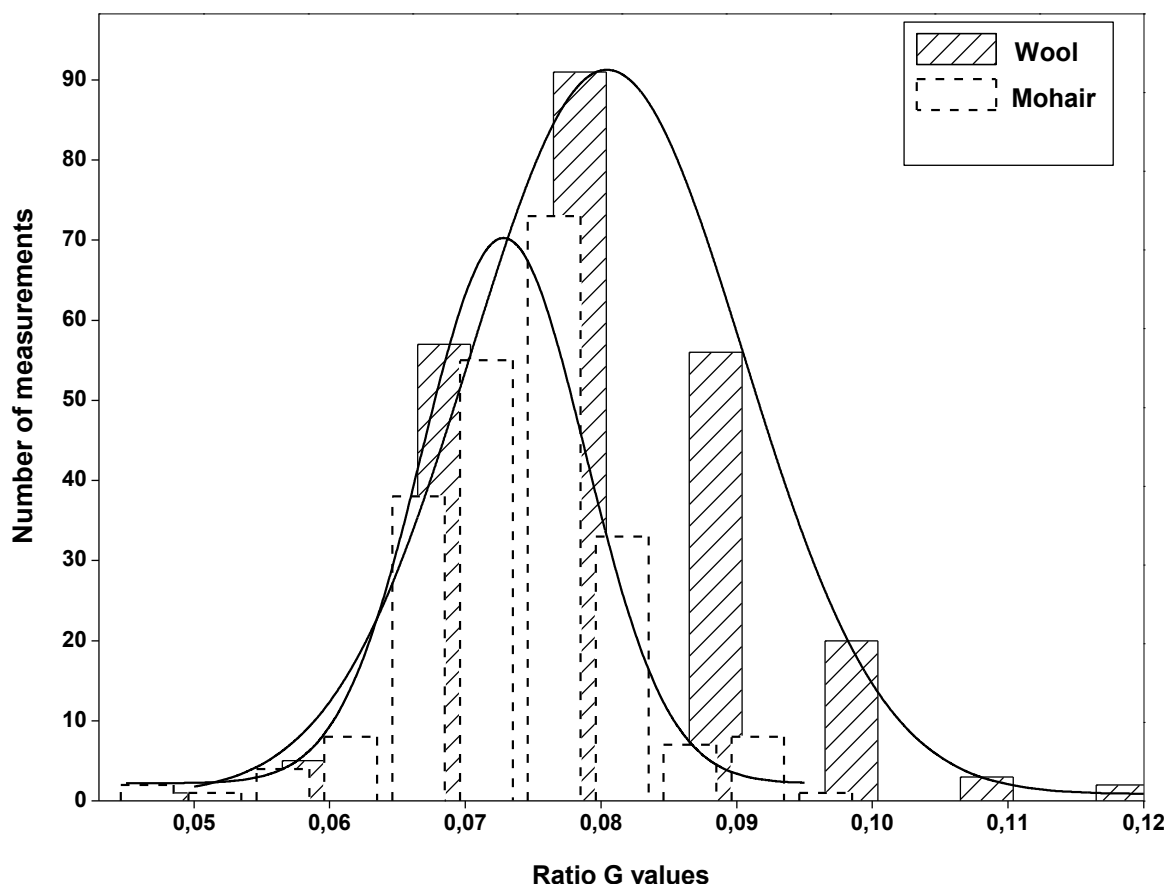


**Figure 4.15: Ratio G distribution for wool and mohair.**

Quantitative analysis of blends of the two animal fibres, wool and mohair, using ratio G, does not seem possible at the moment but further research studies involving a relatively large number of pure wool and mohair of various origins, together with wool/mohair blend samples of different quantities, would be important.

Despite the great overlap observed in the respective band ratios, the application of ratiometric analysis for some of Raman chemical band relative intensities, particularly ratios A and D, seem to hold a potential in detecting fraudulent mislabelling in mohair products. However, a need for an extensive amount of research involving a considerably large number of pure and blended animal fibre samples, would provide the more conclusive results.

#### 4.2.1.3.1 Reproducibility of the Ratiometric Analysis

To investigate the reproducibility of the Raman band ratiometric analysis in the classification and declaration of mohair and wool fibre samples, a random selection of the pre-determined mohair samples, from those contained in Table 3.1, was made and re-analysed. Three fibre bundles were drawn from each sample container, with one spectrum acquired from each of the three fibre bundles.

**Table 4.12: The possible application of Ratio A in practice.**

SAMPLE ID	Spectral acquisitions			Mean ( $\sigma$ )*
	1	2	3	
1052 Mohair	2.81	2.70	2.73	2.75 (0.05)
1089 Mohair	2.71	2.72	2.74	2.72 (0.01)
1006 Mohair	2.69	2.81	2.85	2.78 (0.07)
Texas Int. Mohair INC-#705	2.82	2.94	2.83	2.86 (0.05)
Texas Int. Mohair INC-#748	2.82	2.75	2.78	2.78 (0.03)
TYG1 (Istanbul) Mohair	2.43	2.76	2.58	2.59 (0.13)
BR28 Wool	3.05	3.06	3.00	3.04 (0.03)
BR103 Wool	3.39	3.33	3.36	3.36 (0.02)

\*Standard deviation.

In Table 4.12, the results of ratio A as a criterion for checking the purity of the selected mohair samples, are presented. Despite the few number of spectral measurements involved, the six mohair fibre samples were correctly classified as pure mohair samples, this being concluded from the absence of ratios exceeding 3.1. However, these results, in Table 4.12, also show that solely relying on the application of Ratio A for fibre classification might pose a risk of misidentification and misclassification of some fibre samples, this risk being observed for the BR28 wool sample. The average values were found to be in agreement with those found earlier in this research, wool fibre samples having higher values than those of mohair.

Table 4.13 presents results of the peak height ratio B for wool and mohair.

**Table 4.13: Possible applicability of Ratio B in practice.**

SAMPLE ID	Spectral acquisitions			Mean ( $\sigma$ )*
	1	2	3	
1052 Mohair	0.98	0.94	0.94	0.95 (0.02)
1089 Mohair	0.89	0.86	0.91	0.89 (0.02)
1006 Mohair	0.93	0.91	0.93	0.92 (0.01)
Texas Int. Mohair INC-#705	0.95	0.91	0.92	0.93 (0.02)
Texas Int. Mohair INC-#748	0.92	0.93	0.92	0.92 (0.01)
TYG1 (Istanbul) Mohair	0.89	0.96	0.91	0.92 (0.03)
BR28 Wool	0.95	0.93	0.93	0.94 (0.01)
BR103 Wool	0.94	0.91	0.92	0.92 (0.01)

\*Standard deviation

A considerable overlap in the values of wool and mohair is observed (as shown 4.13), confirming that this band ratio indeed cannot be applied in the identification of these two fibre types. Table 4.14 summarizes results of the ratio C, obtained from wool and mohair fibre samples.

**Table 4.14: Possible application of Ratio C in practice.**

SAMPLE ID	Spectral acquisitions			Mean ( $\sigma$ )
	1	2	3	
1052 Mohair	0,33	0,34	0,34	0.34 (0.01)
1089 Mohair	0,34	0,33	0,37	0.35 (0.01)
1006 Mohair	0,34	0,35	0,35	0.35 (0.01)
Texas Int. Mohair INC-#705	0,36	0,36	0,36	0.36 (0.00)
Texas Int. Mohair INC-#748	0,36	0,37	0,36	0.36 (0.00)
TYG1 (Istanbul) Mohair	0,37	0,38	0,38	0.38 (0.00)
BR28 Wool	0.37	0.37	0.39	0.38 (0.01)
BR103 Wool	0.37	0.38	0.36	0.37 (0.01)

\*Standard deviation

Table 4.14 shows a considerable overlap of individual values between wool and mohair fibre samples, showing that indeed the application of this band ratio in practice can be extremely difficult. Table 4.15 contains results for the ratio D values of wool and mohair fibre samples.

**Table 4.15: Possible application of Ratio D in practice.**

SAMPLE ID	Spectral acquisitions			Mean ( $\sigma$ )*
	1	2	3	
1052 Mohair	0.19	0.20	0.19	0.19 (0.01)
1089 Mohair	0.18	0.17	0.16	0.17 (0.01)
1006 Mohair	0.19	0.20	0.21	0.20 (0.01)
Texas Int. Mohair INC-#705	0.19	0.20	0.20	0.20 (0.00)
Texas Int. Mohair INC-#748	0.19	0.20	0.18	0.19 (0.01)
TYG1 (Istanbul) Mohair	0.20	0.19	0.20	0.20 (0.00)
BR28 Wool	0.23	0.22	0.23	0.23 (0.00)
BR103 Wool	0.23	0.23	0.23	0.23 (0.00)

\*Standard deviation

The application of ratio D in distinguishing between wool and mohair fibres appears to hold a great potential, wool indeed possessing values exceeding the threshold value 0.22 and mohair falling below this value. A good reproducibility of average values is also observed for this peak height ratio, with wool having higher average values than mohair fibre samples. Further studies, however, are highly recommended to investigate the full potential of this band ratio, particularly including chemically treated samples and those from wide range of origins by country. Table 4.16 summarizes the results of ratio E, showing the great overlap of the individual value from wool and mohair. Indeed, the application of this relative intensity ratio seem to be impossible in distinguishing between wool and mohair fibres.

**Table 4.16: Possible application of ratio E in practice.**

SAMPLE ID	Spectral acquisitions			Mean ( $\sigma$ )*
	1	2	3	
1052 Mohair	0,16	0,15	0,16	0.16 (0.01)
1089 Mohair	0,17	0.16	0.17	0.17 (0.01)
1006 Mohair	0,18	0,16	0,17	0.17 (0.01)
Texas Int. Mohair INC-#705	0.15	0.17	0.16	0.16 (0.01)
Texas Int. Mohair INC-#748	0.17	0.17	0.15	0.16 (0.01)
TYG1 (Istanbul) Mohair	0.16	0.16	0.17	0.16 (0.01)
BR28 Wool	0.15	0.15	0.17	0.16 (0.01)
BR103 Wool	0.16	0.17	0.17	0.17 (0.01)

**\*Standard deviation**

Ratio F and G (Tables 4.17 and 4.18) were also found to overlap considerably between those obtained for wool and mohair also confirming that distinguishing between the two fibre types would be extremely difficult.

**Table 4.17: Possible application of Ratio F in practice.**

SAMPLE ID	Spectral acquisitions			Mean ( $\sigma$ )*
	1	2	3	
1052 Mohair	0.10	0.10	0.12	0.11 (0.01)
1089 Mohair	0.12	0.12	0.12	0.12 (0.00)
1006 Mohair	0.12	0.12	0.12	0.12 (0.00)
Texas Int. Mohair INC-#705	0.12	0.12	0.12	0.12 (0.00)
Texas Int. Mohair INC-#748	0.12	0.11	0.11	0.11 (0.01)
TYG1 (Istanbul) Mohair	0.13	0.12	0.13	0.13 (0.01)
BR28 Wool	0.14	0.14	0.14	0.14 (0.00)
BR103 Wool	0.15	0.15	0.15	0.15 (0.00)

**\*Standard deviation**

**Table 4.18: Possible application of Ratio G in practice.**

SAMPLE ID	Spectral acquisitions			Mean ( $\sigma$ )*
	1	2	3	
1052 Mohair	0.07	0.06	0.06	0.06 (0.00)
1089 Mohair	0.07	0.07	0.08	0.07 (0.00)
1006 Mohair	0.06	0.08	0.07	0.07 (0.00)
Texas Int. Mohair INC-#705	0.07	0.07	0.07	0.07 (0.00)
Texas Int. Mohair INC-#748	0.08	0.08	0.08	0.08 (0.00)
TYG1 (Istanbul) Mohair	0.08	0.06	0.08	0.07 (0.01)
BR28 Wool	0.08	0.07	0.07	0.07 (0.00)
BR103 Wool	0.08	0.07	0.08	0.08 (0.00)

**\*Standard deviation**

Although blend composition analysis might seem impossible, the application of the Raman spectroscopy based ratiometric analysis, particularly of the relative intensity ratios A and D, seem to hold a great potential in being applied qualitatively. These ratios could potentially be applied to detect the possibility of counterfeiting in mohair fibre products. However, much thought and experimental work are necessary to discover the full potential of the application of these band ratios, including analysis of blind samples with unknown fibre compositions. Furthermore, realising the full potential of ratiometric analysis will need a considerable number of wool and mohair fibre samples, including those from other speciality fibres of commercial importance, such as cashmere. Also, because textile fibres are all subject to various, and in some instances rather rigorous, treatments before they reach the consumer in the form of a wide variety of textile materials, it would be important that samples that have undergone various treatments be analysed. The advantages of Raman spectroscopic ratiometric analysis over microscopic fibre examination is that no errors may arise from sampling because this method offers an advantage of being easier to conduct, potentially cheaper and fast compared to the existing microscopic based fibre analysis. At this stage, however, it does not seem possible that Raman spectroscopy can replace the existing CSH SEM based method for animal fibre blend composition analysis but could be used in conjunction with it.



The ratiometric analysis-based method was partially validated with known fibre samples, consisting of three wool and one mohair sample, with the results summarized in Table 4.19. One fibre bundle was drawn from the wool samples, with two spots (2 cm apart) along the length of the each bundle being selected and five spectra were acquired from each of the two spots. Two fibre bundles were randomly drawn from the mohair sample (TXSK Texas mohair sample), with two spots selected from each fibre bundle. Ratios B, C, E, F and G were again found to overlap considerably, proving that indeed they cannot be useful in distinguishing between wool and mohair fibre samples. As evident in the table, the mohair sample could easily be classified or declared as a pure mohair sample, with this being based on the values of the ratios A and D. An important observation was that wool samples possessed values of ratio A which considerably overlapped with those of mohair, i.e. falling below the threshold of 3.1. This shows that indeed solely relying on the application of ratio A poses a risk of misclassification of pure wool samples as being pure mohair.

**Table 4.19: Ratiometric analysis validation results.**

<b>Sample ID</b>	<b>A</b>	<b>B</b>	<b>C</b>	<b>D</b>	<b>E</b>	<b>F</b>	<b>G</b>
<b>TSXK mohair sample</b>	2.91	0.96	0.39	0.20	0.15	0.13	0.08
	2.89	0.93	0.39	0.19	0.15	0.13	0.08
	2.87	0.94	0.39	0.20	0.16	0.13	0.08
	2.80	0.95	0.40	0.19	0.14	0.12	0.08
	2.79	0.93	0.39	0.19	0.15	0.13	0.08
	2.41	0.89	0.38	0.20	0.16	0.13	0.08
	2.41	0.89	0.38	0.19	0.16	0.13	0.08
	2.44	0.89	0.38	0.20	0.17	0.13	0.08
	2.41	0.89	0.38	0.19	0.17	0.13	0.08
	2.44	0.89	0.38	0.19	0.16	0.13	0.08
	2.41	0.88	0.37	0.19	0.17	0.12	0.08
	2.74	0.94	0.39	0.18	0.16	0.13	0.07
	2.76	0.93	0.39	0.18	0.16	0.13	0.07
	2.76	0.93	0.39	0.18	0.16	0.13	0.08
	2.75	0.92	0.39	0.18	0.16	0.13	0.08
	2.37	0.91	0.38	0.18	0.16	0.14	0.08
	2.36	0.90	0.37	0.18	0.16	0.13	0.07
	2.35	0.90	0.38	0.19	0.16	0.13	0.08
	2.38	0.91	0.38	0.19	0.17	0.13	0.07
	2.39	0.92	0.39	0.19	0.17	0.12	0.07

<b>Sample ID</b>	<b>A</b>	<b>B</b>	<b>C</b>	<b>D</b>	<b>E</b>	<b>F</b>	<b>G</b>
<b>W54 wool</b>	<b>2.99</b>	<b>0.95</b>	<b>0.35</b>	<b>0.24</b>	<b>0.15</b>	<b>0.12</b>	<b>0.07</b>
	<b>2.95</b>	<b>0.94</b>	<b>0.35</b>	<b>0.24</b>	<b>0.16</b>	<b>0.11</b>	<b>0.07</b>
	<b>2.91</b>	<b>0.96</b>	<b>0.35</b>	<b>0.24</b>	<b>0.16</b>	<b>0.11</b>	<b>0.07</b>
	<b>2.95</b>	<b>0.95</b>	<b>0.35</b>	<b>0.25</b>	<b>0.16</b>	<b>0.12</b>	<b>0.07</b>
	<b>2.95</b>	<b>0.94</b>	<b>0.35</b>	<b>0.24</b>	<b>0.16</b>	<b>0.12</b>	<b>0.07</b>
	<b>2.69</b>	<b>0.95</b>	<b>0.36</b>	<b>0.24</b>	<b>0.18</b>	<b>0.11</b>	<b>0.07</b>
	<b>2.74</b>	<b>0.96</b>	<b>0.36</b>	<b>0.23</b>	<b>0.18</b>	<b>0.12</b>	<b>0.06</b>
	<b>2.69</b>	<b>0.94</b>	<b>0.36</b>	<b>0.23</b>	<b>0.18</b>	<b>0.11</b>	<b>0.07</b>
	<b>2.74</b>	<b>0.95</b>	<b>0.36</b>	<b>0.24</b>	<b>0.18</b>	<b>0.11</b>	<b>0.08</b>
	<b>2.70</b>	<b>0.95</b>	<b>0.35</b>	<b>0.23</b>	<b>0.17</b>	<b>0.11</b>	<b>0.07</b>
<b>OSP51 wool</b>	<b>3.03</b>	<b>0.97</b>	<b>0.38</b>	<b>0.23</b>	<b>0.16</b>	<b>0.16</b>	<b>0.08</b>
	<b>2.84</b>	<b>0.95</b>	<b>0.39</b>	<b>0.23</b>	<b>0.16</b>	<b>0.14</b>	<b>0.08</b>
	<b>2.84</b>	<b>0.94</b>	<b>0.39</b>	<b>0.22</b>	<b>0.16</b>	<b>0.15</b>	<b>0.08</b>
	<b>2.81</b>	<b>0.94</b>	<b>0.39</b>	<b>0.22</b>	<b>0.15</b>	<b>0.16</b>	<b>0.08</b>
	<b>3.04</b>	<b>0.95</b>	<b>0.41</b>	<b>0.22</b>	<b>0.15</b>	<b>0.15</b>	<b>0.07</b>
	<b>3.02</b>	<b>0.96</b>	<b>0.40</b>	<b>0.23</b>	<b>0.15</b>	<b>0.16</b>	<b>0.06</b>
	<b>2.97</b>	<b>0.93</b>	<b>0.39</b>	<b>0.23</b>	<b>0.14</b>	<b>0.16</b>	<b>0.08</b>
	<b>3.01</b>	<b>0.96</b>	<b>0.41</b>	<b>0.22</b>	<b>0.15</b>	<b>0.16</b>	<b>0.09</b>
	<b>3.04</b>	<b>0.95</b>	<b>0.39</b>	<b>0.23</b>	<b>0.16</b>	<b>0.16</b>	<b>0.07</b>
	<b>3.04</b>	<b>0.97</b>	<b>0.41</b>	<b>0.23</b>	<b>0.16</b>	<b>0.16</b>	<b>0.08</b>
	<b>2.86</b>	<b>0.95</b>	<b>0.41</b>	<b>0.23</b>	<b>0.15</b>	<b>0.15</b>	<b>0.08</b>

<b>Sample ID</b>	<b>A</b>	<b>B</b>	<b>C</b>	<b>D</b>	<b>E</b>	<b>F</b>	<b>G</b>
<b>OSP26 wool</b>	<b>2.89</b>	<b>0.96</b>	<b>0.41</b>	<b>0.23</b>	<b>0.15</b>	<b>0.15</b>	<b>0.08</b>
	<b>2.86</b>	<b>0.95</b>	<b>0.40</b>	<b>0.22</b>	<b>0.15</b>	<b>0.15</b>	<b>0.08</b>
	<b>2.86</b>	<b>0.95</b>	<b>0.41</b>	<b>0.22</b>	<b>0.15</b>	<b>0.16</b>	<b>0.08</b>
	<b>2.85</b>	<b>0.95</b>	<b>0.41</b>	<b>0.22</b>	<b>0.15</b>	<b>0.15</b>	<b>0.08</b>
	<b>2.85</b>	<b>0.94</b>	<b>0.39</b>	<b>0.22</b>	<b>0.15</b>	<b>0.15</b>	<b>0.08</b>
	<b>2.84</b>	<b>0.94</b>	<b>0.40</b>	<b>0.23</b>	<b>0.16</b>	<b>0.15</b>	<b>0.08</b>
	<b>2.86</b>	<b>0.95</b>	<b>0.39</b>	<b>0.22</b>	<b>0.16</b>	<b>0.14</b>	<b>0.08</b>
	<b>2.86</b>	<b>0.94</b>	<b>0.40</b>	<b>0.22</b>	<b>0.16</b>	<b>0.16</b>	<b>0.08</b>
	<b>2.87</b>	<b>0.95</b>	<b>0.40</b>	<b>0.22</b>	<b>0.15</b>	<b>0.14</b>	<b>0.08</b>

#### **4.2.1.4 Spectral Database Development and Partial Validation for Wool and Mohair.**

This section of this thesis deals with the development and partial validation of a simple in-house Raman spectral database of wool and mohair fibre samples. About 50 scoured wools and 50 scoured mohair samples, with all the details contained in Table 3.1, were used in calibrating the current in-house Raman spectral database and was partially validated with a few wool and mohair. The main aim of this section was to develop and validate a Raman spectral database for wool and mohair fibre samples of different origins. This was also to demonstrate the potential Raman spectral library searching tools bear in distinguishing between different types of animal fibres, especially wool and mohair. The results presented in this research are based on the verification of fibre samples rather than their identification, this being because of the fact that all the samples tested are known.

The extremely large amount of data which can be generated in a single Raman, gas chromatographic (GC), mass spectroscopic (MS) or FTIR spectrum necessitates computer-assisted data processing and interpretation. Consequently, spectral databases or library systems are included in most commercial spectroscopic instruments. The FT Raman system, from Bruker, used in this study, was purchased with such spectral libraries which includes a spectral database for natural animal fibres. The Bruker natural animal fibre database contains Raman spectra acquired from wool, mohair, cashmere and Angora rabbit hair, with differently pigmented fibre samples included. It has previously been shown that differently pigmented fibres display different Raman spectral features (Schrader *et al.*, 2000). The Bruker spectral database includes spectral entries acquired from the dark brown, black, baige, and white sheep wool, with white cashmere and white silver mohair fibres. The acquisition conditions (laser power, spectral resolution and the acquisition time) under which these spectra were acquired or the state in which the samples were in, are unknown and these factors are likely to significantly influence the spectral searching results and may lead to misclassification and misidentification of materials of unknown identity. Various spectral search algorithms have been developed in the past which help in comparing an unknown or query spectrum to each of the reference spectra in the database. These algorithms help in calculating and returning a value popularly referred to as the hit quality Index (HQI), this being calculated to determine the existence of a correlation between a spectrum of an unknown material (query or test spectrum) and the spectra from known materials or compounds in the reference spectral

database (Boruta, 2012). The list of possible candidate matches of the unknown (i.e. query or test spectrum), popularly referred to as the hit list, is arranged such that the highest HQI values are at the top of the list and the higher the HQI value the closer the unknown spectrum to the material/compound in the reference database. When a few spectra produced in the current study were matched with this database (Bruker spectral database), using the HQI spectrum correlation search algorithm, less than 40% of the tested spectra were correctly classified or identified as belonging to the correct fibre type, i.e. wool or mohair. The reason for the low classification accuracy might be in the difference of the acquisition conditions from which the query and the reference spectra were acquired, and it was because of this that the development of a new in-house spectral database for wool and mohair fibre samples from different origins, was necessary.

All spectral matching in this study was conducted using the HQI spectrum correlation search algorithm using an uncomplicated sample-to-sample spectral matching without any modelling. In this search algorithm, i.e. the spectrum correlation, the sum of the squared deviations between the query spectrum and the result spectrum from the data points of the spectral range defined is calculated. The summation can be limited to a spectral range selected by the user. It also allows for spectral normalization to be conducted before any spectral search can be conducted.

A minimum of six spectra from each sample were acquired and averaged using the averaging using OPUS 7.2 software. The current spectral database contains approximately 100 average wool and mohair spectra which have been baseline corrected and were all recorded using the Nd-YAG laser, emitting at 1064 nm. The signal to noise ratio of the spectra was good and smoothing was not found to be necessary. The library entries were loaded and named as fibre type (i.e. wool or mohair) followed by the sample ID. All spectra, whether reference or query, used in this analysis were normalization based on the intensity of the CH<sub>2</sub> & CH<sub>3</sub> bending modes (around 1450 cm<sup>-1</sup>), in the 1375-1508 cm<sup>-1</sup> spectral region. In the pre-processing stage truncation, which includes excluding all parts of the spectra which are likely not overlap between the query and reference or database spectra (Khan and Madden, 2012), was also conducted in this study. It was noted that there are spectral sections or regions that appeared to vary considerably, and which were found to influence the spectral search results namely the 0-450 cm<sup>-1</sup> and the 1800-3600 cm<sup>-1</sup> region. The only important or characteristic

spectral feature occurring in these regions is the very strong CH<sub>2</sub> asymmetric stretch, occurring around 2932 cm<sup>-1</sup>, and was found to vary, particularly the relative peak heights, even between spectra of the same fibre sample. Park *et al* (2017) argued that the strongest bands have the greatest influence on the HQI scores, the reason being the fact that the HQI classification-based algorithms put strong emphasis in comparing band intensity and area rather than peak wavenumbers. As a step towards optimizing the performance of the current wool and mohair spectral database, Figure 4.16 (a & b) is an example of the spectral search results for the same spectrum of the TXSK (Texas) mohair sample with (a) 450-3600 cm<sup>-1</sup> spectral region searched and (b) the 450 cm<sup>-1</sup>-1800 cm<sup>-1</sup> spectral region searched, respectively. The obviously observable difference is in the first hit, which is the BR82 wool sample in (a) and the Texas International Mohair INC- #708 in (b). The strong influence of the strongest bands in HQI is also observed in the decrease in HQI values, after the exclusion of the spectral region containing the strong band (2932 cm<sup>-1</sup>), from 987 in (a) to 976 in (b). Furthermore, the number of mohair spectra in the top ten entries of the hit list also improved, with only two mohair entries in (a) as opposed to the four in (b).

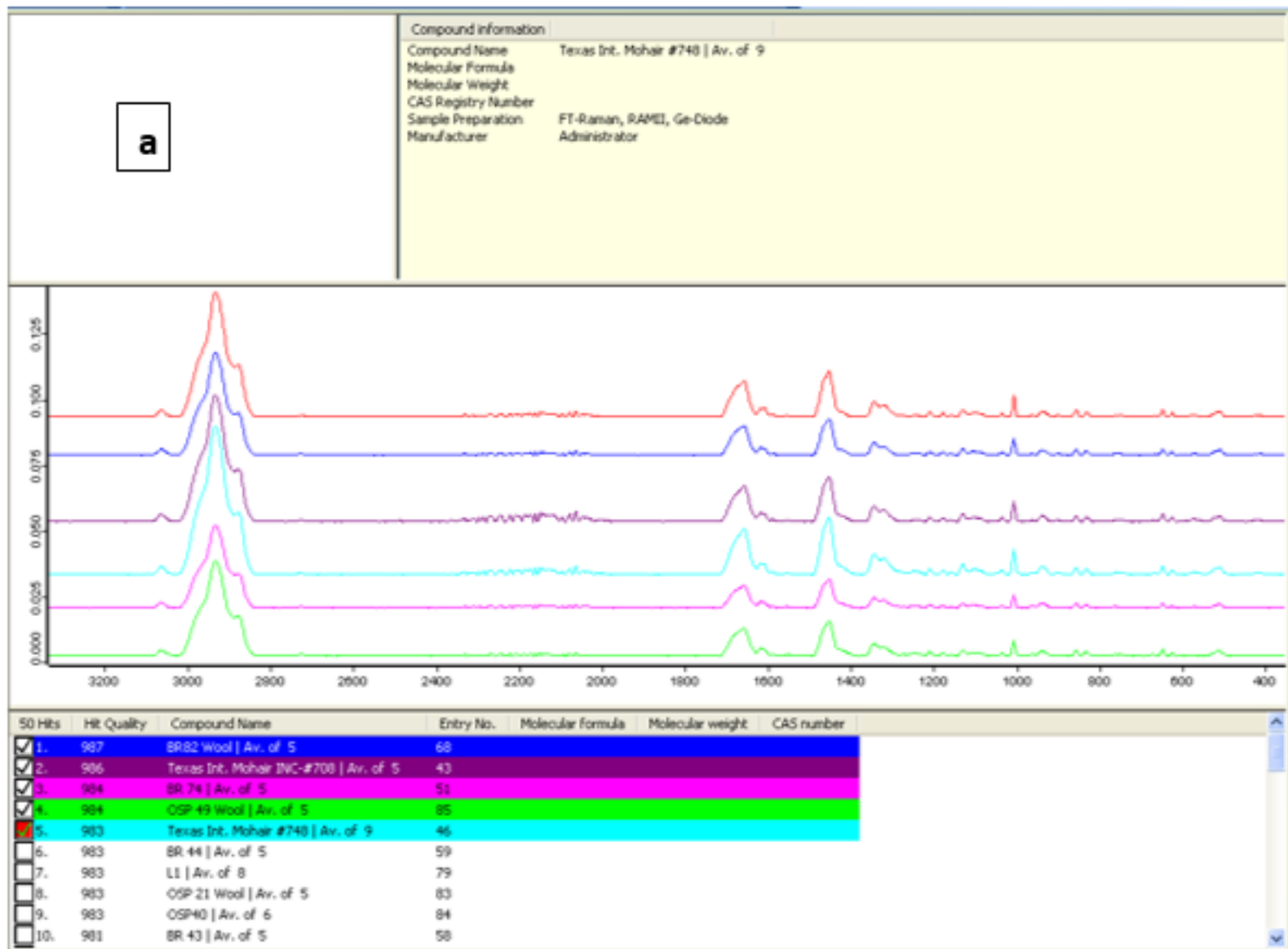


Figure 4.16(a): The influence of the strongest band in the HQI matching for the same spectrum.



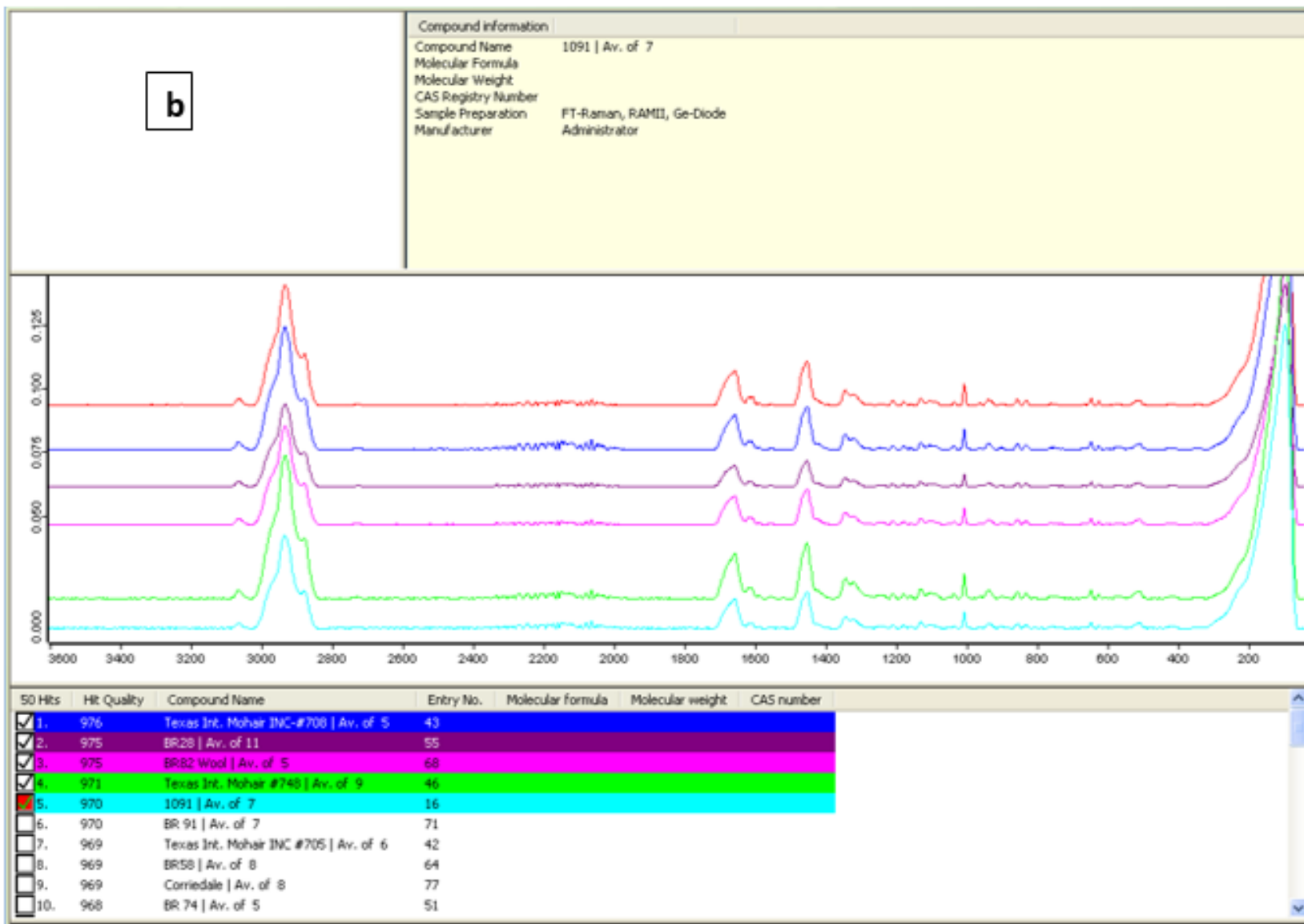
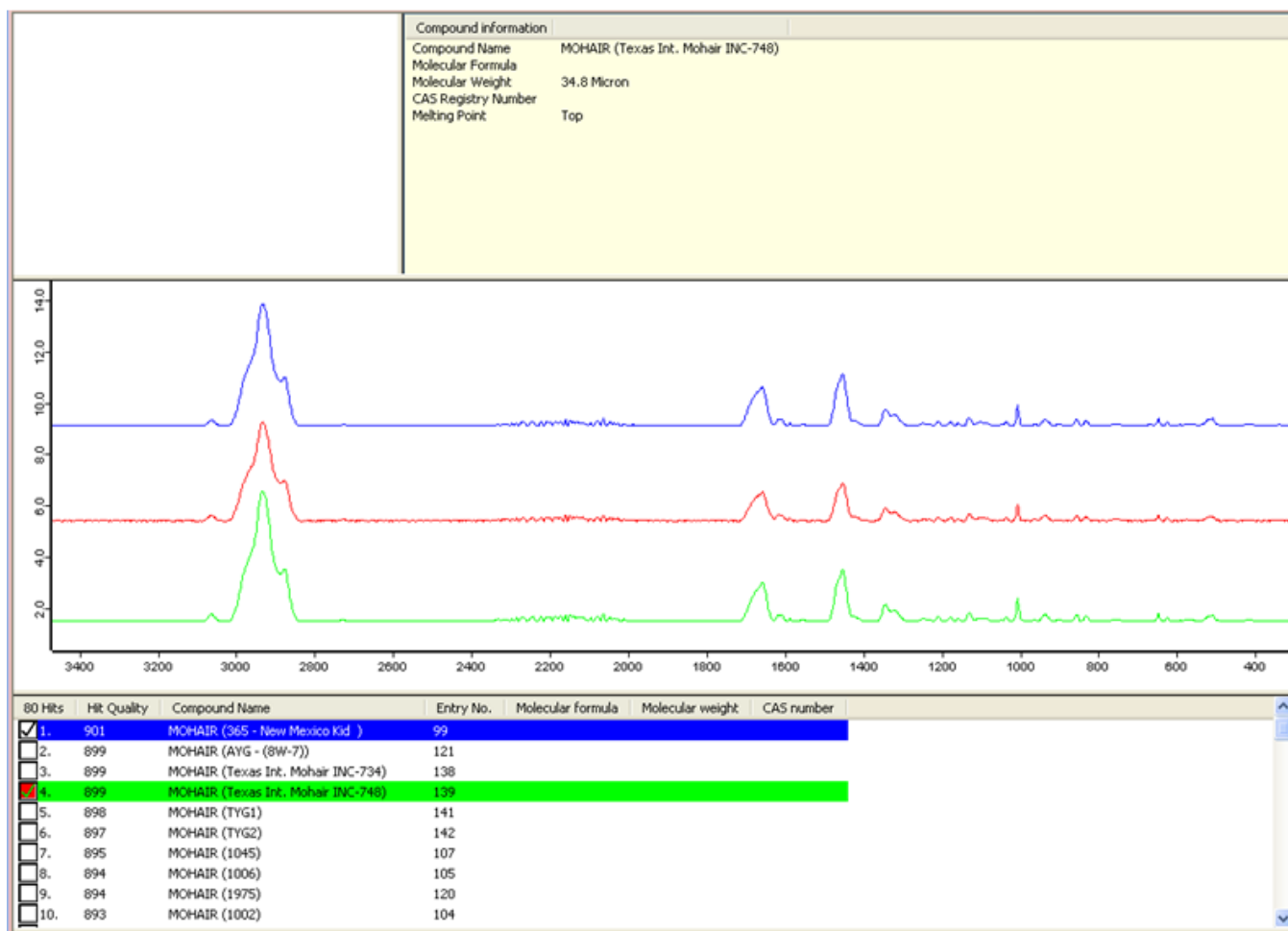


Figure 4.16(b): The influence of the strongest band in the HQI matching for the same spectrum.

The current study initially investigated several spectral searching conditions to achieve the optimum conditions. Searching the region  $450\text{-}1800\text{ cm}^{-1}$  with the second derivative and applying the vector normalization provided satisfactory results. Consequently, the results to be presented in the following section were performed with under these conditions. All the reference or database spectra are averages of a minimum of five normalized individual spectra while all the test or query spectra are the normalized individual spectra.

Figure 4.17 is an example of spectral matching for one of the mohair samples (Texas International Mohair INC- #748). When the spectral range  $450\text{-}3600\text{ cm}^{-1}$  was searched, Vector normalization and the second derivative selected, the exact match of this spectrum was found at the 9<sup>th</sup> position of the hit list (result not shown). In Figure 4.16 the search conditions Spectral region  $450\text{-}1800\text{ cm}^{-1}$ , Second derivative and Vector normalization were used. The query spectrum, in both cases, was not the perfect match of the first hit of the hit list, however, the improvement (from 9<sup>th</sup> to 4<sup>th</sup>) in the hit list position, of the actual match, was observed. This improvement in the hit list is most likely due to the fact that the spectral features occurring in the region  $1800\text{-}3600\text{ cm}^{-1}$  tend to vary in both wavenumber (position) and intensity. It is worth mentioning that in both these cases the top ten of the hit list was entirely made up of all mohair spectra, resulting in the decision making about whether the test spectrum belongs to the wool or mohair fibre class an easy task.



**Figure 4.17: Examples of spectral search result, with the red, blue and green spectra as the query, the first hit of the hit list and the actual match, respectively.**

This study also found out that the exact match of the query spectrum was sometimes not even in the top ten of the hit list, despite the dominance (in the hit list) by spectra of fibre samples belonging to the same fibre class as the query. Figure 4.18 (a-d) contains spectral search results of the 1052 mohair sample and notably none of the first hits was the exact match (i.e. the 1052 mohair spectrum). In Figure 4.18 (c) the exact match was found in the 14<sup>th</sup> position of the hit list, however, even in this case the hit list is entirely made up of mohair spectra, making it easy to classify the fibre type, to which the query spectrum belongs. Generally, this study has shown that finding the exact match of the query spectrum might not be possible using the currently developed wool and mohair spectral library. This is due to the great similarity of the spectral features, and probably the overlapping intensities and band positions, shared by mohair and wool samples from different countries and different fibre

dealers. This observation is in agreement with that of Park *et al.*, (2016), that the HQI based spectral classification is vulnerable to the intensity.

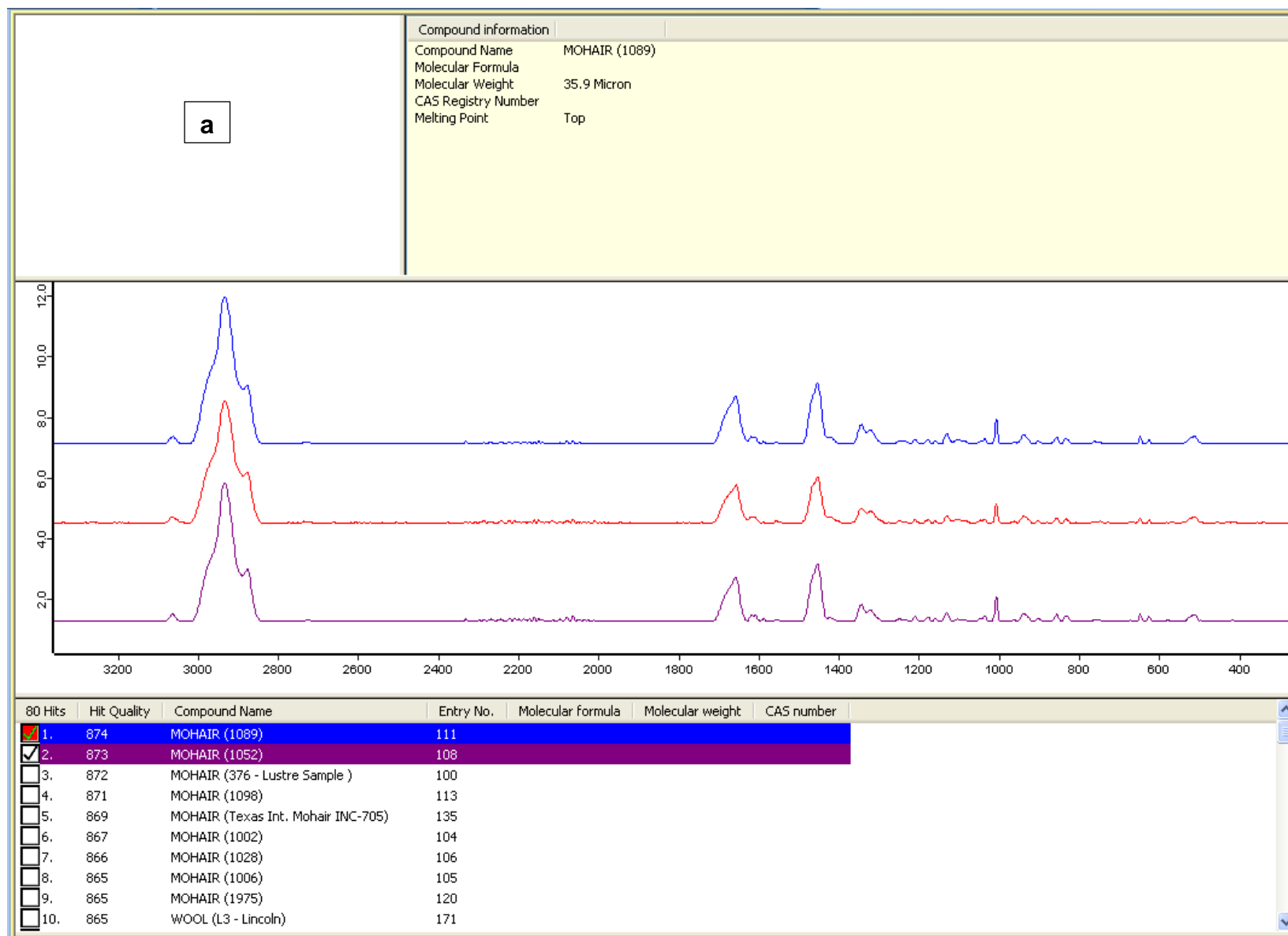


**Figure 4.18(a): Search result of the first query spectrum of the 1052 mohair.**

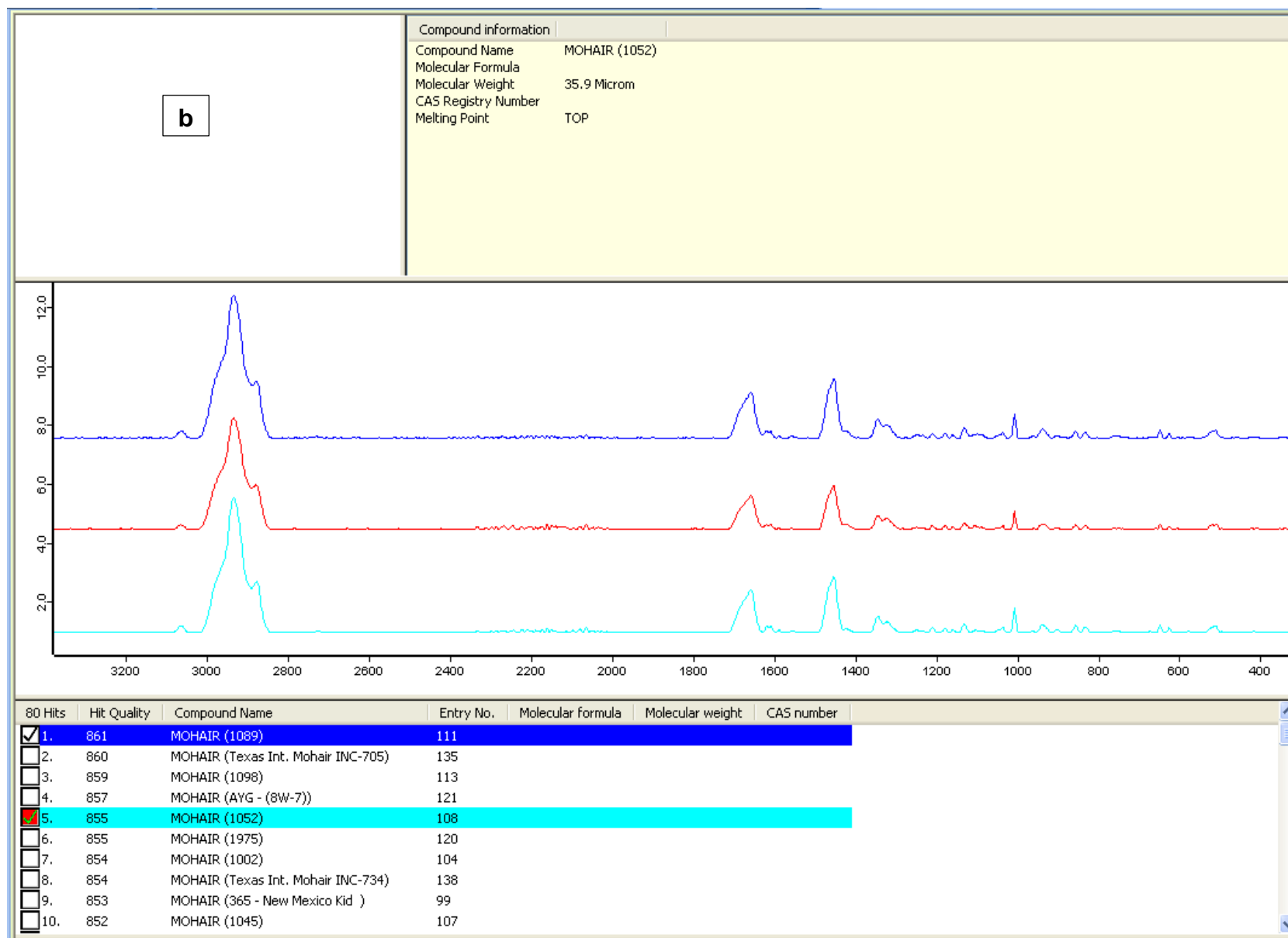


**Figure 4.18(b): Search result of the second query spectrum of the 052 mohair.**

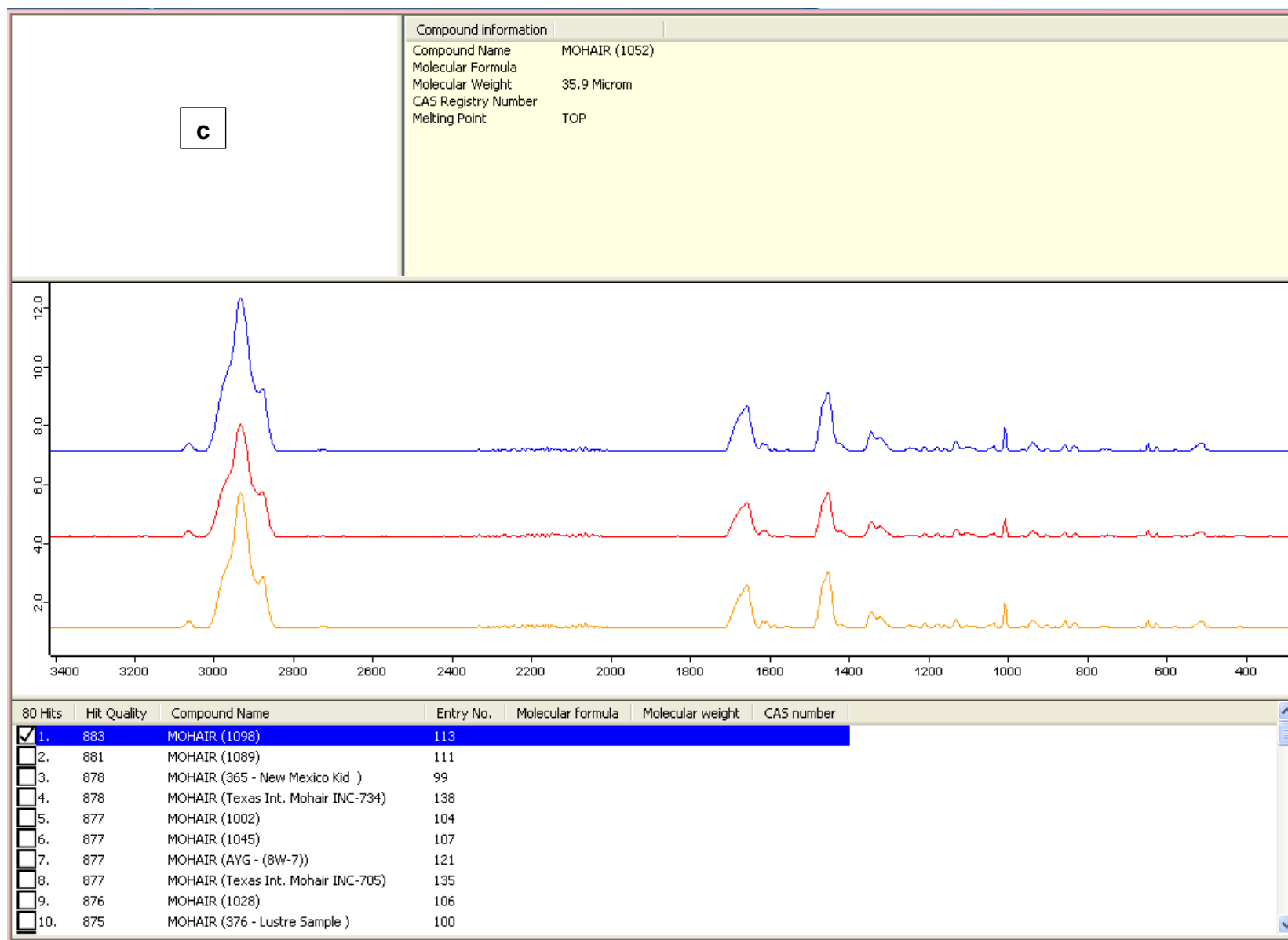


Figure 4.18(c): Search result of the third query of the 1052 mohair.

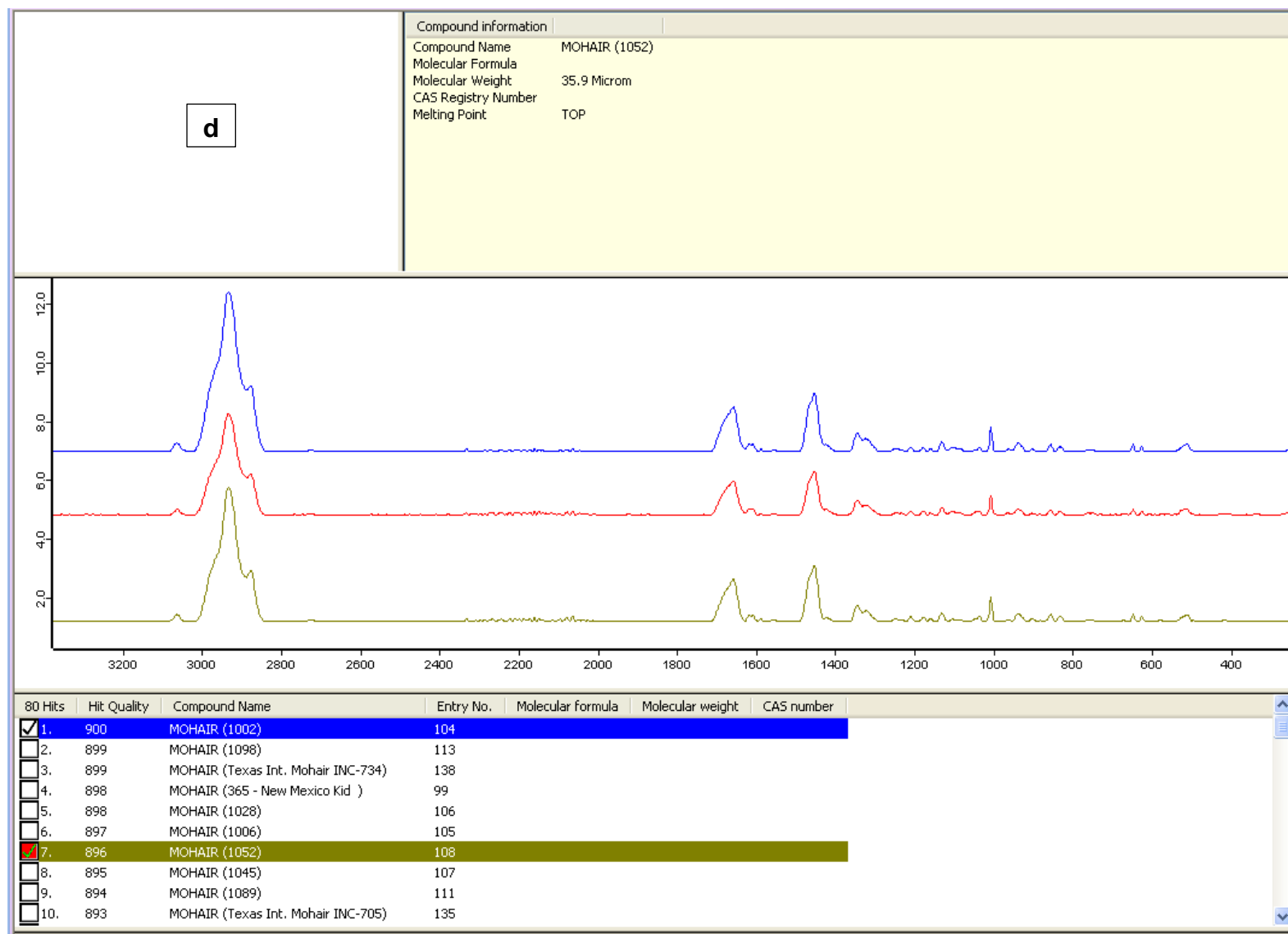
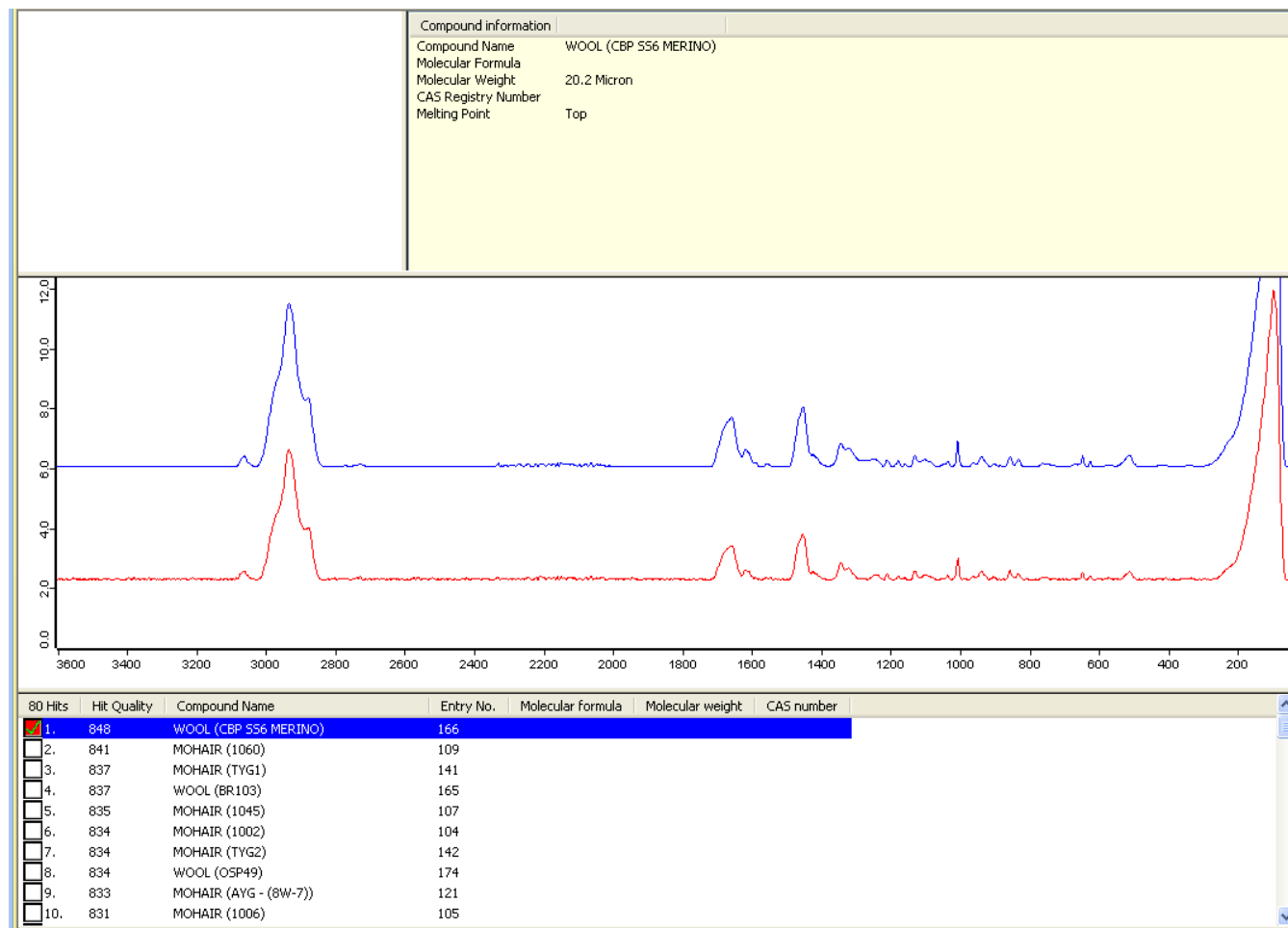


Figure 4.18(d): Search result for the fourth query spectrum of the 1052 mohair.



Occasionally, the hit list was found to be dominated by spectra of fibre samples which does not belong to the fibre class of the query (see Figure 4.19) despite the first hit of the hit list being the exact match. In Figure 4.19 match result of the CBP SS4 merino wool are shown.



**Figure 4.19: Spectral search result for CBP SS4 merino wool.**

This fibre sample did not have an average spectrum in the database rather an average spectrum from a similar fibre sample, CBP SS6 merino wool, was added in the database. This analysis showed that all the spectra from this sample (all three) matched exactly with the CBP SS6 merino wool as the first hit of the top ten.

Table 4.20 contains some of the spectral search results for the four of the seven wool and mohair samples examined. A minimum of three query or test spectra from each of these samples were acquired and matched with the database. Spectra tested here had their average spectra on the database but were not included in constructing the average spectrum

(left out for this purpose). The only exception was the CBP SS4 Merino sample which was not represented in the database (only the average spectrum of the CBP SS6 Merino sample was in the database). An important fact to emerge from this section of results is that the first hit of the hit list hardly matched with the query spectrum. However, the top ten of the hit list, was always dominated or entirely made up of spectra of the fibre samples which belong to the same fibre type as the query. This implies that the group to which the query belongs may have been identified, leading to the classification as wool or mohair, rather than the exact sample from which it was acquired. Because of this, this study used a simple classification method based on the number of spectra of the fibre type/class dominating the top ten of the hit list being the fibre class to which the query spectrum belongs. This is combined with the average HQI values for each of the fibre classes in the top ten entries of the hit list, a similar classification method to that of hit quality index (HQI)-voting developed by Lee *et al.*, (2013). No special software was necessary for the analysis in this section, HQI data were manually exported from the OPUS software spectral image into excel for average calculations.

**Table 4.20: Spectral matching results of normalized spectra.**

Sample ID	Query number	Number of wool spectra (HQI)*	Number of mohair spectra (HQI)‡	HQI of the first hit
	1	2 (894)	8 (897)	904
Texas International Mohair INC- #748	2	2 (898)	8 (900)	905
	3	0 (0)	10 (897)	901
	4	0 (0)	10 (903)	908
	1	1 (865)	9 (874)	874
	2	0 (0)	10 (856)	861
1052 Mohair sample	3	0 (0)	10 (878)	883
	4	0 (0)	10 (897)	900

\*‡ Number of wool and mohair spectra in the top ten of the hit list, respectively, their average HQI in <sup>0</sup>.

Sample ID	Query number	Number of wool spectra (HQI)*	Number of mohair spectra (HQI)‡	HQI of the first hit
Texas	1	1 (876)	8 (879)	882
International Mohair INC- #705	2	1 (876)	8 (878)	883
	3	1 (874)	10 (880)	885
	1	6 (856)	4 (855)	857
TYG1 Turkey Mohair sample	2	0 (0)	10 (877)	879
	3	0 (0)	10 (876)	877
	1	6 (856)	4 (846)	871
CBP SS4 Merino wool	2	3 (840)	7 (834)	848
	3	8 (866)	2 (841)	874

**Table 4.20: continued...**

**\*\*‡ Number of wool and mohair spectra in the top ten of the hit list, respectively, their average HQI in ().**

Notably, even in cases where query or test spectra were represented in the database, verification of the test spectrum as being from a certain sample was extremely difficult using the current database. When the query spectrum was not represented in the database (the case of the CBP SS4 wool sample), the first hit always belonged to the same fibre type and from the same dealer as the query spectrum. The results in Table 4.17 indicates that the classification of query spectra as wool or mohair was achieved with good accuracy (above 90 % of the query spectra being classified correctly), with a very few cases where the classification was not satisfactory (e.g. Query 1 of the TYG1 sample), where wool spectral entries dominated the top ten of the hit list.

The main challenge of this section of this research study, however, is based on the fact that a very small number of spectra was available to validate the database; this stems from the

frequently experienced equipment breakdown. This study was also challenged greatly by the lack of strong ability in the field of algorithm development on the side of the researcher. Collaborative research work towards developing a suitable search algorithm for the currently developed Raman spectral database would be beneficial and is highly recommended for the future research studies. The Raman spectral match results of this study indicates that there might be success in the classification of wool and mohair fibre samples with the application of multivariate or chemometric based methods. Methods such as cluster analysis and principal component analysis (PCA) will be assessed for their application in the current spectral database. This comes from the general observation that spectra belonging to the same fibre class as query spectra formed a cluster or group of identified spectra at the top of the hit list.

#### 4.2.2 Micro-Raman Fibre Analysis

A repeated Raman experiment using a different excitation laser wavelength (514.5 nm) was conducted to characterize wool and mohair single fibres, with the aim to distinguish between them. One of the advantages of Raman spectroscopy is the availability of different excitation wavelengths one can select from to analyse different materials. Zhou (2015) stated that the Raman spectrum and its specific spectral band positions are mainly related to the material's unique chemical structure and are independent of the laser excitation wavelength used in acquiring the spectrum. This section of the thesis provides results obtained from the Raman micro-spectroscopic analysis of wool and mohair single fibres. The micro-Raman instrument, with the operating parameters described in section 3.4.2.2 was used. This instrument is equipped with an excitation laser wavelength of 514.5 nm, which provides an improved scattering efficiency (Zhou, 2015) compared to that of the 1064 nm excitation laser wavelength used in the FT Raman spectrophotometer. A stronger Raman signal is expected when using the lower wavelength excitation laser (Tuschel, 2016). Fibre samples analysed in this investigation were selected from those contained in the Table 3.1.

Highly identical spectral information (Figure 4.20 a and b) was also observed from the wool and mohair fibres. Like in the case of FT Raman spectroscopic results presented earlier, there were no new band assignments or any new spectral features which could help distinguish between the two fibre types, with all the bands observed earlier (Table 4.1) being observed in this micro-Raman spectroscopic analysis. Expectedly, spectral features or bands were notably stronger or more pronounced compared to the FT Raman spectra. However, the risk of fluorescence was strongly observed and consequently, the weaker Raman bands were difficult to analyse, especially extracting peak heights or intensities as some were either suppressed or ill-defined. Band positions tended to vary within spectra of the same sample, with similar variation observed between wool and mohair. Table 4.20 contains band positions at maximum peak heights for the selected chemical bands:

**Table 4.20: Micro-Raman spectral positions of selected bands for wool and mohair.**

Band assignment	This study (cm <sup>-1</sup> )	Reference
CH <sub>2</sub> asymmetric stretch	2932 ± 2	Carter <i>et al.</i> , (1994)
CH <sub>2</sub> & CH <sub>3</sub> bending	1449 ± 2	Jurdana <i>et al.</i> , (1994)
Amide I	1652 ± 2	Rintoul <i>et al.</i> , (2000)
Phe & Trp	1002 ± 2	Carter <i>et al.</i> , (1994)
Skeletal C-C stretch	935 ± 1	Church <i>et al.</i> , (1997)
Tyr	642 ± 1	Carter <i>et al.</i> , (1994)
Phe	621 ± 2	Carter <i>et al.</i> , (1994)
S-S stretch	509 ± 2	Carter <i>et al.</i> , (1994)

The only possible difference observed between wool and mohair was that based on the peak heights of each of the Raman chemical bands. However, these were found to vary significantly, even within spectra acquired from the same fibre sample. Hence, relative peak height ratios (see Table 4.21) were determined between wool and mohair as a means of distinguishing between them.

**Table 4.21: Micro-Raman relative peak heights for wool and mohair fibres.**

Band ratio	Wool		Mohair	
	Mean	95% conf. limits (q)	Mean	95% conf. limits (q)
A	5.08	0.15	4.88	0.25
B	1.54	0.06	1.41	0.11
C	0.69	0.04	0.74	0.05
D	0.47	0.01	0.38	0.02
E	0.50	0.02	0.47	0.04
F	0.21	0.02	0.19	0.02
G	0.14	0.01	0.13	0.01

The peak height of the very strong CH<sub>2</sub> asymmetric stretch (near 2932 cm<sup>-1</sup>) relative to the CH<sub>2</sub> & CH<sub>3</sub> bending modes, was found to be stronger in wool spectra than in the mohair fibre spectra. However, the means comparison, using the statistical student t-test, showed that the observed difference is statically insignificant ( $p > 0.05$ ). The few number of samples involved, and also the biasness in the mohair selection may have influence the results. A large number of samples from different regions will be included in the next research studies, to investigate the potential of this band ratio in the classification of wool and mohair.

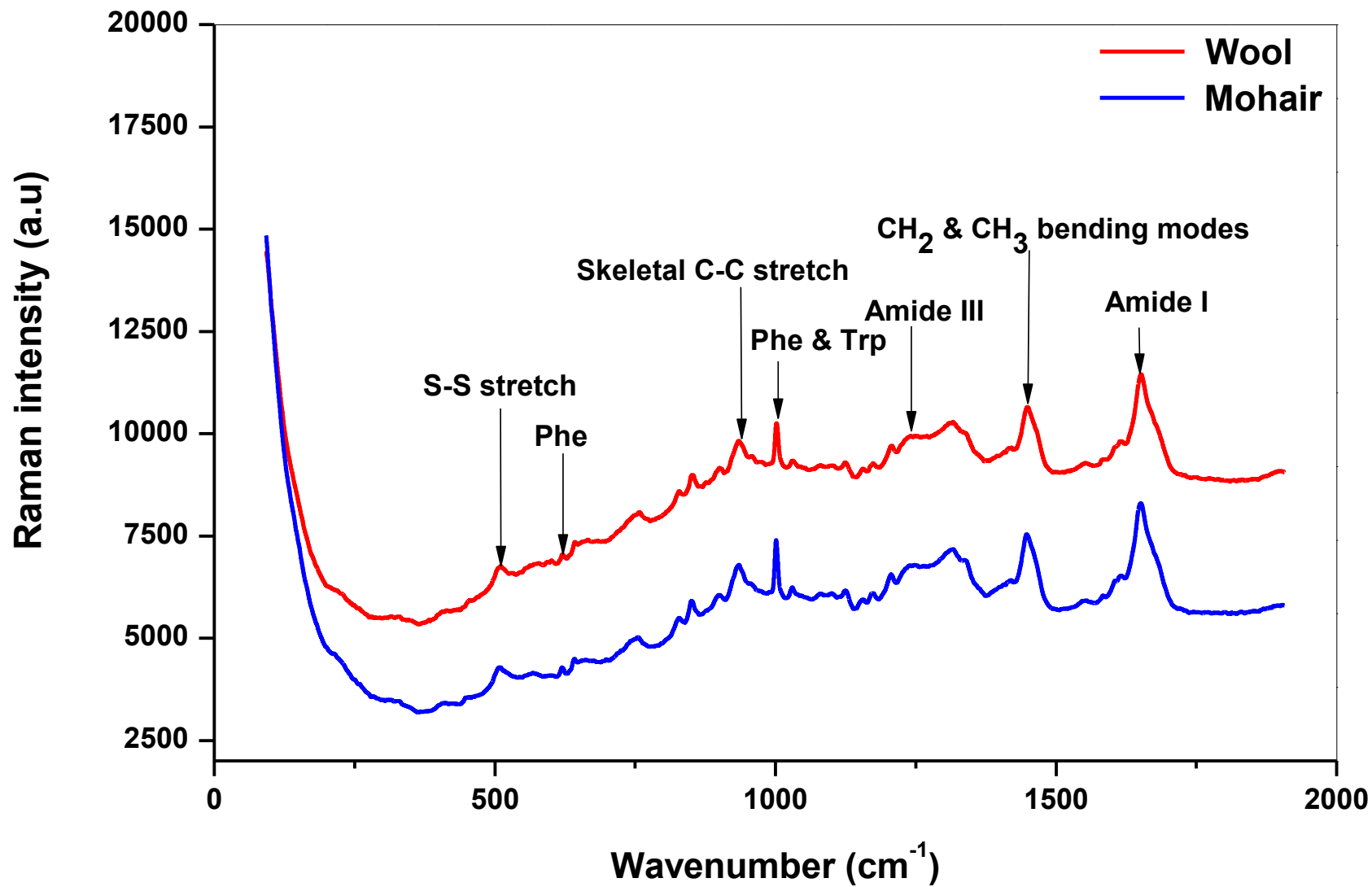
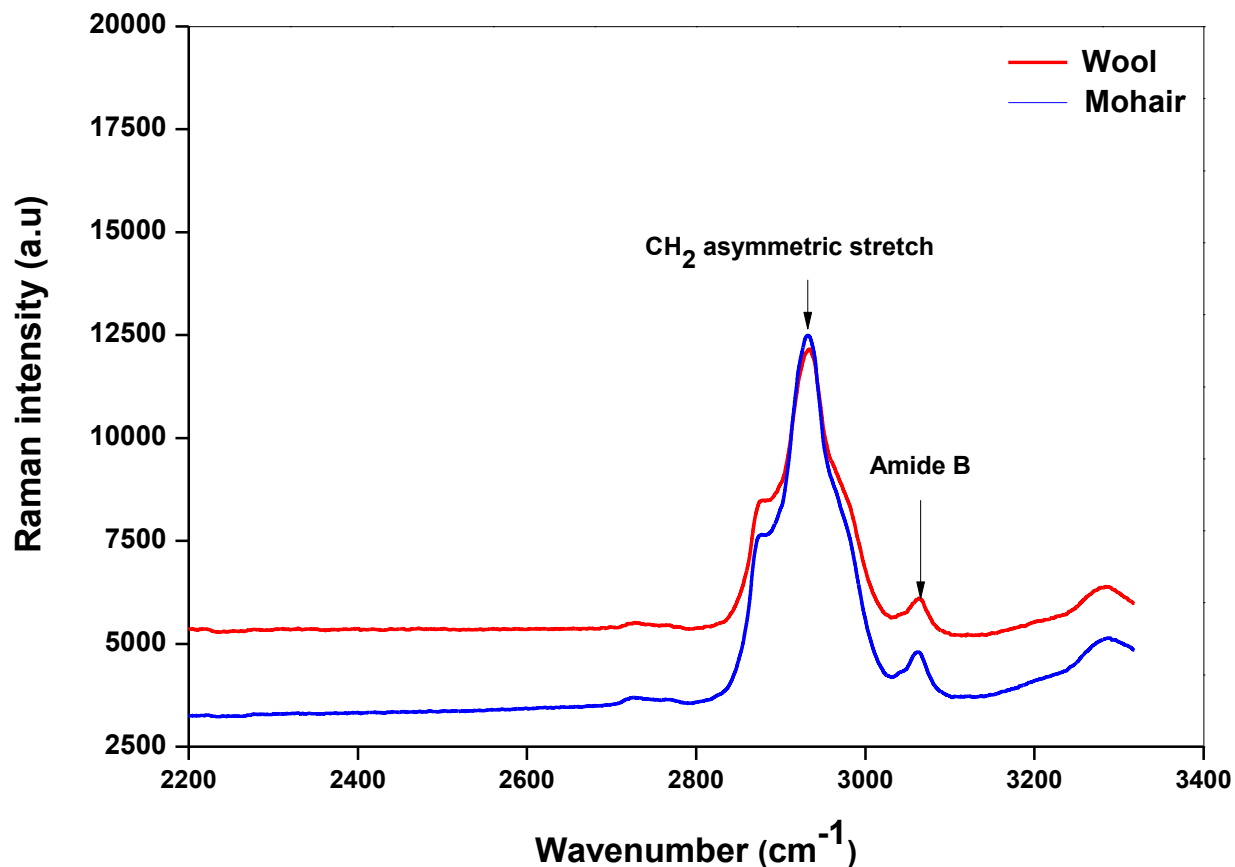


Figure 4.20(a): Wool (red) and mohair (blue) spectra over the spectral range 0-2000  $\text{cm}^{-1}$ .





**Figure 4.20 (b): Wool (red) and mohair (blue) spectra over a spectral range of 2200-3400  $\text{cm}^{-1}$ .**

This investigation also proved that a great overlap of the individual ratio A values exists between wool and mohair fibres. The peak heights of the amide I (around  $1655 \text{ cm}^{-1}$ ) relative to the peak heights of the  $\text{CH}_2$  &  $\text{CH}_3$  bending modes (near  $1450 \text{ cm}^{-1}$ ) (i.e. ratio B) were found to be higher in wool fibres compared to mohair spectra, although the means comparison proved the difference as statistical insignificant ( $p > 0.05$ ). Furthermore, the individual values were found to overlap considerably (see the box whisker plots in Figure 4.21), casting a great doubt of the application of this band ratio in the classification of the two fibre types, wool and mohair. This Raman band intensity ratio is usually related to the secondary structure of keratin fibres, and the lack of difference is to be expected for the wool and mohair fibres, since both of these fibres are dominated by the  $\alpha$ -helical secondary structure when in their natural state.

The ratio C was also found to overlap greatly between wool and mohair individual values, with the mean values of  $0.69 \pm 0.04$  (95% confidence limits) and  $0.74 \pm 0.05$  (95% confidence limits), for both wool and mohair, respectively. This study also looked at the applicability of the ratio D, as a potential tool for classification of wool and mohair single fibres. The individual values varied considerably in both wool and mohair fibres, with wool ranging from 0.39 to 0.53 and mohair from 0.30 to 0.43. The mean values of  $0.47 \pm 0.01$  and  $0.38 \pm 0.02$  (95% confidence limits), were found to be statistically significant ( $p < 0.05$ ). A fair overlap (see Figure 4.22) of the individual values was also observed for this band ratio, between wool and mohair. This band ratio appears to hold a great potential in classifying wool and mohair fibre samples, despite the observed overlap. More experimental work, however, including a considerable number of animal fibres of different origins and those which have undergone different processing stages, is necessary towards realizing the full potential of this band ratio in animal fibre identification. A correlation of this Raman band ratio with the content of the amino acid cystine determined using chromatographic or electrophoretic methods would also be important and is planned for future research.

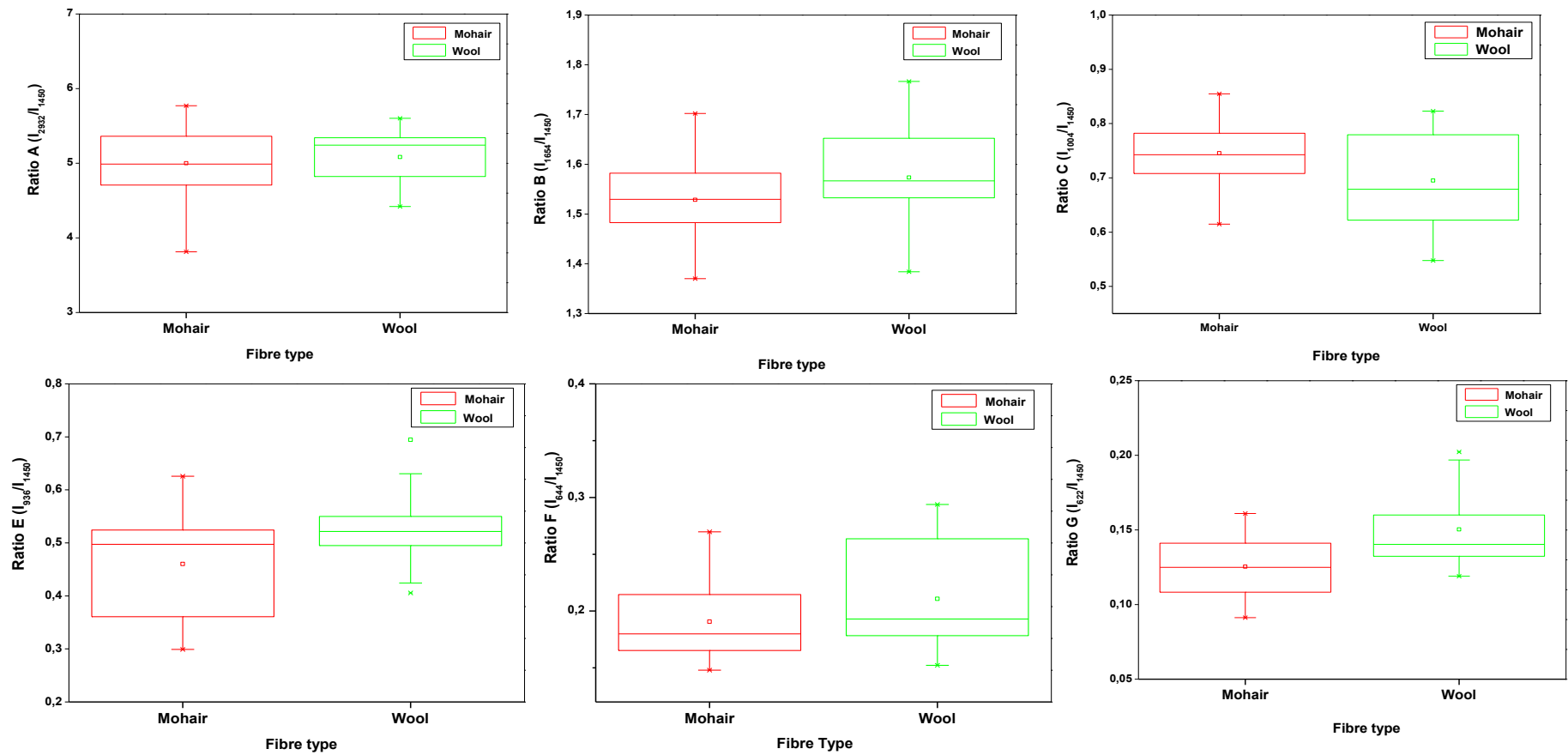
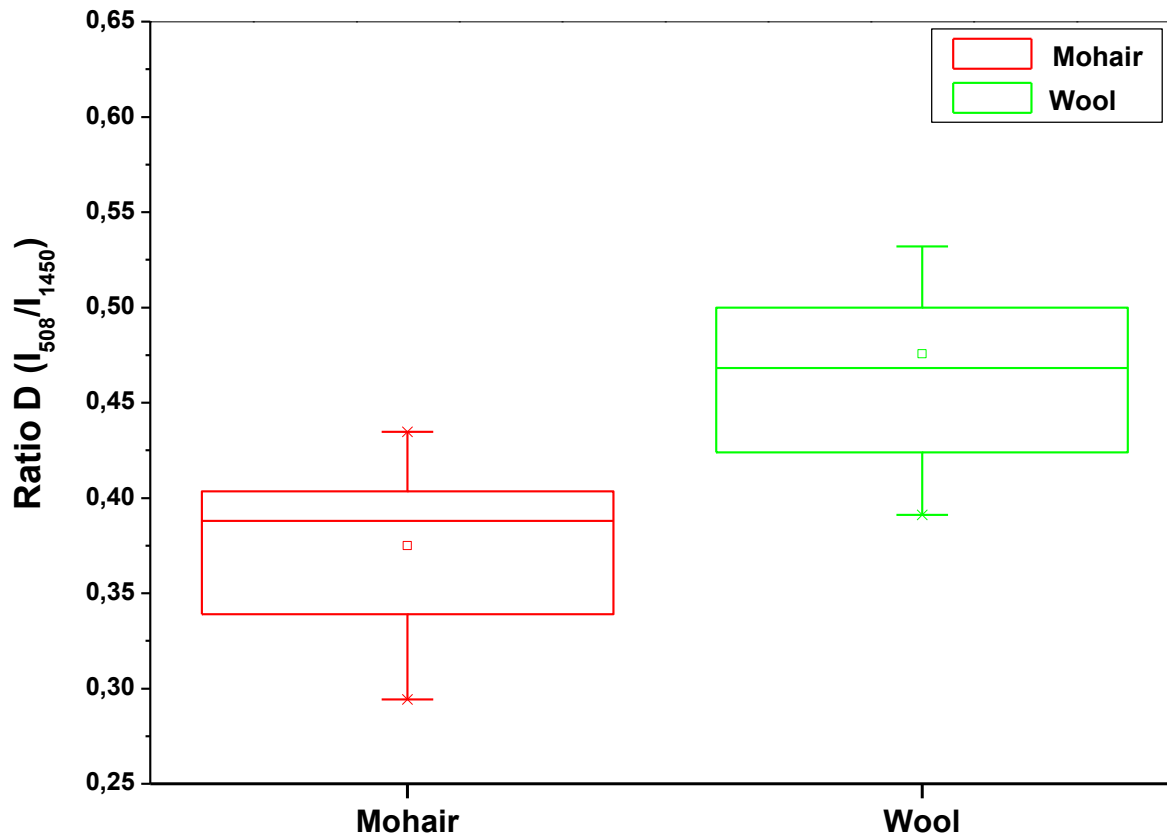


Figure 4.21: Box whisker plots of micro-Raman peak height ratios (A-G) for wool and mohair fibres.



**Figure 4.22: Box whisker of the ratio D values for wool and mohair.**

This band ratio appears to hold a great potential in classifying wool and mohair fibre samples, despite the observed overlap. More experimental work, including a considerable number of animal fibres of different origins and those which have undergone different processing stages, is necessary towards realizing the full potential of this band ratio in animal fibre identification. A correlation of this Raman band ratio with the content of the amino acid cystine determined using chromatographic or electrophoretic methods would also be important. The mean values of these relative peak heights skeletal C-C stretching vibration (ratio E), which is also related to the secondary structure of keratin fibres, were also determined and found to be statistically insignificantly different ( $p > 0.05$ ). The band ratios F and G were found to overlap considerably, between wool and mohair fibres with mean values of  $0.21 \pm 0.02$  and  $0.14 \pm 0.01$  (95% confidence limits) for wool and  $0.19 \pm 0.02$  and  $0.13 \pm 0.01$  for mohair

fibres, respectively. The means comparison with the application of the student t-test, showed that these are statistical insignificant ( $p > 0.05$ ).

The mohair samples analysed in this study were the lustre samples (\* labelled in Table 3.1) prepared at the Council for Scientific and Industrial Research (CSIR). These samples were always found to possess high relative intensities or peak heights compared to any other mohair sample in Table 3.1. This observation was also noticed for the analysis on the FT Raman system, with the 1064 nm wavelength excitation and may be related to their unknown composition. A comprehensive amino acid analysis of these samples would be essential and important in understanding the composition of these mohair samples.

## 4.3 FTIR MICROSCOPIC EXAMINATION OF WOOL AND MOHAIR FIBRES

### 4.3.1 Introduction

Another well established and recognized technique in qualitative, and occasionally quantitative, analysis of organic materials, is that employing infrared spectroscopy, particularly in the mid-infrared (MIR) region. IR spectroscopy exploits the fact that molecules rotate and vibrate at specific frequencies, depending on their discrete energy levels (Houck, 2009). The IR spectrum is acquired through the exposure of the sample to infrared radiation, over a range of energies within the IR region. IR spectroscopic methods have been widely adopted, especially in the forensic examination of biological materials and in hair research (Pande, 1994), mainly due to its speed and non-destructive nature. Nevertheless, this technique has not been widely applied for characterization of animal fibres mainly due to the fact that these materials produce diffuse and poorly defined spectra. The development of Fourier Transform Infrared (FTIR) instruments, together with IR microscopes, has opened up the possibility for IR analysis of single fibres.

### 4.3.2 Amide Band Analysis for Distinguishing Between Wool and Mohair

High quality FT-IR spectra of wool and mohair fibres were acquired using the Bruker ATR-FTIR LUMOS system described in section 3.4.2.3. Figure 4.23 contains average spectra of wool and mohair fibres. Visually, there were no unique spectral features present in one of the two fibres, which could aid the identification of the two fibre types. Two amide bands dominate the IR spectrum of animal or protein fibres namely the amide I and the amide II. These bands occur at spectral regions  $1600-1700\text{ cm}^{-1}$  and  $1500-1570\text{ cm}^{-1}$ , respectively (Liu *et al.*, 2008). The amide I band is predominantly (80 %) due to contributions from the C=O stretching vibration of the peptide backbone. The amide II is 40-60 % due to the in-plane bending of the N-H bending and 18-40 % C-N stretching vibrations of the backbone and is found between  $1510-1580\text{ cm}^{-1}$ . These two amide bands are sensitive to hydrogen bonding and therefore sensitive to the differences in conformation of the secondary protein structure. Other chemical bands characterizing the IR spectra of keratin fibres includes the amide III ( $\sim 1230-1270\text{ cm}^{-1}$ )

and the S-O stretching vibrations in the spectral range 1030-1100  $\text{cm}^{-1}$ . The strong  $\text{CH}_2$  &  $\text{CH}_3$  bending modes (around 1450  $\text{cm}^{-1}$ ) in a wool Raman spectrum only appear as weak feature in the IR spectrum.

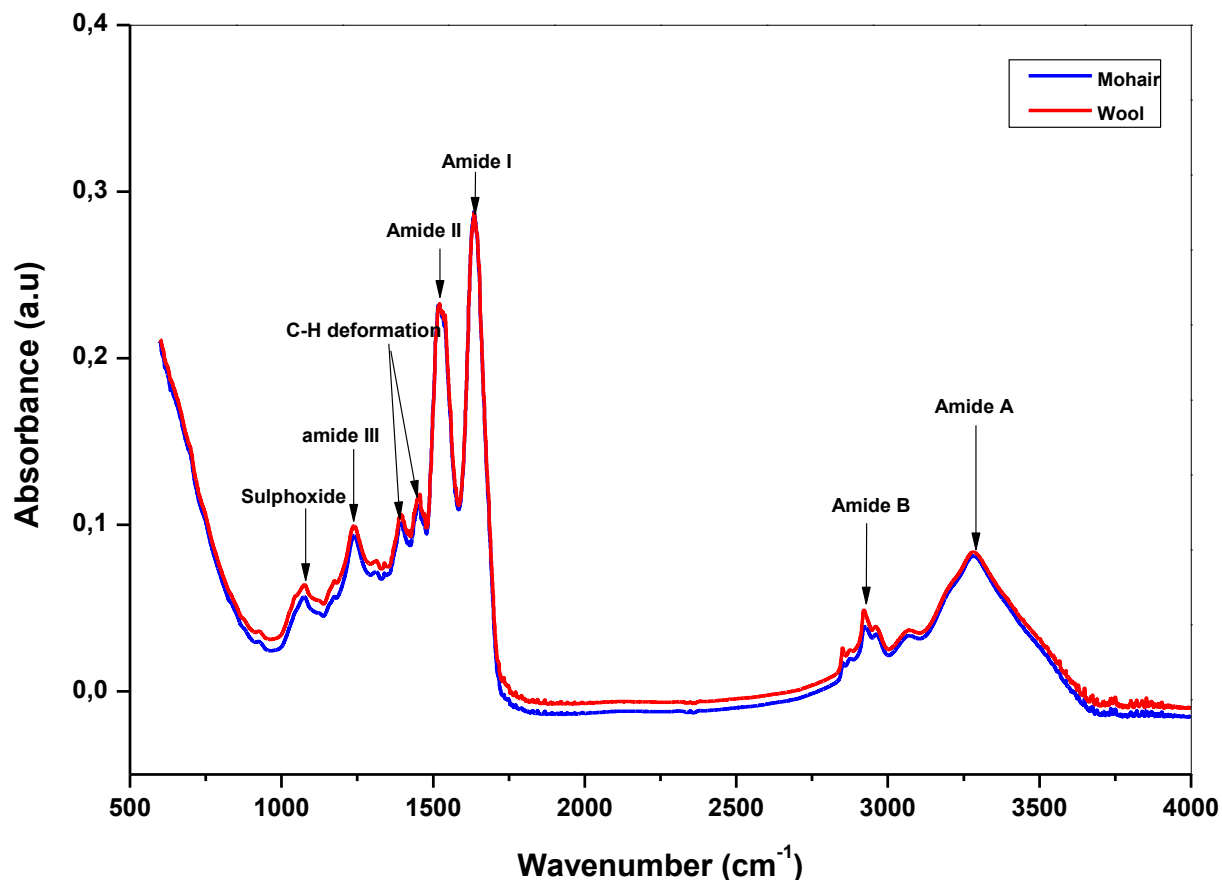


**Figure 4.23: Wool and mohair FTIR spectra in the spectral range 500-4000  $\text{cm}^{-1}$ .**

Liu *et al.*, (2008) with the application of the FTIR for wool and cashmere fibre analysis, noted that between different animal fibres, the peak positions, band shape and the peak heights may differ claiming that these could form basis for distinguishing between different animal fibre types including wool and cashmere fibre samples. In the current study the application of band area ratio of the amide I to that of the amide II (amide I/II) was determined and investigated for the possibility of differentiating between wool and mohair untreated fibres. The absorbance values were determined from eight average wool and eight average mohair spectra using the curve fitting procedure, with Table 4.22 summarizing the results. This band ratio has been selected for study because it

could be easily determined and since it is highly sensitive to any variations of the protein peptides (Hopkins *et al.*, 1991).

**Table 4.22: Amide I/II ratios for wool and mohair.**

Fibre type	Amide I/II ratio		
	Mean	Std Dev ( $\sigma$ )	Confidence limit ( $q$ )
Wool	1.20	0.04	0.02
Mohair	1.21	0.02	0.01

Mohair values ranged from 1.14 to 1.31 while wool was found to range from 1.13-1.45 and it is this observed overlap of the individual values between wool and mohair fibres which lead to a conclusion that the application of this amide band ratio in distinguishing between the two fibre types seem extremely impossible. The comparison of the mean values of the ratios of the two amide bands, using the student t-test, showed that indeed these values are not significantly different ( $p > 0.05$ ). Because of this impossible applicability of this band ratio in distinguishing between wool and mohair, this study investigated other IR bands for the possible differences between the two fibre types, including the investigation of the possible differences in the protein secondary structural conformation.

#### 4.3.3 FTIR Spectral Curve Fitting Results

Notably, the two fibre types shared identical spectral features and components, implying that their possible identification cannot be based on the absence or presence of IR bands in one fibre which could not be found on the other. A curve fitting or deconvolution of IR bands was also adopted with a view of studying the secondary structure of the two fibres. The combination of previous literature (Carr and Lewis (1993); Jones *et al.*, (1998); Wojciechowska *et al.*, (2004); Panaiotou (2004)) and the application of second derivative spectral analysis were useful in locating the exact



positions (wavenumbers) for each band and its components before curve fitting was conducted. The major bands in fingerprint region, spectral range 900-1800  $\text{cm}^{-1}$ , were selected for this section of the results. This spectral region contains IR bands such as the amide bands I, II and III, the  $\text{CH}_2$  &  $\text{CH}_3$  bending modes and the cysteic acid vibrations. Figures 4.19 (a and b) contain examples for some of the wool and mohair curve fitting results, respectively. Prior to curve fitting, the three spectra acquired from each fibre were averaged and the curve fitting was performed on the resulting average spectrum. A linear baseline subtraction was conducted using Origin Lab 8.0 software and the components were all fitted with 100% gaussian shaped bands. The curve fitting accuracy was quantified by the coefficient of determination (COD) ( $R^2$ ) and the reduced chi-squared values and these were always found to be 0.999 for all the curve fitting results obtained in this research, see Table 4.23.

**Table 4.23: The accuracy of wool and mohair FTIR spectral gaussian curve fitting.**

Statistic	Mohair		Wool	
	COD ( $R^2$ )	Reduced Chi-squared values	COD ( $R^2$ )	Reduced Chi-squared values
Average	0.999	$3.09 \times 10^{-6}$	0.999	$1.96 \times 10^{-6}$
Standard deviation ( $\sigma$ )	$2.22 \times 10^{-6}$	$2.04 \times 10^{-6}$	$1.11 \times 10^{-6}$	$2.04 \times 10^{-6}$

The band positions (wavenumbers) are summarized later in Table 4.24 for both wool and mohair found in this study with reference to which each band was compared. The centre of the cysteic acid band (typically centred around 1040  $\text{cm}^{-1}$ ) component was found to range between 1035-1048  $\text{cm}^{-1}$  in both wool and mohair spectra, with the peak heights and band area individual values considerably overlapping between the two fibre types. A closer look at other characteristic cystine oxidation by-products, the cystine monoxide (1077  $\text{cm}^{-1}$ ), cystine dioxide (around 1123  $\text{cm}^{-1}$ ) and the  $\nu_a$  (S-O) band at 1170  $\text{cm}^{-1}$ , all showed considerable variation in their band positions. The cystine

monoxide ( $1077\text{ cm}^{-1}$ ) component varied from  $1070$  to  $1081\text{ cm}^{-1}$ , while that of the cystine dioxide ( $1125\text{ cm}^{-1}$ ) band component ranged from  $1115$  to  $1130\text{ cm}^{-1}$ . The position (wavenumber) of the  $\nu_a$  (S-O) ( $1177\text{ cm}^{-1}$ ) band component has also been found to vary considerably within each fibre type, ranging from  $1168$  to  $1180\text{ cm}^{-1}$ .

The position of the Amide III band ranged between  $1235$  and  $1240\text{ cm}^{-1}$  in spectra of both wool and mohair fibres, while that of the CH<sub>2</sub> and CH<sub>3</sub> bending modes was found to range between  $1449$ - $1455\text{ cm}^{-1}$ . In Figure 4.24 second order derivative (in the  $1500$ - $1720\text{ cm}^{-1}$  spectral range) spectra of wool and mohair obtained in this study are shown.

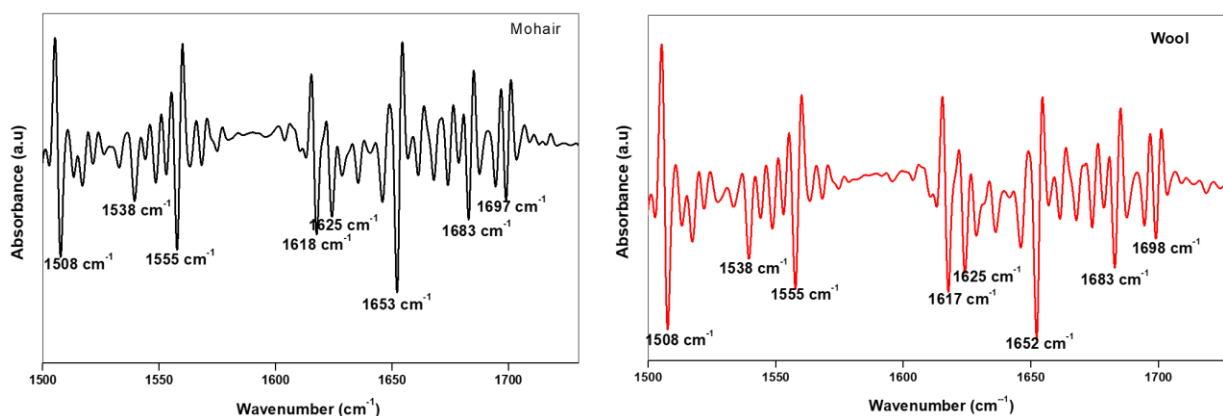


**Figure 4.24: FTIR second derivative spectra of mohair and wool in the  $1500$ - $1750\text{ cm}^{-1}$  spectral range.**

Notably, the centres of the peak maxima for the amide I and II bands were consistently found around  $1652$  and  $1550\text{ cm}^{-1}$ , respectively, indicating the dominance of the  $\alpha$ -helical secondary structure. Other band components in the amide I and II range include the  $\beta$ -pleated sheet ( $\sim 1670\text{ cm}^{-1}$ ), disordered conformation (around  $1645\text{ cm}^{-1}$ ), the amide II component of the  $\beta$ -sheet conformation ( $1531\text{ cm}^{-1}$ ) and the Tyrosine (Tyr) band around  $1508\text{ cm}^{-1}$  (Sowa *et al.*, 1995).

**Table 4.24: IR spectral band positions for wool and mohair fibres.**

Band component	Wool	Mohair	Reference
$\nu_s(\text{S-O})$ , cysteic acid	1044	1044	Church <i>et al.</i> , (1997)
$\nu_s(\text{S-O})$ , cysteic acid monoxide	1073	1073	Jones <i>et al.</i> , (1998)
$\nu_s(\text{S-O})$ , cystine monoxide	1119	1117	Jones <i>et al.</i> , (1998)
$\nu_s(\text{S-O})$ , cystine dioxide	1176	1175	Robbins (1967)
Amide III	1238	1239	Signori and Lewis (1997)
CH <sub>2</sub> & CH <sub>3</sub> bending modes	1453	1453	Signori and Lewis (1997)
Amide II (unodered)	1514	1513	Sowa <i>et al.</i> , (1995)
Amide II ( $\beta$ -sheet)	1537	1537	Sowa <i>et al.</i> , (1995)
Amide II ( $\alpha$ -helical streucture)	1553	1550	Wojciechowska <i>et al.</i> , (2004)
Amide I (unordered )	1612	1611	Wojciechowska <i>et al.</i> , (2004)
Amide I (Turns)	1626	1624	Wojciechowska <i>et al.</i> , (2004)
Amide I ( $\alpha$ -helical streucture)	1652	1652	Wojciechowska <i>et al.</i> , (2004)
Amide I ( $\beta$ )	1678	1678	Wojciechowska <i>et al.</i> , (2004)

The band area values relative to that of the CH<sub>2</sub> & CH<sub>3</sub> bending modes (around 1454 cm<sup>-1</sup>), for some of the major IR bands namely S-O (1040), amide III (1239 cm<sup>-1</sup>), amide II (1531 and 1550 cm<sup>-1</sup>), and amide I (1626, 1650 and 1673 cm<sup>-1</sup>), for both wool and mohair were determined with the intention of distinguishing between the two fibre types. The band area and peak height results from wool and mohair are summarized in Table 4.25.

**Table 4.25: Band areas and heights determined by curve fitting.**

Band component	Wool		Mohair	
	Band area	Peak height	Band area	Peak height
$\nu_s(\text{S-O})$ , cysteic acid	0.71	0.02	0.78	0.02
$\nu_s(\text{S-O})$ , cystine monoxide	2.22	0.03	2.23	0.03
$\nu_s(\text{S-O})$ , cystine dioxide	0.78	0.02	0.78	0.02
$\nu_s(\text{S-O})$ , cystine dioxide	2.49	0.03	2.66	0.03
Amide III ( $1239 \text{ cm}^{-1}$ )	2.19	0.04	2.41	0.04
$\text{CH}_2$ & $\text{CH}_3$ bending modes	4.50	0.08	4.40	0.09
Amide II ( $1515 \text{ cm}^{-1}$ )	3.91	0.10	4.12	0.11
Amide II ( $1531 \text{ cm}^{-1}$ )	2.89	0.08	2.36	0.09
Amide II ( $1555 \text{ cm}^{-1}$ )	6.17	0.11	6.26	0.12
Amide I ( $1614 \text{ cm}^{-1}$ )	4.33	0.10	4.74	0.10
Amide I ( $1624 \text{ cm}^{-1}$ )	3.79	0.08	3.90	0.10
Amide I ( $1650 \text{ cm}^{-1}$ )	7.29	0.17	8.23	0.19
Amide I ( $1673 \text{ cm}^{-1}$ )	3.26	0.07	3.81	0.08

Each of the determined band area and peak height was compared, using the student t-test, for the two fibre types. The observed minor differences were proved to be statistically insignificant ( $p > 0.05$ ). The band area of the cysteic acid (around  $1040 \text{ cm}^{-1}$ ) band component has been associated with the content of the cysteic acid (Panaiotou, 2004). In the current research these were compared between wool and mohair, using

the student t-test, with the aim of distinguishing between them two fibres. A considerable variation of the individual values was observed for both fibre types, wool ranging between 0.40 and 1.08 while for mohair ranged from 0.30 to 1.14. Keratin fibres with high content of the amino acid cystine are expected to possess low content of cysteic acid while the low cystine content should be accompanied by high content of cysteic acid. The comparison of the mean values between wool (0.71) and mohair (0.78) showed that the observed difference is statistically insignificant ( $p > 0.05$ ). Because of the observed overlap between the values of wool and mohair, this study can conclude that the two fibres cannot be distinguished using the FTIR cysteic acid band ( $1040 \text{ cm}^{-1}$ ).

#### 4.3.4 Secondary Structure Analysis for Wool and Mohair.

The band area ratios of the amide I band components  $1650 \text{ cm}^{-1}$  and  $1673 \text{ cm}^{-1}$  to that of the  $\text{CH}_2$  &  $\text{CH}_3$  bending modes ( $1455 \text{ cm}^{-1}$ ) have been previously used to estimate (quantitatively) the contents of the  $\alpha$ -helical and  $\beta$ -sheet secondary structures, respectively, in keratin fibres (Panaiotou, 2004). In the current study these ratios were determined with the aim of establishing a method for distinguishing between wool and mohair fibres. Table 4.26 contains a summary of the results:

**Table 4.26: Summary of the secondary structure analysis.**

<b>Fibre type</b>	<b><math>\alpha</math>-helix content</b>	<b><math>\beta</math>-sheet content</b>
Wool	$1.64 \pm 0.10$	$0.79 \pm 0.08$
Mohair	$1.87 \pm 0.15$	$0.91 \pm 0.07$

**Average  $\pm$  standard error of the mean (SEM).**

The individual values of the  $\alpha$ -helix content were found to vary and overlap considerably between wool and mohair fibres, wool ranging from 0.95 to 2.42 while mohair ranged from 1.18 to 2.53. The individual values were found to vary greatly between fibres of the same sample, possibly due to the varying ratios of the IFs/matrix occurring in different fibres (Marshall *et al.*, 1991).

The means comparison proved that the observed difference in the  $\alpha$ -helical content between wool and mohair is statistically significant ( $p < 0.05$ ). However, the observed great overlap in the individual seem to cast a doubt on the possible application of the secondary structure contents in distinguishing between the two fibre types. A study involving a larger number of wool and mohair fibres appears to be necessary to be able to reach a sound and final conclusion.

The individual values of the  $\beta$ -sheet secondary structure content also varied and overlapped considerably between wool and mohair fibres, with the wool values ranging between 0.55 and 1.53 for wool while these ranged between 0.48 and 1.68 for mohair fibres. These observed variations may probably be attributed to the variations of the secondary structure existing from fibre to fibre of the same sample. The mean values of the  $\beta$ -sheet content (see Table 4.23) were statistically compared for significance of the observed difference, with the student t-test proving them to be statistically insignificant ( $p > 0.05$ ).

## CHAPTER FIVE

### 5.1 CONCLUSIONS

The development of reliable, fast and cheaper methods for distinguishing between wool and speciality animal fibres, such as mohair, remain of paramount importance in the textile industry. This study was aimed at investigating the potential of vibrational spectroscopic techniques, particularly Raman spectroscopy in distinguishing between wool and mohair. This section of this research outlines the conclusions drawn from this research study, outlining the results of the investigations performed in the framework of this thesis.

#### **Conclusions for objective 1:**

FT Raman spectra of high quality from wool and mohair fibres samples were obtained with ease and with good reproducibility. No sample degradation was observed throughout the investigation, even at the maximum laser power (500 mW). This study has confirmed that indeed wool and mohair share similar basic chemistry, showing highly similar Raman and IR spectral features with identical spectral positions and band shapes in both fibre types. In their natural state, keratin fibres such as wool and mohair, are strongly dominated by the  $\alpha$ -helical secondary structure, this being confirmed by the band positions of the amide I ( $1654\text{ cm}^{-1}$ ), the skeletal C-C stretch ( $936\text{ cm}^{-1}$ ) and the amide III ( $1243\text{ cm}^{-1}$ ). Raman spectral curve fitting confirmed this dominance of the  $\alpha$ -helical secondary structure and also showed that both fibres prefer the gauche-gauche-gauche (GGG) conformation, their spectra being dominated by the band component at around  $508\text{ cm}^{-1}$ .

#### **Conclusions for objective 2:**

In terms of the second objective of this thesis, this study found that no relationship exists between the Raman relative peak heights/intensities and the mean fibre diameter (MFD) of wool/mohair fibres, for all the Raman bands analysed. Despite the small number of samples involved in this analysis, it is worth noting that the spectral information gathered here has been obtained with good reproducibility, and apart from

the minor variations in peak positions, average values of the relative peak height ratios differed significantly between wool and mohair. The application of Raman spectroscopic ratiometric analysis, particularly that based on ratios A and D, seem to be potentially the method for detecting if some fraudulent adulteration has taken place in pure mohair fibre products. This research is, however, challenged by the lack of blind samples of pure and blended wool and mohair samples.

### **Conclusions for objective 3:**

An in-house spectral database of high-quality Raman spectra for wool and mohair has been established with the aim of possibly identifying unknown animal fibres. This database contains about 100 average FT Raman spectra from wool and mohair fibre bundles. The search results of spectrum correlation search algorithm, based on the application of HQI, provided good accuracy in classifying known wool and mohair, with more than 90% test spectra being classified successfully. However, very few test spectra were involved in the validation, and more work still needs to be done in future studies on the performance of the current database. This study concludes that, a spectral search algorithm based on multivariate or chemometrics, rather than on the HQI, would be more suitable for the classification of animal fibres such as wool and mohair using the current database.

### **Conclusions for objective 4:**

Micro-Raman spectra of single fibres from wool and mohair single fibres were obtained with easy and good reproducibility. The micro-Raman spectra of wool and mohair single fibres also did not show any chemical band that was specific to one fibre type, which would enable their identification. A peak height based ratiometric analysis showed a great overlap of individual values for ratios A, B, C, E, F and G, confirming their application in distinguishing between the two fibres is might be impossible. This analysis confirmed the existence of the possible differences in the peak height ratio D.



**Conclusions for objective 5:**

High quality spectra of wool and mohair single fibres have been acquired easily and with good reproducibility from the FTIR-LUMOS micro-spectrometer. The ratios of the peak heights of the amide I to those of amide II (Amide I/Amide II) were determined for the two fibre groups. These ratios could not distinguish between the wool and mohair fibres used in this study, these possessing a great overlap. The FTIR based cysteic acid content and the secondary structure ( $\alpha$ -helix and  $\beta$ -sheet) could not distinguish between wool and mohair, showing considerable variations and overlap of the individual values. This study supports the results of the previously published research and also concludes that distinguishing between animal fibres such as wool and mohair, using IR techniques, is an extremely difficult task.

## 5.2 RECOMMENDATIONS FOR THE FUTURE

- The current research has recognized a potential fibre identification method of wool and mohair, using the Raman peak height based ratiometric analysis, particularly the application of band ratios A and D (based on the relative peak height ratios  $I_{2932}/I_{1450}$  and  $I_{508}/I_{1450}$ , respectively). Because of the time constraints (and the frequent break down of the FT Raman system experienced), only a limited number of samples were involved in the validation of the ratiometric analysis for wool and mohair fibre identification. A validation on a larger number of wool and mohair samples, including samples of unknown identities, i.e. blind samples (pure and blended samples), is highly recommended as the next step towards realizing the full potential of the ratiometric analysis method.
- These observed differences in the relative peak height ratios, particularly ratios A and D, are believed to be the result of differing compositions of the amino acids and lipids responsible for those Raman chemical bands. A comprehensive correlation study of the amino acid internal and external lipid analysis determined using chromatographic or electrophoretic methods with the relative intensities of the respective Raman bands for wool and mohair fibre samples, particularly those used in this study, is highly recommended.
- A chemometric-based spectral classification model such as cluster analysis or principal component analysis (PCA), is recommended for the identification and classification of wool and mohair fibres. The spectral searching results of the Raman database developed in this research has shown that although the first hit could not be an exact match (i.e. the query and the first hit of the library belong to the same sample), for most of the search results, the following four hits always belonged to the same fibre class as the query spectrum, i.e. wool or mohair. The inclusion of a wide range of animal fibre samples other than wool and mohair fibres will be assessed, these including cashmere, Angora rabbit hair, camel hair, etc.

- It is common knowledge that chemical treatments are most likely to degrade or affect the chemical makeup of protein fibres. Spectral analysis of chemically treated animal fibre samples is also recommended for the future research studies. This is because fibre identification and blend composition analysis are often required for finished products which have undergone chemical processing, such as dyeing and bleaching.

### 5.3 REFERENCES

AATCC Technical Manual. (1971). *Fibres in Textile-Identification*, 49.

Abduallah, A. (2006). Investigating the Effect of Dyeing on the Surface of Wool Fibres with Atomic Force Microscope (AFM), MSc Dissertation, Stellenbosch University, South Africa.

Ainsworth, W.D. and Zhang, L. (2005). Microscope Analysis of Animal Fibre Blends Training of Operatives, SGS. [Online] Available at: [http://www.sgs.com/~media/Global/Documents/Third%20Party%20Documents/Third%20Party%20Technical%20and%20Research%20Papers/TP\\_M25\\_Fibre%20Type%20Discrimination](http://www.sgs.com/~media/Global/Documents/Third%20Party%20Documents/Third%20Party%20Technical%20and%20Research%20Papers/TP_M25_Fibre%20Type%20Discrimination). [Accessed 07 April 2015].

Akhtar, W., Edwards, H.G.M., Farwell, D.W. and Nutbrown, M. (1997). Fourier-Transform Raman Spectroscopic Study of Human Hair, *Spectrochimica Acta (A)*, **53**, pp. 1021-1031.

Anon. (1989). Fibre Identification, *Text. Asia*, **20**(4), pp. 138-138.

Appleyard, H.M. (1960). *Guide to the Identification of Animal Fibres*, Leeds: Wool Industries Research Association.

Bahi, A., Jones, J.T., Carr, C.M., Ulijn, R.V. and Shao, J. (2007). Surface Characterization of Chemically Modified Wool, *Text. Res. J.*, **77**(12), pp. 937-945.

Baker, J., Lentz, H., Kritikos, D., Schamber, F., and Lee, R. (1998). Wool and Cashmere Fibre Identification Study Using Scanning Electron Microscopy, *Microscopy and Microanalysis*, **4**(S2), pp. 264-265.

Baldwin, K.J., Batchelder, D.N. and Webster, S. (2001). Raman Microscopy: Confocal and scanning Near-Field, In "*Handbook of Raman Spectroscopy- From the Research to the Process Line*", I.R. Lewis and H.G.M Edwards (eds.), New York: Mercel Dekker: pp. 145-190.

Barani, H. and Haji, A. (2015). Analysis of Structural Transformation in Wool Fibre Resulting from Oxygen Plasma Treatment Using Vibrational Spectroscopy, *J. Mol. Struc.*, **1079**, pp. 35–40.

Barańska, H., Łabudzinska, A., and Terpinski, J. (1987). *Laser Raman Spectrometry: Analytical Applications*, Chichester: Ellis Horwood Limited.

Bauters, M. (1985). Study of the Proteins Extracted by Formic Acid from Wool and Mohair. In: *Proc. 7<sup>th</sup> Int. Wool Text. Res. Conf.*, Tokyo: Society of Fibre Science and Technology, **1**, pp. 162-170.

Bendit, E.G. (1966). Infrared Absorption Spectrum of Keratin. I. Spectra of  $\alpha$ - and  $\beta$ -, and Super Contracted Keratin, *Biopolymers*, **4**, pp. 539-559.

Bereck, A. (1990). Bleaching of Pigmented Speciality Fibres. In: *Proc. 2<sup>nd</sup> Int. Symp. On Speciality Fibres*, Aachen: Schrift. der Deutsches Wollforschungsinstitutet, **106**, pp. 20-58.

Berndt, H., Kalbe, J., Kuroпка, R., Meyer-Stork, S. And Höcker, H. (1990). Progress and Limitations of the DNA Analysis in the Fine Animal Fibre Identification. In: *Proc. 2<sup>nd</sup> Int. Symp. Speciality Animal Fibres*, Aachen: Schrift. der Deutsches Wollforschungsinstitutet, **106**, pp. 259-265.

Blankenburg, G., Henning, H.J., Philipen, H. and Zahn, H. (1979). *A Note on the Determination of the Cashmere Content in Blends of Cashmere and Wool*, IWTO Tech. Rep. No. 8, Paris: International Wool Textile Organization.

Boruta, M. (2012). *FT-IR Search Algorithm- Assessing the Quality of a Match*, Spectroscopy Magazine, **27**(8). Accessed 07 February 2017, URL: <http://www.spectroscopyonline.com/ft-ir-search-algorithm-assessing-quality-match?id=&pageID=1&sk=&date>.

Bradbury, J.H. (1976). The Morphology and Chemical Structure of Wool, *Pure and Appl. Chem.*, **46**, pp. 247-253.

Bradbury, J.H. and Chapman, G.V. (1964). The Chemical Composition of Wool, *Aust. J. Biol. Sci.*, **17**, pp. 960-972.

Bradbury, J.H., Chapman, G.V. and King, L.R. (1965). The Chemical Composition of Wool. Part II: Analysis of the Major Histological Components Produced by Ultrasonic Disintegration, *Aust. J. Biol. Sci.*, **18**, pp. 353-364.

Brenner, L., Squires, P.L., Gary, M. and Tumosa, C.S. (1985). A Measurement of Human Hair Oxidation by Fourier Transform Infrared Spectroscopy, *J. Forensic Sci.*, **13**(2), pp. 420-426.

Burns, D.A. and Ciurczak, E.K. (2001). *Handbook of Infrared Analysis*, 2<sup>nd</sup> Ed., New York: Marcel Dekker.

Bryson, W.G., McNeil, S.J., McKinnon, A.J. and Rankin, D.A. (1992). *The Cell Membrane Complex of Wool- A Critical Assessment of the Literature*, Wool Research Organization of New Zealand (WRONZ).

Carr, C.M. and Lewis, D.M. (1993). An FTIR Spectroscopic Study of the Photodegradation and Thermal Degradation of Wool, *J. Soc. Dyers Color.*, **109**(1), pp. 21-24.

Carter, E.A. and Edwards, H.G.M. (2001). Biological Applications of Raman Spectroscopy. In: H.-U. Glemlich, and B. Yan, ed(s)., *"Infrared and Raman Spectroscopy of Biological Materials"*, New York: Marcel Dekker, INC, pp. 421-473.

Carter, E.A., Fredericks, P.M., Church, J.S. and Denning, R.J. (1994). FT-Raman Spectroscopy of Wool- I. Preliminary Studies, *Spectrochimica Acta*, **50A**(11), pp. 1927-1936.

Cebeci-Maltaş, D., Ben-Amotz, D., Alam, M.A., Wang, P. and Pinal, R. (2017). *Photobleaching Profile of Raman Peaks and Fluorescence Background*, European Pharmaceutical Review, Accessed 07 December 2019, URL <<https://www.europeanpharmaceuticalreview.com/article/70503/raman-peaks-fluorescence-background/>>.

Chalmers, J.M., Edwards, H.G.M. and Hargreaves, M.D. (2012). *Infrared and Raman Spectroscopy in Forensic Science*, Chichester: John Wiley & Sons Ltd.

Chalmers, J.M. and Everall, N.J. (1993). Vibrational Spectroscopy. In: B.J. Hunt, and M.I. James, ed(s), *"Polymer Characterization"*, New York: Blackie Academic & Professional.

Cho. L.-L. (2007). Identification of Textile Fibre by Raman Micro-Spectroscopy, *Forensic. Sci. J.*, **6** (1), pp. 55-62.

Church, J.S., Corino, G.L. and Woodhead, A.L. (1997). The Analysis of Merino Wool Cuticle and Cortical Cells by Fourier Transform Raman Spectroscopy, *Biopolymers*, **42**(1), pp. 7-17.

Church, J.S., Corino, G.L. and Woodhead, A.L. (1998). The Effects of Stretching on Wool Fibres as Monitored by FT-Raman Spectroscopy, *J. Mol. Struc.*, **440**, pp. 15-23.

Church, J.S., Davie, A.S., James, D.W., Leong, W.-H. and Tucker, D.J. (1994). Determination of Wool Wax in Raw Wool by Raman Spectroscopy, *JAOCS*, **71**(10), pp. 1163-1167.

Church, J.S. and Leong, W.H. (1995). The Analysis of Wool Textile Blends Using FT-IR Photo-Acoustic and FT-Raman Spectroscopies. In: *Proc. 9<sup>th</sup> Int. Wool Text. Res. Conf.*, Biella: Cita' Deglia Studi Biella, **II**, pp. 114-122.

Church, J.S. and Millington, K.R. (1996). Photodegradation of Wool Keratin: Part I. Vibrational Spectroscopic Studies, *Biospectrosc.*, **2**(4), pp. 249-258.

Church, J.S., O'Neill, J.A. and Woodhead, A.L. (1999). A Comparison of Vibrational Spectroscopic Methods for Analyzing Wool/Polyester Textile Blends, *Text. Res. J.*, **69**(9), pp. 676-684.

Clark, M.J. and Hickie, T.S. (1975). The Quantitative Analysis of Binary Mixtures of Fibres by Methods of Infrared Spectroscopy, *J. Text. Inst.*, **66**(7), pp.243-248.

Cohen, J. (1988). *Statistical Power Analysis for the Behavioural Sciences*, 2<sup>nd</sup> Ed., Lawrence Erlbaum Associates: USA.

Corfield, M.C. and Robson, M. (1955). The Amino Composition of Wool, *Biochem. J.*, **59**(1), pp. 62-68.

Crewther, W.G., Fraser, R.D.B., Lennox, F.G. and Lindley, H. (1965). The Chemistry of Keratins, *Advances in Protein Chemistry*, **20**, pp. 191-346.

Crossley, J.A., Gibson C.T., Mapledoram, L.D., Huson, M.G., Myhra, S., Pham, D.K., Sofield, C.J., Turner, P.S. and Watson, G.S. (2000). Atomic Force Microscopy Analysis of Wool Fibre Surfaces in Air and Under Water, *Micron*, **31**, pp. 659-667.

Darskus. R.L. and Gillespie. J.M. (1971). Breed and Species Differences in the Hair Proteins of Four Genera of Caprini, *Aust. J. Biol. Sci.*, **24**, pp. 515-524.

David, C. (2012). Raman Spectroscopy for proteins. Accessed 24 May 2017, URL: [http://www.horiba.com/fileadmin/uploads/Scientific/Documents/Raman/HORIBA\\_webinar\\_proteins.pdf](http://www.horiba.com/fileadmin/uploads/Scientific/Documents/Raman/HORIBA_webinar_proteins.pdf).

Davidson, R.S. and King, D. (1983). A New Method of Distinguishing Wool from Polyester-Fibre and Cotton Fabrics, *J. Text. Inst.*, **74**(6), pp. 382-384.

Department of Agriculture, Forestry and Fisheries. (2016). A Profile of the South African Mohair Market Chain. Accessed 09 May 2018, URL: <<http://www.daff.gov.za/Daffweb3/Portals/0/Statistics%20and%20Economic%20Analysis/Statistical%20Information/Trends%20in%20the%20Agricultural%20Sector%202016.pdf>>.

Dobb, M.G., Johnston, F.R., Nott, J.A., Oster, L., Sikorski, J. and Simpson, W.S. (1961) Morphology of the Cuticle of Wool Fibres and Other Animal Fibres, *J. Text. Inst.*, **52**(4), pp. T153-T170.

Douthwaite, F.J., Lewis, D.M. and Schumacher-Hamedat, U. (1993). Reaction of Cysteine Residues in Wool with Peroxy Compounds, *Text. Res. J.*, **63**(3), pp. 177-183.

Dowling, L.M., Ley, K.F. and Pearce, A.M. (1990). The Protein Composition of Cells in the Wool Cortex. In: *Proc. 8<sup>th</sup> Int. Wool Text. Res. Conf.*, Christchurch: Wool Research Organization of New Zealand, **1**, pp. 205-214.

Edwards, H.G.M., Hunt, D.E. and Sibley, M.G. (1998). FT-Raman Spectroscopic Study of Keratotic Materials: Horn, Hoof and Tortoiseshell, *Spectrochimica Acta Part A*, **54**, pp. 745-757.



EEC Working Party on Textile Names and Labelling. (1988). EEC Inter-Laboratory Tests on Methods of Analysis of Fibre Mixtures, *J. Text. Inst.*, **79**, pp. 155-188.

El-Alfy, M.D. and Blakey, P.R. (1980). The Identification of Animal Fibre by Plasma-Etching and the SEM, *J. Text. Inst.*, **71**(3), pp. 168-170.

Ferraro, J. R., Nakamoto, K. and Brown, C. W. (2003). *Introductory Raman Spectroscopy*, 2<sup>nd</sup> Ed., London: Academic Press.

Feughelman, M. (1997). “*Mechanical Properties and Structure of Alpha-Keratin Fibres: Wool, Human Hair and Related Fibres*”, Sydney: University of New South Wales Press.

Fienberg, S. (1989). *The Evolving Role of Statistical Assessment as Evidence in the Courts*, New York: Springer-Verlag.

Fraser, R.D.B. and Macrae, T.P. (1980). Molecular Structure and Mechanical Properties of Keratins, In: *Symp. of the Soc. for Exp. Bio.*, **34**, pp. 211-246.

Fredericks, M. (2012). Forensic Analysis of Fibres by Vibrational Spectroscopy. In: J.M. Chalmers, H.G.M. Edwards, and M.D. Hargreaves, ed(s). “*Infrared and Raman Spectroscopy in Forensic Science*”, Chichester: John Wiley and Sons Ltd.

Frenkel, M.J., Gillespie, J.M. and Reis P.J. (1974). Factors Influencing the Biosynthesis of the Tyrosine-rich Proteins of Wool, *Aust. J. Biol. Sci.*, **27**, pp. 31-38.

Füchtenbusch, D. and Baumann, H. (1985). Systematic Treatment of Wool with Amines. In: *Proc. 7<sup>th</sup> Int. Wool Text. Res. Conf.*, Tokyo: Society of Fibre Science and Technology, **IV**, pp. 411-419.

Gale, D.J., Logan, R.I. and Rivett, D.E. (1987). Detection of Desmosterol in the Internal Lipids of Wool Fibres, *Text. Res. J.*, **57**, pp. 539-542.

Gallimore, P.J., Davidson, N.M., Kalberer, M., Pope, F.D. and Ward, A.D. (2018). 1064 nm Dispersive Raman Micro-Spectroscopy and Optical Trapping of Pharmaceutical Aerosols, *Anal. Chem.*, **90**, pp. 8838-8844.

Geng, R.-Q., Yuan, C. and Chen, Y.-L. (2012). Identification of Goat Cashmere and Sheep Wool by PCR-RFLP Analysis of Mitochondrial 12S rRNA Gene, *Mitochondrial DNA*, **23**(6), pp. 466-470.

Ghen, W.L. and Fujishige, S. (1996). Bilateral Structure of Wool Fibre Studied with Differential Staining Method, *Sen-i Gakkaishi*, **52**(2), pp. 48-53.

Gillespie, J.M. and Frenkel, M.J. (1975). The Tyrosine-Rich Proteins of Keratins: Occurrence, Properties and Regulation of Biosynthesis. In: *Proc. 5<sup>th</sup> Int. Wool Text. Res. Conf.*, Aachen: Schrift. der Deutesches Wollforschungsinstitutet, **II**, pp. 265-276.

Gillespie, J.M. and Marshall, R.C. (1980). Variability in the Proteins of Wool and Hair. In: *Proc. 6<sup>th</sup> Int. Wool Text. Res. Conf.*, Pretoria: South African Wool and Textile Research Institute, **II**, pp. 67-77.

Giri, C.C. (2002). Scanning Electron Microscope and its Application in Textiles, *Colourage*, **49**(3), pp. 29-42.

Gochel, M., Pirotte, F. and Knott, J. (1995). Development of a Method for the Automatic Identification of Keratineous Fibres by Gas Chromatography Analysis of the Profile of Their Internal Fatty Acids. In: *Proc. 9<sup>th</sup> Int. Wool Text. Res. Conf.*, Biella: Cita' Deglia Studi Biella, **II** pp. 528-535.

Gohl E.P.G. and Vilensky L.D. (1983). *Textile Science*, Melbourne: Longman Cheshire Pty Ltd.

Gralen, N. (1950). The Cuticle of Wool, *J. Soc. of Dyers and Col.*, **66**(9), pp. 465-470.

Greaves, P. (1990). Fibre Identification and Quantitative Analysis of Fibre Blends, *Rev. Prog. Coloration*, **20**, pp. 32-39.

Greaves, P. (1992). Fibre Content Testing, *Wool Science Review*, **68**, pp. 1-24.

Greaves, P.H. and Saville B.P. (1995). *Microscopy of Textile Fibres*, Oxford: BIOS Scientific Publishers Ltd.

Greaves, P. (2005). Identification and Analysis of Speciality Fibres: Further Considerations, *Wool Record*, **4**, pp. 45-45.

Green, D.B., Happey, F., Williams, B.A. and Bromage, B. (1983). The Application of Computer-Assisted IR Spectroscopy to Some Analytical Problems in Wool Textiles. In: *Proc. 5<sup>th</sup> Int. Wool Text. Res. Conf.*, Aachen: Schrift. der Deutesches Wollforschungsinstitutet, **V**, pp. 501-512.

Günzler, H. and Gremlich, H. (2002). *An Introduction to IR Spectroscopy*, Federal Republic of Germany: WILEY-VCH.

Haylett, T. and Swart, L.S. (1969). Studies on the High-Sulphur Proteins of Reduced Merino Wool, Part III: The Amino-Acid Sequence of Protein SCMKB-IIIB2, *Text. Res. J.*, **39**, pp. 917-929.

Hamlyn, P.F., Nelson, G. and McCarthy, B.J. (1990). Applied Molecular Genetics- New Tools for Animal Fibre Identification. In: *Proc. 2nd Int. Symp. On Speciality Animal Fibres*, Aachen: Schrift. der Deutesches Wollforschungsinstitutet, **106**, pp. 249-258.

Hamlyn, P.F. (1998). Analysis of Animal Fibres, *Textile Magazine*, Issue 3, pp. 14-17.

Hamlyn, P.F., Nelson, G., Kibria, I., Broadbent, E. and McCarthy, B.J. (1995). DNA-Based Techniques for Special Fibre Analysis. In: *Proc. 9<sup>th</sup> Int. Wool Text. Res. Conf.*, Biella: Cita' Deglia Studi Biella, **II**, pp. 513-518.

Hamlyn, P.F., Nelson, G., Holden, L. and McCarthy, B.J. (1993). *Species-Specific DNA Probes for the Identification of Wool and Goat Fibres*, IWTO Tech. Report No. 12, Nice: International Wool Textile Organization.

Hallegot, P. and Corcuff, P. (1993). High-SPartial-Resolution Maps of Sulphur from Human Hair Sections: An EELS Study, *J. Microsc.*, **172**(9), pp. 131-136.

Halliday, L.A. (2002). Wool Scouring, Carbonizing and Effluent Treatment. In: W.S. Simpson and G.H. Crawshaw, ed(s)., *Wool: Science and Technology*, Cambridge: Woodhead Publishing Ltd.

Howari, F.M. (2003). Comparison of Spectral Matching Algorithms for Identifying Natural Salt Crusts, *J Appl. Spectrosc.*, **70**(5), pp. 782-787.

Hermann, S., Wortmann, G., Schanabel, D. and Wortmann, F.–J. (1995). Application of Multivariate Analysis Methods for the Characterization and Identification of Textile Animal Fibres. In: *Proc. 9<sup>th</sup> Int. Wool Text. Res. Conf.*, Biella: Cita' Deglia Studi Biella, **II**, pp. 519-527.

Herrero, A.M. (2008). Raman Spectroscopy for Monitoring Protein Structure in Muscle Food Systems, *Critical Reviews in Food Science and Nutrition*, **48**, pp. 512-523.

Herrero, A.M. (2007). Raman Spectroscopy a Promising Technique for Quality Assessment of Meat and Fish: A Review, *Food Chem.*, **107**, pp:1642-1651.

Hillbrick, L.K. (2012). *Fibre Properties Affecting the Softness of Wool and Other Keratins*, PhD thesis, Deakin University, Australia.

Höcker, H. (1990). Methods of Analysis of Animal Fibres at DWI: State of the Art. In: *Proc. 8<sup>th</sup> Int. Wool Text. Res. Conf.*, Christchurch: Wool Research Organization of New Zealand, **II**, pp. 374-384.

Hogg, L.J., Edwards, H.G.M., Farwell, D.W. and Peters, A.T. (1994). FT Raman Spectroscopic Studies of Wool, *J. Soc. Dyers Colour*, **110**(4), pp. 196-199.

Houck, M.M. (2009). *Identification of Textile Fibres*, Philadelphia, Woodhead Publishing Ltd in Association with the Textile Institute.

Hudson, P.B., Clapp, A.C. and Kness, D. (1993). *Joseph's Introductory Textiles*, 6<sup>th</sup> Ed., Florida: Harcourt Brace Jonanovich College Publishers.

Hughes, V.L. and Nelson, G. (2001). Surface Modification of Cashmere Fibres by Reverse Proteolysis, *AATCC Review*, **1**(3), pp. 39-43.

Hunter, L. (1993). *Mohair: A Review of Its Properties, Processing and Applications*, Port Elizabeth: CSIR Division of Textile Technology.

ISO 18074 (2015). Identification of Some Animal Fibres by DNA Analysis Method- Cashmere, Wool, Yak, and Their Blends.

ISO 17751 (2007). Textile- Quantitative Analysis of Animal Fibres by Microscopy- Cashmere, Wool, Speciality Fibres and Their Blends, Switzerland.

IWTO 58-00 (2000). Scanning Electron Microscopy Analysis of Speciality Fibres and Sheep's Wool and Their Blends.

Jasper, W.J. and Kovacs, E.T. (1994). Using Neural Networks and NIR Spectrophotometry to Identify Fibres, *Text. Res. J.* **64**(8), pp. 444-448.

Javkhlantugs, N., Ankhbayar, E., Tegshjargal, K., Enkhjargal, D. and Ganzorig, C. (2009). AFM Study of Untreated and Treated Fibers of Mongolian Goat Cashmere, *Materials Science Forum*, **610-613**, pp 175-178.

Ji, W., Bai, L., Ji, M. And Yang, X. (2011). A Method for Quantifying Mixed Goat Cashmere and Sheep Wool, *Forensic Sci. Int.*, **208**, pp. 139-142.

Jin, M. and Hu, J. (2005). The Breeding Situation of the Developing Trend of Liaoning Cashmere Goat, *Chin. J. Anim. Sci.* **41**(3), pp. 54-56.

Jones, D.C., Carr, C.M., Cooke, W.D. and Lewis, D.M. (1998). Investigating the Photo-Oxidation of Wool Using FT-Raman and FT-IR Spectroscopies, *Text. Res. J.*, **68**(10), pp. 739-748.

Jones, L.N., Cholewa, M., Kaplin, I.J., Legge, G.E., Ollerhead, R.W. (1990). Elemental Distribution in Keratin Fibre/Follicle Sections. In: *Proc. 8<sup>th</sup> Int. Wool Text Res. Conf.*, Christchurch: Wool Research Organization of New Zealand, **1**, pp. 246-255.

Jones, L. and Rodgers, G. (2006). *Structure and Composition of Wool*, The Australian Wool Education Trust licensee for educational activities University of New England, Accessed 11 October 2020, <https://libraryguides.vu.edu.au/harvard/internet-websites>.

Joubert, F.J. and Burns, M.A. (1967). The Fractionation of High-Sulphur Proteins of Reduced Merino Wool by Column Chromatography, *Journal of South African Chemical Institute*, **20**, pp. 161-173.

Joy, M. and Lewis, O. M. (1999). The use of Fourier Transform Infrared Spectroscopy in the Study of the Surface Chemistry of Keratin Fibres, *J. Soc. Cosmet. Chem.*, **13**, pp. 249-261.

Kadikis, A. (1987). Comments on Quantitative Fibre Mixture Analysis by Scanning Electron Microscopy, *Tex. Res. J.*, **57**(11), pp. 676-677.

Kalbé, J., Kuroпка, R., Meyer-Stork, L.S., Sauter, S.L., Höcker, H., Berndt, H., Riesner, D. and Henco, K. (1988). Isolation and Characterization of High Molecular Weight DNA from Hair Shafts of Wool and Fine Animal Hair Fibre, *Biol. Chem.*, **369**(1), pp. 413-416.

Kaufmann, R., Phan, K.H. and Wortmann, F.J. (2005). Determination of High Sulphur and High Glycine/Tyrosine Proteins in Wool Fibre Cross Section. In: *Proc. 11<sup>th</sup> Int. Wool Text. Res. Conf.*, Leeds: Department of Colour & Polymer Chemistry.

Kerkhoff, K., Cescütti, G., Kruse, L. And Mussig, J. (2009). Development of a DNA-Analytical Method for the Identification of Animal Hair Fibres in Textiles, *Text. Res. J.*, **79**(1), pp. 69-75.

Kerkhoff, K., Kruse, L., Rüggeberg, H., Cescütti, G. and Müssig, J. (2006). DNA Analytical Identification of Animal Hair Fibres in Textiles, *Melliand English*, **85**(5), pp. E 83.

Ki-Hoon, K. (2008). Classification of Unidentified Fibres in Identified Cashmere and the Date Control. In: *Proc. 4<sup>th</sup> Int. Cashmere Determination Techniques Symp.*, Erdos: Inner Mongolia Erdos Cashmere Group Co. Ltd, pp. 271-276.

Körner, A. (1988). Lipids in the Analysis of Fine Animal Fibres. In: *Proc. 1<sup>st</sup> Int. Symp. Speciality Animal Fibres*, Aachen: Schrift. der Deutsches Wollforschungsinstitutet, **103**, pp. 104-127.

- Kumar, S., Verma, T., Mukherjee, R., Ariese, F., Somasundaram, K. and Umopathy, S. (2016). Raman and Infra-Red Microspectroscopy: Towards Quantitative Evaluation for Clinical Research by Ratiometric Analysis, *Chem. Soc. Rev.*, pp. 1-47.
- Kurabayashi, T., Kikuchi, N., Tanno, T. And Watanbe, M. (2009). Significance of Terahertz Spectrometry for Textile Article of Wool. In: *Proc. 34<sup>th</sup> Int. Conf. On Infrared, Millimeter and Terahertz Waves*, Busan: IEEE, pp. 1-2.
- Kurabayashi, T., Suzuki, K., Yodokawa, S., Kosaka, S. and Ando K. (2010). Identification of Textile Fibre by Terahertz Spectroscopy. In: *Proc. 35<sup>th</sup> Int. Conf. on Infrared, Millimeter and Terahertz Waves*, Rome: IEEE, pp. 1-2.
- Kusch, P. and Arns, W. (1983). Electron Scanning Microscopic Investigation to Distinguish Between Sheep Wool and Goat Hair (e.g. Mohair), *Milliand Textilberichte*, **64**(6), pp. 427-429.
- Kuzuhara, A. (2017). A Raman Spectroscopic Investigation of the Mechanism of the Reduction in Hair with Thioglycerol and the Accompanying Disulphide Conformational Changes, *Int. J. Cosmetic Sci.*, **40**, pp. 34-43.
- Kuzuhara, A. and Hori, T. (2003). Reduction Mechanism of Tioglycolic Acid on Keratin Fibres Using Micro-spectrophotometry and FT-Raman Spectroscopy, *Polymer*, **44**, pp. 7963-7970.
- Kuzuhara, A. (2007). A New Method of Internal Structural Analysis of Keratin Fibres Using Raman Spectroscopy”, in T.S. Nemeth, ed., *Biopolymer Research Trends*, New York: Nova Science Publishers, Inc.
- Lang, P.L., Katon, J.E., O’Keefe, J.F. and Scheiring, D.W. (1986). The Identification of Fibres by Infrared and Raman Microscopy, *Microchem. J.*, **34**, pp. 319-331.
- Lang, P.L., Katon, J.E., Scheiring, D.W. and O’Keefe, J.F. (1986). Application of Infrared and Raman Microscopy to Polymer Characterization, *Polym. Mater. Sci. Eng.*, **54**, pp. 381-385.
- Langley, K. D. and Kennedy, T. A. (1981). The Identification of Speciality Fibres, *Text. Res. J.*, **51**, pp. 703-709.

Langley, K.D. (2003). Identifying Rare and Speciality Fibres, *Wool Record*, **10**, pp. 61-61.

Laopa, P.S., Vilaivan, T. and Hoven, V.P. (2013). Positively Charged Polymer Brush-Functionalized Filter Paper for DNA Sequence Determination Following Dot-Blot Hybridization Employing a PyrrolidinyI Peptide Nucleic Acid Probe, *Analyst*, **138**, pp. 269-277.

Laumen, H., Wortmann, G. and Wortmann, F.J. (1990). A Contribution to the Objective Evaluation of Gel Electrophoretical Protein Patterns of Fine Animal Hairs. In: *Proc. 2<sup>nd</sup> Int. Symp. Speciality Animal Fibres*, Aachen: Schrift. der Deutsches Wollforschungsinstitutet, **106**, pp. 269-284.

Leaver, I.H., Hester, R.E. and Girli, R.B. (1987). Analytical Potential of Raman Spectroscopy in Wool Textile Research, *Text. Res. J.*, **58**(7), pp. 182-184.

Leeder, J.D., Bishop, D.G. and Jones, L.N. (1983). Internal Lipids of Wool Fibres, *Text. Res. J.*, **53**, pp. 402-407.

Leeder, J.D., Holt, L.A., Rippon, J.A. and Stapleton, I.W. (1990). Diffusion of Dyes and Other Reagents into the Wool Fibre. In: *Proc. 8<sup>th</sup> Int. Wool Text. Res. Conf.*, Christchurch: Wool Research Organization of New Zealand, **IV**, pp. 227-236.

Lester, E.P, Lemkin, P.F. and Lipkin, E.E. (1981). New Dimensions in Protein Analysis, *Anal. Chem.*, **53**(3), pp. 390-404.

Ley, K.F. and Crewther, W.G. (1980). The Proteins of Wool Cuticle. In: *Proc. 6<sup>th</sup> Int. Wool Text. Res. Conf.*, Pretoria: South African Wool Textile Research Institute, **II**, pp. 13-28.

Ley, K.F., Crewther, W.G., Flanagan, G.F., Jones, L.N. and Marshall, R.C. (1988). Release of Cuticle from Wool by Agitation in Solutions of Detergents, *Aust. J. Biol. Sci.*, **41**, pp. 163-176.

Lippert, J.L., Tyminski, D. and Desmeules, P.J. (1975). Determination of the Secondary Structure of Proteins by Laser Raman Spectroscopy, *J. Am. Chem. Soc.*, **98**(22), pp. 7075-7080.



Liu, K., Luo, J., Zhong, Y. and Chai, X. (2019). Identification of Wool and Cashmere SEM Image Based on SURF Features, *J. Eng. Fibres and Fabrics*, **14**, pp.1-9.

Liu, X., Ma, N., Wen, G. and Wang, X. (2008). FTIR Spectrum and Dye Absorption of Cashmere and Native Fine Sheep Wool. In: *Proc. 4<sup>th</sup> Int. Cashmere Determination Technique Symp.*, Erdos: Inner Mongolia Erdos Cashmere Group Corporation, pp. 253-264.

Liu, X.R., Zhang, L.P., Wang, J.F., Wu, J.P. and Wang, X.R. (2013). Use of Visible and Near Infrared Reflectance Spectroscopy to Identify Cashmere and Wool, *Guang Pu Xue Yu Guang Pu Fen Xi*, **33** (8), pp. 2092-2095.

Liu, H. and Yu, W. (2005). Study of the Structure Transformation of Wool Fibre with Raman Spectroscopy, *J. Appl. Polymer Sci.*, **103**, pp. 1-7.

Logan, R.I., Rivette, D.E., Tucker, D.J. and Hudson, A.H.F. (1989). Analysis of the Intercellular and Membrane Lipids of Wool and other Animal Fibres, *Text. Res. J.* **59**(3), pp. 109-113.

Ma, H., Hong, X., Gao, A. and Liu, T. (2008). Research and Discussion on the Identification Techniques for Cashmere and Yak Fibres. In: *Proc. 4<sup>th</sup> Int. Cashmere Determination Technique Symp.*, Erdos: Inner Mongolia Erdos Cashmere Group Corporation, pp. 174-187.

Marshall, R.C. (1981). Analysis of Protein from Single Wool Fibre by Two-Dimensional Polyacrylamide Gel Electrophoresis, *Text. Res. J.* **51**(1), pp. 106-108.

Marshall, R.C. (1990). Protein and Fibre Chemistry of Wool. In: *Proc. 8<sup>th</sup> Int. Wool Text. Res. Conf.*, Christchurch: Wool Research Organization of New Zealand, pp. 169-185.

Marshall, R.C., Orwin, D.F.G. and Gillespie, J.M. (1991). Structure and Biochemistry of Mammalian Hard Keratins, *Electron Microsc. Rev.*, **4**, pp. 47-83.

Marshall, R.C. and Gillespie, J.M. (1990). Human Hair: Normal Composition and Chemically Induced Changes In: *Proc. 8<sup>th</sup> Int. Wool Text. Res. Conf.*, Christchurch: Wool Research Organization of New Zealand, pp.256-265.

Marshall, R.C. and Gillespie, J.M. (1988). 'Variations in the Proteins of Wool and Hair', In Roger, G.E., Reis, P.J., Ward, K.A. and Marshall, R.C. (Eds), '*The Biology of Wool and Hair*', Dordrecht: Springer, pp. 117-125.

Marshall, R.C. and Gillespie, J.M. (1982). Comparison of Samples of Human Hair by Two-Dimensional Electrophoresis, *J. Forensic. Sci. Soc.* **22**, pp. 377-385.

Marshall, R.C., Frenkel, M.J. and Gillespie, J.M. (1977). High-Sulphur Proteins in Mammalian Keratins: A Possible Aid in Classification, *Aust. J. Zool.*, **25**, pp. 121-132.

Marshall, R.C. and Ley, K.F. (1986). Examination of Proteins from Wool Cuticle by Two-Dimensional Gel Electrophoresis, *Text. Res. J.*, **56**(7), pp. 772-774.

Marshall, T., Paviour, S.M. and Williams, K.M. (1986). A Simplified Method for the Electrophoretic Analysis of Hair Proteins, *J. Biochem. Biophys. Methods*, **14**, pp. 53-58.

Marshall, R.C., Zahn, H. and Blankenburg, G. (1984). Possible Identification of Speciality Fibres by Electrophoresis, *Text. Res. J.*, **54**(2), pp. 126-128.

Maxwell, J. M. and Huson, M. G. (2004). Scanning Probe Microscopy Examination of the Surface Properties of Keratin Fibres, *Micron*, **36**, pp 127-136.

McCain, S.T., Willett, R.M. and Brady, D.J. (2008). Multi-Excitation Raman Spectroscopy Technique for Fluorescence Rejection, *Opt. Express*, **16**, pp. 10975-10991.

McGregor, B.A. and Tucker, D.J. (2010). Effects of Nutrition and Origin on the Amino Acid, Grease, and Suint Composition and Colour of Cashmere and Guard Hairs, *Journal of Applied Polymer Science*, **117**, pp. 409-420.

McGregor, B. A. (2011). *Improving Production Efficiency, Quality and Value-Adding of Rare Natural Animal Fibres*, Canberra: Rural Industries Research and Development Corporation.

McGregor, B.A. (2012). *Properties, Processing and Performance of Rare Natural Animal Fibres- A Review and Interpretation of Existing Research Results*, Canberra: Rural Industries Research and Development Corporation.

McGregor, B. A., Liu, X. and Wang, X. G. (2017). Comparisons of the Fourier Transform Infrared Spectra of Cashmere, Guard Hair, Wool and other Animal Fibres, *J. Text. Inst.*, **109**(6), pp. 813-822.

Michielsen, S. (2001). Application of Raman Spectroscopy to Organic Fibres and Films. In I.R. Lewis, and H.G.M. Edwards, ed(s)., In *“Handbook of Raman Spectroscopy- From the Research Laboratory to the Process Line”*, New York: Mercel Dekker, pp.749-798.

Mikhonin, A.V., Ahmed, Z., Ianoul, A. and Asher, S.A. (2004). Assignments and Conformational Dependencies of the Amide III Peptide Backbone UV Resonance Raman Bands, *J. Phys. Chem. B.*, **108**, pp. 19020-19028.

Molloy, J. and Naftaly, M. (2013). Wool Textile Identification by Terahertz, *J. Text. Inst.*, **105**(8), pp. 794-798.

Mozaffari-Medley, M. (2003). *Colour Matching of Dyed Wool by Vibrational Spectroscopy*, MSc dissertation, Queensland University of Technology, Australia.

Musango, K.J., Dumini, L. and Batinge, B. (2017). Understanding Sustainability of Mohair Value Chain in South Africa, Accessed 05 July 2020, URL: [https://www.google.co.za/search?sxsrf=ALeKk00WJ1CIE3b6IKUBdmByyGDtP2IrpA%3A1596197869039&ei=7QskX4b8AcTVkgWUpbv4DA&q=Understanding+Sustainability+of+Mohair+Value+Chain+in+South+Africa&og=Understanding+Sustainability+of+Mohair+Value+Chain+in+South+Africa&gs\\_lcp=CgZwc3ktYWIQDFCpkQxYqZEMYMuaDGgAcAB4AIAB0QSIAdEEkgEDNS0xmAEAoAEC0AEBggEHZ3dzLXdpesABAQ&scient=psy-ab&ved=0ahUKEwjGpua3vPfqAhXEqqQKHZTSDs8Q4dUDCAw](https://www.google.co.za/search?sxsrf=ALeKk00WJ1CIE3b6IKUBdmByyGDtP2IrpA%3A1596197869039&ei=7QskX4b8AcTVkgWUpbv4DA&q=Understanding+Sustainability+of+Mohair+Value+Chain+in+South+Africa&og=Understanding+Sustainability+of+Mohair+Value+Chain+in+South+Africa&gs_lcp=CgZwc3ktYWIQDFCpkQxYqZEMYMuaDGgAcAB4AIAB0QSIAdEEkgEDNS0xmAEAoAEC0AEBggEHZ3dzLXdpesABAQ&scient=psy-ab&ved=0ahUKEwjGpua3vPfqAhXEqqQKHZTSDs8Q4dUDCAw).

Nakamura, A., Arimoto, M., Takeuchi, K. and Fujii, T. (2002). A Rapid Extraction Procedure of Human Hair Proteins and Identification of Phosphorylated Species, *Biol. Pharm. Bull.* **25**(5), pp. 569-572.

Nakamura, K., Era, S., Ozaki, Y., Sogami, M., Hayashi, T. and Murakami, M. (1997). Conformational Changes in Seventeen Cystine Disulphide Bridges of Bovine Serum Albumin Proved by Raman Spectroscopy, *FEBS Letters*, **417**, pp. 375-378.

Nelson, G., Hamlyn, P.F., McCarthy, B.J. (1990). Developments in DNA-Based Speciality Fibre Analysis. In: *Proc. 8<sup>th</sup> Int. Wool Text. Res. Conf.*, Christchurch: Wool Research Organization of New Zealand, **II**, pp. 385-401.

Nelson, G., Hamlyn, P.F. and Holden, L. (1992). A Species-Specific DNA Probe for Goat Fibre Identification, *Text. Res. J.*, **62**(10), pp. 590-595.

Notayi, M. (2014). *Characterization of Animal Fibres*, MSc Dissertation, Nelson Mandela Metropolitan University, South Africa.

OriginLab® Corporation. (2007). OriginLab 8.0 Software, Northampton: OriginLab Corporation.

Paluzzi, S., Mormino, M., Vineis, C., Tonin, C., Patrone, E., Barboro, P. and Balbi, C. (2004). Anti-keratin Monoclonal Antibodies for Identifying Animal Hair Fibres, *Text. Res. J.*, **74**(5), pp. 458-464.

Panaiotou, H. (2003). *Vibrational Spectroscopy of Keratin Fibres A Forensic Approach*, PhD thesis, Queensland University of Technology, Australia.

Pande, C.M. (1994). FT-Raman Spectroscopy-Applications in Hair Research, *J. Soc. Cosmet. Chem.*, **45**(9), pp. 257-268.

Paolella, S., Bencivenni, M., Lambertini, F., Prandi, B., Faccini, A., Tonetti, C., Vineis, C. and Sforza, S. (2013). Identification and Quantification of Different Species in Animal Fibres by LC/ESI-MS Analysis of Keratin-Derived Proteolytic Peptides, *J. Mass Spectrom.*, **48**, pp. 919-926.

Park, J-K., Park, A., Yang, S.K., Baek, S-J., Hwang, J. and Chwaa, J. (2017). Raman Spectrum Identification Based on the Correlation Score Using the Weighted Segmental Hit Quality Index, *Analyst*, **142**, pp. 380-388.

Perez, F.R. (2001). Application of IR and Raman Spectroscopy to the Study of Mediaval Pigments. In: R. Lewis, and H.G.M. Edwards, ed(s), "*Handbook of Raman Spectroscopy: From the Research to the Process Line*", New York: Mercel Dekker, Inc, pp. 835-862.

Phan, K.H. and Wortmann F.-J. (1987). Characterization of Speciality Fibres by Scanning Electron Microscopy. In: *Proc. 1<sup>st</sup> Int. Symp. Speciality Animal Fibres*, Aachen: Schrift. der Deutches Wollforschungsinstitutet. **103**, pp. 137-162.

Phan, K. H. and Wortmann, F.-J., (1996). Identification and Classification of Cashmere, In: *Metrology and Identification of Speciality Animal Fibres, European Fine Fibre Network*, Occ. Publication No. 4, Aachen: Schrift. der Deutches Wollforschungsinstitutet, pp. 45–58.

Phan, K.H. And Wortmann, F.-J. (1997). *Microscopic Analysis of Wool/Cashmere Blends Results of the 1995 CCMI Round Trial*, IWTO Tech. Report No. 25, Boston: International Wool Textile Organization.

Phan, K.H., Wortmann, F.-J. and Arns, W. (1995). Characterization of Cashmere. In: *Proc. 9<sup>th</sup> Int. Wool Text. Res. Conf.*, Biella: Cita' DegliaStudi Biella, **II**, pp. 571-579.

Phan, K.H., Wortmann, F.-J., Wortmann, G. and Arns, W. (1988). Bivariate Microscopical Characterization of Speciality Animal Fibres, DWI Report.

Phan, K.H., Arns, W., Wortmann, F.-J. and Hocker H. (1991). *Cashmere- An Operational Definition*, IWTO Tech. Report No. 4, Lisbon: International Wool Textile Organization.

Phan, K.H., Rütten, S. And Posescu, C. (2008). Yak and Sheep's Wool: The Fibres Hidden Behind Cashmere, In: *Proc. 4<sup>th</sup> Int. Cashmere Determination Technique Symp.*, Erdos: Inner Mongolia Erdos Cashmere Group Corporation, pp. 49-55.

Phillips, T.L., Horr, T. J., Huson, M.G. and Turner, P.S. (1995). Imaging Wool Fibre Surfaces with a Scanning Force Microscope, Australia, *Text. Res. J.*, **65**(8), pp. 445-453.

Pielesz, A., Freeman, H.S., Weselucha-Birczynska, A., Wysocki, M. and Włochowicz, A., (2003). Assessing Secondary Structure of a Dyed Wool Fibre by Means of FTIR and FTR Spectroscopies, *Journal of Molecular Structure*, **651–653**, pp. 405–418.

Popescu, C. and Höcker, H. (2007). Hair – The Most Sophisticated Biological Composite Material, *Chem. Soc. Rev.*, **36**, pp. 1282–1291.

Popescu, C. and Wortmann, F.-J. (2010). ‘Wool – Structure, Mechanical Properties and Technical Products Based on Animal Fibres’, in Mussig, J. (Ed.) *“Industrial Applications of Natural Fibres: Structure, Properties and Technical Applications”*, Chichester: John Wiley & Sons, pp. 255-266.

Potts, W. J. JR. (1963). *“Chemical Infrared Spectroscopy- Techniques”*, United States of America: John Wiley & Sons, Inc.

Rane, P.P. and Barve, S.S. (2010). Evaluating Protein Patterns of Speciality Fibres for Identification to Combat False Labelling, *Int. J. Zool. Res.*, pp. 1-7.

Reis, P.J. and Schinckel, P.G. (1963). Some of Sulphur-Containing Amino Acids on the Growth and Composition of Wool, *Aust. J. Biol. Sci.*, **16**, pp. 218-230.

Rintoul, L., Carter, E.A., Stewart, S.D. and Fredericks, P.M. (2000). Keratin Orientation in Wool and Feathers by Polarized Raman Spectroscopy, *Biopolymers (Biospectroscopy)*, **51**, pp. 19-28.

Rivett, D.E., Logan, R., Tucker, D. And Hudson, A. (1988). The Lipid Composition of Animal Fibres. In: *Proc. 1<sup>st</sup> Int. Symp. Speciality Animal Fibres*, Aachen: Schrift. der Deutesches Wollforschungsinstitutet, **103**, pp. 128-136.

Robbins, C. (1967). Infrared Analysis of Oxidized Keratins, *Text. Res. J.*, **37**(9), pp. 811-813.

Robson, D., Weedall, P.J. and Harwood, R.J. (1989). Cuticular Scale Measurements Using Image Analysis Techniques, *Text. Res. J.*, **59**, pp. 713-719.

Robson, D. and Weedall, P.J. (1990). Cuticular Scale Pattern Description Using Image Processing and Analysis Techniques. In: *Proc. 8<sup>th</sup> Int. Wool Text. Res. Conf.*, Christchurch: Wool Research Organization of New Zealand, **II**, pp. 402-410.

Robson, D. (1997). Animal Fibre Analysis Using Imaging Techniques-Part I: Scale Pattern Data, *Text. Res. J.*, **67**(10), pp. 747-752.

Robson, D. (2000). Animal Fibre Analysis Using Imaging Techniques-Part II: Addition of Scale Height Data, *Text. Res. J.*, **70**(2), pp. 116-120.

Rouse, J.G. and Van Dyke, M.E. (2010). A Review of Keratin-Based Biomaterials for Biomedical Applications, *Materials*, **3**, pp. 999-1014.

Sagar, A.J.G., Calvert, E., McCarthy, B.J. and Sagar, B.F. (1990). Characterization of Keratin Fibres by Chemical Analysis. In: *Proc. 2<sup>nd</sup> Int. Symp. On Speciality Animal Fibres*, Aachen: Schrift. der Deutches Wollforschungsinstitutet, **106**, pp. 147-162.

Sawbridge, M. and Ford, J.E. (1987). *Textile Fibres-Under the Microscope*, Manchester: Shirley Institute Publication S.50.

Shah, R.C. and Ghandhi, R.S. (1968). Infrared Analysis of Oxidized Keratins, *Text. Res. J.*, **38**(2), pp. 874-875.

Schrader B., Schultz H., Andreev G.N., Klump H.H. and Sawatzki J. (2000). Non-Destructive NIR-FT-Raman Spectroscopy of Plant and Animal Tissues of Food and Works of Art, *Talanta*, 53(1), 35-45.

She, F.H., Chow, S., Wang, B. and Kong, L.X. (2001). Identification and Classification of Animal Fibres Using Artificial Neural Networks, *J. Text. Eng.*, **47**(2), pp 35-38.

She, F.H., Kong, L.X., Nahavandi, S. and Kouzani, A.Z. (2002). Intelligent Animal Fibre Classification with Artificial Neural Networks, *Text. Res. J.*, **72**(7), pp. 594-600.

Shelton, M. (1993). *Angora Goat and Mohair Production*, San Angelo: Mohair Council of America.

Shenai, V.A. and Dalvi, M.C. (1989). Wool Fibres- A Review, *Text. Dyer and Printer Special Article*, 25.

Shi, X.-J. and Yu, W.-D. (2011). Intelligent Animal Fibre Classification with Artificial Neural Networks, *Int. J. Model. Identif. Control*, **12**(1/2), pp. 107-112.

Slater, K. (1993). Chemical Testing and Analysis-A Review of Recent Literature on Chemical Testing and Analysis Developments, *Text. Prog.*, **25**(1), pp. 1-168.

Sich, J. (1990). Fibre Identification with Both Scanning Electron Microscope and Light Microscope. In: *Proc. 2<sup>nd</sup> Int. Symp. Speciality Animal Fibres*, Aachen: Schrift. der Deutsches Wollforschungsinstitutet, **106**, pp. 91-103.

Signori, V. and Lewis, D.M. (1997). FTIR Investigation of the Damage Produced on Human Hair by Weathering and Bleaching Processes: Implementation of Different Sampling Techniques and Data Processing, *International J. Cosmet. Sci.*, **19**, pp. 1-13.

Sikorski, J. (1963). *Fibre Structure*, 1<sup>st</sup> Ed., Manchester: Butterworth and co. Ltd.

Simonds, D.H. (1958). The Amino Acids Components of Keratins: A Comparison of the Chemical Composition of the Merino Wools of Differing Crimp with that of Other Animal Fibres, *Textile Res. J.*, **28**, pp. 314-317.

Skinkle, J.H. (1936). The Determination of Wool and Mohair by Scale Size and Diameter, *Amer. Dyest. Rep.*, **25**, pp. 620-621.

Smith, J.R. (1998). A Quantitative Method for Analysing AFM Images of the Outer Surfaces of Human Hair, *J. Microscopy*, **191**, pp. 223–228.

Smuts, L., Hunter, L. and Gee, E. (1980). *Identification of Mohair in Blends with Other Animal Fibres by Using their Frictional Properties*. Tech. Rep. No. 457, Port Elizabeth: SAWTRI.

Smuts, S. and Slinger, R.I. (1972). *The Influence of Fibre Friction on the Handle of Wool and Mohair*, Tech. Rep. No. 163, Pot Elizabeth: SWTRI.

Sowa, M.G., Wang, J., Schultz, C.P., Ahmed, M.K. and Mantsch, H.H. (1995). Infrared Spectroscopic Investigation of In-vivo and Ex-vivo Human Nails, *Vibrational Spectrosc.*, **10**, pp. 49-56.

Speakman, P.T. and Horn, J.C. (1987). Distinguishing Between Different Animal Fibres by Electrophoresis of Polypeptides Dissolved for Them, *J. Text. Inst.*, **78**(4), pp. 308-311.



Stapleton, I.W. (1992). *Alpaca as a Textile Fibre: Fact or Fiction- A Review and Interpretation of Published Research Findings on Alpaca*, Textile Fibre Research Institute.

Stein, S.E. and Scott, D.R. (1994). Optimization and Testing of Mass Spectral Library Search Algorithms for Compound Identification, *J. Am. Soc. Mass Spectrom.*, **5**, pp. 859-866.

Stephani, G. and Zahn, H. (1985). Investigation of Blends of Fone Animal Hairs by Two-Dimensional SDS-Polyacrylamide Gel Electrophoresis. In: *Proc. 7<sup>th</sup> Int. Wool Text. Res. Conf.*, Tokyo: Society of Fibre Science and Technology, **II**, pp. 195-204.

Stewart, K., Spedding, P.L., Otterburn, M.S. and Lewis, D.M. (1997). Isolating Cuticle Layer of Wool: A Comparison of Methods, *JSDC*. **113**, pp. 32-34.

Straussburger, J. (1985). Quantitative Fourier Transform Infrared Spectroscopy of Oxidized Hair, *J. Soc. Cosmetic Chem.*, **36**, pp. 61-74.

Stuart, B. (20014). "*Infrared Spectroscopy: Fundamentals and Applications*", Chichester: John Wiley & Sons Ltd.

Subramanian, S., Karthik, T. and Vijayaraaghavan, N.N. (2005). Single Nucleotide Polymorphism for Animal Fibre Identification, *J. Biotechn.*, **116**, pp. 153-158.

Sugeta, H., Go, A. and Miyazawa, T. (1972). S-S and C-S Stretching Vibrations and Molecular Conformations of Dialkyl Disulphide and Cystine, *Chem. Lett.*, **1**, pp. 83-86.

Sugeta, H., Go, A. and Miyazawa, T. (1973). Vibrational Spectra and Molecular Conformations of Dialkyl Disulphides, *Bull. Chem. Soc. Jpn.*, **46**, pp. 3407-3411.

Tang, M., Zhang, W., Zhou, H., Fei, J., Yang, J., Lu, W., Zhang, S., Ye, S. and Wang, X. (2014). A Real-Time PCR Method for Quantifying Mixed Cashmere and Wool Based on Hair Mitochondrial DNA, *Text. Res. J.*, **84**(15), pp. 1612-1621.

Teasdale, D.C. (1988). Multivariate Analysis in Fibre Characterization and Identification. In: *Proc. 1<sup>st</sup> Int. Symp. On Speciality Animal Fibres*, Aachen: Schrift. der Deutsches Wollforschungsinstitutet, **103**, pp. 23-38.

The Textile Institute. (1970). "*Identification of Textile Materials*", 6<sup>th</sup> Ed., London: C. Tinling Co.Ltd.

Thiry, M.C. (2007). Detecting-The Art and Science, In: *AACTT Review*, pp. 18-21.

Tonetti, C., Vineis, C., Aluigi, A. and Tonin, C. (2012). Immunological Method for the Identification of Animal Hair Fibres, *Text. Res. J.*, **82**(8), pp. 766-772.

Tuchel, D. (2016). Selecting an Excitation Wavelength for Raman Spectroscopy, *Spectroscopy*, **31**(3), pp. 14-23.

Tucker, P.A. (1997). Scale Height of Chemically Treated Wool and Hair Fibres, *Text. Res. J.*, **68**(3), pp. 229-230.

Tucker, D.J., Hudson, A.H.F., Logan, R.I. and Rivett, D.E. (1990). Integral Lipids of Goat Fibres. In: *Proc. 8<sup>th</sup> Int. Wool Text. Res. Conf.*, Christchurch: Wool Research Organization of New Zealand, **II**, pp. 364-373.

Tucker, D.J., Hudson, H.F., Ozolins, G.V., Rivett, D.E. and Jones, L.N. (1988). Some Aspects of the Structural and Composition of Speciality Animal Fibres. In: *Proc. 1<sup>st</sup> Int. Symp. Speciality Animal Fibres*, Aachen: Schrift. Der Deutsches Wollforschungsinstitutet, **103**, pp. 71-101.

Tucker, D.J., Rivett, D.E., Restall, B.J. and Hudson, A.H.F. (1985). The Non-Protein Contents of the Cashmere Fibre. In: *Proc. 7<sup>th</sup> Int. Wool Text. Res. Conf.*, Tokyo: Society of Fibre Science and Technology, **II**, pp. 223-235.

Tucker, D.J., Hudson, A.H.F., Laudani, A., Marshall., R.C. and Rivett, D.F. (1989). Variation in Goat Fibre Proteins, *Aust. J. Agric. Res.*, **40**, pp. 675-683.

Tungol, M. W., Bartick, E. B. and Montaser, A. (1990). The Development of a Spectral Data Base for the Identification of Fibres by Infrared Microscopy, *Applied Spectroscopy*, **44**(4), pp. 543-549.

Varley, A.R. (2006). A Modified Method of Cuticle Scale Height Determination for Animal Fibres, *AATCC Review*, pp. 38-41.

Veldsman, D.P. (1980). Latest Trends in Processing Mohair. In: *Proc. 5<sup>th</sup> Int. Wool Text. Res. Conf.*, Pretoria: South African Wool and Textile Research Institute, **1**, pp. 195-212.

Vineis, C., Tonetti, C., Paoella, S., Pozzo, P.D. and Sforza, S. (2013). A UPLC/ESI-MS Method for Identifying Wool, Cashmere and Yak Fibres, *Text. Res. J.*, **83**(9), pp.953-958.

Von-Bergen, W. (1963). "*Wool Handbook*", 3<sup>rd</sup> Ed., New York: John Wiley & Sons, Inc.

Wang, H., Liu, X. and Wang, X. (2005). FTIR and Thermal Analysis of Cashmere and other Animal Fibres. In: *Proc. 3<sup>rd</sup> Int. Cashmere Determination Technique Sermina-Paper Collection*, Erdos: Inner Mongolia Erdos Cashmere Group Co. Ltd, pp. 217-228.

Wang, K., Li, R., Ma, J.R., Y. K. Jian, Y.K. and Che, J.N. (2013). Extracting Keratin from Wool by Using L-Cysteine, *Green Chem.*, **18**(2), pp. 476-481.

Ward, W.H., Binkley, C.H. and Snell, N.S. (1955). Amino Acid Composition of Normal Wools, Wool Fractions, Mohair, Feather, and Feather Fractions, *Text. Res. J.*, **25**(4), pp. 314-325.

Weideman, E., Gee, E., Hunter, L. and Turpie, D.W.F. (1987). The Use of Fibre Scale Height in Distinguishing Between Mohair and Wool, *SAWTRI Bulletin*, **21**(3), pp. 7-13.

Weideman, E. and Smuts, S. (1985). A Study of Scale Geometry and Friction of Wool and Mohair, *Proc. Electron Microscopy Soc.*, **15**, South Africa, pp. 51-51.

Weston, G.J. (1955). The Infrared Spectrum of Paracetic Acid-Treated Wool, *Biochimica Et Biophysica Acta*, **17**, pp. 462-464.

Whiffer, D. H. (1966). "*Spectroscopy*", London: Longmans Green and Co Ltd.

Wilcox, C. (2018). 'The Global Wool Market: The Good, the Bad and the Prospects', 87<sup>th</sup> IWTO Congress, Hong Kong, 13-16 May 2018, Online URL:

[https://www.woolbrokers.org/images/presentations/wilcox\\_2018\\_iwto\\_hong\\_kong.pdf](https://www.woolbrokers.org/images/presentations/wilcox_2018_iwto_hong_kong.pdf).

Wildman, A.B. (1954). “*The Microscopy of Animal Textile Fibres, Including Methods for the Complete Analysis of Fibre Blends*”, Leeds: Wool Industries Research Association.

Wilkinson, B.R. (1990). Speciality Animal Fibres. In: *Proc. 8<sup>th</sup> Int. Wool Text. Res. Conf.*, Christchurch: Wool Research Organization of New Zealand, **II**, pp. 355-363.

Wilson, A.S., Edwards, H.G.M., Farwell, D.W. and Janaway, R.C. (1999). Fourier Transform Raman Spectroscopy: Evaluation as a Non-destructive Technique for Studying the Degradation of Human Hair from Archaeological and Forensic Environments, *J. Raman Spec.*, **30**, pp. 367-373.

Wilson, R.H. and Lewis, H.B. (1927). The Cystine Content of Hair and Other Epidermal Tissues, *J. Biol. Chem.*, **73**, pp. 543-553.

Wilrich, C., Wortmann, G., Wortmann, F.-J. and Höcker, H. (1995). Gel Electrophoresis as a Mean for the Damage Assessment of Wool. In: *Proc. 8<sup>th</sup> Int. Wool Text. Res. Conf.*, Christchurch: Wool Research Organization of New Zealand, **II**, pp. 289-295.

Wojciechowska, E., Włochowicz, A. and Wesełucha-Birczyńska, A. (1999). Application of Fourier-Transform Infrared and Raman Spectroscopy to Study Degradation of Wool Fibre Keratin, *J. Molec. Struc.*, **511-512**, pp. 307-318.

Wojciechowska, E., Rom, M., Włochowicz, A., Wjsocki, M. and Wesełucha-Birczyńska, A. (2004). The Use of Fourier Transform Infrared (FTIR) Raman Spectroscopy (FTR) for the Investigation of Structural Changes in Wool Fibre Keratin after Enzymatic Treatment, *J. Molec. Struc.*, **704**, pp. 315-321.

Wortmann, F.J. (1991). Quantitative Fibre Mixture Analysis by Scanning Electron Microscopy-Part III: Round Trial Results on Mohair/Wool Blends, *Text. Res. J.* **61**(7), pp. 371-374.

Wortmann, F.J. and Arns, W. (1986). Quantitative Fibre Mixture Analysis by Scanning Electron Microscopy-Part I: Blends of Mohair and Cashmere with Sheep Wool, *Text. Res. J.*, **56**(7), pp. 442-446.

Wortmann, F.J. and Phan, K.H. (1999). Cuticle Scale Heights of Wool and Speciality Fibres and their Changes Due to Textile Processing, *Text. Res. J.*, **69**(2), pp. 139-144.

Wortmann, F.J. and Phan, K.H. (2006). What is 100 Cashmere? *Wool Record*, **10**, pp. 25-25.

Wortmann, F.J. and Wortmann, G. (1992). Quantitative Fibre Mixture Analysis by Scanning Electron Microscopy-Part IV: Assessment of Light Microscopy as an Alternative Tool for Analysing Wool/Speciality Fibre Blends, *Tex. Res. J.*, **62**(7), pp. 423-431.

Wortmann, F.J. and Phan, K.H. (2004). The Accurate Analysis of Speciality Fibre/Wool Blends, *Wool Record*, **10**, pp. 51-51.

Wortmann, F.J. and Wortmann, G. (1988). Chemical Characterization of Fine Animal Hair. In: *Proc. 1<sup>st</sup> Int. Symp. Speciality Animal Fibres*, Aachen: Schrift. der Deutsches Wollforschungsinstitutet, **103**, pp. 39-70.

Wortmann, F.J. and Wortmann, G. (1990). Wool Contaminations in Cashmere, In: *Proc. 2<sup>nd</sup> Int. Symp. On Speciality Animal Fibres*, Aachen: Schrift. der Deutsches Wollforschungsinstitutet, **106**, pp. 138-146.

Wortmann, F. J, Wortmann, G. and Greven, R. (2000). Mechanical Profilometry of Wool and Mohair Fibres, *Text. Res. J.*, **70**(9), pp. 795-801.

Wortmann, F. J, Wortmann, G. and Roes, J. (1989). Light Microscopic Analysis of Yak and Cashmere. In: *Proc. 2<sup>nd</sup> Int. Symp. On Specialty Animal Fibres*, Aachen: Schrift. der Deutsches Wollforschungsinstitutet, DWI Rep. **102**, pp. 104-112.

Wortmann, F.-J., Wortmann, G., Arns, W. and Phan, K.-H. (1988). Analysis of Specialty Fibre/Wool Blends by Means of Scanning Electron Microscopy (SEM). In:

*Proc. 1st Inter. Symp. On Speciality Animal Fibres*, Aachen: Schrift. der Deutsches Wollforschungsinstitutet, **103**, pp. 163-188.

Wortmann, F.J., Phan, K.H. and Augustine, P. (2003). Quantitative Fibre Analysis by Scanning Electron Microscopy-Part V: Analysis of Pure Fibre Samples and Samples with Small Admixtures According to Test Method IWTO-58, *Text. Res. J.*, **73**(8), pp. 727-732.

Wortmann, F.J., Wortmann, G. and McCarthy, B. (2007). Cashmere/Yak Blends: A Vexing Analytical Problem, *Wool Record*, **4**, pp. 33-33.

Wortmann, G., Körner, A. and Wortmann, F.J. (1986). IWTO Tech. Report No. 10, pp. 1-7.

Wortmann, G., Phan, K.-H. and Wortmann, F.-J. (2000). Electrophoretical Differentiation of Animal Hair: Shahtoosh. In: *Proc. 10<sup>th</sup> Int. Wool Text. Res. Conf.*, Aachen: Schrift. der Deutsches Wollforschungsinstitutet, **III**, pp. 1-3.

Wozney, K.M. and Wilson, P.J. (2012). Real –Time PCR Detection and Quantification of Elephantid DNA: Species Identification for Highly Processed Samples Associated with the Ivory Trade, *Forensic Sci. Int.*, **219**, pp 106-112.

Wu, G.F., Zhu, D.S. and He, Y. (2008). Identification of Fine Wool and Cashmere Using Vis/NIR Spectroscopy Technology, *Guang Pu Xue Yu Guang Pu Fen Xi*, **28**(6), pp. 1260-1263.

Yang, H., Yang, S., Kong, J., Dong, A. and Yu, S. (2015). Obtaining Information About Protein Secondarys in Aqueous Solution using Fourier Transform IR Spectroscopy, *Nature Protocols*, **10**(3), pp. 382-396.

Yao, J., Liu, Y., Yang, S. and Liu, J. (2008). Characterization of Secondary Structure Transformation of Stretched and Slenderized Wool Fibers with FTIR Spectra, *J. Eng. Fibres and Fabrics*, **3**(2), pp. 1-10.

Yiping, J., Rui, W., Souting, Y., Yi, Z. and Yunhui, Y. (2008). Study on Identifying Blend Ratio of Wool and Cashmere by Computer Image Recognition Technology. In:

*Proc. 4<sup>th</sup> Int. Cashmere Determination Tech. Symp.*, Erdos: Inner Mongolia Erdos Cashmere Group Co. Ltd, pp. 66-72.

Yoshioka, Y. (2008). DNA Analysis for Animal Fibres. In: *Proc. 4<sup>th</sup> Inter. Cashmere Determination Techniques Symposium*, Erdos: Inner Mongolia Erdos Cashmere Group Co. Ltd, pp. 282-287.

Žemaitytė, R., Jonaitienė V., Milašius, R., Stanys, S. and Ulozaitė, R. (2006). Analysis and Identification of Fibre Constitution of Archaeological Textiles, *Materials Science J. (Madziagotyra)*, **12**(3), pp. 258-261.

Zhang, J., Palmer, S. and Wang, X. (2010). Identification of Animal Fibres with Wavelet Texture Analysis, *Proceedings of the World Congress on Engineering*, London, **1**, pp. 742-747.

Zhou, P. (2015). *Choosing the Most Suitable Laser Wavelength for Your Raman Application*, BWTEK Inc, accessed 21 September 2017, URL: <<https://bwtek.com/wp-content/uploads/2015/07/raman-laser-selection-application-note.pdf>>.

Zhong, Z. and Xiao, C. (2008). Fabric Composition Testing. In J. HU, ed., “*Fabric Testing*”, Oxford: Woodhead Publishing Limited, pp. 48-87.

Zoccola, M., Lu M., Mossotti, R., Innocenti, R. and Montarsolo A. (2013). Identification of Wool, Cashmere, Yak and Angora Rabbit Fibre and Quantitative Determination of Wool and Cashmere in Blend: A Near Infrared Spectroscopy Study, *Fibres and Polymers*, **14**(8), pp. 1283-1289.

## APPENDICES

### Appendix I (a): Wool and mohair (all Texas) samples for micro Raman analysis.

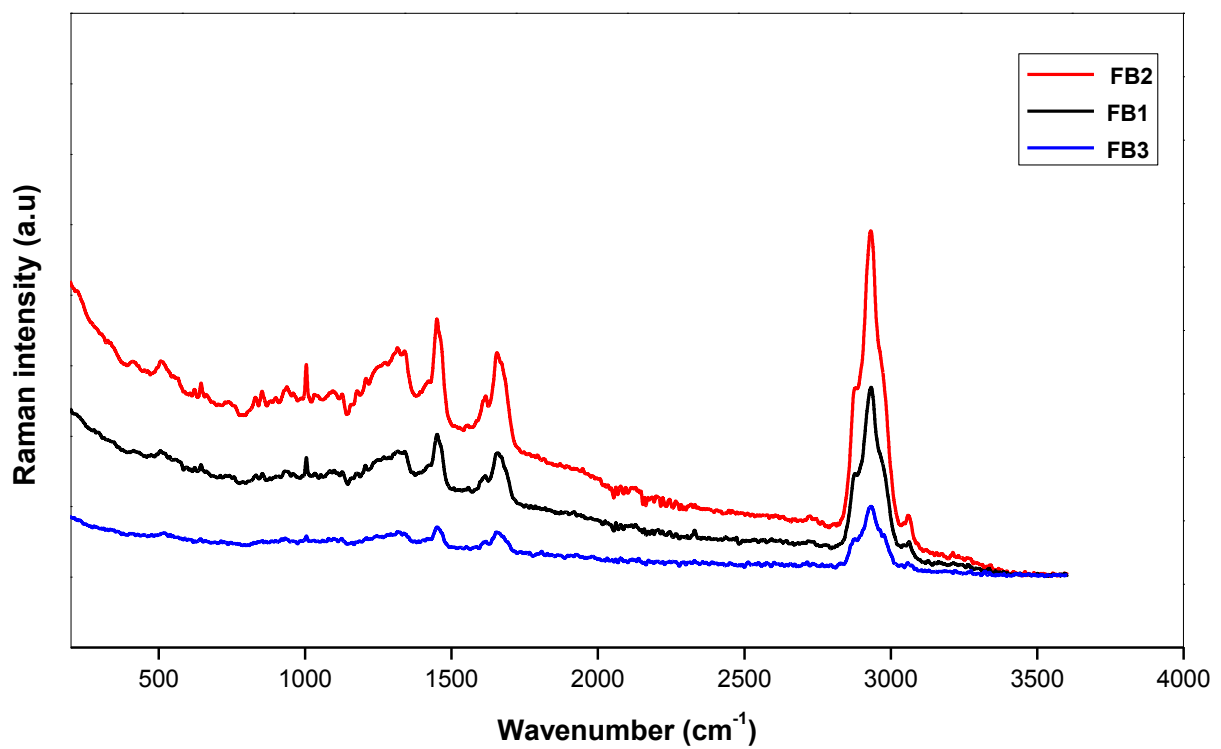
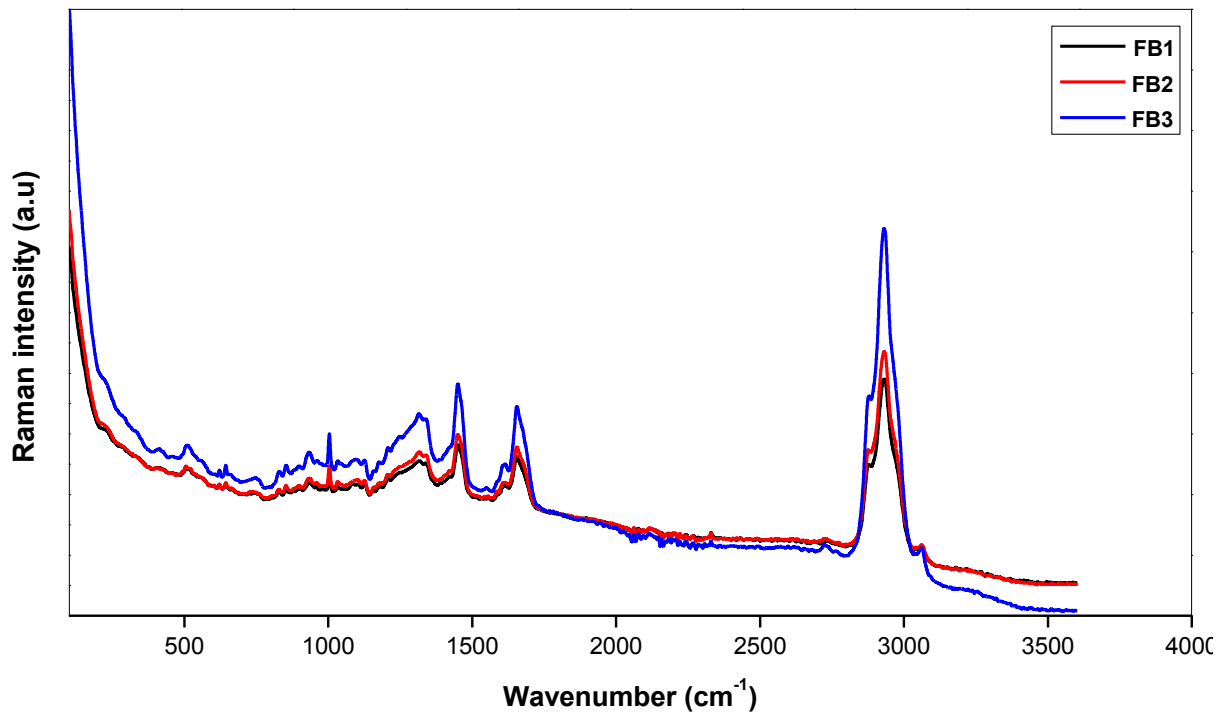
Wool samples	Mohair samples
BR11	1048 (Texas mohair)
Lincoln3	742 (Texas mohair)
Lincoln4	1126 (Texas mohair)
Romney marsh	146 (Texas mohair)
Corriedale	

### Appendix I (b): Wool and mohair samples analysed using the FTIR-LUMOS.

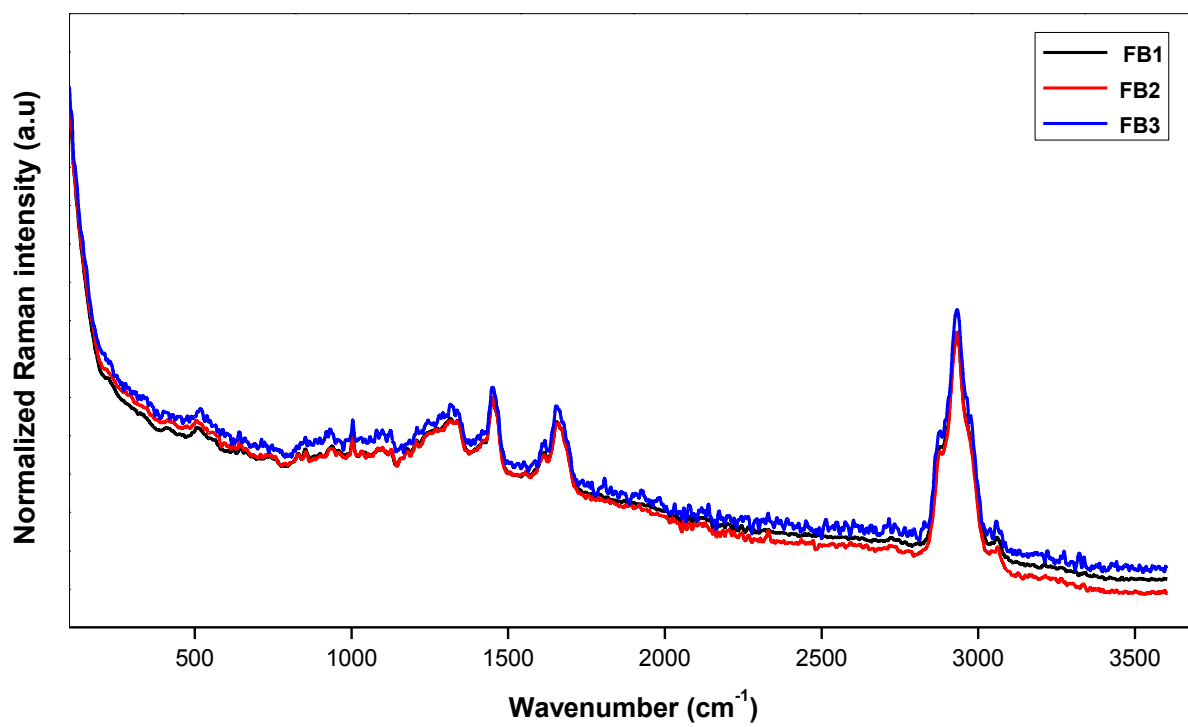
Wool	Mohair
Dorset horn (DH)	146
W38	1048
W52	1078
BR59	712
Corriedale	742
Lincoln3	1002
Romney marsh	SB
W56	TYG1



Appendix II (a) Effect of sample thickness on the band absolute intensities



## Appendix II (b): Effect of Sample Thickness on Normalized Raman Intensity



## Appendix III: FT Raman curve fitting results

### a) Amide I

#### Mohair

##### Peaks

	Area	Center	Width	Height
1	2,44218	1586,2557	9,8893	0,19704
2	7,26651	1605,41965	15,53731	0,37316
3	1,14008	1617,43547	7,06892	0,12868
4	13,76397	1622,39674	25,43161	0,43183
5	39,92611	1650,94767	20,30578	1,56884
6	15,91548	1668,22116	18,01786	0,70478
7	24,57008	1681,05676	23,04818	0,85057
8	7,82373	1695,47083	20,98938	0,29741

##### Statistics

DF	126
COD (R <sup>2</sup> )	0,99962
ReducedChiSq	1,31632E-4

##### Peaks

	Area	Center	Width	Height
1	28,78514	1653,40147	16,21986	1,41599
2	26,54472	1670,04913	17,55084	1,20676
3	11,93015	1684,52034	14,68444	0,64823
4	0,18113	1694,66662	5,98081	0,02416
5	0,93599	1616,85421	5,3012	0,14088
6	11,74993	1608,51002	16,87807	0,55546
7	2,37001	1586,66827	10,79261	0,17521
8	12,92169	1636,35309	18,98176	0,54315

##### Statistics

DF	97
COD (R <sup>2</sup> )	0,99985
ReducedChiSq	5,79497E-5

##### Peaks

	Area	Center	Width	Height
1	36,08594	1653,30427	18,56314	1,55105
2	20,10986	1670,2756	16,84759	0,95238
3	18,84002	1684,48789	18,80319	0,79945
4	5,05141	1698,82718	16,56334	0,24334
5	13,44958	1633,32334	22,19123	0,48358
6	2,17631	1618,51217	8,55935	0,20287
7	10,76037	1607,28396	16,39264	0,52374
8	2,42407	1586,70463	10,42597	0,18551

##### Statistics

DF	100
COD (R <sup>2</sup> )	0,99952
ReducedChiSq	1,90861E-4

#### Wool

##### Peaks

	Area	Center	Width	Height
1	1,06851	1585,87884	7,09736	0,12012
2	9,38462	1607,7419	17,23021	0,43458
3	2,096	1617,70865	8,14815	0,20524
4	8,78311	1633,66571	21,67786	0,32328
5	27,90254	1654,13241	16,46055	1,35251
6	19,80431	1669,90328	15,59947	1,01295
7	18,43106	1684,74335	17,25237	0,8524
8	3,51194	1699,03279	13,15844	0,21295

##### Statistics

DF	97
COD (R <sup>2</sup> )	0,99927
ReducedChiSq	2,49369E-4

*Peaks*

	Area	Center	Width	Height
1	0,82864	1585,51427	6,19584	0,10671
2	6,0206	1606,43075	16,57477	0,28982
3	2,9104	1617,20777	8,88018	0,2615
4	12,62555	1641,64418	23,62715	0,42636
5	23,94737	1654,66226	15,83253	1,20683
6	12,47519	1668,00433	13,53897	0,73519
7	15,79271	1678,99316	15,33807	0,82154
8	8,87068	1691,22546	14,60492	0,48462

*Statistics*

DF	97
COD (R <sup>2</sup> )	0,99996
ReducedChiSq	1,23837E-5

*Peaks*

	Area	Center	Width	Height
1	0,93577	1586,33732	6,14892	0,12143
2	8,00143	1607,86301	16,3853	0,38963
3	1,83628	1617,96291	7,64846	0,19156
4	22,62912	1644,8684	32,05964	0,56318
5	19,41357	1654,06751	15,73741	0,98427
6	14,82702	1669,20005	14,8233	0,79808
7	18,76581	1683,71639	17,92547	0,83529
8	2,63581	1698,1927	12,44905	0,16893

*Statistics*

DF	97
COD (R <sup>2</sup> )	0,99886
ReducedChiSq	3,66479E-4

**b) S-S stretch**

Mohair

*Peaks*

	Area	Center	Width	Height
1	5,33317	507,09975	13,48187	0,31563
2	0,15168	514,41948	4,93772	0,02451
3	3,39147	520,57401	12,09687	0,22369
4	0,61642	492,37705	8,2114	0,0599
5	2,97369	533,26026	15,94164	0,14883
6	0,0331	541,27159	3,03353	0,00871

*Statistics*

DF	54
COD (R <sup>2</sup> )	0,99907
ReducedChiSq	1,80602E-5

*Peaks*

	Area	Center	Width	Height
1	0,24798	493,11988	4,22636	0,04682
2	2,09826	504,91837	9,69067	0,17276
3	2,33577	515,83908	11,25705	0,16556
4	0,6319	524,03447	6,70861	0,07515
5	0,6876	532,11971	8,2057	0,06686
6	0,16545	539,93349	3,99614	0,03303

*Statistics*

DF	--
COD (R <sup>2</sup> )	0,99443
ReducedChiSq	4,96077E-5

*Peaks*

	Area	Center	Width	Height
1	0,32865	492,69236	5,20098	0,05042
2	5,07104	507,70011	13,16102	0,30743
3	0,16237	515,41022	3,99252	0,03245
4	2,47728	521,01847	9,48397	0,20841
5	2,85384	534,74428	15,60246	0,14594
6	0,19572	541,19365	4,50619	0,03466

*Statistics*

DF	48
COD (R <sup>2</sup> )	0,99706
ReducedChiSq	5,27048E-5

## Wool

### Peaks

	Area	Center	Width	Height
1	3,51729	506,65983	10,61913	0,26428
2	0,69722	514,84905	5,80256	0,09587
3	0,27021	493,05271	4,36345	0,04941
4	1,88412	521,68252	10,28532	0,14616
5	0,14598	536,27548	5,41747	0,0215
6	0,13096	540,50524	3,14111	0,03326

*Statistics*

DF	50
COD (R <sup>2</sup> )	0,99267
ReducedChiSq	6,51813E-5

### Peaks

	Area	Center	Width	Height
1	0,26756	492,66145	5,8411	0,03655
2	5,59443	507,68274	13,38568	0,33347
3	0,22984	515,61038	5,84684	0,03136
4	3,30032	522,11216	13,38534	0,19673
5	0,29841	533,53128	6,11007	0,03897
6	0,45672	540,32278	6,39063	0,05702

*Statistics*

DF	47
COD (R <sup>2</sup> )	0,99883
ReducedChiSq	2,16865E-5

### Peaks

	Area	Center	Width	Height
1	4,32309	507,78543	12,42174	0,27769
2	0,18668	514,93321	4,6208	0,03223
3	0,32382	492,19818	5,91005	0,04372
4	0,67893	533,14528	9,72109	0,05573
5	0,29412	540,85263	5,11436	0,04589

*Statistics*

DF	50
COD (R <sup>2</sup> )	0,99854
ReducedChiSq	1,54822E-5

#### Appendix IV: A t-test comparison of the disulphide content values from wool and mohair.

##### Descriptive Statistics

	N	Mean	SD	SEM
MOHAIR	54	0,16708	0,03203	0,00436
WOOL	50	0,1976	0,04416	0,00624
Difference		-0,03052		

##### t-Test Statistics

	t Statistic	DF	Prob> t
Equal Variance Assumed	-4,05651	102	9,76424E-5
Equal Variance NOT Assumed	-4,00787	88,86731	1,27133E-4

Null Hypothesis: mean1-mean2 = 0  
 Alternative Hypothesis: mean1-mean2 <> 0  
 At the 0.05 level, the difference of the population means is significantly different with the test difference(0)

#### Appendix V: Variation in relative intensities of the same spot along a fibre bundle

The averages (of five spectra) of the relative intensities for each Raman band are presented with the standard deviation values in brackets. A minimum of five spectra were acquired from each spot (S) along the length of each fibre bundle (B).

Sample ID	Different fibre bundles	CH <sub>2</sub> asym. Stretch	CH <sub>2</sub> & CH <sub>3</sub> bending	Amide I	Phe & Trp	Skeletal C-C stretch	Tyr	Phe	S-S stretch
Texas International Mohair INC-	B1S1	4.613 (0.021)	1.752 (0.009)	1.564 (0.016)	0.678 (0.011)	0.261 (0.003)	0.231 (0.005)	0.137 (0.003)	0.342 (0.006)
	B1S2	4.42 (0.028)	1.754 (0.005)	1.603 (0.008)	0.676 (0.003)	0.279 (0.006)	0.231 (0.004)	0.134 (0.004)	0.348 (0.004)
	B1S3	4.812 (0.013)	1.765 (0.004)	1.624 (0.004)	0.661 (0.008)	0.270 (0.004)	0.221 (0.006)	0.127 (0.004)	0.346 (0.005)

<b>#728</b>	B2S1	5.071 (0.047)	1.772 (0.007)	1.662 (0.010)	0.662 (0.007)	0.274 (0.005)	0.231 (0.005)	0.134 (0.001)	0.334 (0.004)
	B2S2	4.716 (0.048)	1.766 (0.014)	1.640 (0.013)	0.651 (0.007)	0.272 (0.002)	0.232 (0.003)	0.133 (0.001)	0.338 (0.003)
	B2S3	5.098 (0.010)	1.769 (0.003)	1.635 (0.005)	0.682 (0.004)	0.276 (0.004)	0.230 (0.004)	0.132 (0.002)	0.342 (0.002)
<b>New Mexico Kid Mohair - 365</b>	B1S1	4.496 (0.006)	1.763 (0.011)	1.610 (0.004)	0.604 (0.005)	0.270 (0.003)	0.198 (0.004)	0.117 (0.004)	0.376 (0.004)
	B1S2	4.375 (0.003)	1.769 (0.004)	1.636 (0.004)	0.596 (0.003)	0.279 (0.003)	0.203 (0.004)	0.120 (0.001)	0.379 (0.003)
	B2S1	4.944 (0.040)	1.768 (0.013)	1.641 (0.011)	0.577 (0.009)	0.265 (0.003)	0.190 (0.002)	0.108 (0.004)	0.368 (0.008)
	B2S2	5.219 (0.035)	1.772 (0.001)	1.654 (0.009)	0.591 (0.008)	0.255 (0.004)	0.202 (0.009)	0.122 (0.004)	0.372 (0.007)

**B1S1- Bundle 1 Spot 1; B1S2-Bundle 1 Spot 2; B1S3-Bundle 1 Spot 3.**

<b>Sample ID</b>	<b>Different fibre bundles</b>	<b>CH<sub>2</sub> asym. Stretch</b>	<b>CH<sub>2</sub> &amp; CH<sub>3</sub> bending</b>	<b>Amide I (1654 cm<sup>-1</sup>)</b>	<b>Phe &amp; Trp (1004 cm<sup>-1</sup>)</b>	<b>Skeletal C-C stretch</b>	<b>Tyr (644 cm<sup>-1</sup>)</b>	<b>Phe (622 cm<sup>-1</sup>)</b>	<b>S-S stretch (508 cm<sup>-1</sup>)</b>
<b>CBP SS6 Merino Wool</b>	B1S1	5.175 (0.033)	1.819 (0.069)	1.749 (0.055)	0.636 (0.019)	0.313 (0.015)	0.242 (0.011)	0.127 (0.004)	0.456 (0.013)
	B1S2	5.633 (0.049)	1.788 (0.007)	1.629 (0.012)	0.618 (0.009)	0.305 (0.009)	0.226 (0.009)	0.121 (0.003)	0.436 (0.007)
	B2S1	5.017 (0.080)	1.786 (0.005)	1.659 (0.019)	0.702 (0.012)	0.308 (0.016)	0.287 (0.008)	0.128 (0.010)	0.448 (0.019)
	B2S2	4.993 (0.030)	1.770 (0.008)	1.671 (0.012)	0.680 (0.008)	0.302 (0.003)	0.291 (0.003)	0.132 (0.011)	0.459 (0.011)
	B2S3	5.247 (0.047)	1.757 (0.009)	1.662 (0.029)	0.700 (0.009)	0.307 (0.008)	0.280 (0.009)	0.140 (0.013)	0.435 (0.007)

<b>W56 Wool</b>	B1S1	4.733 (0.032)	1.748 (0.009)	1.711 (0.006)	0.591 (0.013)	0.339 (0.009)	0.176 (0.004)	0.114 (0.003)	0.450 (0.007)
	B1S2	4.791 (0.016)	1.750 (0.008)	1.626 (0.007)	0.583 (0.008)	0.319 (0.007)	0.173 (0.004)	0.116 (0.004)	0.420 (0.005)
	B1S3	4.610 (0.028)	1.747 (0.004)	1.549 (0.006)	0.590 (0.004)	0.320 (0.003)	0.181 (0.001)	0.118 (0.003)	0.427 (0.004)
	B2S1	4.662 (0.035)	1.753 (0.012)	1.652 (0.021)	0.557 (0.010)	0.312 (0.006)	0.179 (0.007)	0.115 (0.008)	0.468 (0.004)
	B2S2	4.579 (0.023)	1.748 (0.007)	1.665 (0.007)	0.595 (0.011)	0.316 (0.004)	0.196 (0.002)	0.118 (0.013)	0.464 (0.011)
	B2S3	5.202 (0.016)	1.761 (0.007)	1.610 (0.007)	0.593 (0.006)	0.323 (0.008)	0.175 (0.006)	0.114 (0.006)	0.398 (0.003)



